

Assessment of contact pressure and sliding velocity on the Tribological Performance of TPU Seal Materials for the Establishment of a Rating System

Master's Thesis

of

Ines Jölly, BSc

submitted to

**Chair of Materials Science and Testing of Plastics,
Montanuniversitaet Leoben**

with the support of

Polymer Competence Center Leoben GmbH



Supervision:

Dipl.-Ing. Dr. mont. István Gódor
Dipl. Ing. Andreas Hausberger

Revision:

Univ.-Prof. Dipl.-Ing. Dr.mont. Gerald Pinter

2011

Affidavit:

I declare in lieu of oath, that I wrote this thesis and performed the associated research myself, using only literature cited in this volume.

Leoben, 08 June 2011

Acknowledgement

The research work of this thesis was performed at the Polymer Competence Center Leoben GmbH (PCCL, Austria) within the framework of the COMET-program of the Austrian Ministry of Traffic, Innovation and Technology with contributions by the Montanuniversitaet Leoben (Chair of Mechanical Engineering, Chair of Materials Science and Testing of Plastics) and SKF Economos GmbH. The PCCL is funded by the Austrian Government and the State Governments of Styria and Upper Austria.

Many thanks to Univ.-Prof. Dipl.-Ing. Dr. mont. Gerald Pinter (Head of the Chair of Materials Science and Testing of Plastics, Montanuniversitaet Leoben, Austria) for establishing the scientific background of this research, thus making it possible.

I would also like to express great gratitude to Dipl.-Ing. Andreas Hausberger (Polymer Competence Center Leoben GmbH, Austria), who has been my mentor and supervisor for the current research and a constant source of motivation and support.

Furthermore, I'd like to thank in particular Dipl.-Ing. Dr. mont. István Gódor (Chair of Mechanical Engineering, Montanuniversitaet Leoben, Austria) for his technical expertise, especially in the field of tribology, and who was a great asset during the experimental section of this research. Many regards to Ass. Prof. Dipl.-Ing. Dr. mont. Florian Grün (Chair of Mechanical Engineering, Montanuniversitaet Leoben, Austria) for providing further technical support.

Moreover, I want to mention Dipl.-Ing. Dr. mont. Gerald Pilz (Chair of Materials Science and Testing of Plastics, Montanuniversitaet Leoben, Austria), who was always open for healthy discussion, but further contributed to this thesis as a reference of polymer characterization.

This thesis simply wouldn't be, if not for Dipl.-Ing. Dr. mont. Thomas Schwarz, who through SKF Economos GmbH, Judenburg, Austria granted access to required funds, materials and imminent data and Dipl.-Ing. Mario Mitterhuber (SKF Economos GmbH, Judenburg, Austria), who helped to acquire relevant materials.

Conclusively, many thanks to the PCCL -Team and the team of the Chair of Materials Science and Testing of Plastics for providing support in the organisational and experimental accomplishment of this work and for establishing a cooperative work environment.

Abstract

Over the previous years, Thermoplastic Polyurethanes (TPU) have firmly established themselves as high performance engineering materials on account of their excellent mechanical and processing properties. Accordingly, TPUs have now been utilized as seal materials for quite some time.

Mechanical seal performance is critically dependant on the tribology of the seal material, hence a reliable testing procedure to determine and compare the friction and wear related properties is of outermost importance.

The aim of this thesis is to develop a tribological benchmark testing methodology for TPU seal materials, using a precise rotary tribometer. The testing procedure in the Ring on Disc (RoD) mode, based on the standard ASTM D3702 (ASTM International Standard D 3702-94, 1999), is adapted to polymeric materials. The test specimen is a polymer disc, which slides on a ring shaped steel counterpart at dry contact at room temperature. During our former research the present test configuration was already used for the tribological characterization of seal materials.

The methodology has to investigate the influence of the main performance parameters, the sliding velocity v and the normal pressure p (in short: PV-parameters) on the materials' tribological behaviour. Therefore, a procedure was set up by progressively varying p at constant values of v and reversed varying v at constant values of p . The results demonstrate a strong dependency between friction related parameters and variations in PV-parameters. Additionally, friction and wear mechanisms of the tested materials can be further investigated by optical investigation of the worn surfaces along with an analysis of thermo-mechanical material parameters.

Conclusively, a significant tribological performance rating can be achieved via PV-step tests in correlation with contact surface formations, deterioration mechanisms and thermo-mechanical bulk characteristics. A relative PV-limiting value can be defined and the accumulation of damage mechanisms as well as the initiation of tribological failure can be analyzed.

Kurzfassung

Thermoplastische Polyurethane (TPU) haben sich aufgrund ihrer guten Verarbeitbarkeit in Kombination mit verbesserter mechanischer Stabilität in den letzten Jahren immer mehr als Ersatz für technische Elastomere in einem breiten Anwendungsspektrum etabliert. Besonders in der Dichtungsindustrie bewähren sie sich wegen ihrer herausragenden Ölbeständigkeit und den guten tribologischen Eigenschaften.

Das Laufverhalten und die daraus resultierende Lebensdauer von Dichtungen werden in großem Maße vom tribologischen Eigenschaftsspektrum des verwendeten Materials beeinflusst, was die Notwendigkeit einer geeigneten Charakterisierung und Bewertung von Dichtungsmaterialien unterstreicht.

Dazu soll im Rahmen der vorliegenden Masterarbeit eine umfassende tribologische Evaluierung von TPU-Dichtungsmaterialien mit dem Ziel der Entwicklung einer Benchmark-Testmethodik auf Modellniveau durchgeführt werden. Die Untersuchungen werden auf einem Rotationstribometer mit einer Ring-Scheibe-Testkonfiguration basierend auf der Norm ASTM D3702 (ASTM International Standard D 3702-94,1999) durchgeführt. Das zugrundeliegende Modellprüfsystem, bestehend aus der zu charakterisierenden Polymerscheibe, die unter einer bestimmten Flächenpressung auf einem Stahlring als Gegenkörper rotiert, wird im Rahmen der Arbeit, aufbauend auf den Inhalten früherer Forschungsprojekte, an elastomere Dichtungsmaterialien angepasst.

Des Weiteren wird eine Testmethodik entwickelt, die gezielt den Einfluss von Flächenpressung (p) und Gleitgeschwindigkeit (v), den sogenannten PV-Parametern, als limitierende Faktoren bei der tribologischen Performance der Materialien untersucht. Generell werden dazu die Reaktionen der Materialien auf Veränderungen der PV-Parametern mit Laststufen- und Drehzahlstufentests gezielt untersucht. Neben dem tribologischen Eigenschaftsprofil werden noch optische Untersuchungen der Laufflächen und thermomechanische Festkörpereigenschaften zur Bewertung hinzugezogen. Eine signifikante Abhängigkeit des tribologischen Laufverhaltens von den PV-Parametern kann gezeigt werden, was als Ansatz verwendet wird um eine PV-Einsatzgrenze bzw. Schadensgrenze für die untersuchten Dichtungsmaterialien zu definieren.

Table of Contents

1.	Introduction & Motivation	7
2.	Theoretical Background	9
2.1	Tribological Principles	9
2.1.1	<i>Overview of Tribological Materials' Testing</i>	9
2.1.2	<i>Definition and Significance of PV-application limits</i>	10
2.1.3	<i>Introduction to Elastomer Tribology</i>	12
2.1.4	<i>Tribological Impact Parameters- PV-dependency</i>	14
2.2	Thermoplastic Polyurethanes as High Performance Sealing Materials	15
2.2.1	<i>General Overview of Thermoplastic Polyurethanes</i>	15
2.2.2	<i>Specifications and Relevance in Sealing Industry</i>	17
3.	Experimental	21
3.1	Review of Tested Materials	21
3.2	Bulk Characterization	21
3.2.1	<i>Thermomechanical Bulk Properties</i>	21
3.2.2	<i>Thermal Bulk Properties</i>	24
3.3	Tribological Surface Characterization	25
3.3.1	<i>Experimental Set Up: RoD-Device at Rotary Tribometer TE93</i>	25
3.3.2	<i>Description of the Tribological Profile - Calculated parameters</i>	28
3.3.3	<i>Optical Investigations of Specimen and Counterpart</i>	29
3.3.4	<i>Set Up of Standard Testing Methodology</i>	30
3.3.5	<i>Development of a Benchmark Testing Methodology- PV-Step-Tests</i>	33
3.3.6	<i>Supplementary Tribological Characterization based on PV-Step-Tests</i>	34
3.3.7	<i>PV-Rating and definition of a PV-application limit</i>	35
4.	Results	41
4.1	Bulk Properties	41
4.1.1	<i>Dynamical Mechanical Analysis</i>	41

4.1.2	<i>Thermal Analysis via DSC</i>	45
4.2	Results and Approval of the Improvements on Specimen Geometry and the Test Configuration.....	47
4.2.1	<i>Geometrical optimization of RoD-specimens</i>	47
4.2.2	<i>Improvements of the Test Configuration</i>	47
4.3	General Tribological Profile of Tested Materials.....	49
4.3.1	<i>Tribological Performance of the unfilled material</i>	49
4.3.2	<i>Tribological Performance of the filled material</i>	50
4.3.3	<i>Comparison of the filled and unfilled material</i>	51
4.4	PV-dependency of Tribological Material Characteristics	53
4.4.1	<i>Evaluation of Load Step Tests</i>	53
4.4.2	<i>Evaluation of Speed Step Tests</i>	59
4.4.3	<i>Summary and Comparison of PV-Step Tests</i>	65
4.4.4	<i>Impact of varying contact pressure or sliding speed on the Surface Formation-Approach to define a phenomenological wear model</i>	67
4.5	PV-Rating and Definition of a PV-limiting value	78
4.5.1	<i>PV-Rating based on Results from PV-Step tests</i>	78
4.5.2	<i>PV-limit based on Investigations of worn Surfaces</i>	84
4.5.3	<i>Correlations with Thermo-Mechanical Material Characteristics</i>	88
4.5.4	<i>Approach to define a PV- application limit</i>	92
4.5.5	<i>Characterization of operational range by composing PV-diagrams</i>	93
5.	Conclusion	97
6.	Perspectives	100
7.	References	102
8.	Appendix	109
8.1	List of Figures.....	109
8.2	List of Tables.....	118
8.3	List of Abbreviations	120

8.4	Table of Context.....	122
8.4.1	<i>DMA-Analysis.....</i>	122
8.4.2	<i>DSC-measurements.....</i>	124
8.4.3	<i>Development and Adaptation of the ASTM D3702 Testing methodology for TPU materials.....</i>	127
8.4.4	<i>Standard tribological characterization- Constant load tests.....</i>	134
8.4.5	<i>Load step tests.....</i>	141
8.4.6	<i>Speed step tests.....</i>	159
8.4.7	<i>Advanced PV-step tests of the filled material</i>	176

1. Introduction & Motivation

In nearly all fields of mechanical engineering the tribological in-service behaviour has a major effect on the lifetime of diverse machine elements (Czichos and Habig, 2003). The resistance to tribological loading is essential to maintain the functionality of the seal, especially in regards to dynamical seal design. Leak tightness and stable running behaviour requires undamaged contact surfaces, conjointly with thermo-mechanical stability and sufficient resistance to tribological stresses of the seal (Flitney, 2007). Hence a detailed tribological characterization of sealing materials is of crucial importance.

Investigations of the operational behaviour of machine elements generally start with a tribological assessment of the components. Thus, the main influential parameters besides the operational conditions have to be well known for the specific application to set up a model testing procedure. Conventionally, appropriate component testing calls for the similitude of the tribological system at model and operational conditions since evaluated parameters depend to a high degree on the tribological system as a whole (Czichos and Habig, 2003). The in-service-performance of seals is highly dependent on the applied contact pressure (p) and the sliding velocity (v) (Jones, 2004). Moreover, the testing procedure has to be tailored for the selected sealing material. Polymers particularly are very temperature sensitive and elastomeric solutions additionally suffer from low modulus and hence low mechanical stability.

The aim of this research work is thus to assess the PV-dependency on the tribological performance of TPU sealing materials and to develop an accurate benchmark testing methodology.

In Figure 1 below the contents are schematically demonstrated. Firstly, the task is to adapt and develop the tribological testing procedure based on the ASTM Standard D3702 (ASTM International Standard D 3702-94, 1999), for metallic materials to elastomeric materials (Gódor et al, 2009). Subsequently, the tribological profile, focusing on the PV-dependency of pattern materials, is characterized. Accordingly, an appropriate testing methodology is developed or adapted by gradually varying either the contact pressure or the sliding velocity. Friction and wear related parameters are assessed in detail.

Additionally, the surface formation and the contact conditions are investigated to approve the PV-dependency on the tribological performance. The precise examination of the worn surfaces enables to describe friction and wear phenomena of the tested materials.

Thermo-mechanical bulk properties are analyzed additionally for a better understanding of the TPUs complex heterogeneous structure. An attempt is made to correlate the tribological profile of the pattern materials to the thermo-mechanical features. Especially the effect of elevated temperatures is of outermost importance. Bulk softening highly affects the tribological performance (Gódor et al, 2009).

Via combining tribological test results, optical surface investigations and thermo-mechanical analysis, a benchmark testing methodology can be defined to classify the tribological performance of elastomeric sealing materials (Figure 1.1-1).

Moreover, the investigated parameters can be used to define and identify tribological failure mechanisms on top of formulating a PV-application limit. PV-limits are already known for describing the operational behaviour of journal bearings and are used in their design (Mäurer, 2002).

Based on the collected data friction and wear mechanisms of TPU materials can be further investigated and linked to their morphology.

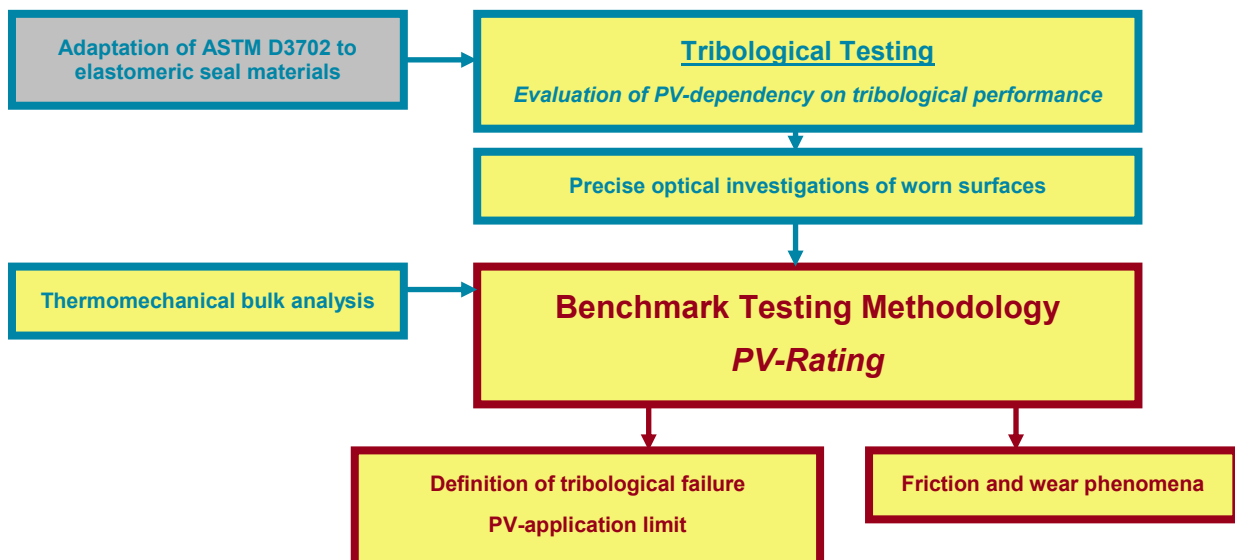


Figure 1.1-1: Contents of Masters Thesis

2. Theoretical Background

2.1 Tribological Principles

2.1.1 Overview of Tribological Materials' Testing

Tribological performance is highly complex, henceforth requires an extensive understanding of the influencing parameters and their interactions. It can definitely not be solely defined as substrate property. Tribological behaviour hence is designated as system characteristic (Grellmann, 2007). Figure 2.1-1 schematically presents the Tribological System.

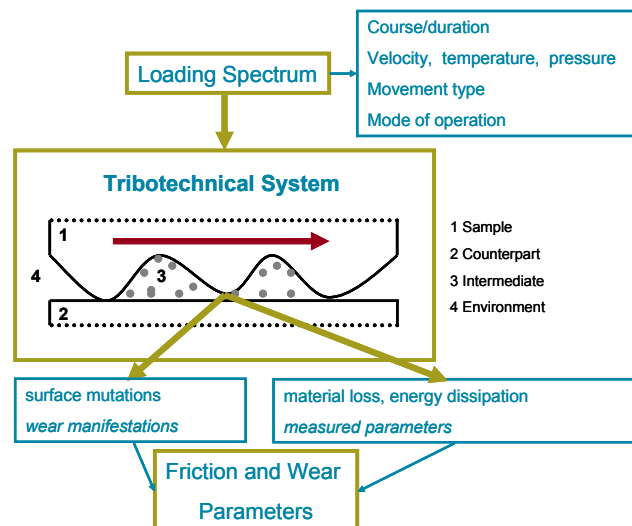


Figure 2.1-1: Schematical demonstration of the Tribological System (Czichos and Habig, 2003)

It mainly consists of the tribological pairing (sample, counterpart and intermediate) and its environment. A complex loading spectrum is applied and subsequently friction and wear phenomena occur. The system characteristic of a tribological operation has to be considered in regards to the development of suitable testing procedure of tribological materials, by means of equivalence in damage mechanisms.

In the field of engineering component testing generally starts at materials' level and advances to actual service trials. Comprehensive assignments from model experimentations to real application can be made by developing appropriate pattern testing procedures. Especially in tribology, the model testing configuration has to accurately

fit the real application conditions, otherwise assignments are invalid due to the system character of tribological phenomena. For that reason, a multitude of model testing configurations are developed in tribological testing. Some examples and their applications are demonstrated in Figure 2.1-2.

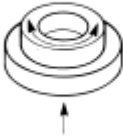


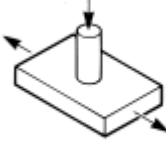

				
Ring on Disc	Pin on Disc	Block on Ring	Pin on Plate	Rolling Contact Fatigue
seals, plain bearings	seals, plain bearings	brakes	piston ring /cylinder liner, plain bearings	gears

Figure 2.1-2: Acknowledged tribological model testing configurations and equivalent application examples (Copyright © 2009 Phoenix Tribology Ltd, PLINT Tribology Products, www.phoenix-tribology.com, Newbury, England, 2011-04-27)

The key of an appropriate tribological characterization therefore is, first, to choose an appropriate model testing configuration and, then, to precisely set up a testing methodology and assess impact parameters, which exactly approximate the real application. Only if these conditions are met, an equivalent loading model is feasible, and an approach to correlate tribological material characteristics with the materials tribological performance in end-use application can be implemented.

2.1.2 Definition and Significance of PV-application limits

Tribological tests on component level do not reflect the operational behaviour of tribologically loaded devices. Anyhow, the influence of the main loading parameters on operation, contact pressure and sliding velocity, can be evaluated from model. The crucial impact of those parameters on the materials tribological performance enables to draw correlations between model testing and operational behaviour. A feasible implementation is constituted by the definition of a PV-application limit and respectively a PV-operating range (Mäurer, 2002). Especially in the plain bearing industry the so called PV-diagrams are fundamental and are conventionally specified in prod-

uct catalogues (Iigus GmbH Köln, Germany; SKF Group, Göteborg, Sweden). A schematical PV-diagram is shown in Figure 2.1-3.

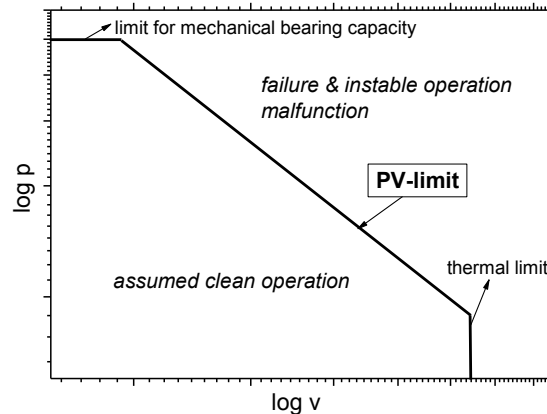


Figure 2.1-3: Schematical PV-diagram as reported at Mäurer (2002)

Notwithstanding, the implementation and modus operandi of PV-diagrams are not standardized in any way. The definition and modelling of the PV-limit strongly depends on the application and requirements of the machine element in practice. The PV-limit therefore is a critical accessory to the tribological system at hand (Mäurer, 2002). It is only valid for a specific tribological pairing - assignments to other pairings are not permitted by means of different frictional behaviour, heat transmission, contact surface temperatures and temperature-dependent material properties (Müller and Deters, 2004). Furthermore, the PV-limit only describes an application limit, but cannot declare the functionality of the tribological system (Müller and Deters, 2004).

Specifications about admissible operating conditions are of crucial significance, since the PV-limit only assesses the short-term characteristics of the tribological pairing. More durable performance can introduce failure due to the thermal overstress (Mäurer, 2002). The occurring temperatures in the rubbing contact generally influence the PV-limit to a significantly high degree. It is reported that the PV-settings in tribological performance mainly affect the arising frictional force, which is correlated with heat accumulation. Heat accumulation itself has a major effect on the wear, and thus is responsible for failure initiation (Davim and Cardoso, 2006; Schneider, 2000). As a result, the PV-limit is, in most cases, evaluated in accordance with frictional heat accumulation and contact surface temperatures (Schneider, 2000; Mäurer, 2002; Iigus GmbH, 2010). An approach for an accurate account of system temperature is absolutely vital in regards to the definition of the PV-limit, especially in polymer tribology when regarding the low thermal conductivity of polymers (Schneider, 2002). Other

estimations of the PV-limit, as described in literature, are based on the definition of tolerable wear and wear rates (Mäurer, 2002), conjointly mechanical stability, life-time predictions (rating life equation by SKF Group, 2004), friction and wear mechanisms (e.g. transfer film formation as described at Jones, 2004).

2.1.3 Introduction to Elastomer Tribology

Elastomers are conventionally characterized by highly nonlinear viscoelastic/hyperelastic behaviour, strong hysteresis, low rigidity and cyclic softening processes (Röthemeyer and Sommer, 2006), which have a vital impact on their tribological performance.

The sliding of elastomers on a rigid base under unlubricated conditions efforts high frictional work, on account of the soft elastomeric bulk and the resulting expanded contact area (Johnson et al, 1971). It is not a real sliding process, since it is mainly affected by deformation. In a strict sense, it can be described as caterpillar-like movement (Uetz and Wiedmeyer, 1985). This motion is described in greater detail by Schallamach (Schallamach, 1971; Fukahori, 2010). He assigns the caterpillar-like movement as local buckling instability in accordance with cyclic compressive stresses and shear deformations of surface asperities of the rubber face. Furthermore, stick-slip-processes are elucidated for elastomeric materials, especially in lower sliding velocity regimes (Hausberger, 2009) and can possibly be related with Schallamach's theory under certain conditions (Fukahori, 2010). The severe frictional heat accumulation in the rubbing groove has to be highlighted as another crucial tribological characteristic of rubbers. Frictional energy dissipation significantly contributes to cyclic deformation processes and strong internal damping of rubber henceforth. The frictional force thus features the same temperature dependency as the dynamical mechanical properties and is mainly a bulk property of rubber (Persson, 1998).

Rubber friction on rigid bases thus is generally dominated by adhesion and deformation/hysteresis processes. The distinct adhesion of the tribological pairing arises from expanded contact areas and provokes high frictional forces. The hysteresis part is caused by energy dissipation via the internal friction of rubber (Persson, 1998). Figure 2.1-4 schematically presents both mechanisms.

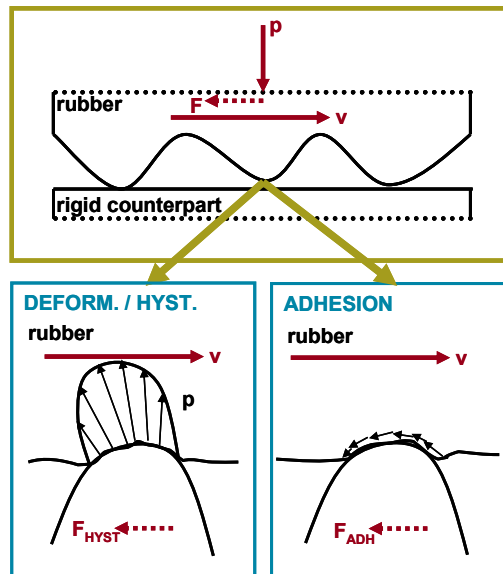


Figure 2.1-4: Adhesion and deformation part of friction of elastomers (Müller, 2002)

The occurring wear mechanism is critically dependent on the loading spectrum and system parameters. Conventionally, wear models, based on adhesion, abrasion and fatigue, are described in literature (Uetz and Wiedmeyer, 1985; Zhang, 2004; Myshkin, 2005; Gódor et al, 2009). Figure 2.1-5 schematically depicts the main mechanisms.

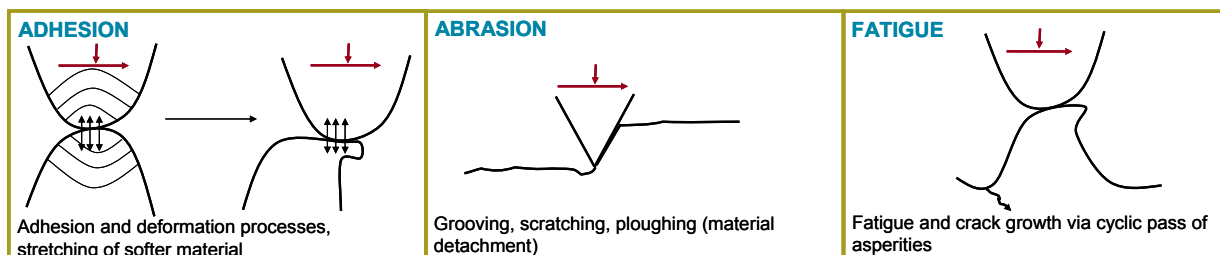


Figure 2.1-5: Common wear mechanisms of elastomers in dry sliding contact (Uetz and Wiedmeyer, 1985; Myshkin et al, 2005)

In adhesive/frictional wear regimes the strong adhering contact spots of the rubber are stretched during the sliding process. Overloads cause tearing of the stretched areas and roll-like wear particles are formed (Uetz and Wiedmeyer, 1985; Zhang, 2004).

Abrasions in rubber performance are described as grooving, cutting, scratching or ploughing with or without material detachment and respectively wear particle formation. Abrasive wear is generated by harder particles (three-body-abrasion) or asperities (two-body-abrasion) (Myshkin et al, 2005).

Fatigue wear is described as crack growth, indicating failure due to the cyclic pass of asperities (compression/expansion cycles, shear stresses) and can be related with Schallamach wave-formations (Zhang, 2004). Further fatigue mechanisms are related to delamination processes, explaining fatigue as detachment of surface layers on account of crack growth in subsurface areas due to tribological loading (Martínez, 2010; Da Silva et al, 2007) and are derived from Suh's theory of delamination wear (Suh, 1973).

2.1.4 Tribological Impact Parameters- PV-dependency

In most engineering applications the main varying loading parameters are contact pressure, sliding velocity and the occurring contact face temperatures. Their influence on the tribological operation of rubbers and generally polymers is crucially dependent on the viscoelastic transitions and morphological changes in the operating range. Increasing contact pressures generally result in lower frictional forces and higher wear, due to a better load distribution on the expanded contact area as long as the occurring deformations are of elastic nature (Myshkin, 2005). Elevated sliding velocities cause a lowering in the frictional force and a rise in wear, too. At higher testing rates bulk stiffening occurs, which leads to fewer contact spots and shorter contact times, resulting in lower COF values for adhesive friction (Myshkin, 2005). Viscoelastic materials are conventionally characterized by a strong time-temperature-dependency. The frictional heat accumulation in the contact faces therefore is of immense importance, influencing tribological performance and introducing failure mechanisms. With increasing speed and pressure setting, the energy dissipation and the resulting heat build-up are rising (Myshkin, 2005).

Further important influencing parameters on the rubber's tribological performance are, e.g., the surface conditions (surface roughness), sliding conditions (dry, lubricated) the chemical composition (molecular mass) and the composition of the rubber compound (fillers, additives) and are described in greater detail by Uetz and Wiedmeyer, 1985.

2.2 Thermoplastic Polyurethanes as High Performance Sealing Materials

2.2.1 General Overview of Thermoplastic Polyurethanes

Originally, polyurethanes were invented by Otto Bayer in 1937. From that point on, they played an important role as high performance materials. Polyurethanes conventionally are formed by polyaddition from a broad variety of chemicals (Holden et al, 2004). Specifically, polyurethane elastomers consist of three main components (Drobny, 2007):

- a polyester or polyether high molecular diol
- a chain extender (water, low-molecular weight diol)
- a bulky diisocyanate

Conventionally, polyurethane elastomers cannot be melted. Only a few compositions with specific diisocyanates can be used for forming (linear) thermoplastic polyurethanes (Drobny, 2007). The most common diisocyanate in TPU-chemistry is diphenylmethane-4,4'-diisocyanate (MDI) (Figure 2.2-1).

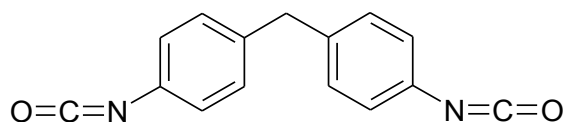


Figure 2.2-1: Diphenylmethane-4,4'-diisocyanate (MDI)

The first TPUs were synthesized in the late fifties. TPUs are overall categorized in polyether-types (better low temperature properties, hydrolytic stability) and polyester-types (better physical properties, oil resistance) (Walker and Rader, 1988).

Over the past years, much effort was spent to declare structure-property-relationships and use this for tailoring new materials. The elastomeric structure of TPUs is a result of their domain structure - TPUs generally owe a multiblock structure of phase separated systems. The domain structure mainly consists of hard and soft segments. The soft segments form a kind of elastomeric matrix responsible for elastomeric properties. They consist of flexible polyether- or polyesterdiol chains and are characterized by low polarity and melting points. The hard segments act as multifunctional tie points by means of functioning as both reinforcing fillers and physical cross-

links (intermolecular attraction via hydrogen bonds (Frick et al, 2010)). They are composed from the bulky diisocyanates. Low molecular diols act as chain extenders. Hard domains are polar and have higher melting points. Figure 2.2-2 points out the multiblock structure of TPUs (Holden et al, 2004).

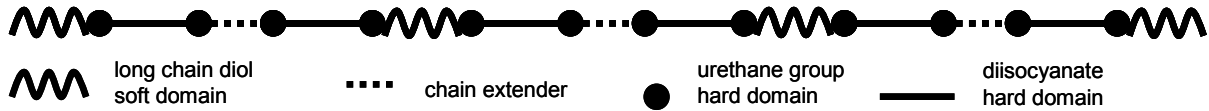


Figure 2.2-2: Multiblock structure of phase-separated TPU system

The soft domain features an amorphous structure, whereas the hard domains are semi crystalline. A continuous phase is partially formed by dispersion of the hard domains in the soft domains (Walker and Rader, 1988). At room temperature the system is phase separated due to difference in polarity, melting ranges and crystallinity between hard and soft domains. Exceeding the melting point of the hard segments, reversible phase mixing occurs, which elucidates the thermoplastic character of TPUs (Holden et al, 2004). Phase mixing and phase separation is of crucial importance for the physical properties of TPUs (Frick et al, 2010).

To focus on the thermal transitions of TPU, conventionally a glass transition range at rather low temperatures of the soft domains (elastomeric character) and several endothermic transition by means of melting processes of hard domains (thermoplastic character) are depicted (Schwarz, 1993). The glass transition shifts to higher temperatures with increasing hard segment content (dissolving of hard domains) (Crawford et al 1998). Crystallinity is attributed to hydrogen bondings between the hard segments and the resulting restricted mobility of chains (Hepburn, 1991). Hard domains conventionally consist of spherulithic crystalline and paracrystalline structures (crystalline structures of lower order) (Drobny, 2007), which can be influenced by heat treatment by means of annealing (Schwarz, 1993). The temperature application range is restricted to the melting region of the hard domains (Schwarz, 1993). The hard domains are generally responsible for the TPUs thermo-mechanical stability and exhibit a vital impact on a great variety of bulk properties, e.g. correlations with the wear performance and the hard segment order are described by Crawford, 1998. With increasing hard domain content, the elastomeric character decreases (Holden et al, 2004). Conventionally, the property profile of TPU materials is thus dominated by

hydrogen-bondings, molecular weight, crystallization, phase mixing and phase composition (Drobny, 2007).

The mechanical properties are characterized with nonlinear hyperelastic behaviour, time-temperature-dependence, hysteresis and softening (Qi and Boyce, 2005). Deformation processes generally introduce orientation and rotating of hard domain structures along with shear and stretch processes of soft domains (Sarva and Hsieh, 2009). Mechanisms like strain aging, in accordance with morphology changes due to strain, resulting in some degree of phase mixing, are further described (Crawford, 1998). Moreover, cyclic softening, also described as “Mullins effect” in elastomer engineering (Hofmann, 1998), is described as a result of the multiphase-structure, assuming the hydrogen bonds functionalizing as fillers (Schwarz, 1993; Boyce et al, 2006). A more detailed assessment of the structure-property relationship is not allocated within the scope of the thesis at hand, but can be found in the cited literature.

Conclusively, today’s available TPU grades depict a Shore Hardness between 70 ShA and 80 ShD, tensile strengths between 25 and 75 MPa. Compared to (polyurea) elastomers they are characterized by higher compression sets (10 to 50 %) and higher mechanical damping. TPUs are distinguished for elevated wear resistance and improved resistance to apolar media, especially fuel and mineral oil and greases (Drobny, 2007). Typical application examples are bearing bushes, bellows, seals and coupling elements in mechanical engineering, e.g. automotive industry. Further examples would be shoe soles, hoses and tubes for different markets (Walker and Rader, 1988; Holden et al, 2004).

2.2.2 Specifications and Relevance in Sealing Industry

TPU application in Seal Engineering

Polyurethane elastomers are conventionally used in the sealing industry since the 1980s, on account of their improved mechanical stability and resistance to mineral oils (Schwarz, 1993). TPUs additionally are distinguished for easy processability and consequently easy design (Drobny, 2007). Compared to the originally used technical rubbers, e.g. NBR, HNBR, FKM, MVQ, etc., and high performance thermoplasts, e.g. PTFE, TPUs indeed feature advanced mechanical stability, e.g. by means of tearing

resistance or tensile strength, but are afflicted with higher compression set levels (irreversible deformation, plastic flow) and a low temperature-application-range (Schwarz, 1993; Flitney, 2007).

Seal failure mainly depends on the tribo-mechanical material capacity (Gódor et al, 2009). The tribological performance thus is of outermost importance for seals function. Furthermore, this exemplifies another verification for the beneficial usage of TPU in seal applications. TPUs are characterized by good abrasion resistance (low wear performance). Additionally, the use of fillers can balance the rather high COF values and the tendency to Stick-Slip-Operation, which negatively affect the seals quality (Gódor et al, 2009). Consequently, it improves the applicability for dynamical seals.

Over the previous years, TPUs have established their role as appropriate material for hydraulic and pneumatic reciprocating seals, e.g. hydraulic cylinder seals, but also for O-rings and in most cases will not require back-up rings due to their elevated strength (Flitney, 2007). Figure 2.2-3 briefly outlines some TPU seal applications.

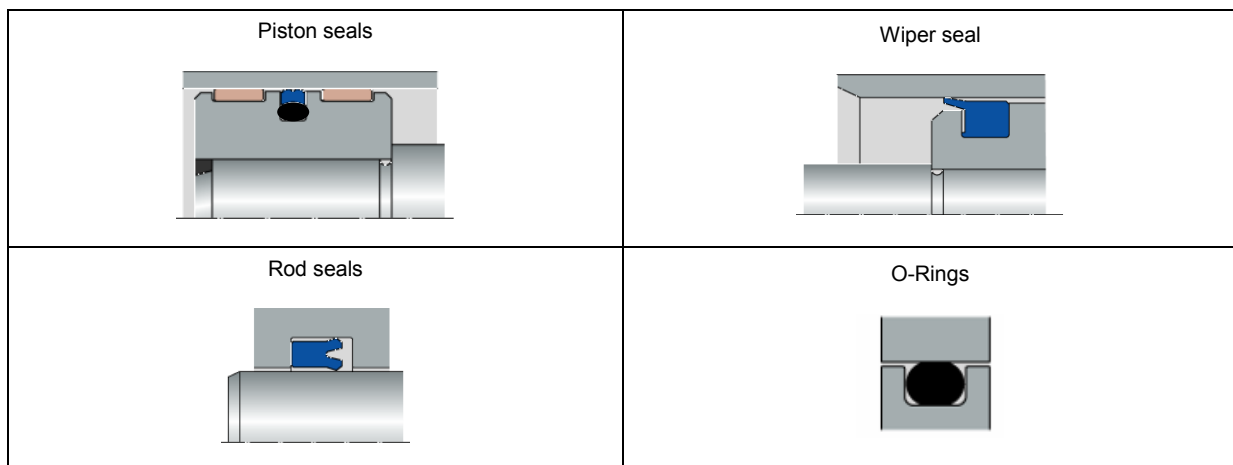


Figure 2.2-3: Examples for reciprocating seals/O-rings of TPU materials (SKF Group Homepage, Hydraulic seals, www.skf.com, Göteborg, Sweden, 2011-04-26)

Outline of Tribological Profile

The tribological profile of TPU in dry sliding contact to steel counterparts can be described as typical elastomeric frictional operation (Gódor, 2009). It is characterized by high occurring frictional forces compared to more rigid thermoplasts and requires a distinct run-in for achieving tribological stable performance (Uetz and Wiedmeyer, 1985). Frequently, the tribological performance is critically dependent on material's rigidity and its molecular weights (Gódor, 2009; Beck and Truss, 1998). The wear

performance thus is improving, with higher mechanical stability by means of higher hard domain content (Holden et al, 2004). The TPUs tribological operation range is crucially limited to the thermal stability of the matrix system, since frictional heat accumulation entails morphological changes, which are unfavourable for stable performance (Gódor, 2009). Furthermore, it typically tends to stick-slip- processes, especially at low sliding velocities (Hausberger, 2009).

The rubbing contact area of TPU generally depicts strongly adhering and sliding regions. The occurring wear mechanisms thus are based on adhesion processes and are characterized by high frictional forces. The formation of roll-like wear particles is exemplified at adhesive/frictional operation (Gódor, 2009) based on the wear model of Reznikovskij and Brodskij (Zhang, 2004), which is schematically demonstrated in Figure 2.2-4.

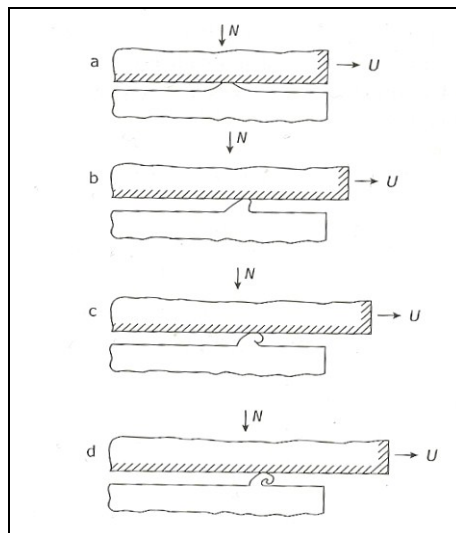


Figure 2.2-4: Adhesive/Frictional wear of Rubber (Zhang, 2004)

At more severe loadings fatigue mechanisms are further described for TPU materials. Wave like formations, similar to Schallamach's theory on rubber sliding (Schallamach, 1971), and more severe prow formations, due to partial melting of contact spots and respectively strong adhering regions, are depicted at Martínez (2010) and are also described at Da Silva et al (2007).

Moreover, delamination is also exemplified as a possible wear mechanisms occurring at dry sliding TPU-metal contacts. The delamination theory is based on the theory of Suh (Suh, 1973) explaining material detachment by means of sheared sheets (Mar-

tínez, 2010). The above outlined fatigue wear mechanisms are schematically summarized in Figure 2.2-5.

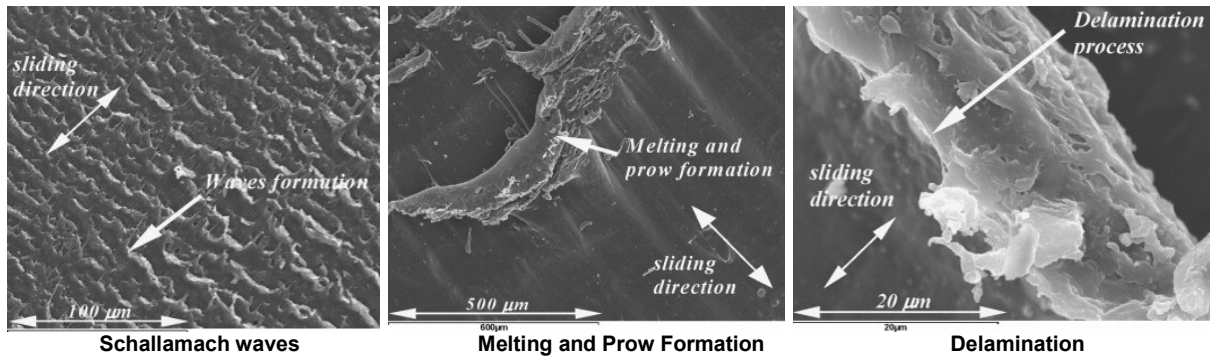


Figure 2.2-5: Wear mechanisms described for TPU materials (Martínez et al, 2010)

At abrasive operational conditions, especially at higher counterpart roughness, sub-surface cracking and a kind of ploughing (Martínez, 2010) is described at the worn TPU faces.

Conclusively, the tribological performance and operational range is critically dependent on bulk properties of the TPU-system and the system parameters, influencing the occurring frictional and wear mechanisms.

3. Experimental

3.1 Review of Tested Materials

Within the framework of this masters thesis two TPU pattern materials, a filled and an unfilled system, are investigated. The filled one contains stiffening or lubricating fillers. The overall filler content is less than 10%. The matrices of both materials differ in their morphological structure, e.g. different hard domain content and structure, which results in contrasting surface and bulk properties. The materials are provided by the SKF Economos GmbH, Judenburg, Austria. Further information about the formulation and characteristics are strictly confidential. Table 3.1-1 below presents a short overview of both TPU-systems:

Table 3.1-1: Overview of TPU unfilled and filled

		TPU unfilled	TPU filled
Colour	[-]	white	black
Density	[g/cm ³]	1,20	1,23
Shore A	[-]	95	95
Shore D	[-]	47	48

3.2 Bulk Characterization

3.2.1 Thermomechanical Bulk Properties

Dynamical Mechanical Analysis

The dynamical mechanical analysis is commonly used to describe the viscoelastic behaviour of polymers over a wide frequency and temperature range. The influence of temperature and loading rates can be investigated in a relatively consolidated test (Grellmann et al, 2007). The focus on the DMA-characterization for the research work at hand is to compare the viscoelastic response of the pattern TPU-materials and to investigate possible correlations to the materials tribological profile (as described in chapter 4.5.3).

The tests are performed at the Mettler Toledo DMA device DMA/DTA 861 SDTA (Mettler Toledo GmbH, Vienna) with a force limit of 40 N at tensile mode (Figure 3.2-1). Measurements in the tensile mode generally provide the most applicable results on account of the uniaxial loading and the constant stress distribution (Ehrenstein, 1998). The bar shaped specimens (2x4 mm, 25 mm length) are cut out from a moulded plate. They are fixed on the tensile device at a gauge length of 19,5 mm. The measurements are performed in standard atmosphere, temperature control is realized via nitrogen purge gas flushing. The overall testing process is displacement controlled.

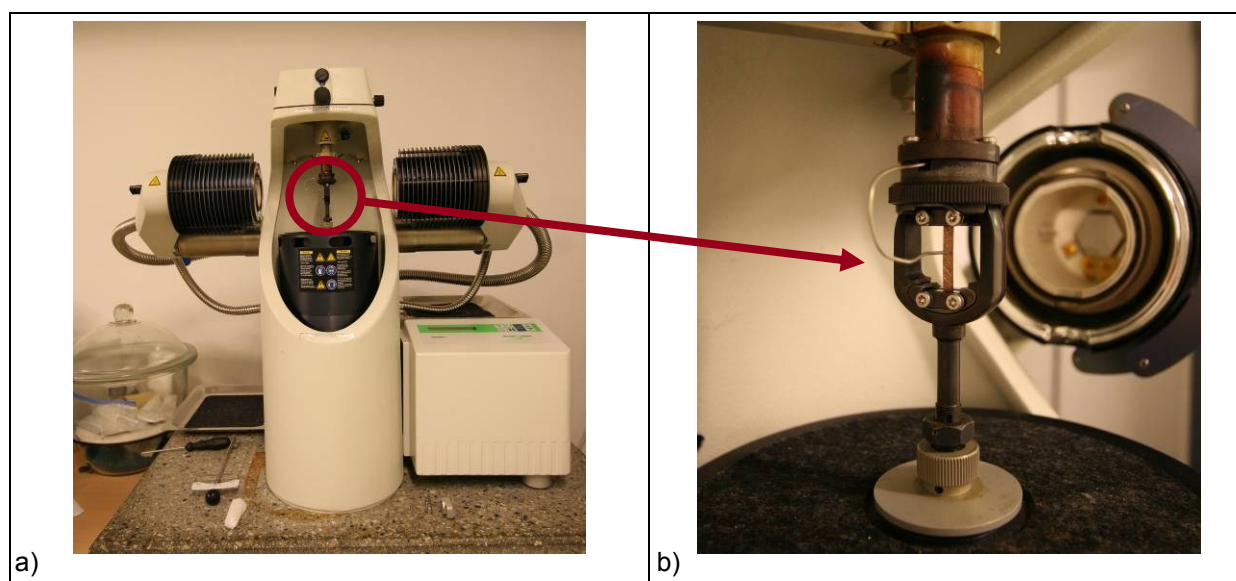


Figure 3.2-1: a) Mettler Toledo DMA 861 SDTA, b) Tensile Device for DMA 861 SDTA

Initially, amplitude sweeps are executed to identify the linear viscoelastic (lve) limit on account that DMA-assessment of polymeric materials is only valid for the lve-range (Ehrenstein, 1998). Based on those results, the setting parameters for amplitude, frequency and temperature are selected to ensure that the lve-limit, as well as the force limit of the testing machine is not exceeded. For the tested amplitude range at two frequencies, both materials do not overrun the lve-limit, due to their high elasticity. A detailed evaluation of the amplitude sweeps is demonstrated in the appendix (see section 8.4.1). Summing up, an strain amplitude of 0,1 % is selected for the subsequent tests to assert that the lve-limit is not exceeded at higher frequencies or lower temperatures, when stiffening of the bulk occurs. Further testing conditions are based on corresponding literature (Ehrenstein, 1998; Grellmann et al, 2007).

Subsequently, the influence of frequency and temperature on the materials behaviour is investigated via frequency sweeps at different temperatures. The tests are carried out at an strain amplitude of 0,1 % in a frequency range of 1 to 300 Hz at temperatures from -80 °C up to 180 °C. The increasing modulus with increasing frequencies is demonstrated in dependency of testing temperatures.

Based on the data of amplitude and frequency sweeps temperature scans are executed at range from -60 °C up to 180 °C with a heating rate of 2 °C/min. This analysis assesses the glass transition of the soft segments as well as softening by means of melting of the hard segments at elevated temperatures. Its coverage over a broad range of material characteristics is essential to declare the temperature-dependent mechanical stability of TPU which can be used further to describe tribological phenomena (see section 4.5.3). The tests are run at low frequencies (2 Hz, 10 Hz) with amplitudes of 0,1 %. The temperature dependency of the storage modulus E' , the loss modulus E'' and the loss factor $\tan\delta$ is demonstrated. To examine E' the tangent method on logarithmic scale is used, E'' and $\tan\delta$ are characterized by their temperature-dependent maximum (Ehrenstein, 1998). Figure 3 summarizes the testing procedure of the DMA-analysis.

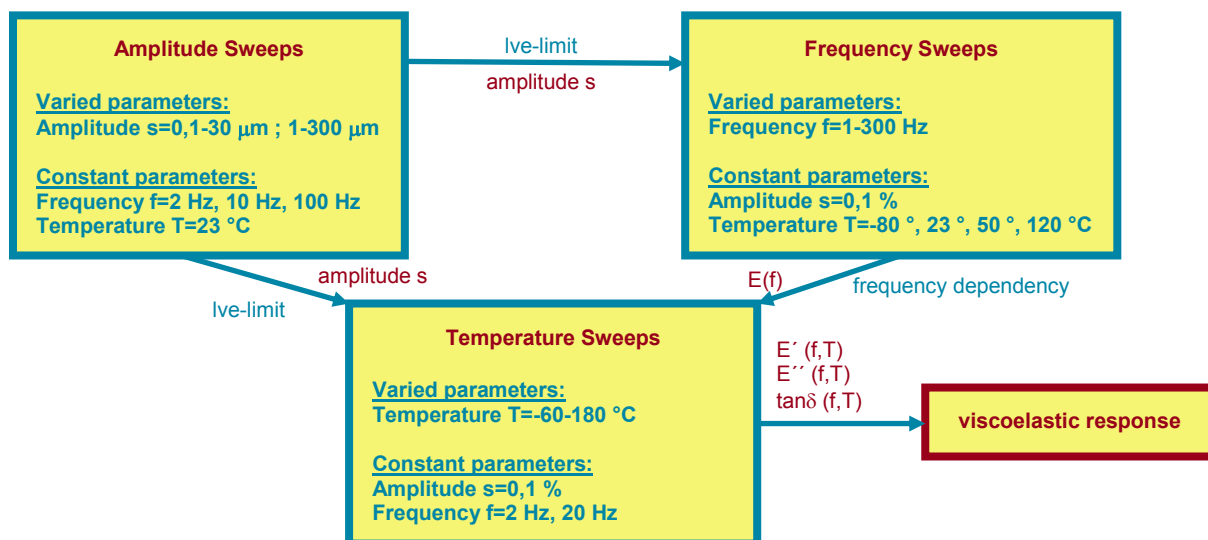


Figure 3.2-2: Testing procedure of DMA-analysis

3.2.2 Thermal Bulk Properties

Differential Scanning Calorimetry

Differential Scanning Calorimetry (DSC) is commonly used to characterize changes of the molecular orientation and morphology, e.g. glass transition, crystallization, melting and phase segregation of TPU (Holden, 2004) and is essential for a better understanding of its complex multi-phase-structure. TPU differ in their thermal response compared to chemically crosslinked products (Holden et al, 1996). Generally three different phases can be described: amorphous soft segments, amorphous hard domains and crystalline hard domains (Schwarz, 1993). The formation of the crystalline hard segments, their proportion and their length determine the melting point and thus affect the thermal stability of the TPU system (Holden, 2004) to a high degree.

Within the scope of this research work, DSC analysis is performed to compare the thermal response of the matrix of the filled and unfilled TPU pattern material. The tests are achieved via a Mettler Toledo heat flux calorimetry device DSC 822^e (Mettler Toledo GmbH, Vienna) (Figure 3.2-3a). A testing procedure is assembled, analyzing temperature induced morphological characteristics in the temperature range from 30 up to 300 °C. Figure 3.2-3b presents the testing methodology schematically.

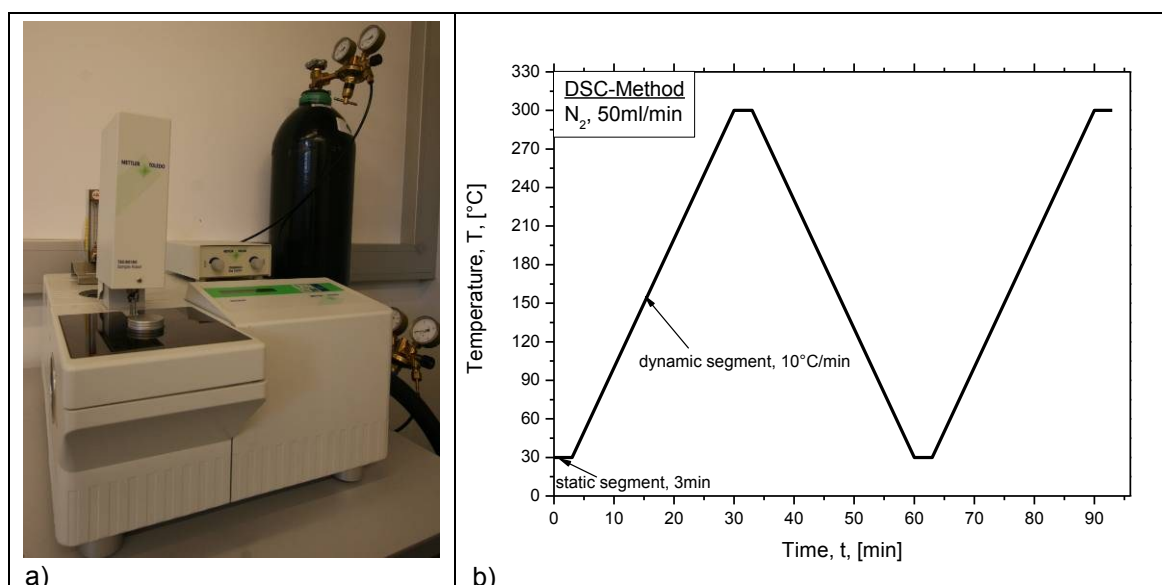


Figure 3.2-3: Mettler Toledo DSC 822^e; b) Testing Methodology for TPU analysis

The specimens are heated up from 30 up to 300 °C in nitrogen purge gas atmosphere with gas flux of 50 ml/min, and subsequently cooled. Each dynamic segment is

separated by static segments of 3 min. Subsequently, a second run is carried out. In the first run the influence of processing and after-treatment, e.g. annealing, can be analyzed. During the subsequent cooling crystallization processes might occur. The second heating run demonstrates thermal substrate properties (Ehrenstein, 1998). A heating/cooling rate of 10 °C/min is selected to focus on crystallite melting (Ehrenstein, 1998). All specimens are prepared with the same procedure in order to ensure reproducibility: A 60 μm thick slice having a weight of 6 +/-1 mg from the bearing surface of the RoD-Specimen (see section 0) is sectioned with the automatic microtome Leica RM 2255 (Leica Microsystems, Vienna, Austria). The specimens are put in DSC 40 μl aluminium crucibles sealed with aluminium lids with holes for degassing for analysis. The overall testing procedure is similar to the method described by Frick et al (2010).

3.3 Tribological Surface Characterization

3.3.1 Experimental Set Up: RoD-Device at Rotary Tribometer TE93

The precise rotary Tribometer Plint TE93 (Phoenix Tribology Ltd., Newbury, England) is commonly used for tribological characterization of materials at component level in the present research work. It is a Ring on Disc-system (RoD) based on the ASTM D3702 (ASTM International Standard D3702-94, 1999) for thrust washer testing in rubbing contact. The test configuration is depicted in Figure 3.3-1.

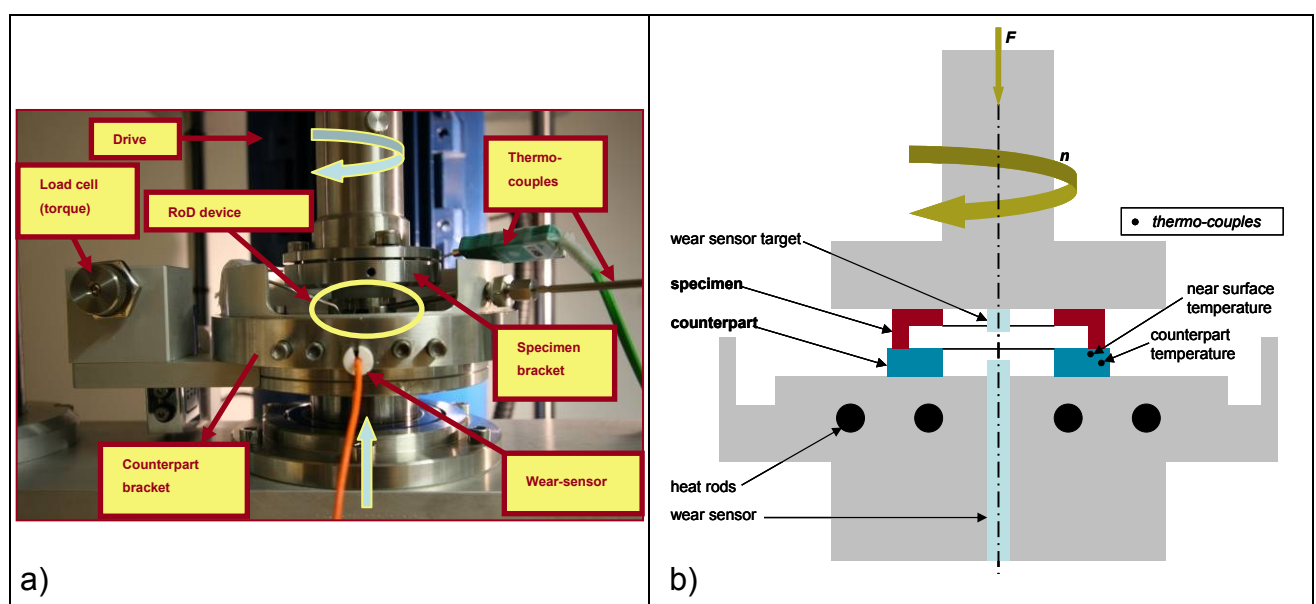


Figure 3.3-1: a) Tribometer TE93, b) Test configuration TE 93 (schematically)

Briefly, a normal load is applied on the specimen disc via a pneumatic device using air bellows. The rotating disc is pressed on the stationary counterpart, also called “ring”. A torque is thus transmitted from the specimen to the counterpart and the air bearing bracket performs an unhindered movement. The resulting frictional torque can be measured via a load cell (Figure 3.3-2a). Additionally, the wear of the specimen is measured by a wear sensor (capacitance distance sensor) (Figure 3.3-1b) and friction related heat accumulation is determined via two thermo-elements in the counterpart (Figure 3.3-2b). The temperature of the system can be increased using four heating rods.

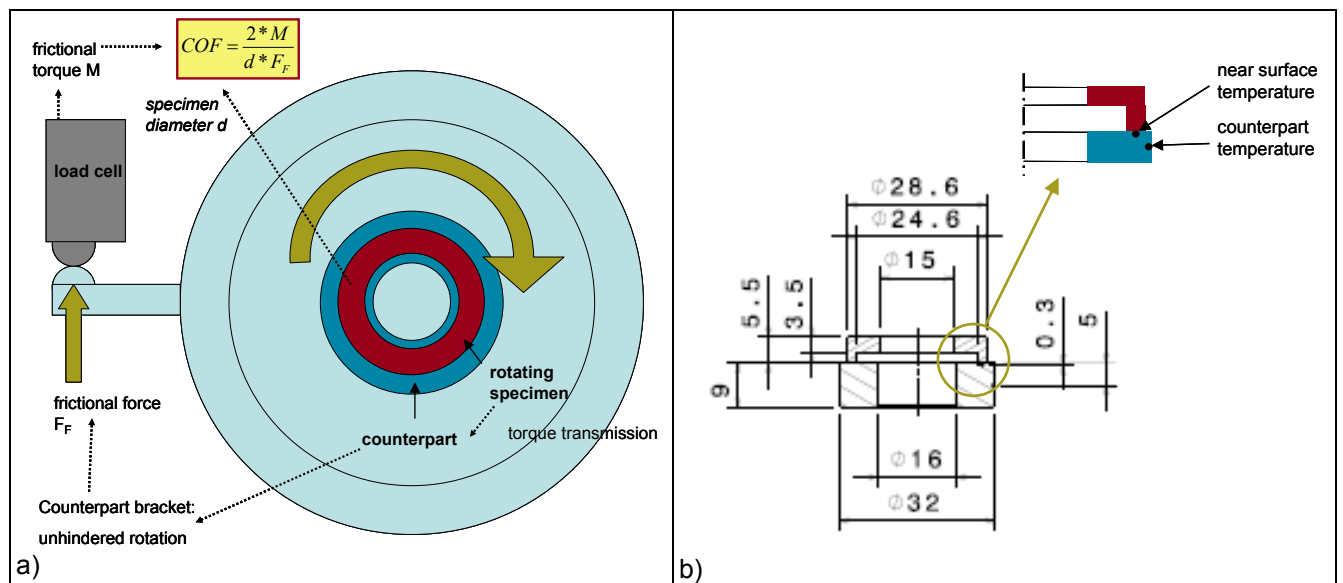


Figure 3.3-2: TE 93; Scheme of a) Frictional torque measuring at RoD-device, b) Temperature measuring

Conclusively, parameters like frictional torque, wear and sample temperatures are measured online, whereas the normal load, the rotational speed, the testing temperature and the test duration are controlled parameters.

Adaptation of the Experimental Setup for Elastomeric Seal Materials

Elastomeric sealing materials differ significantly in their property profile from metallic ones. The main differences are the thermal and mechanical stability, which highly impact the design of the test configuration. As a result the testing procedure based on the ASTM D3702 (ASTM International Standard D 3702-94, 1999) has to be adapted to elastomeric materials which has already been a task of former research projects (Gódor et al, 2009; Hausberger, 2008). First the specimen bracket is im-

proved in order to be used for elastic material testing. Originally, the ASTM D3702 sample is fixed with one bolt to the bracket. Due to large deformations of the elastomeric specimens and softening at rather low temperatures (compared to metals) a bracket with four crabbing bolts is designed and the specimen geometry (revised as RoD standard) is improved to avoid deformations and slipping from the testing track (Hausberger, 2008). Secondly, the geometry of the specimen is further improved during the present research to gain more mechanical stability. Therefore, a thicker specimen with a broader contact surface is designed. Figure 3.3-3 demonstrates the geometrical innovations. The new geometry is denoted RoD BB and is utilized for the tribological tests within the framework of the research work at hand.

To further stabilize the tribological running, some improvements at the upper specimen bracket are made. With the standard configuration the specimen holder is mounted on the socket flange by a self aligning ball bearing to balance tilting movements. The improved configuration uses a ball scraper instead of the rolling bearing for more precise compensation of tilting. Furthermore, the new bracket is dimensioned more rigid. Accordingly, large deformations and unstable running can be avoided especially for softer materials. Actual design drawings of the above described device and of the optimized specimen geometry are demonstrated in the appendix (chapter 8.4.3).

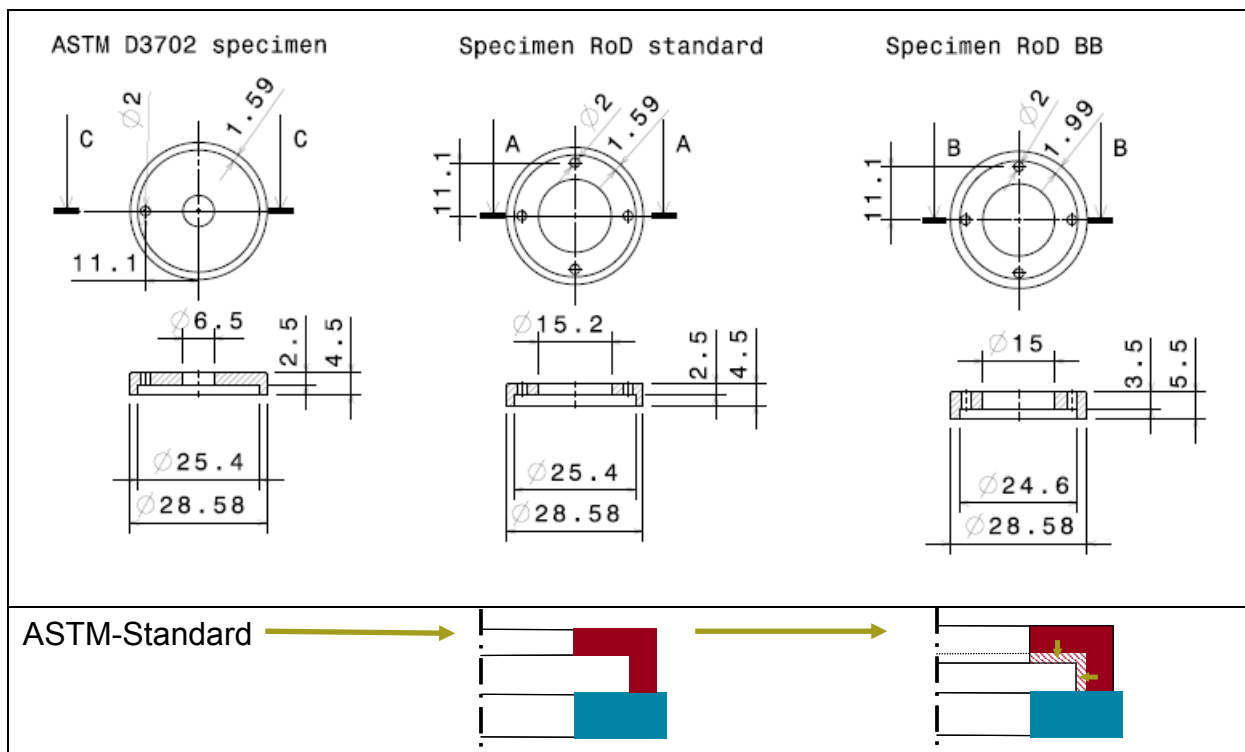
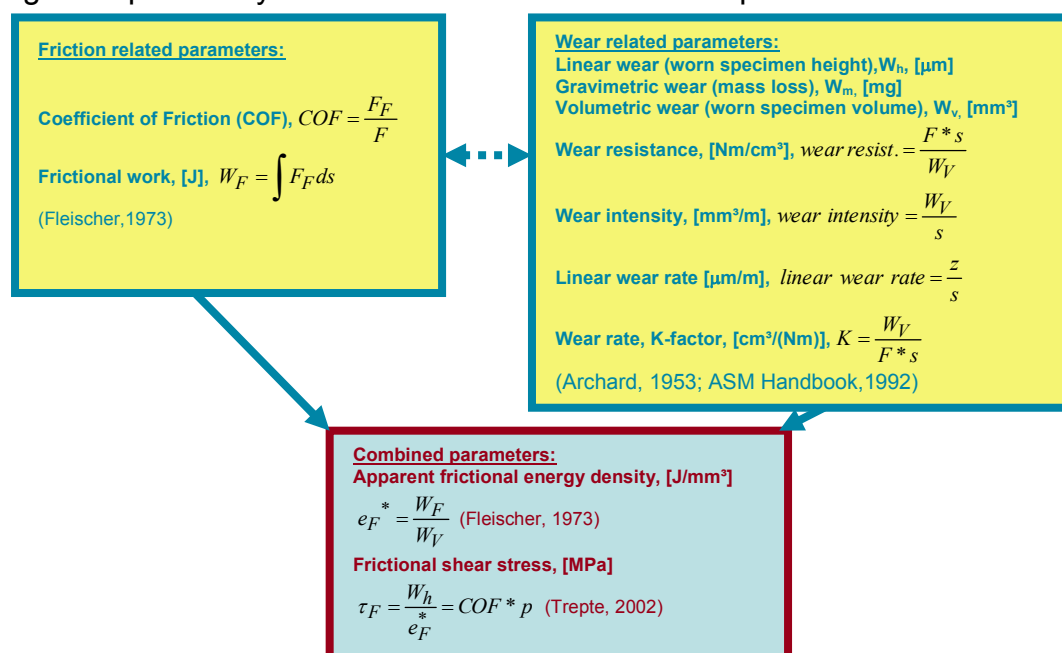


Figure 3.3-3: Geometrical optimization of RoD- specimen (schematically)

3.3.2 Description of the Tribological Profile - Calculated parameters

During tribological testing parameters like frictional torque, frictional heat accumulation and wear are measured depending on the setting parameters such as normal load, testing speed, testing temperature, lubrication and testing time or distance. Additionally, surface (e.g. surface roughness) and bulk properties (e.g. thermal stability, mechanical stability) influence the tribological profile (Müller, Deters, 2004). Considering the impact of all these factors friction and wear related indicators can be derived (Trepte, 2002). Usually, it is distinguished between friction and wear related parameters (Czichos and Habig, 2003). Figure 3.3-4 presents the above described correlation schematically as well as the calculated friction and wear related parameters to assess the tribological performance of the tested materials (GfT Arbeitsblatt 7, 2002). Friction related parameters are directly evaluated from the measured frictional force and the extrapolated measured temperatures. The calculation of wear related parameters is of more crucial complexity, due to the defective measurement technique. The wear, measured via capacitance distance sensor, is influenced by material's wear, material's deformation, polymer creep and thermal expansion. For further verification the measured wear is compared to the calculated wear, derived from the mass loss. Within the scope of the current testing series no significant differences between calculated and measured wear could be detected. Albeit, wear data suffers from marginal repeatability as a result of all the above cited phenomena.



(F...normal load, F_F ...frictional force, p...contact pressure, s...sliding distance, z...linear wear)

Figure 3.3-4: Derived parameters from TE93 testing

3.3.3 Optical Investigations of Specimen and Counterpart

The tribological profile of materials is critically dependent on the surface formation of specimen and counterpart. Optical investigations are an essential tool to characterize the tribological performance and approve the validity of certain calculated parameters. As a result, microscopic investigations of specimen and counterpart after the tribological tests are carried out and evaluated in detail.

Before testing, the surface roughness of the steel counterpart is determined via white light confocal microscopy (DIN 4768, 1990). The surface roughness has to be held constant in a range between $R_a = 0,02 \mu\text{m}$ to $0,05 \mu\text{m}$ for all testing series within the framework of this research work to guarantee reproducible adhesive contact conditions (Hausberger, 2008). The measuring of the surface roughness parameters are performed on the white light confocal microscope MPR1080 (Fries Research and Technology GmbH, Germany).

After testing, both the worn surface of the specimen and the counterpart are investigated via light microscopy to approve reproducibility of the test results and to investigate typical friction and wear phenomena of TPU. The analysis of the specimens is executed on the upright light microscope Olympus BX51 (Olympus Soft Imaging Solutions GmbH, Münster, Germany) at magnifications of 50x1 to 200x1. Figure 3.3-5/6 depicts the conventionally used micrograph settings for specimens/counterparts and adjustment within the scope of the current research work, unless otherwise stated.

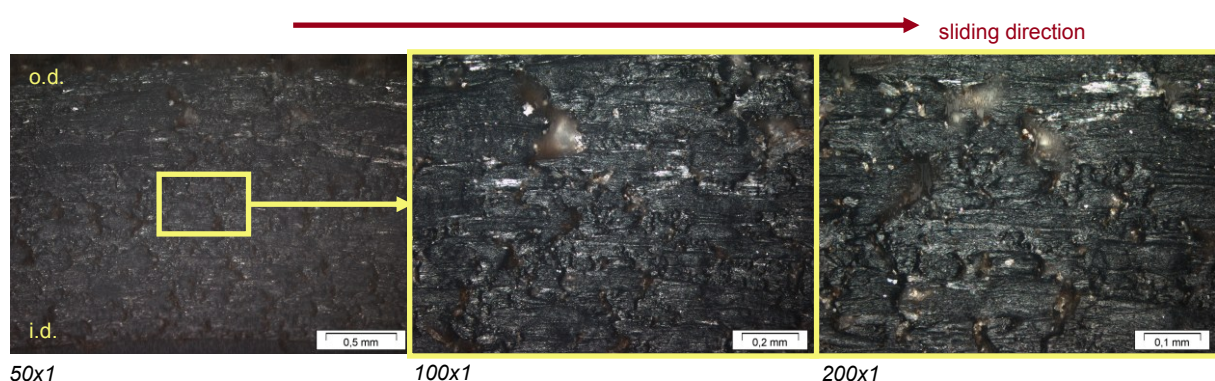


Figure 3.3-5: Schematic demonstration of adjustment of specimen micrographs

The wear tracks of the counterparts are studied with the stereo microscope Zeiss Stemi 2000C (Carl Zeiss MicroImaging GmbH, Germany). The range of the magnification is set between 3,25x1 and 20x1 to attain an appropriate impression of the surface.

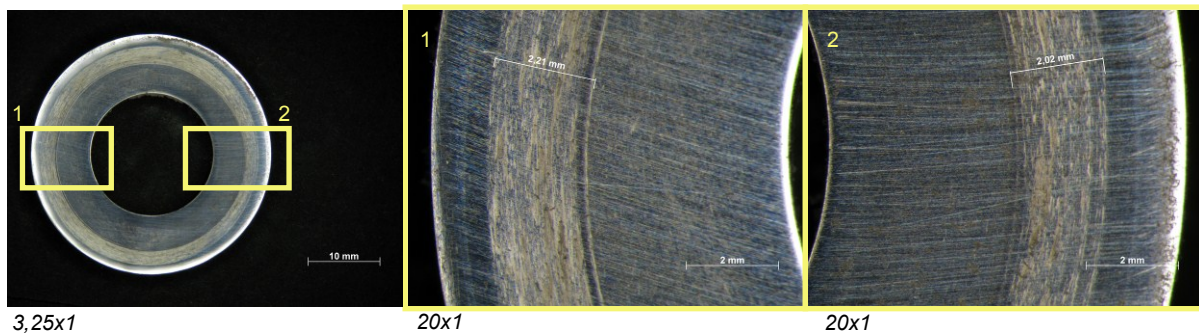


Figure 3.3-6: Schematic demonstration of adjustment of counterpart micrographs

Additionally, for certain tests the surfaces are further analysed via SEM to achieve more detailed information about the friction and wear mechanisms. Large differences in the height of the structure of the sample surface contribute to the image formation at the image plane at SEM micrography (Kämpf, 1986). The Zeiss DSM 962 with Si(Li)-szintilator and LaB6-cathode SEM is utilized for that purpose (Carl Zeiss MicroImaging GmbH, Germany). The relevant parts of the worn surfaces are cut out and bonded to a microscope slide using a conductive C-adhesive. To reinforce the conductivity, Ag-paste is brushed on the sample to link sample with object plate. Subsequently, the sample is evacuated for at least 24 hours and then sputtered with gold on the Bal-Tec Sputter Coater SCD 005 (Leica Microsystems, Vienna, Austria). The micrographs are recorded at an acceleration voltage of 3kV with a working distance of 6 to 9 mm at magnification levels from 50x1 to 5000x1. The conventionally used picture adjustment is similar to that of the specimens' light micrographs.

3.3.4 Set Up of Standard Testing Methodology

In tribological engineering it is of absolute importance to define compelling testing parameters to sufficiently approach application conditions. The results depend on the setting parameters of the system to a crucial degree (Czichos and Habig, 2003). Setting up a kind of reference test (standard test) is substantial for tribological characterization. A standard testing procedure with the tribometer TE93 is developed henceforth. Based on this methodology different materials can be compared and the effect of varying setting parameters on their tribological profile can be analyzed in detail. Briefly, the reference methodology is a constant load test at $p=1$ MPa and $v=100$ rpm at room temperature in dry contact. The following section describes this methodology from the specimen preparation to the evaluation of results in more detail:

- Specimen/Disc preparation

The TPU discs are manufactured by fine turning from an injection molded rod on the SKF Seal Jet® NG 040 (SKF Economos GmbH, Judenburg). The surface roughness R_a of the turned bearing surface is approximately 3 to 4 μm (Hausberger, 2009). The surface formation after the turning process is depicted in Figure 3.3-7 and 3.3.8.

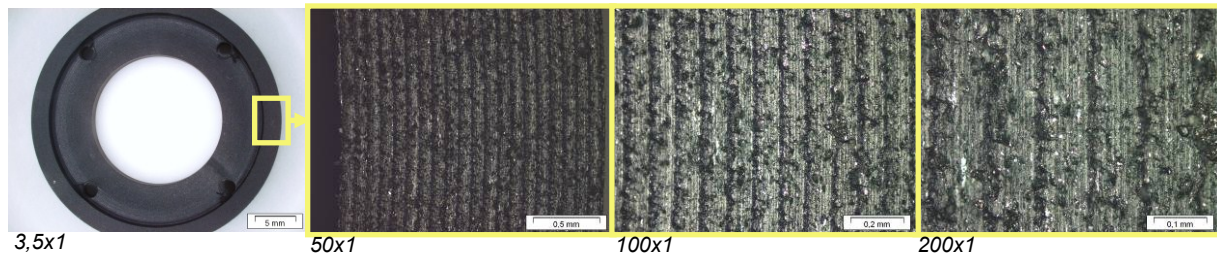


Figure 3.3-7: Turning grooves at the filled TPU specimen

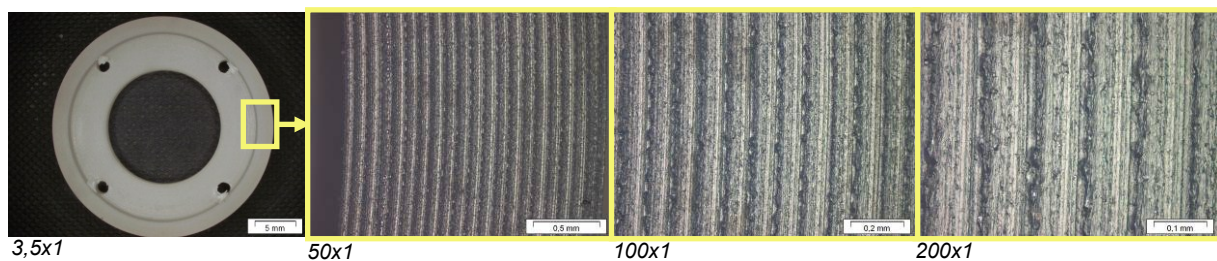


Figure 3.3-8: Turning grooves at the unfilled TPU specimen

The specimens are stored for at least three days in the laboratory at standard condition (50 % rel. humidity, 23 °C) to compensate possible moisture absorption from transporting.

- Counterpart/Ring preparation

The counterparts are steel rings (heat treated 34CrNiMo6) with an average hardness of 630 to 700 HV (Gódor et al, 2009). The surface is polished on a Buehler Phoenix Beta polishing machine (Buehler GmbH, Düsseldorf, Germany). It shows parallel grinding grooves with a center line average roughness R_a of 0,02 to 0,05 μm (Hausberger,2008) (investigated with a white light confocal microscope MPR 1080 (Fries Research and Technology GmbH, Germany)).

- Cleaning of ring and disc

The polymeric discs are dryly dusted off whereas the steel counterpart is cleaned with acetone.

- Running the test, Evaluation of results

Initially, the disc is weighed on a Mettler Toledo XP/XS laboratory scale (Mettler Toledo GmbH, Vienna, Austria). Afterwards, both ring and disc are fixed. Subsequently, the normal load of 50 N is applied and the tribological pairing performs a run-in-phase of 600 s with a testing speed of 50 rpm. Next the main load of 166 N (equivalent to a contact pressure of 1 MPa) is applied with a rate of 10 N/min and the testing speed is raised to 100 rpm with a rate of 1 rpm/s. Following to the load ramp, the test runs for four hours except for possible dropout on account of exceeding the tolerable wear of 1500 μm or the tolerable torque of 5 Nm. Figure 3.3-9 schematically represents the methodology.

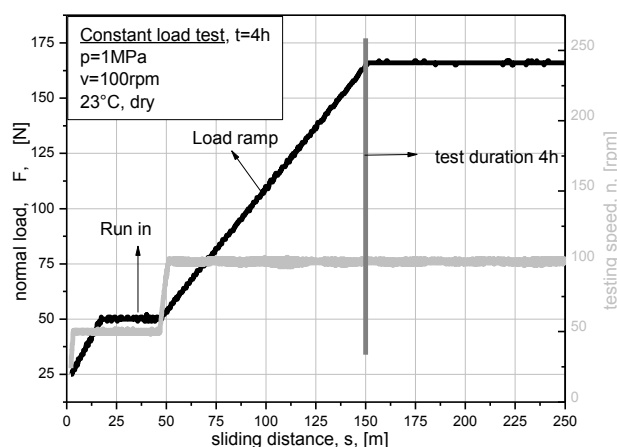


Figure 3.3-9: Constant load test at 1 MPa and 100 rpm for TPU sealing materials

The setting parameters ($p=1$ MPa, $v=100$ rpm, $T=23$ °C, $t=4$ h) are held constant during the test. The frictional torque, the wear path and the temperatures at two positions in the counterpart are measured online. The local rubbing surface temperature is assumed to attain values of at least 30 °C more than the measured near surface temperature (Grün, 2007; Grün et al, 2008). After the test, the specimen is weighed again to calculate the loss of mass. Based on the gravimetric wear, diverse friction and wear related parameters are determined (see section 3.3.2). Deriving parameters from the gravimetric wear is critical since the specimens absorb moisture and are temporarily dried during the friction test on account of heat accumulation and further measuring inaccuracies.

3.3.5 Development of a Benchmark Testing Methodology- PV-Step-Tests

Contact pressure (p) and sliding velocity (v) (in short: PV-parameters) influence the operational behaviour of seals to an outermost degree (Jones, 2004). Setting up a testing methodology on component level to assess the impact of the PV-parameters is critically important henceforth. In the journal bearing industry the performance of bearings relates specifically to PV-limits (Mäurer, 2002).

Accordingly, a testing methodology to evaluate PV-dependency is developed within the scope of this research work. Altogether, two procedures are defined, a load step test at constant speed and a speed step test at constant loads (Figure 3.3-10), providing detailed information on the influence of altering either speed or load in a distinct adjustment. Supplementary, the step tests are performed gradually (Figure 3.3-11). Combined with optical investigations after every step more detailed information about the surface formation at altering PV-conditions is gained.

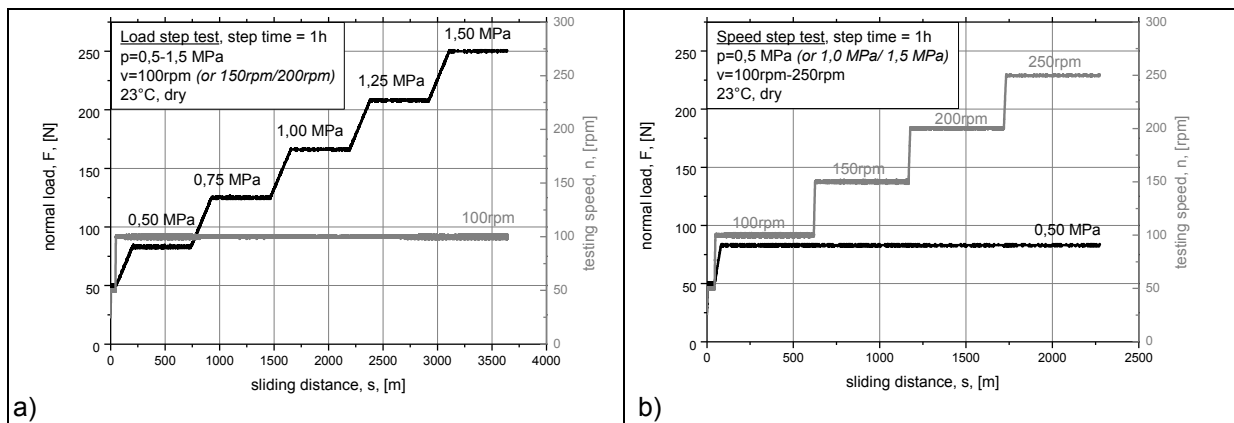


Figure 3.3-10: Schematical representation of a) load step tests, b) speed step tests

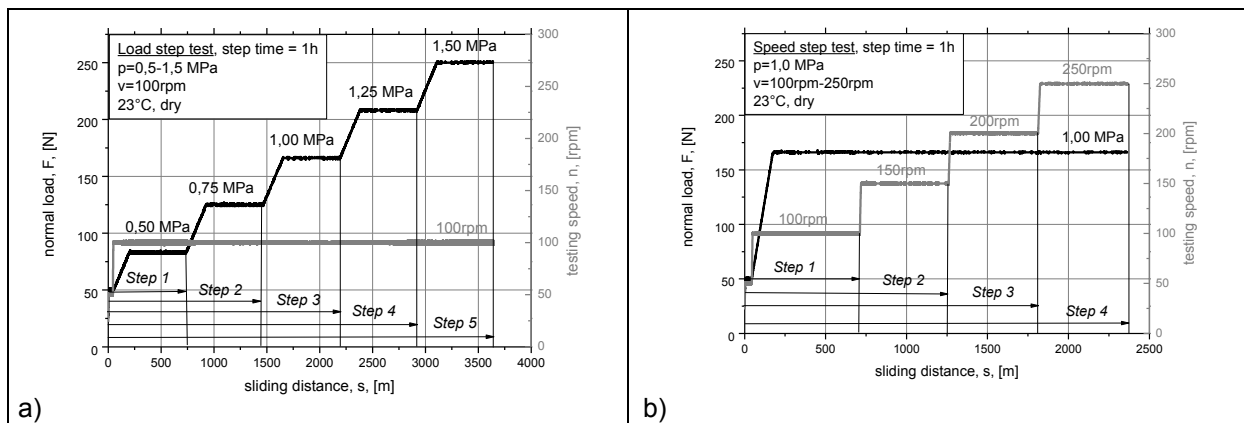


Figure 3.3-11: Schematical representation of gradual performance of a) load step tests, b) speed step tests

The load step tests are performed at progressive load levels of 0,5 to 1,5 MPa with an increment of 0,25 MPa (totally five steps) at a constant testing speed of either 100, 150 or 200 rpm. The program starts with a run-in for ten minutes at 50 N (equating to 0,3 MPa) and 50 rpm. The load is then applied at a rate of 2 N/min and the step length is set to 6000 revisions. Furthermore, a step condition defining a tolerable wear for every step, to ensure that materials showing high wear are able to perform all steps even at shorter distances, is composed. The COF and two measured temperatures in the counterpart (near surface, middle of counterpart) are consulted to declare the frictional phenomena in dependency of the PV-parameters, conjointly the linear wear rate, defined as the ratio of linear wear to sliding distance, is observed to assess wear related characteristics. Albeit, it has to be highlighted that especially during load step tests the gradually altering contact conditions and the resulting surface formation depending on the altering contact pressure have to be considered in the evaluation of the results.

The speed step tests equate to the load step tests concerning the procedure and evaluation, except for the variation of speed at constant load levels. The tests are carried out at speed steps from 100 to 250 rpm with an increment of 50 rpm (totally 4 steps) at constant load levels of either 0,5; 1,0 or 1,5 MPa. The testing speed is applied with a rate of 1 rpm/min.

3.3.6 Supplementary Tribological Characterization based on PV-Step-Tests

Advanced PV-Step-Tests for High Performance Materials

The above described PV-step tests can easily be used as an appraisal to rate sealing materials in a PV-range relevant to the application. For further investigations, the PV-setting parameters have to be adapted. Within the scope of this research, no failure mechanisms can be declared from the standard PV-step tests conducted with the filled material. As a result the PV-levels are increased to a maximum contact pressure of 2,5 MPa and a maximum speed of 400 rpm to assess tribological phenomena in greater detail.

Advanced constant load tests to define and approve the PV-application limit

The PV-step tests highlight critical stages of the materials performance, e.g. failure mechanisms, high wear, intolerable frictional heat accumulation, etc. Considering those effects combined with optical investigations and thermo-mechanical material properties, enables to define a PV-limiting value. PV-limiting values are restricted to certain testing parameters and cannot be regarded as a characteristic of materials (Mäurer, 2002). Further constant load tests at critical PV-levels are thus performed to approve the certainty of the estimated PV-limiting value and to set up the validity extent in regards to a certain testing time of four hours.

3.3.7 PV-Rating and definition of a PV-application limit

Definition of Tribological Failure

Tribological failure has many aspects and can certainly not be reduced to material failure, since it is characterized by the tribological system as a whole (Czichos and Habig, 2003). As a result, failure and damage are defined by the specific application and indicate the state, at which the function of the component or machine element is negatively affected or at worst fails. Within the scope of the current research, a tribological characterization of sealing materials is outlined, therefore damage limits and failure mechanisms are defined by the seal's operation with tribological loadings. Sealing failure is generally denoted as leakage and restrictions in their operational lifetime (mechanical failure) (Flitney, 2007).

The issue is simplified, since only the operational conditions at the seal lip are investigated by the RoD-testing methodology on a component level. Additionally, only dry sliding operations at room temperature are analyzed. Incontrovertibly, it is a crucial task to identify damage inducing parameters during tribological operation. The structural properties and thus the thermo-mechanical stability of polymers are highly time- and temperature-dependent, denoted as viscoelasticity (Cahn et al, 1993). Moreover, loading conditions are very complex. Tribological loadings conventionally consist of a combination of compression, tensile, shear and thermal stresses, related to indentations of surface asperities (Czichos and Habig, 2003).

Correlating thermo-mechanical properties of TPU materials in combination with tribological loadings and requirements on seal design, possible failure mechanisms and causes can be declared, which are briefly summarized in Figure 3.3-12.

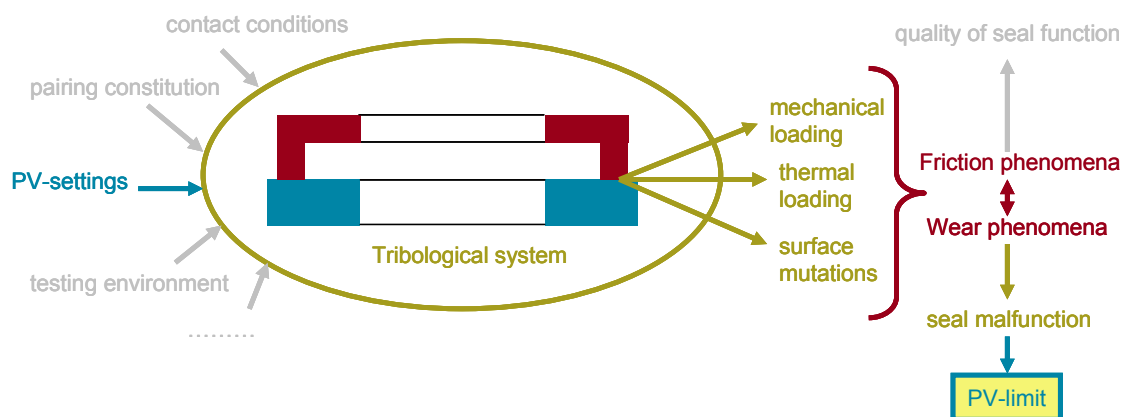


Figure 3.3-12: Review of tribological loading conditions on the TPU-sample in a RoD-testing configuration and their effect on failure

For the current research, contact pressure and sliding velocity are set as input parameters. Other influential parameters (contact conditions, surface roughness, testing temperature, etc.) are held constant during the tests (as is described in chapter 3.2.), to exclusively attribute failure to PV-settings. During operation the rubbing contact of the tribological pairing is exposed to mechanical loadings (tensile, compression, shear at high rates) and thermal loadings respectively, in accordance with energy dissipation/hysteretic heat-up. The loading conditions provoke certain surface formations, which either serve to stabilize the system or, e.g. at severe wear stages, induce failure. Heat accumulation conventionally decreases the mechanical and especially the tribological resistance of the elastomeric specimen due to bulk softening at elevated temperatures, thus negatively affects the performance of the material (Thomine et al, 2007). The performance and operational behaviour of the sealing material is characterized by parameters derived from friction and wear (see section 3.2.2.). Frictional phenomena characterize the quality of the seal's function (Gódor et al, 2009), whereas wear phenomena directly affect the fatigue life by inducing leakage.

Conclusively, those PV-settings for the component testing system, which affect severe wear and surface formations and can be related with malfunction of the seal, have to be identified. Conventionally, approaches to define PV-limits in correlation

with tolerable wear levels, unfavourable surface mutations and thermo-mechanical material damage are outlined in the following sections. The causes of failure based on observation of the PV-step tests reveal application limits valid for an operation time of 4 h at the currently employed testing configuration (related to the constant load tests described in section 3.2.2.), which is- allocated to seal operation- an adequate testing time.

Assessment of tolerable wear to perform a PV-rating

The first attempt to define a PV-application limit is based on a tolerable wear level. The linear wear rate (described in chapter 3.3.1.3) is considered to define an appropriate limit (Ashby and Jones, 1995), but should be verified by assessment of further parameters, since it mainly reflects not only wear mechanisms, but likewise polymer creep (Da Silva and Sinatora, 2007) and thermal expansion. Therefore, the results of load and speed step tests are summarized and averaged over the PV-setting. The linear wear rate is either determined by evaluating the slope of the measured wear or by numerical results derived from mass loss. Both methods do not differ significantly. Considering the fact that the PV application limit should guarantee clean operation over a testing time of 4 h, a linear wear rate of 0,5 $\mu\text{m}/\text{m}$ is defined as critical wear rate. The value is based on the tolerable wear of the RoD-specimen of 2000 μm before the ligament is completely worn (see appendix section 8.4.3.) and respectively the testing rigs' limit of 1700 μm wear. A maximum wear of approximately 1080 μm can be achieved with a wear rate of 0,5 $\mu\text{m}/\text{m}$ at a sliding speed of 100 rpm, at 150 rpm approximately 1600 μm .

Assessment of optically investigated surface mutations to define PV-limit

Unfavourable surface mutations can cause leakages even at low wear stages. An optical investigation of the surfaces has to be indisputably correlated with the test results. It is worth pointing out that an assessment on the surface mutations is solely a phenomenological method to rate the materials' tribological performance and to indicate failure initiation. The systematics (picture adjustment, settings) for micrography are demonstrated in section 3.3.1.4.

Correlations with thermo-mechanical bulk properties

Frictional phenomena are invariably correlated with heat accumulation. Especially, in polymer tribology an assessment of the temperatures at the rubbing contact is of outermost importance, on account of polymers sensitive response to thermal loadings. At rubbing contact thermal loadings cause softening/deformation, hysteresis, dispersion and respectively melting/flow processes of surface layer/asperities. Those phenomena can be considered using thermo-mechanical material properties. The correlations are valid as long as the heat build-up is attributed to dissipation and does not impact adhesion (Myshkin et al, 2005). The PV-application limit hence can be defined based on the thermo-mechanical material behaviour, since a significant change of the thermo-mechanical characteristics can negatively affect the tribological performance and introduce failure mechanisms. DSC- and DMA-measurements are carried out within the scope of the research at hand for precisely that reason. A conclusive composition of the DSC- and DMA-measurements is depicted in the appendix (section 8.4.1 and 8.4.2) and is further described in section 4.1 and 4.2.

Assessment of heat accumulation and melting processes in the rubbing contact at the testing configuration at hand

The current methodology determines frictional heat accumulation via temperature measurements at two positions in the counterpart (Gódor et al, 2006). Based on the FEM- simulations of a PTFE bronze composite/steel pairing at a RoD model testing configuration, outlined by Grün (2007) and Grün et al (2008), the real contact temperature area is assumed to level out at values of 30 to 40 °C higher than the measured near surface temperature. For the TPU/steel pairing, used in the research work at hand, those results are adopted and the real contact temperature is even expected to slightly overrun the 30 to 40 °C level due to higher frictional work of the current model system. Moreover, the real temperature in the single contact spots is approximately higher and partial melting is expected even at “low” overall contact temperatures (Figure 3.3-13). Partial melting of asperities affects the tribological bearing capacity and conjointly the stability and can introduce failure. The debris of a lubricating polymer film on the counterpart possibly indicates and certifies such melting processes as well as prow-like formations on the stressed surface (Da Silva et al, 2007).

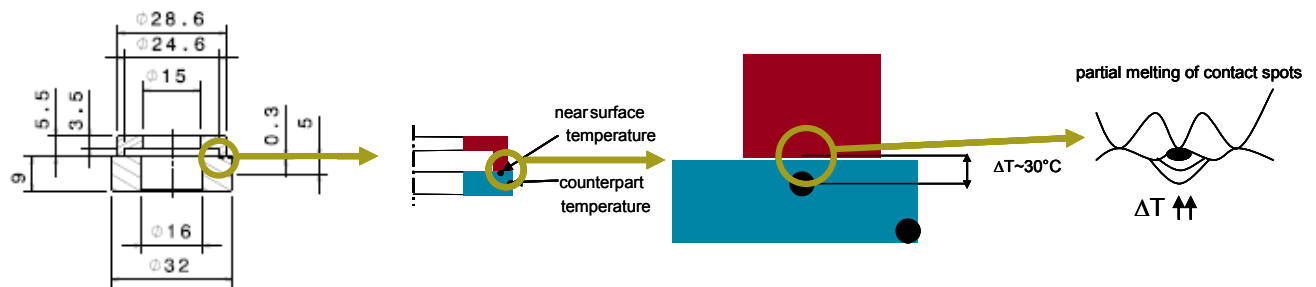


Figure 3.3-13: Assumptions made on the frictional heat accumulation in the rubbing contact for the tribological system at hand

Attempt and procedural method to compose a PV-diagram

Conventionally, PV-diagrams are used to apply identification to the ignition map of journal bearing applications (Müller and Deters, 2004). A more detailed background on the modus operandi and their relevance in mechanical engineering to characterize tribologically stressed components is given in the theoretical review in section 2.1.2.3. The current approach combines frictional heat accumulation with regards to melting of the TPU sliding face, the occurring surface mutations in relation with appearing wear mechanisms and the linear wear rate resulting from the measured material detachment. The maximum tolerable pressure is defined as the limit of mechanical bearing capacity. An overrun of this limit results in severe mechanical fatigue. The limitation of the maximum tolerable sliding velocity is related to a thermal limit in terms of frictional and hysteretic heat-up. Furthermore, the possible testing range of the testing rig influences the validity range of the PV-limit. Certain limiting PV-settings, to characterize the scope of use for the sealing material, are set with rigorous regards on each individual parameter and real operation conditions. Notwithstanding, the approaches are precisely valid for the current tribological systems performance at the component testing configuration at hand with the testing methodologies described within the scope of this thesis. Figure 3.3-14 schematically sums up a PV-diagram.

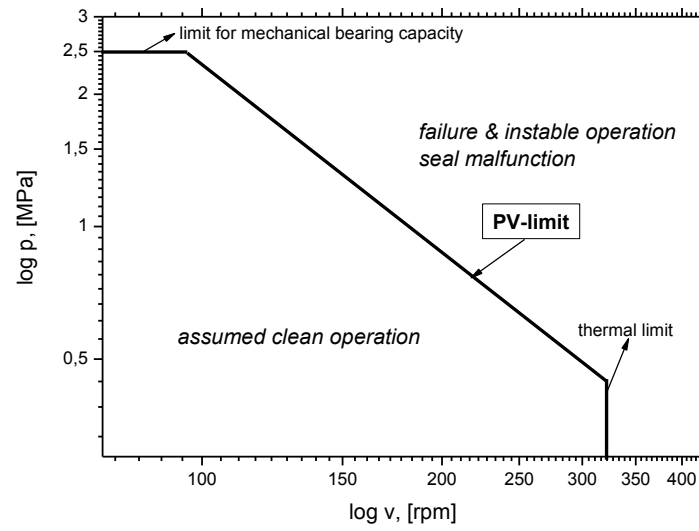


Figure 3.3-14: Schematic PV-diagram for TPU seal materials

4. Results

4.1 Bulk Properties

4.1.1 Dynamical Mechanical Analysis

The main aim of the dynamical mechanical analysis in the research work at hand is to explain the rate and temperature dependency of the pattern materials' properties and to generate material data which can be possibly linked to the tribological profile of the material. Viscoelastic response, in accordance with hard segment content and formation, is emphasized since the hard domains highly affect main bulk softening processes, which is then correlated with mechanical and tribological stability to a high degree (Holden et al, 2004). Therefore, frequency sweeps and temperature sweeps are carried out. The testing procedure is described in section 3.2.1.1. The subsequent chapters briefly sum up the most considerable results. A detailed account of the results is given in the appendix (see section 8.4.1).

Assessment of Rate Dependency

TPU systems are generally noted for rate-dependent stiffening. The initial rubbery type behaviour at certain temperatures is transformed into glassy-type behaviour with increasing strain rate (Sarva and Hsieh, 2009). Within the framework of the present work, frequency sweeps are conducted. The evolution of the modulus as a result of the loading rate can be demonstrated. Additionally, the effect of higher frequency loading can be linked to that of tribological loading because similar mechanisms, e.g. heat accumulation, are occurring (Uetz and Wiedmeyer, 1985). Figure 4.1-1 shows frequency sweeps for the filled and the unfilled TPU system at different temperatures. Both materials are characterized by similar modulus developing. The effect of the filler in dynamical mechanical analysis is negligible since dynamic thermo-mechanical properties are related with the matrix of the rubber material (Hofmann, 1989).

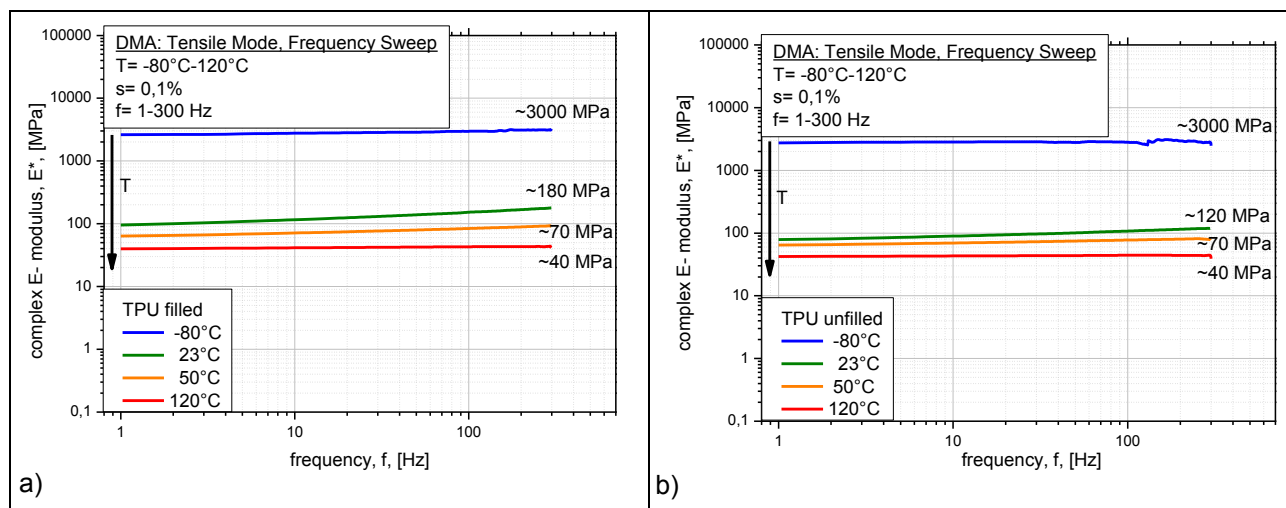


Figure 4.1-1: Frequency Sweeps at different temperatures for the a) filled b) unfilled TPU

At - 80 °C both materials stiffen to a high degree which is affected by the soft domains. The soft domains account for the rubber-like behaviour of TPU (Qi and Boyce, 2005). Remarkable stiffening in the glassy state is typical for rubber products (Sommer and Röthemeyer, 2006).

An indicative impact of the frequency can not be declared based on the tested range. The stiffening occurs at rather small levels. This phenomenon is mainly due to the fact, that no significant viscoelastic transitions could be depicted over the tested temperature range and scarcely rate dependency henceforth. Albeit, the impact of frequency is more distinctive at room temperature. At the testing range from 1 to 300 Hz the modulus nearly doubles (Figure 4.1-2), which follows from viscoelastic transition at this temperature range.

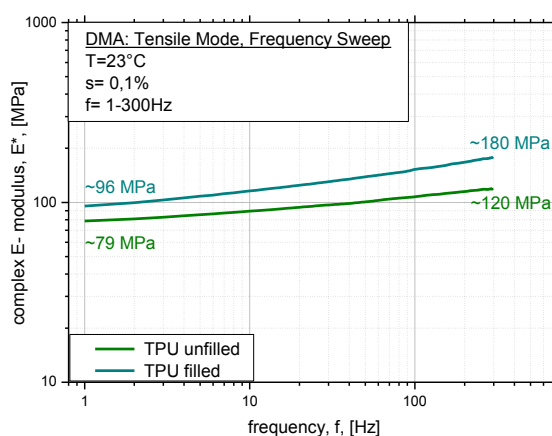


Figure 4.1-2: Comparison of frequency sweeps of filled and unfilled TPU performed at room temperature

This effect decreases at elevated temperatures and during the glassy state. Moreover, the assorted morphology of the matrix of the filled and unfilled system attains importance during viscoelastic transitions. The matrix of the filled system is possibly more crystalline due to differing formation of hard domains and thus behaves more rigid.

Conclusively, the matrix systems of both materials feature a similar thermo-mechanical response and the strain rate induced stiffening of both materials is not remarkable at the tested temperature range.

Assessment of Temperature Dependency

Generally, two transitions, mainly dependent on the block length, the composition, phase mixing and the thermal history, are described for TPU: a glass transition temperature dominated by soft domains at low temperatures and softening by means of melting of the hard domains at elevated temperatures (Holden et al, 2004). The present analysis focuses on the bulk softening processes at elevated temperatures because it mainly affects the thermo-mechanical stability of materials and therefore can be correlated with tribological failure. Bulk softening is highly dependent on the hard segment content and formation (Holden et al, 2004). Figure 4.1-3 demonstrates temperature sweep curves for both materials.

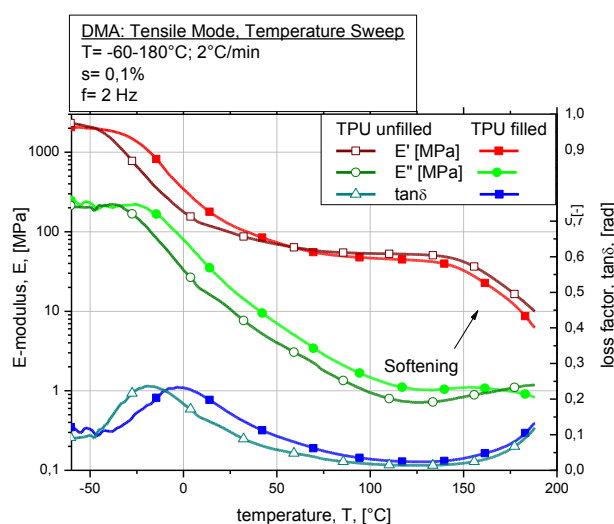


Figure 4.1-3: Temperature Sweeps for the filled and unfilled TPU performed at 2Hz

Significantly the glass transition of E' , E'' and $\tan\delta$ emerge at higher temperatures for the filled system which applies to the differing matrix system (Table 4.1-1). A shift of the glass transition range towards higher temperatures is described as a result of

increased hard segment content in literature (Crawford, 1998). The levels and the trends of storage and loss modulus are similar for both systems, including the loss factor. Bulk softening occurs at elevated temperature of about 150 °C for both materials which indicates similar thermal stability at low frequency loading. Table 4.1-1 summarizes the results.

Table 4.1-1: Comparison of the Results from Temperature Sweeps

Material	Frequency	TPU unfilled		TPU filled	
		2 Hz	20 Hz	2 Hz	20 Hz
Glass Transition (E')	[°C]	-45	-41	-30	-26
Glass Transition (E'')	[°C]	-38	-30	-22	-15
E'_{max}	[MPa]	210	207	200	190
Glass Transition ($\tan\delta$)	[°C]	-19	-9	-3	7
$\tan\delta_{max}$	[-]	0,25	0,25	0,24	0,25
Softening	[°C]	150	150	151	151

Significantly, the glass transition shifts to higher temperatures with the strain rate. This shift is defined as “apparent glass transition”, meaning that glass transition range, which the material mechanically recognizes at the given strain rate (Yi et al, 2005). The shift is only recognised in the glass transition range. In the subsequent rubbery state an impact of the testing frequency is not demonstrated. Rate dependency thus can solely be detected for transition regimes. Figure 4.1-4 declares the impact of frequency on the temperature sweeps.

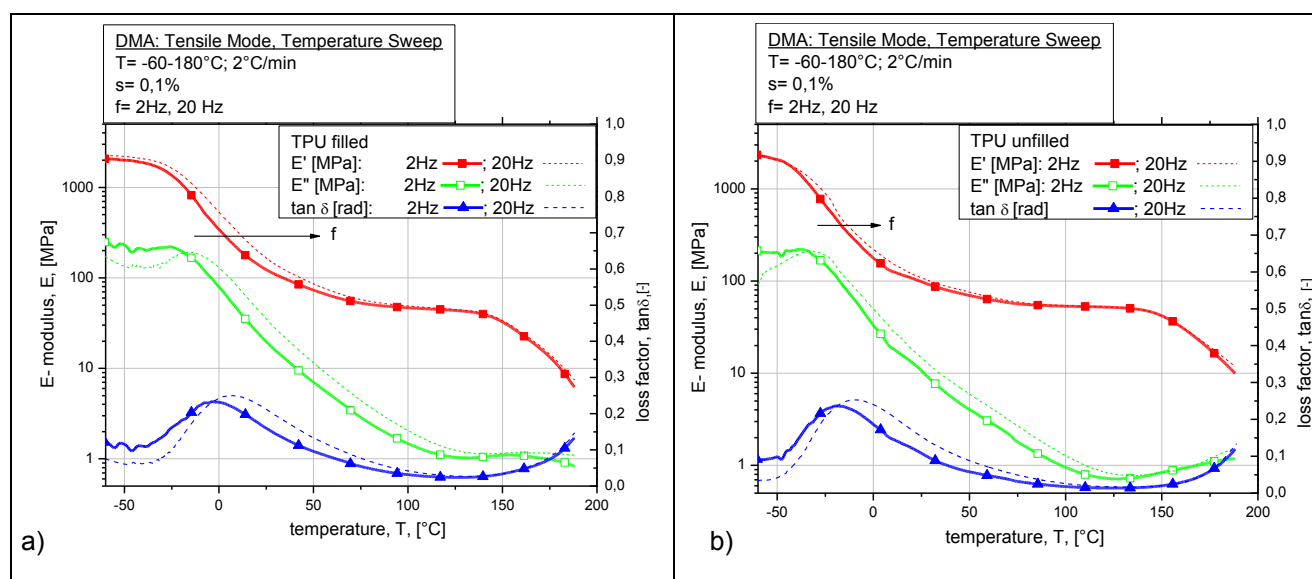


Figure 4.1-4: Temperature sweeps in dependency of the testing frequency for the a) filled, b) unfilled TPU system

Lastly, the thermal stability of the material is conveyed as bulk property and not related to testing parameters, which is critically important for defining a thermal application limit and failure analysis. An attempt to correlate this phenomenon with failure analysis is made in chapter 4.5.3.

4.1.2 Thermal Analysis via DSC

The overall objective of the DSC study on the pattern materials is, first-to perceive a general concept of their thermal response and, secondly, identifying possible morphological changes at critical temperatures evaluated from the tribological tests (described in chapter 4.5.3). Therefore a testing procedure is initiated (see section 3.2.2.1) to investigate bulk softening in accordance with hard segment melting. Figure 4.1-5 and Figure 4.1-6 compare the thermal response of the unfilled and the filled TPU on the basis of their thermal response. A more detailed representation of the results is demonstrated in the appendix (see section 8.4.2). The assumptions derived from the measurements are based on the mechanisms described by Schwarz (1993) and Holden et al(2004).

The unfilled material shows crystalline melting at elevated temperatures of about 240°C. The melting peak is bimodal. It is primarily assumed that paracrystalline structures are melting. Paracrystalline structures, crystalline structures of lower order, as conventionally described at TPU-materials (Holden et al, 2004), can possibly be traced back to processing and annealing conditions. After that crystalline hard domain structures of higher order are melting, demonstrated as a rather narrow sharp peak. No recrystallization or melting processes, ensuing during the second heating run, can be demonstrated on account of the reorientation and destruction of hard domains during the first melting.

The filled material shows hard segment melting at similar temperatures as the unfilled one. The paracrystalline peak is sized wide. Significantly, the main melting peak is very sharp due to a different configuration of the hard domains by means of higher order of crystalline structures. A small melting peak appears at about 110 °C, which possibly can be attributed to processing conditions. Moreover, recrystallization during cooling and a paracrystalline melting in the second heating run can be demonstrated in Figure 4.1-6, but cannot be significantly connoted with morphological phenomena.

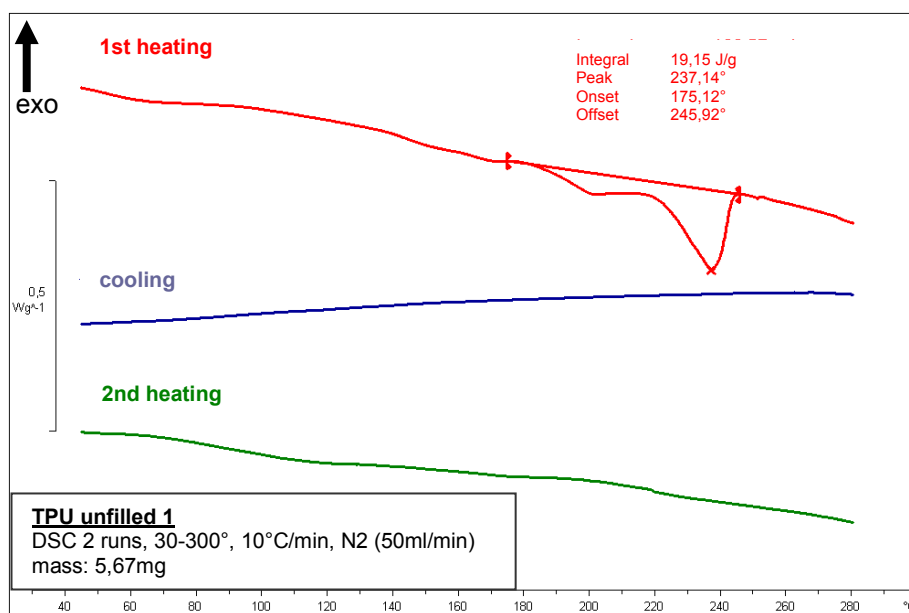


Figure 4.1-5: DSC- measurement for TPU unfilled

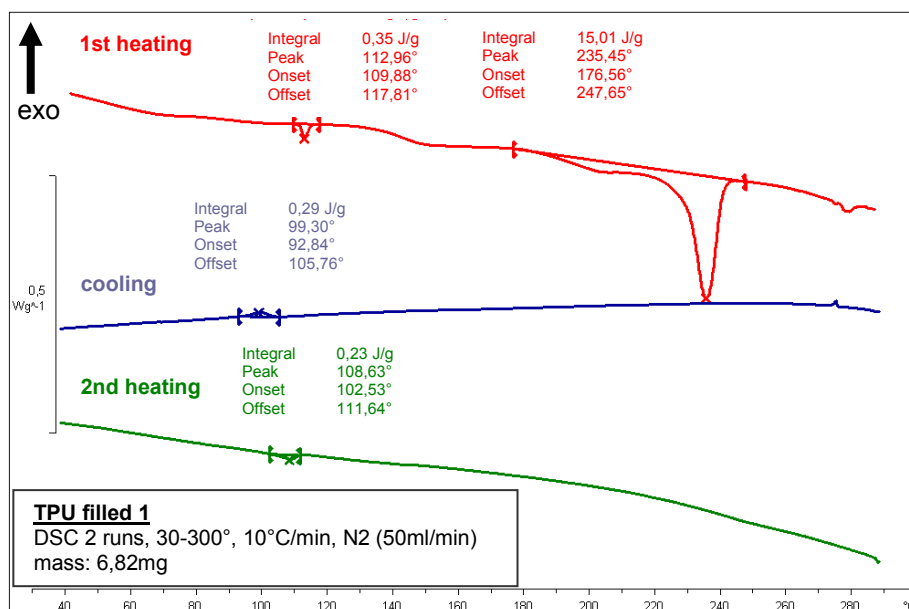


Figure 4.1-6: DSC- measurement for TPU filled

Conclusively, the thermal response of both materials is similar to each other except for a little higher orientation of the hard domains for the filled TPU. With an additional regard on the tribological tests (described as from chapter 4.3), this characteristics can approve a higher thermal stability of the filled material, in case that the better tribological performance of the filled material results not particularly from the filler system.

4.2 Results and Approval of the Improvements on Specimen Geometry and the Test Configuration

4.2.1 Geometrical optimization of RoD-specimens

The geometrical optimization is approved via constant load tests of the unfilled softer material. The improved mechanical stability leads to a more stable and reproducible tribological operation compared to the standard specimen, which is briefly summarized in Figure 4.2-1. Significantly, the tests with the new geometry RoD BB show higher reproducibility. After short peak amplitude due to run-in-phenomena the COF levels out, while it oscillates heavily during the test with the standard geometry. A more detailed evaluation of the test results is demonstrated in the appendix (chapter 8.4.3).

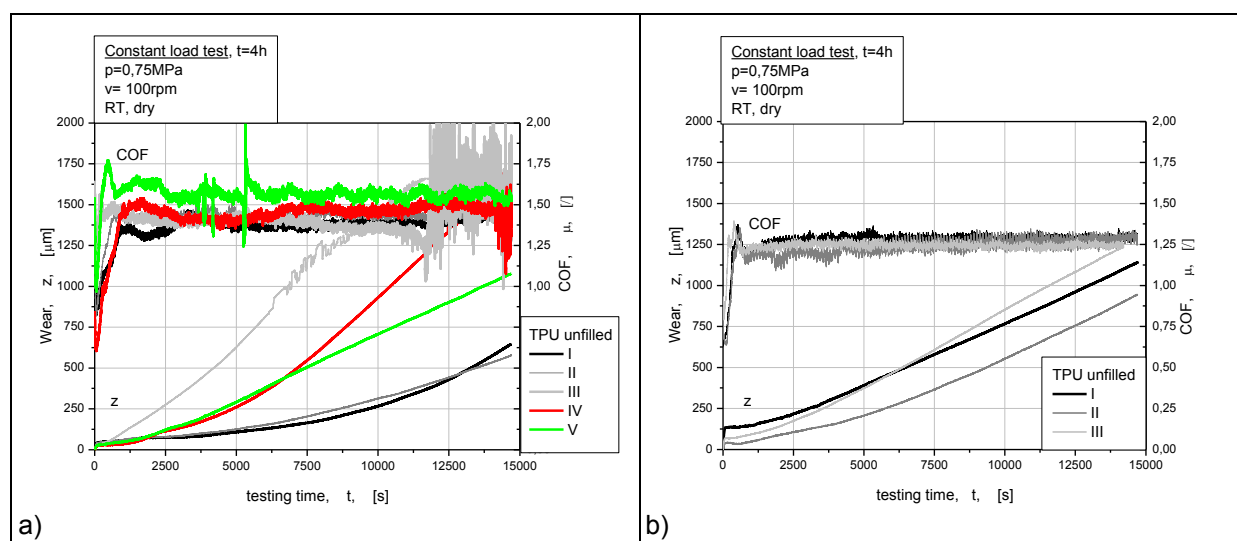


Figure 4.2-1: Impact of geometrical improvements of the testing disc on the tribological profile of TPU unfilled; a) specimen RoD standard, b) specimen RoD BB

4.2.2 Improvements of the Test Configuration

The following section describes the impact of the optimized specimen holder, using a ball scraper instead of a self aligning ball bearing.

Figure 4.2-2 briefly summarizes the impact of the new device on the tribological profile during a speed step test (further described in section 3.3.3) for TPU filled and unfilled. The COF and the wear are demonstrated in dependency of the sliding speed.

For the filled material the stiffer device has nearly no influence on the test results, since the mechanical stability of the material is sufficient for stable performance. For the unfilled material the new device prevents slipping from the original wear track due to large deformation and tilting which results in a more stable running. As a result, the specimen bears higher loadings and shows lower wear.

A detailed evaluation of the tribological tests is represented in the appendix (section 8.4.3).

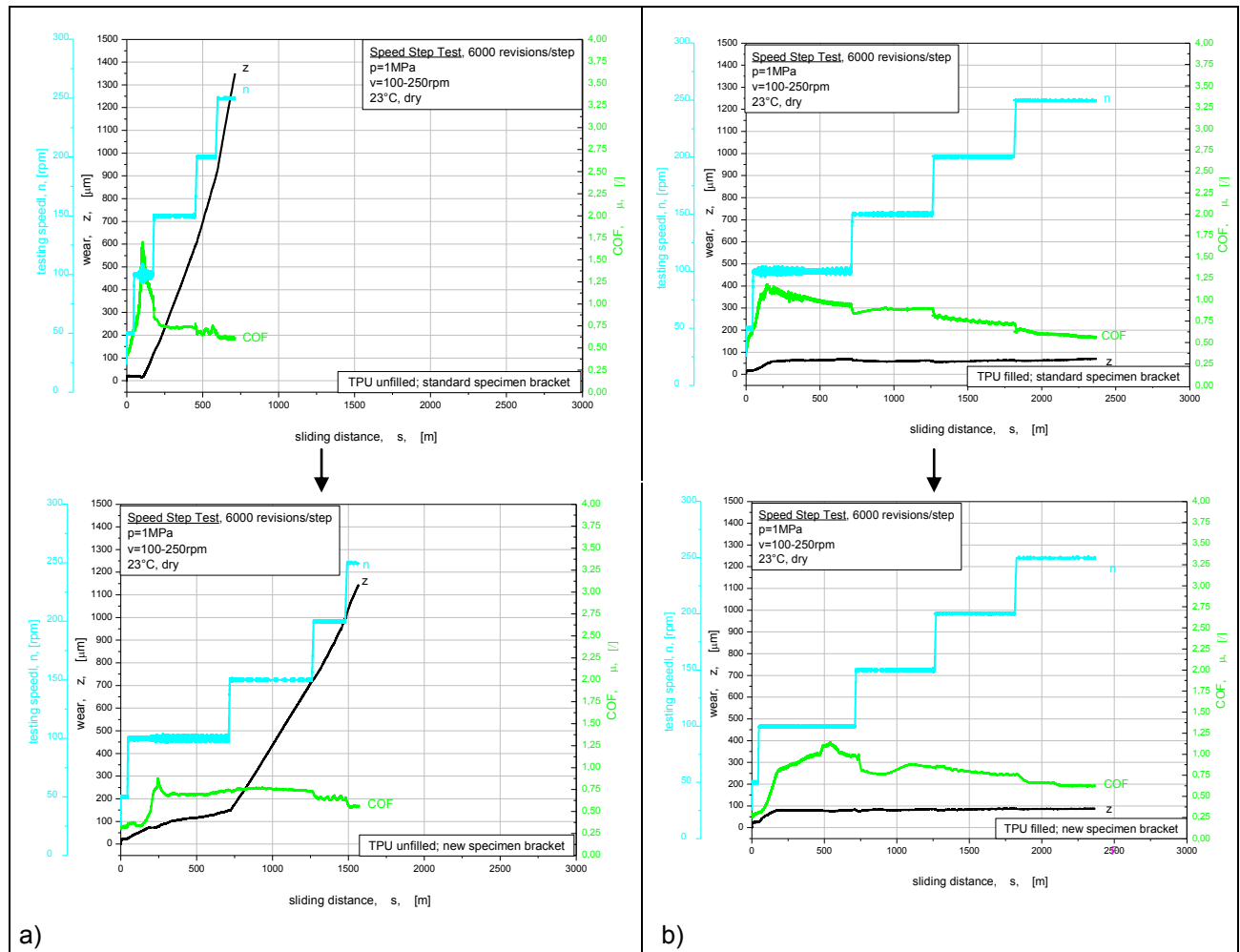


Figure 4.2-2: Impact of the improved upper bracket on the tribological profile at a speed step test of a) TPU unfilled and b) TPU filled

4.3 General Tribological Profile of Tested Materials

In the following chapter the tribological profile of the filled and unfilled TPU system is assessed by means of a constant load test at 100 rpm and 1 MPa for four hours (see chapter 3.3.2.1). A graphical demonstration of the test results is shown in Figure 4.3-1. A more detailed examination can be found in the appendix (chapter 8.4.4).

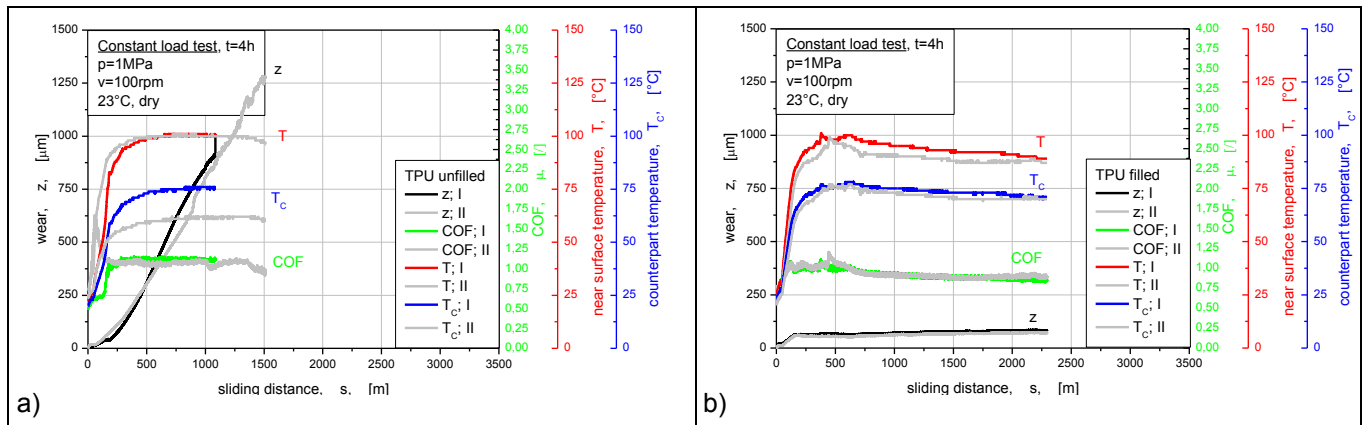


Figure 4.3-1: Constant load test ($p=1\text{ MPa}$, $v=100\text{ rpm}$, $t=4\text{ h}$) for a) TPU unfilled; b) TPU filled

4.3.1 Tribological Performance of the unfilled material

The unfilled material significantly shows marginal resistance to the applied tribological loadings. The wear rapidly increases from the beginning of the test. Accordingly, the test is aborted after approximately two hours running time, since the tolerable wear level of the tribometer is exceeded. The frictional force and conjointly the COF peaks out at the beginning of the test (especially for test No. 2, Figure 4.3-1) due to surface formation processes and then flattens out at a constant level of approximately 1,1 (Table 4.3-1). The tribological operation thus is very stable in spite of high wear. Both measured temperatures (near surface, middle of counterpart) proceed similar to the frictional force. Moreover, it has to be noted that the counterpart temperatures of both tests differ as a possible result of inappropriate positioning of the thermo-element. The optical investigations of the specimens' wear track demonstrate a roughly structured surface indicating higher wear with "puddles" and material accumulations ("prows") oriented perpendicular to the sliding direction. The light micrographs of the first test are depicted as example (Figure 4.3-2 & Figure 4.3-3). The counterpart bearing track reflects a rather balanced load distribution. Moreover, a lubricating film has matured on the surface accounting for stable running at constant

COF-levels. Conclusively, the high wear levels of the unfilled system result from the correlation of low mechanical and tribological stability and conjointly further softening due to frictional heat accumulation.



Figure 4.3-2: Micrographs of unfilled specimen's wear track (Constant load test, $p=1$ MPa, $v=100$ rpm, $t=4$ h, Test No. 1)

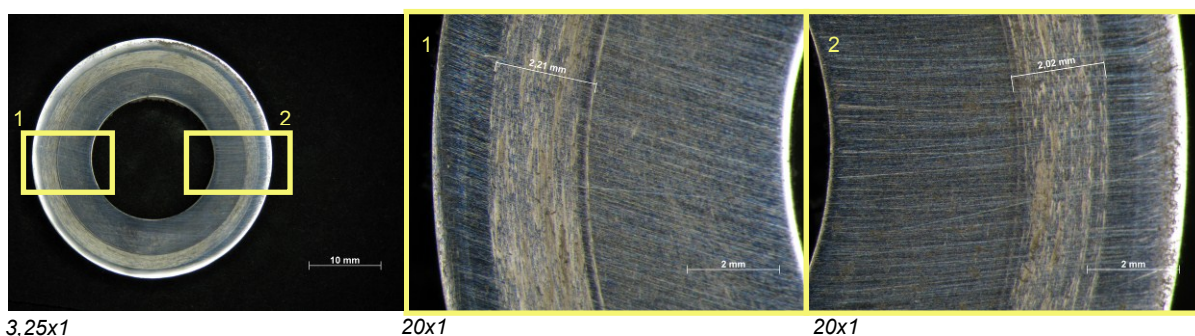


Figure 4.3-3: Micrographs of counterpart's wear track (Constant load test, $p=1$ MPa, $v=100$ rpm, $t=4$ h, Test No. 1)

4.3.2 Tribological Performance of the filled material

The filled material shows scarcely wear. The initial rise of the curve is singly correlated with elastic deformation and run-in processes of the specimen. During the first 500 sliding meters an ideal surface is developed, and, as a result, the temperature increases and the frictional force is at higher levels. As the stability level is reached both the COF and the measured temperatures level out. The frictional heat accumulation relatively decreases in accordance with the formation of a lubricating transfer film on the counterpart and a bearing or lubricating filler network on the specimen (Figure 4.3-4 & Figure 4.3-5). Precisely, on the micrographs of the specimen processing tracks are depicted on the exterior face, whereas a filler network is developed on the interior face. The differing bearing face conditions are due to geometrical relations of the specimen.

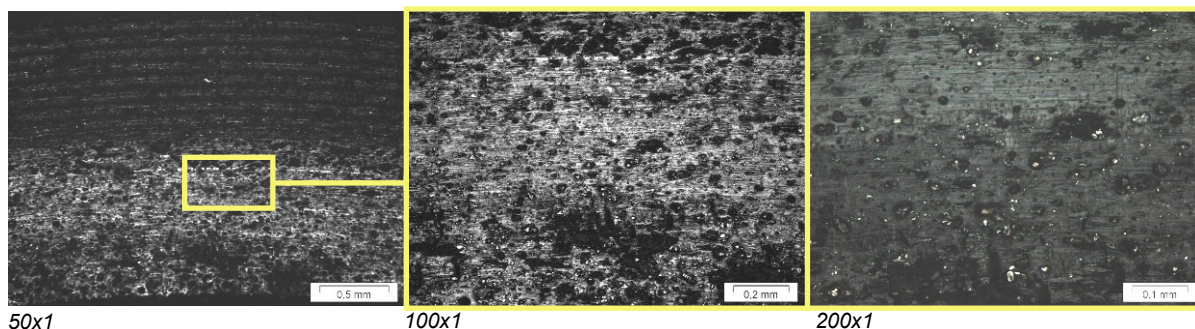


Figure 4.3-4: Micrographs of filled specimen's wear track (Constant load test, $p=1$ MPa, $v=100$ rpm, $t=4$ h, Test No. 1)

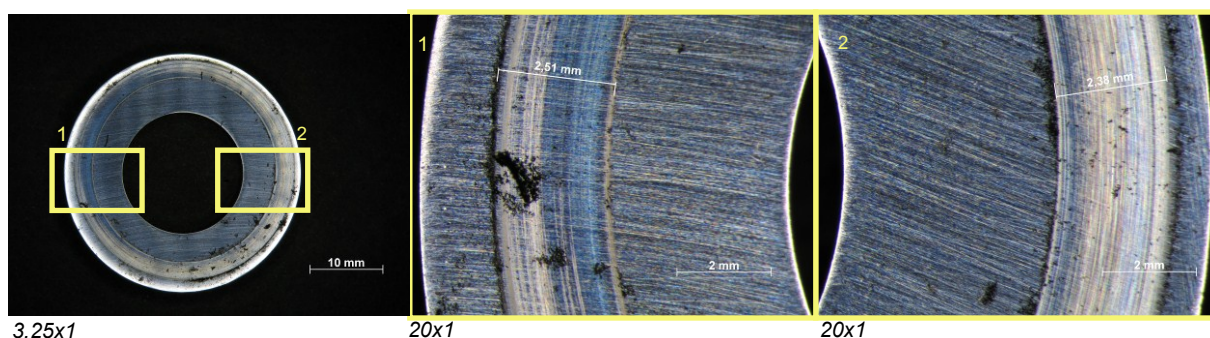


Figure 4.3-5: Micrographs of counterpart's wear track (Constant load test, $p=1$ MPa, $v=100$ rpm, $t=4$ h, Test No. 1)

4.3.3 Comparison of the filled and unfilled material

Table 4.3-1 contrasts a detailed evaluation of the constant load tests for the unfilled and the filled material. Conventionally, the filled system is characterized by lower wear. The wear rate of the filled system is approximately a thousandth of the unfilled ones. The frictional heat accumulation is marginally higher for the filled system, conjointly with the frictional force and the frictional shear stress. This phenomenon is simply due to a permanent tribological stress on the filled TPU's surface layer, whereas new surface layer are continuously incriminated for the unfilled TPU on account of the severe wear characteristic. For the unfilled system the wear track on the surface is dominated by rough structures, indicating failure mechanisms. The lubricating film on the counterpart possibly relates to bulk softening and material debris henceforth. It is permanently building up and breaking down. On account of that, transfer film formation cannot be regarded as a repeatable parameter and barely correlations can be associated with setting parameters for tribological testing

The transfer film on the counterpart of the filled system is correlated with adhesion forces and interactions with the metallic counterface and is characteristic and essential for its operational behaviour. It differentiates from the almost lubricating material

debris of the unfilled material, since barely substrate is smeared on the counterpart. On the bearing track of the filled system a bearing or lubricating structure is developed. Conclusively, the filler network and the more mechanically stable matrix of the filled system induce a better tribological performance and operational behaviour.

Table 4.3-1: Evaluation of constant load ($p=1$ MPa, $v=100$ rpm) tests of TPU filled and unfilled

Constant load test $p=1$ MPa; $v=100$ rpm		TPU filled		TPU unfilled	
		I	II	I	II
Material Parameters					
Density	[g/cm ³]	1,23	1,23	1,20	1,20
Test parameters					
Run in track	[m]	45			
Run in time	[s]	600			
Run in load	[N]	50			
Run in speed	[rpm]	50			
Testing sliding distance	[m]	2155			
Testing time	[h]	4			
Testing force	[N]	166			
Contact pressure	[MPa]	1			
Testing speed	[rpm]	100			
Testing temperature	[°C]	23			
Lubrication		dry			
Wear parameters					
actual sliding distance	[m]	2293,00	2295,00	1091,60	1513,20
mass loss	[mg]	2,61	3,49	288,41	313,94
worn specimen height	[μ m]	12,76	17,07	1445,80	1573,78
worn volume	[mm ³]	2,12	2,84	240,34	261,62
wear rate K	[cm ³ /Nm]	5,57E-09	7,45E-09	1,33E-06	1,04E-06
Wear resistance	[Nm/cm ³]	1,79E+08	1,34E+08	7,54E+05	9,60E+05
Wear intensity	[mm ³ /m]	9,25E-04	1,24E-03	2,20E-01	1,73E-01
Linear Wear Intensity	[mm/m]	5,57E-06	7,44E-06	1,32E-03	1,04E-03
Friction Parameters					
COF	[-]	0,90	0,90	1,12	1,06
Frictional work	[J]	339870,11	343868,61	181122,28	257323,61
near surface temperature	[°C]	93,57	88,62	100,39	99,77
counterpart temperature	[°C]	73,83	71,13	75,09	61,28
Combined Parameters					
Frictional energy density	[J/mm ³]	160168,67	121191,51	753,60	983,59
Frictional Shear stress	[N/mm ²]	0,89	0,90	1,00	1,02

4.4 PV-dependency of Tribological Material Characteristics

In the subsequent sections the PV-dependency of the tribological performance of the tested materials is concisely analysed. A more detailed demonstration of the test results is depicted in the appendix (chapter 8.4.5).

4.4.1 Evaluation of Load Step Tests

Conventional Approach

Variations in the contact pressure have a great impact on the tribological performance, since it directly affects the contact conditions. A significant descent in frictional force is accounted for both materials. The drop of the COF and the coherent incline of temperature with growing normal load are considered to result in a better distribution of the contact pressure on the contacting roughness tops, enlarging the real contact area of the tribological pairing (Uetz and Wiedmeyer, 1985).

Contact pressure dependency of the unfilled material

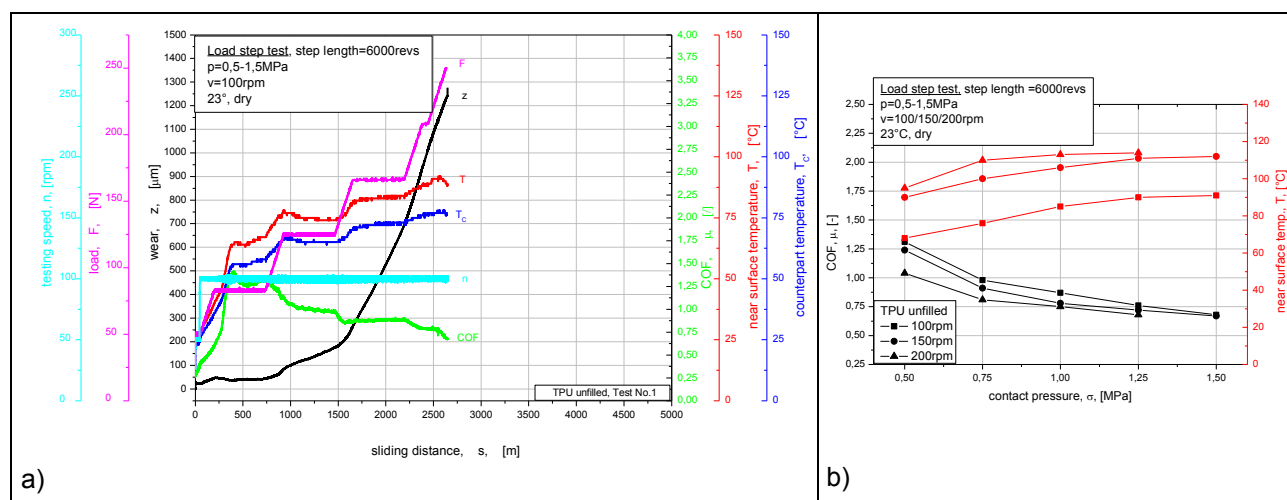


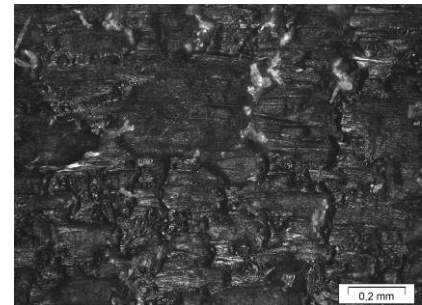
Figure 4.4-1: a) exemplary load step test; b) assessment of contact pressure dependency for the unfilled TPU

Figure 4.4-1a) exemplarily shows the load step test plot of the unfilled material at a testing speed of 100 rpm. Stable frictional and thermal conditions can be achieved for every load step (see temperature and COF plot in Figure 4.4-1a), which confirms the reliability of the present testing methodology to rate the impact of contact pressure on

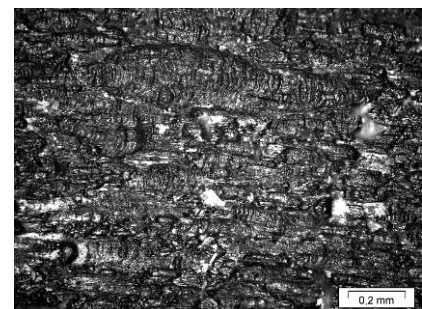
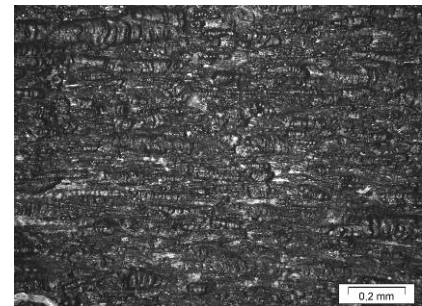
the tribological performance. Additionally, the results show proper reproducibility (see Table 4.4-1), except for some temperature measurements which show high standard deviations in accordance with imprecise positioning of the thermo-elements and differences in counterpart heights due to polishing.

Table 4.4-1: Evaluation and exemplary contact surface micrographs of load step tests of TPU unfilled

Load step test, TPU unfilled							
100 rpm			0,5 MPa	0,75 MPa	1,00 MPa	1,25 MPa	1,50 MPa
COF	[-]	avg	1,31	0,98	0,87	0,76	0,68
		dev	0,00	0,03	0,01	0,04	0,04
near surface temperature	[°C]	avg	67,90	75,59	84,72	89,43	90,74
		dev	4,05	0,93	2,26	1,38	1,13
counterpart temperature	[°C]	avg	59,93	67,02	74,36	78,63	79,40
		dev	4,76	2,41	3,20	2,26	3,35
linear wear rate	[µm/m]	avg	0,04	0,21	0,84	0,96	0,96
		dev	0,06	0,06	0,06	0,11	0,11
150 rpm			0,5 MPa	0,75 MPa	1,00 MPa	1,25 MPa	1,50 MPa
COF	[-]	avg	1,25	0,93	0,84	0,72	0,65
		dev	0,09	0,04	0,04	0,02	0,00
near surface temperature	[°C]	avg	90,11	99,13	106,13	110,91	112,44
		dev	11,63	16,66	14,34	15,82	15,83
counterpart temperature	[°C]	avg	73,34	80,02	83,92	86,50	87,49
		dev	6,41	8,61	5,92	5,44	5,75
linear wear rate	[µm/m]	avg	0,14	0,61	0,81	1,06	1,06
		dev	0,04	0,13	0,01	0,37	0,37
200 rpm			0,5 MPa	0,75 MPa	1,00 MPa	1,25 MPa	1,50 MPa
COF	[-]	avg	1,04	0,81	0,75	0,68	x
		dev	0,04	0,18	0,09	0,00	0,00
near surface temperature	[°C]	avg	95,12	110,34	112,75	114,34	x
		dev	2,81	3,90	0,49	1,75	0,00
counterpart temperature	[°C]	avg	77,83	85,97	88,80	90,35	x
		dev	0,40	2,99	1,02	3,20	0,00
linear wear rate	[µm/m]	avg	0,63	1,11	1,04	1,04	x
		dev	0,13	0,06	0,16	0,16	0,00



TPU unfilled, Test No. 1, 100x1



TPU unfilled, Test No. 2, 100x1

The wear and conjointly the wear rate significantly increase with progressive load steps for the unfilled TPU. The particular load steps and the respective overall testing process cannot be completed due to intolerable high wear (emergency shutdown of the machine). At the tested range damage and failure mechanisms hence occur, especially at the load step tests at elevated sliding velocities (see appendix, chapter 8.4.5). The frictional force and the resulting COF decrease with augmenting contact

pressure. Figure 4.4-1b) traces the impact of the contact pressure on frictional force and heat accumulation by plotting the average COF and the near surface temperature against contact pressure. The drop of the COF with growing normal load is due to a magnification of the real contact area and a better load distribution henceforth. Moreover, bulk softening on account of progressive heat accumulation forwards the formation of lubricating scalings (Figure 4.4-2) on the counterpart.

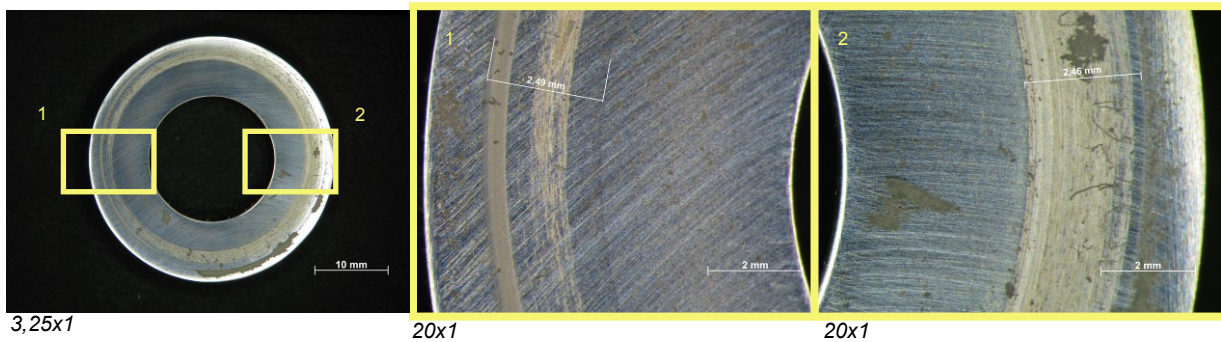


Figure 4.4-2: Wear traces on counterpart of load step test at 200 rpm of TPU unfilled (Test No.1)

For an improved understanding of the impact of contact pressure on the surface formation, the load step test is performed gradually at a testing speed of 100 rpm. Figure 4.4-3 shows the evolution of the contact surface with increasing load steps in greater detail. During the first step the wear is increasing but with a tolerable wear rate. The COF flattens out at rather high levels, which is possibly in accordance with run-in processes. The processing traces on the surface are ablated. Adhesion occurs at the contacting roughness tips of the tribological pairing. On account of its less rigid texture (compared to the counterpart), the roughness tops of the TPU are deformed and oriented, which results in a higher COF-level. These adhering oriented structures are identified on the micrographs as the lighter membrane-like structures. With increasing load the heat accumulation in the rubbing contact rises. As a result the TPU softens and the counterpart peaks partially penetrate the surface. Crudely, abrasion occurs, by means of membrane tearing and roll-like wear particle formation, and the measured wear increases. The surface is now coarsely textured perpendicular to sliding direction (prow formation, Schallamach-waves (Schallamach,1971)). The effect is enforced with load, due to further softening and high deformation. The wear pits get deeper and more extended, which can be demonstrated on the micrographs of step 2 to 5. The overall wear process resembles the commonly described wear mechanisms for adhesion of rubber-like materials (Zhang, 2004).

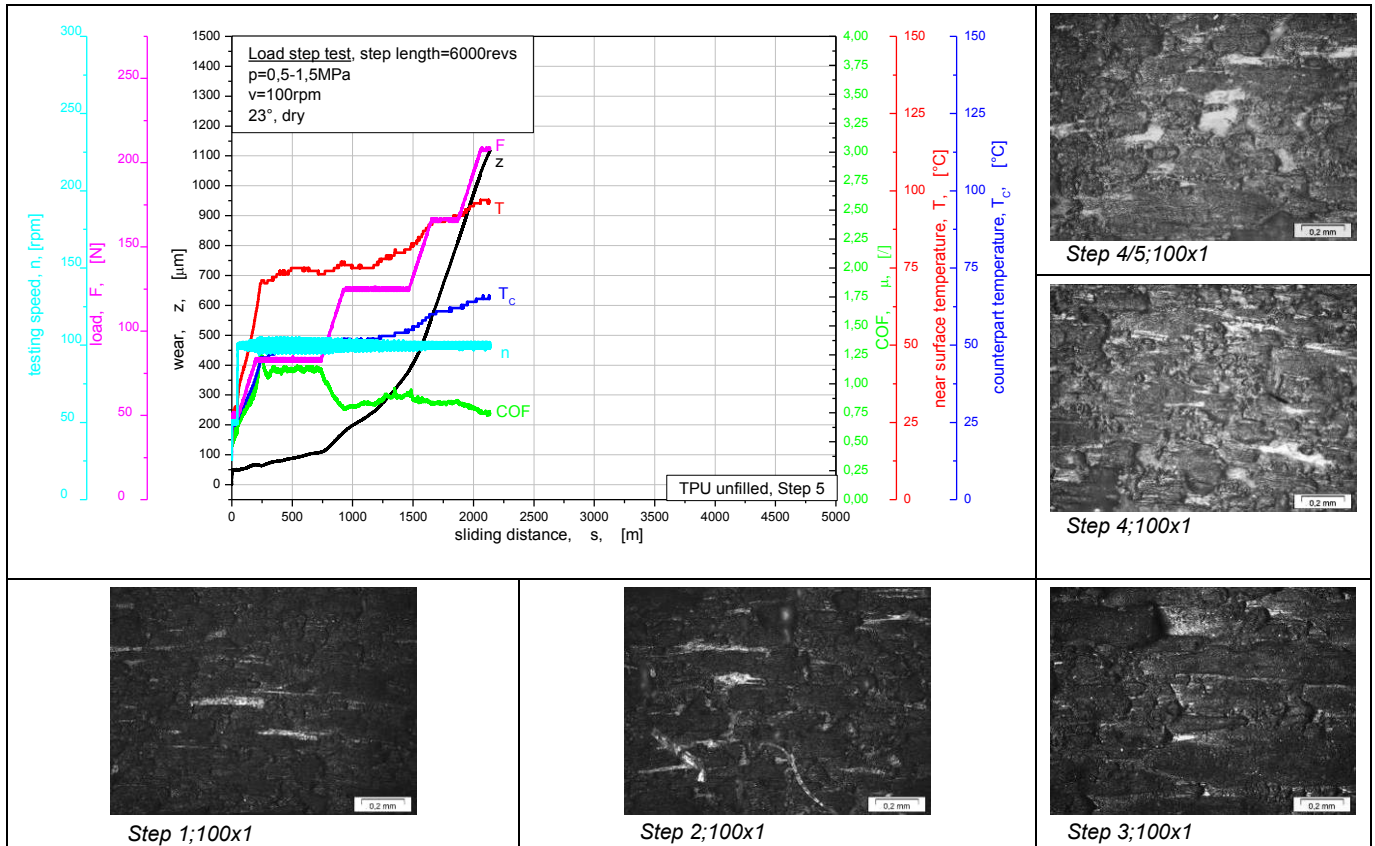


Figure 4.4-3: Gradually performed load step test of TPU unfilled at a testing speed of 100 rpm

Contact pressure dependency of filled material

The impact of the contact pressure on the tribological performance of the filled material is similar to the unfilled TPU (Figure 4.4-1b).

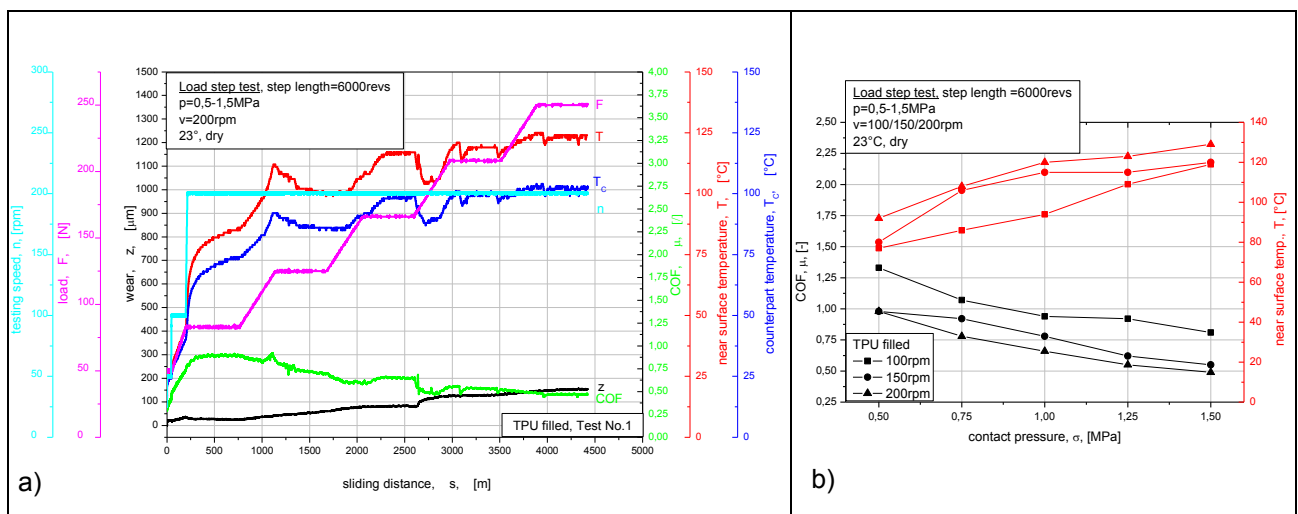


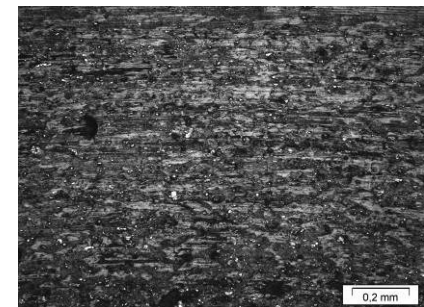
Figure 4.4-4: a) exemplary load step test; b) assessment of contact pressure dependency for the filled TPU

The frictional force thus decreases and conjointly the temperature increases with augmenting load steps. Conclusively, the filled material is more resistant to higher pressure and no failure occurs during the tested range since the wear only marginally or respectively does not rise with progressive load steps (Figure 4.4-4a, Table 4.4-2).

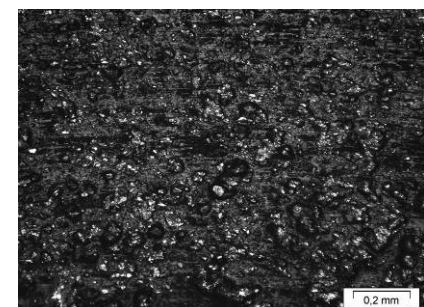
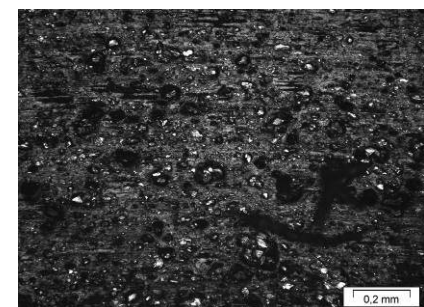
Table 4.4-2: Evaluation and exemplary contact surface micrographs of load step tests of TPU filled

Load step test, TPU filled							
100 rpm			0,5 MPa	0,75 MPa	1,00 MPa	1,25 MPa	1,50 MPa
COF	[-]	avg	1,33	1,10	0,93	0,91	0,81
		dev	0,00	0,04	0,01	0,01	0,00
near surface temperature	[°C]	avg	77,43	86,35	94,04	109,24	118,55
		dev	0,00	1,01	6,10	7,76	0,00
counterpart temperature	[°C]	avg	56,82	64,00	69,14	79,07	83,28
		dev	0,00	0,97	1,12	1,65	0,00
linear wear rate	[μm/m]	avg	0,00	0,01	0,01	0,01	0,02
		dev	0,00	0,00	0,00	0,01	0,00
150 rpm			0,5 MPa	0,75 MPa	1,00 MPa	1,25 MPa	1,50 MPa
COF	[-]	avg	1,12	1,02	0,86	0,79	0,69
		dev	0,29	0,08	0,11	0,19	0,16
near surface temperature	[°C]	avg	80,30	105,50	115,17	115,32	119,76
		dev	0,13	16,93	13,81	5,24	5,52
counterpart temperature	[°C]	avg	63,83	79,16	86,47	87,49	89,84
		dev	5,45	15,79	15,87	12,18	11,40
linear wear rate	[μm/m]	avg	0,00	0,00	0,02	0,02	0,02
		dev	0,00	0,00	0,00	0,01	0,00
200 rpm			0,5 MPa	0,75 MPa	1,00 MPa	1,25 MPa	1,50 MPa
COF	[-]	avg	0,98	0,78	0,66	0,55	0,49
		dev	0,12	0,05	0,03	0,02	0,02
near surface temperature	[°C]	avg	92,08	107,55	120,43	123,15	128,53
		dev	11,65	8,84	5,47	6,45	7,29
counterpart temperature	[°C]	avg	75,97	88,69	97,94	99,60	102,07
		dev	4,33	2,94	0,65	0,57	0,06
linear wear rate	[μm/m]	avg	0,00	0,02	0,01	0,01	0,02
		dev	0,00	0,01	0,01	0,01	0,00

TPU filled, Test No. 1, 100x1



TPU filled, Test No. 1, 100x1



The frictional traces on the counterpart differ significantly from the lubricating film of the unfilled TPUs counterpart. A kind of lubricating transfer film is indeed developed, but it is not only deposited on the counterpart like the unfilled ones but rather an interaction with the metallic counterface due to adhesion evolves.

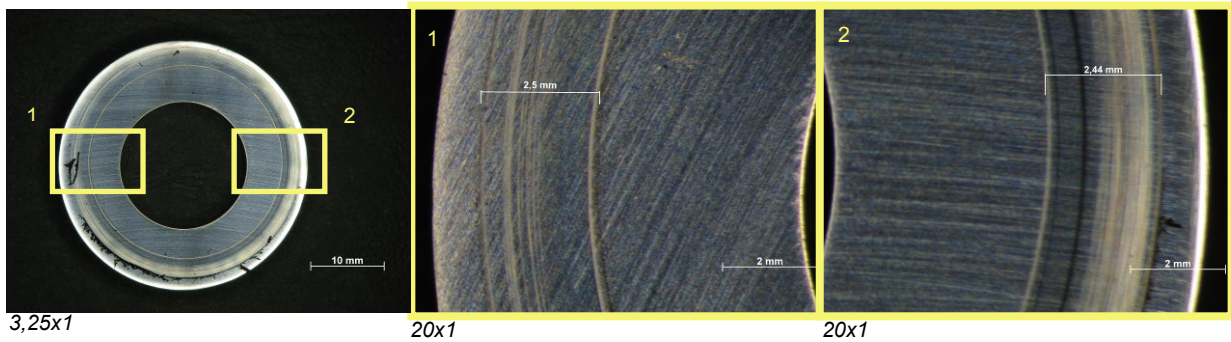


Figure 4.4-5: Wear traces on counterpart of load step test at 100 rpm of TPU filled (Test No.1)

The incrementally performed tests at a testing speed of 100 rpm and the associated wear track micrographs of the TPU sample (Figure 4.4-6). declare the occurring frictional phenomena. During the first two load steps processing traces are still depicted on the surface. The COF is rather high (run-in behaviour). During further tribological operation, the matrix softens and a filler network is dissected and dominates the friction and wear mechanisms due to its bearing and lubricating function. With increasing contact pressure, the dissection of the filler network is enforced. As a result the frictional force descends and the temperature flattens out or respectively slightly diminishes.

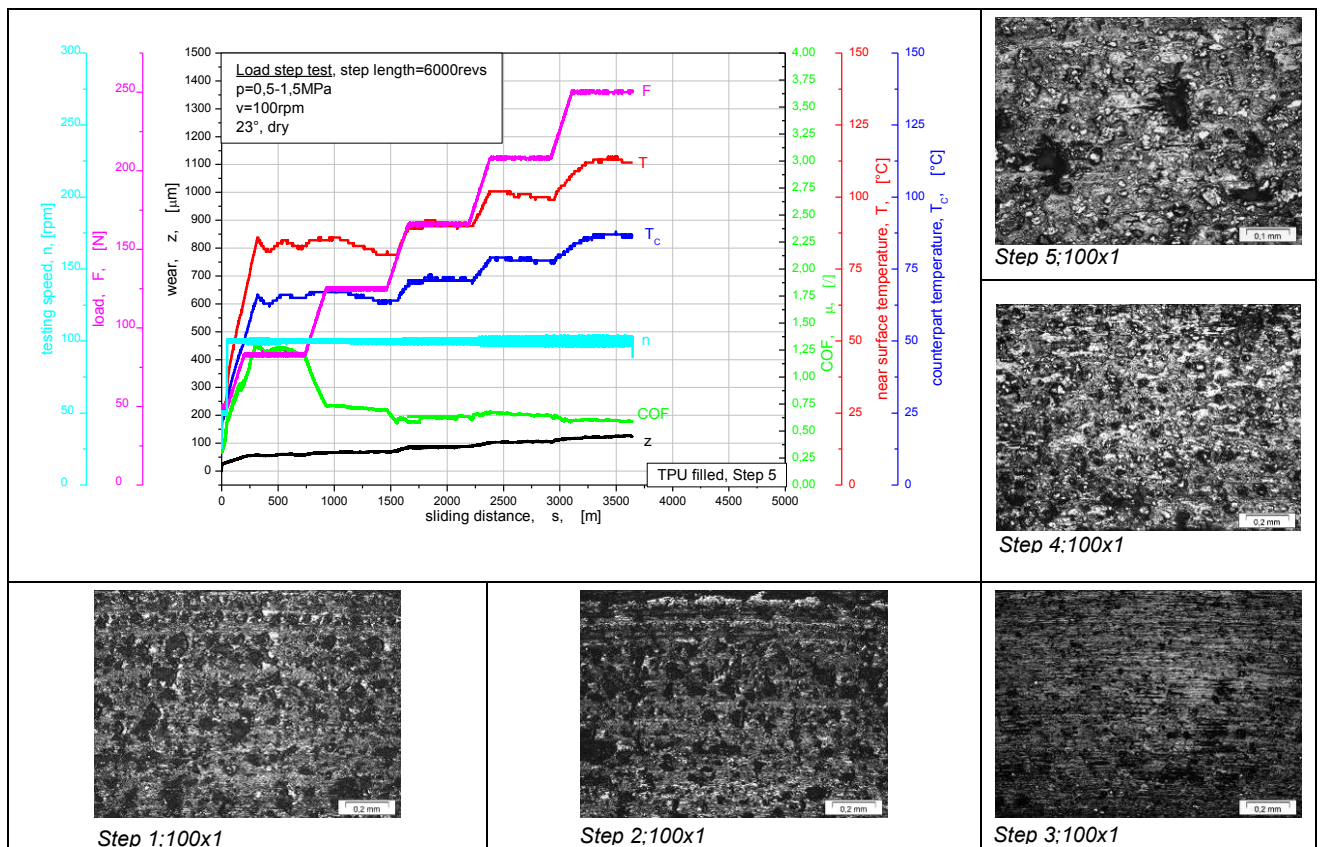


Figure 4.4-6: Gradually performed load step test of TPU filled at 100 rpm

The outcome of the load step tests at elevated velocities is generally the formation of a more distinctive filler network structure on the specimens wear track. The influence of the testing speed is more indistinct for the filled than for the unfilled material due to the advanced tribological resistance of the filled TPU (see micrographs in Table 4.4-2).

4.4.2 Evaluation of Speed Step Tests

Conventional Approach

Generally, the speed step tests are equally approved to rate the PV-dependency of TPU seal materials, as are the load step tests, in accordance with stable tribological conditions at every step and a proper reproducibility of the results (except for temperatures as mentioned in 4.4.1). The speed step tests are characterized a significant drop of the COF with increasing speed steps. Coherently, the measured temperatures and the wear are rising. Those relations are commonly described in polymer tribology (Uetz and Wiedmeyer, 1985) and in conjunction with Stribeck the above cited behaviour is described for mixed friction conditions (Czichos and Habig, 2003). Higher sliding velocities precisely induce bulk stiffening and the resulting subsidence of the roughness asperities of the hard counterpart into the soft elastomeric matrix reduces. The real contact area is therefore smaller and the adhesion forces weaker (Persson, 1997).

Sliding velocity dependency of unfilled material

The unfilled material exposes stable running conditions combined with low wear characteristics only at a rather low sliding velocity of 100 rpm (Figure 4.4-7a). At higher speeds the wear is becoming more severe regarding the wear rate, exposed in Table 4.4-3. With increasing contact pressure, the wear increases further, and even at low sliding velocities of 100 rpm failure mechanisms occur (Table 4.4-3, appendix: chapter 8.4.6). Figure 4.4-7b summarizes the evolution of the COF and the frictional heat build-up as it is described in 0.

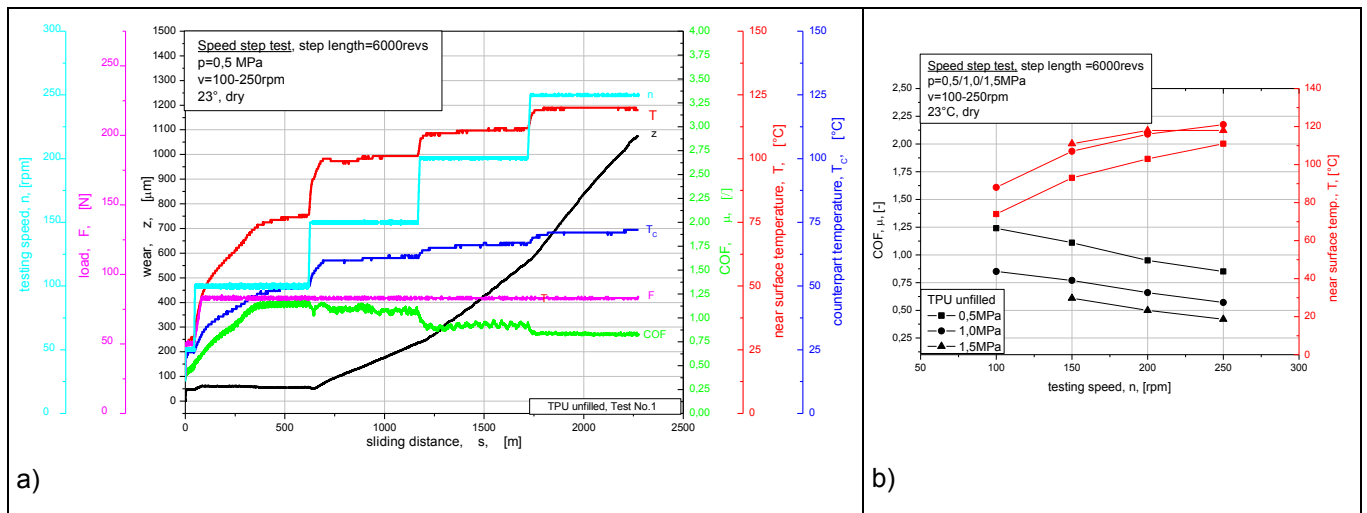
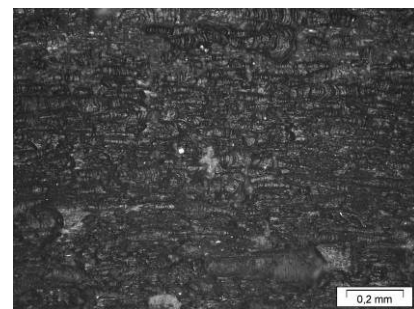


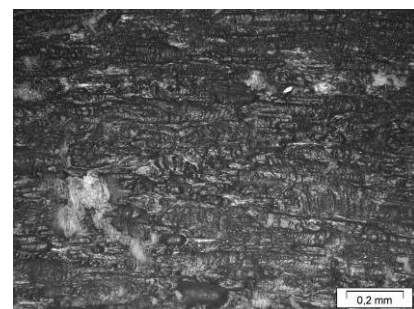
Figure 4.4-7: a) exemplary speed step test; b) assessment of testing speed dependency for the unfilled TPU

Table 4.4-3: Evaluation and exemplary contact surface micrographs of speed step tests of TPU unfilled

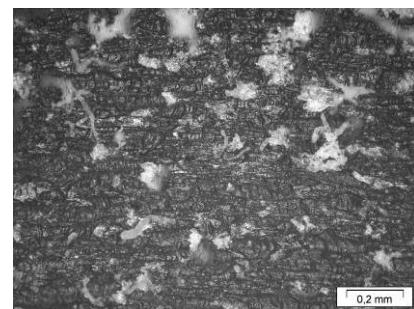
Speed step test, TPU unfilled						
0,5 MPa			100 rpm	150 rpm	200 rpm	250 rpm
COF	[-]	avg	1,24	1,11	0,95	0,85
		dev	0,14	0,03	0,05	0,02
near surface temperature	[$^\circ\text{C}$]	avg	73,66	92,64	103,22	110,63
		dev	4,03	10,61	10,77	13,09
counterpart temperature	[$^\circ\text{C}$]	avg	53,71	67,14	73,72	78,57
		dev	6,88	9,13	10,98	10,51
linear wear rate	[$\mu\text{m}/\text{m}$]	avg	0,02	0,42	0,78	0,87
		dev	0,03	0,09	0,22	0,10
1,0 MPa			100 rpm	150 rpm	200 rpm	250 rpm
COF	[-]	avg	1,09	0,93	0,81	0,71
		dev	0,35	0,28	0,25	0,22
near surface temperature	[$^\circ\text{C}$]	avg	87,77	106,61	115,85	120,73
		dev	11,99	15,36	13,33	13,04
counterpart temperature	[$^\circ\text{C}$]	avg	70,94	79,73	85,76	90,15
		dev	8,74	7,35	5,15	6,26
linear wear rate	[$\mu\text{m}/\text{m}$]	avg	0,26	0,83	1,31	1,64
		dev	0,21	0,14	0,01	0,40
1,5 MPa			100 rpm	150 rpm	200 rpm	250 rpm
COF	[-]	avg	x	0,61	0,50	0,42
		dev	0,00	0,00	0,02	0,02
near surface temperature	[$^\circ\text{C}$]	avg	x	111,36	117,70	118,36
		dev	0,00	10,12	1,66	0,89
counterpart temperature	[$^\circ\text{C}$]	avg	x	79,26	84,10	85,33
		dev	0,00	10,26	12,07	11,53
linear wear rate	[$\mu\text{m}/\text{m}$]	avg	1,21	1,57	2,05	1,59
		dev	0,09	0,91	0,78	0,24



TPU unfilled, Test No. 1, 100x1

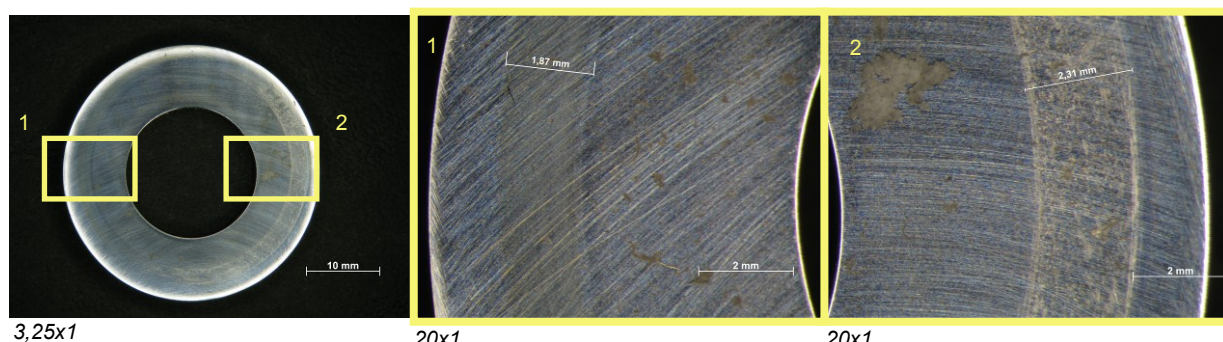


TPU unfilled, Test No. 1, 100x1



TPU unfilled, Test No. 1, 100x1

The micrographs shown in Table 4.4-3 depict a rather smooth textured surface and the formation of small wear pits in accordance with a rather low penetration of the roughness tops of the hard counterpart due to bulk stiffening. With augmenting contact pressure the pits are becoming more profound. The counterpart's penetration into the temperature related softened matrix enlarges. Increasing the testing speed does not influence the formation of the typical lubrication film on the counterpart, which is demonstrated in Figure 4.4-8. The micrographs even represent marginal deposits at the low pressure speed step test.



3,25x1
20x1
20x1
Figure 4.4-8: Wear traces on counterpart of speed step test at 0,5 MPa of TPU unfilled (Test No. 2)

The impact of the sliding velocity is further analysed by gradually performed speed step tests at a contact pressure of 1 MPa. The mutations of the surface during the speed steps are shown in Figure 4.4-9. At relatively low sliding velocities (during Step 1), the wear rate is tolerable and the frictional force is first rather high due to run-in and surface formation processes. The adhesion forces are at high levels at this testing stage. The TPU softens with increasing temperature and is deformed by the roughness peaks of the counterpart in rubbing contact. The contact spots are deformed/stretched by the sliding process, those membrane-like areas are outlined in the micrograph of the first step (Figure 4.4-9). With increasing speed those “adhering membranes” are stripped from the surface. The frictional force thus decreases and the wear rises. The stripped membranes form wear particles. The areas where those “membranes” are stripped, then show a wavy texture in the wear pit (see micrographs of step 2 to 4). The structure of the wear pits attains a finer structure with advanced speed steps, which results in a less coarse surface. This effect is related to bulk stiffening and the formation of smaller wear particles.

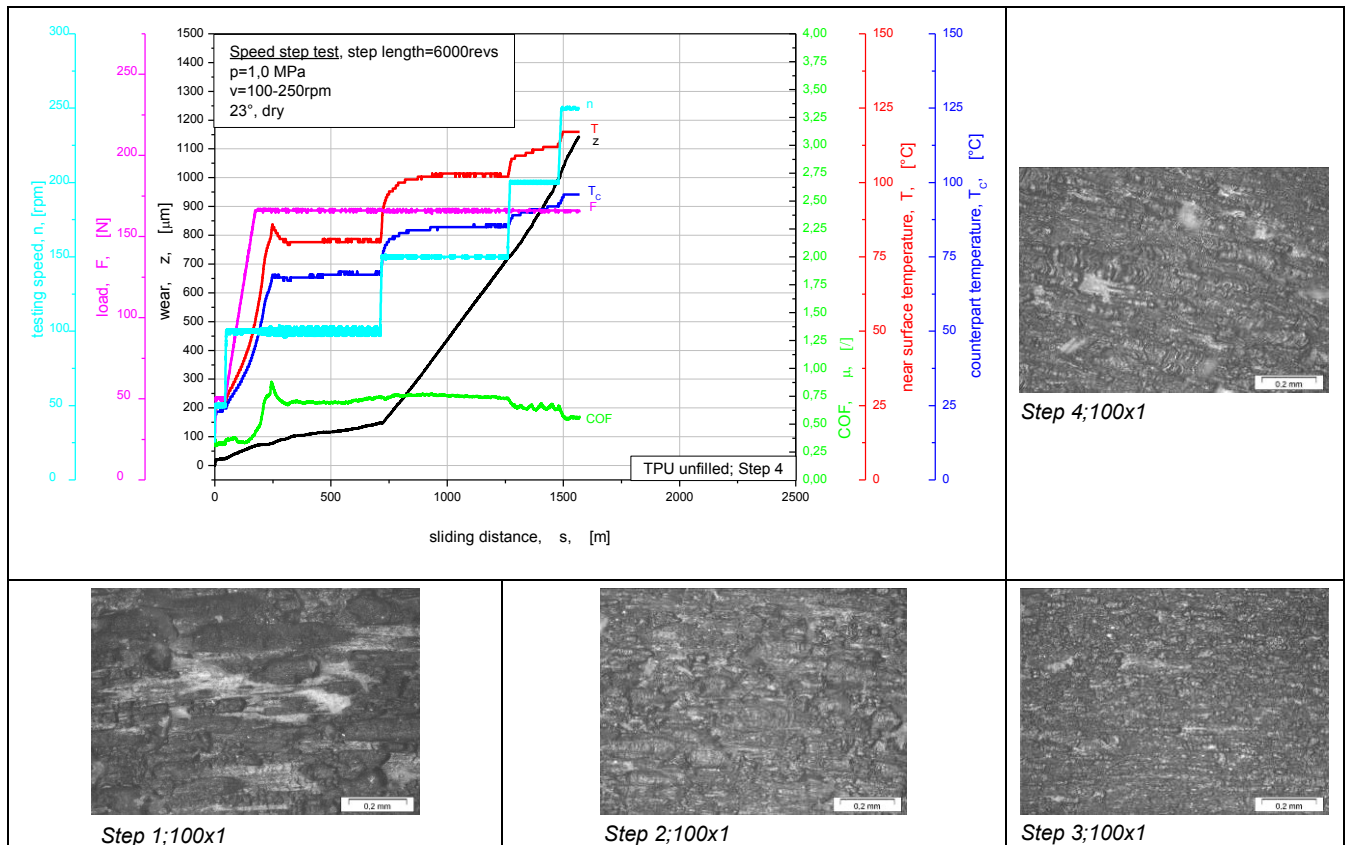


Figure 4.4-9: Gradually performed speed step test of TPU unfilled at a testing load of 1,0 MPa

Sliding velocity dependency of filled material

The filled material shows an attenuated reaction to the speed tests opposed to the unfilled TPU (Figure 4.4-10, Table 4.4-4).

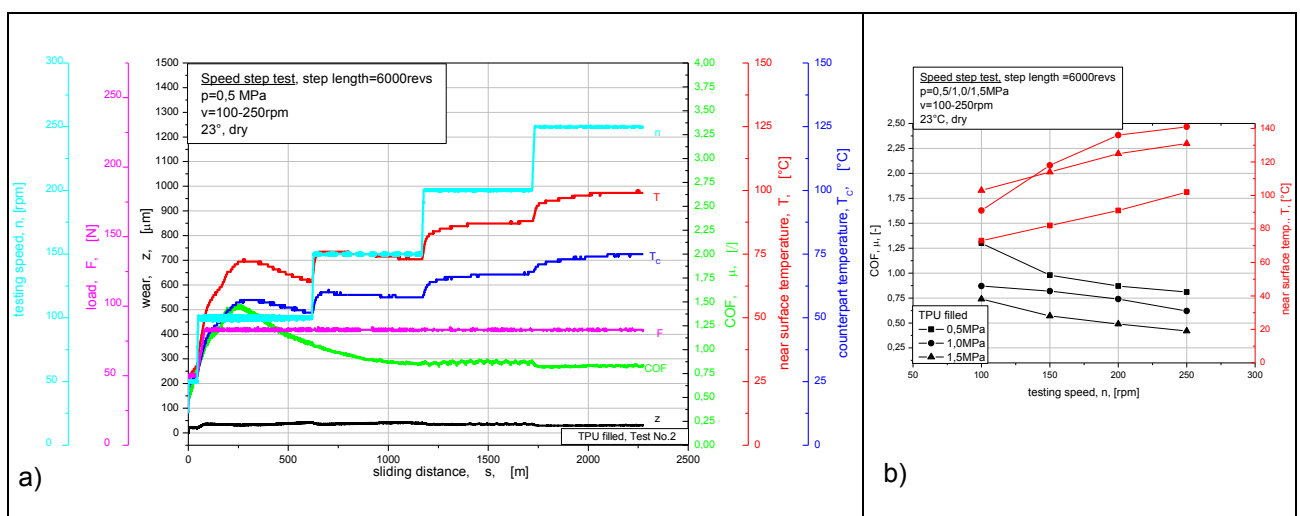
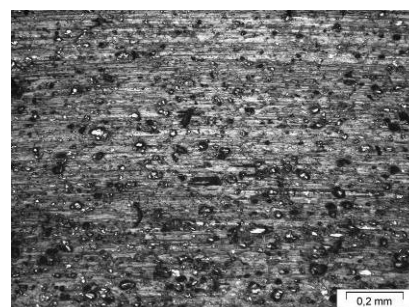


Figure 4.4-10: a) exemplary speed step test; b) assessment of testing speed dependency for the filled TPU

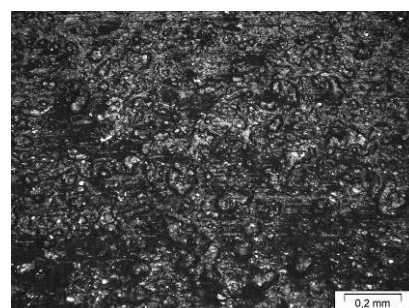
This behaviour is also described in literature for certain TPU systems (Elleuch et al, 2007). In certain cases (appendix, chapter 8.4.6) the material shows a distinctive run in behaviour resulting in higher COF values. Furthermore, the material shows no significant wear over the tested range. With increasing load the friction force drops rapidly and the heat accumulation rises to a high degree.

Table 4.4-4: Evaluation and exemplary contact surface micrographs of speed step tests of TPU filled

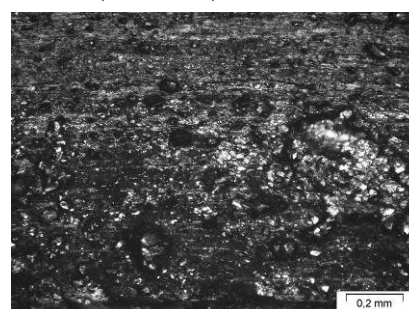
Speed step test, TPU filled						
0,5 MPa			100 rpm	150 rpm	200 rpm	250 rpm
COF	[-]	avg	1,30	0,98	0,87	0,81
		dev	0,00	0,09	0,01	0,02
a) near surface temperature	[°C]	avg	72,86	81,74	91,41	101,95
		dev	4,72	9,62	6,40	4,84
counterpart temperature	[°C]	avg	59,71	66,26	73,44	81,01
		dev	6,32	10,48	9,56	9,68
linear wear rate	[μm/m]	avg	0,00	0,00	0,00	0,00
		dev	0,00	0,00	0,00	0,00
1,0 MPa			100 rpm	150 rpm	200 rpm	250 rpm
COF	[-]	avg	1,09	0,87	0,78	0,70
		dev	0,30	0,08	0,13	0,18
near surface temperature	[°C]	avg	90,76	117,94	135,61	141,42
		dev	17,27	31,69	32,42	27,12
counterpart temperature	[°C]	avg	69,36	88,47	101,53	105,10
		dev	12,65	23,50	25,31	21,69
linear wear rate	[μm/m]	avg	0,00	0,00	0,00	0,00
		dev	0,00	0,00	0,00	0,00
1,5 MPa			100 rpm	150 rpm	200 rpm	250 rpm
COF	[-]	avg	0,74	0,57	0,49	0,42
		dev	0,00	0,03	0,00	0,01
near surface temperature	[°C]	avg	102,83	114,21	125,23	130,86
		dev	0,00	0,52	2,03	2,01
counterpart temperature	[°C]	avg	82,97	92,74	101,34	104,70
		dev	0,00	3,67	2,05	1,88
linear wear rate	[μm/m]	avg	0,02	0,02	0,01	0,01
		dev	0,02	0,01	0,00	0,00



TPU filled, Test No. 2, 100x1



TPU filled, Test No. 2, 100x1



TPU filled, Test No. 2, 100x1

Additionally, a higher contact pressure compels a more distinctive formation of a filler network as it can be seen in Table 4.4-4. The wear track on the counterpart shows approximately the same characteristics as the track formed at the load step tests. On account of that, it is assumed that the formation of the transfer film is rather independent from the PV-conditions. Moreover, it is considered to result from adhesion forces between the tribological faces (Figure 4.4-11).

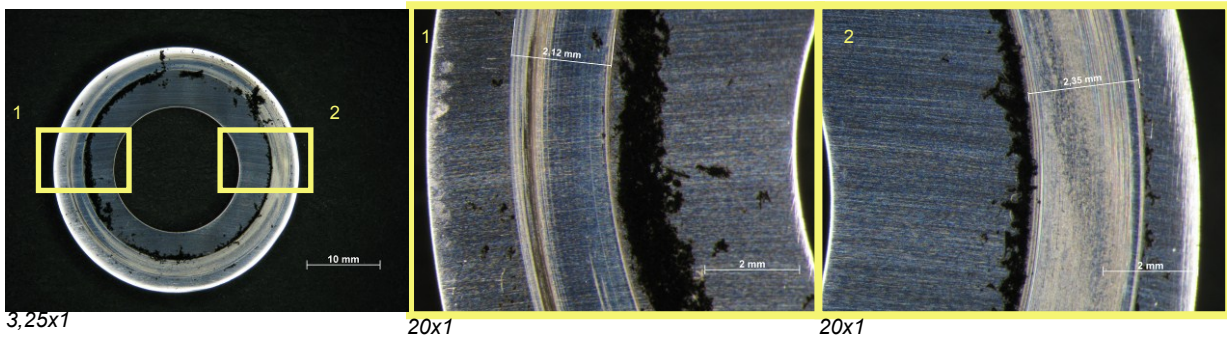


Figure 4.4-11: Wear traces on counterpart of speed step test at 0,5 MPa of TPU filled (Test No.2)

To approve the above described coherences a speed step test at 1,0 MPa is carried out gradually (Figure 4.4-12). With advanced speed steps the heat accumulation escalates. The bulk thus softens and a filler network is dissected. The same procedure is stated for the surface formation at increasing contact pressures (see 0). Hence, the dissection of the bearing or lubricating filler network is indicative for the filled materials tribological operation and cannot be exemplified as a direct result of PV-variations.

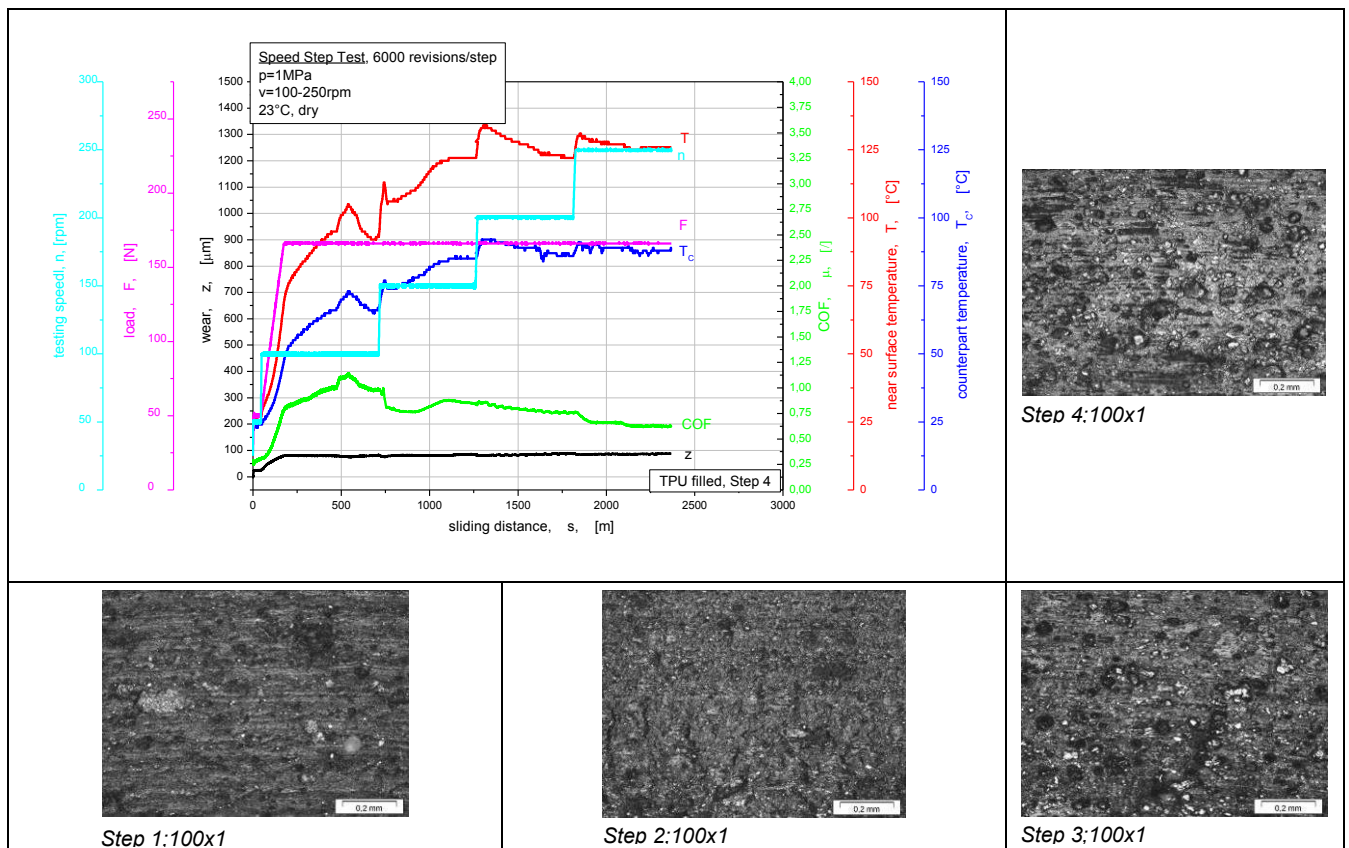


Figure 4.4-12: Gradually performed speed step test of TPU filled at a testing load of 1,0 MPa

4.4.3 Summary and Comparison of PV-Step Tests

The PV-step tests are approved as an accurate testing methodology to assess the influence of contact pressure and sliding velocity on the tribological operational behaviour of TPU materials. Stable frictional conditions, by means of a thermo-mechanical equilibrium, can be achieved for each individual load/speed step during the step tests, allowing a neat and precise evaluation of the PV-dependency of the materials. Additionally, load and speed step tests are slightly comparable to each other at similar PV-settings, notwithstanding different testing procedures and deviations. The frictional response thus is mainly dependent on the PV-settings and does not contribute to the tribological history to a significant degree. Table 4.4-5 statistically summarizes the results for selected PV-settings.

Table 4.4-5: Evaluation of COF, T and linear wear rate for selected PV-levels for TPU filled and unfilled

		TPU unfilled				TPU filled			
p	v		COF	T	wear rate		COF	T	wear rate
[MPa]	[rpm]		[-]	[°C]	[μm/m]		[-]	[°C]	[μm/m]
0,5	100	avg	1,28	74,38	0,07	avg	1,28	78,5	0,00
		dev	0,1	6,09	0,07	dev	0,05	5,32	0,00
0,5	150	avg	1,18	69	0,28	avg	0,97	81,25	0,00
		dev	0,09	38,8	0,17	dev	0,06	5,85	0,00
0,5	200	avg	1	99	0,7	avg	0,93	91,5	0,00
		dev	0,06	8,02	0,17	dev	0,09	6,36	0,00
1	100	avg	0,87	91	0,62	avg	0,86	91,18	0,00
		dev	0,06	7,83	0,46	dev	0,1	4,81	0,01
1	150	avg	0,77	107,43	1,03	avg	0,81	117,57	0,00
		dev	0,03	3,31	0,35	dev	0,03	5,35	0,01
1	200	avg	0,69	114,83	1,24	avg	0,7	126,5	0,01
		dev	0,06	3,19	0,19	dev	0,06	8,31	0,01
1,5	100	avg	0,68	91	1,04	avg	0,72	109,5	0,02
		dev	0,04	1,41	0,24	dev	0,09	8,02	0,01
1,5	150	avg	0,65	112,25	1,32	avg	0,56	117,25	0,02
		dev	0,04	5,85	0,64	dev	0,03	6,55	0,01
1,5	200	avg	0,5	118	2,05	avg	0,49	127	0,01
		dev	0,01	1,41	0,78	dev	0,02	4,97	0,00

The COF and the near surface temperatures show insignificant deviations and jointly good repeatability. The worse reproducibility of the wear rate results can be traced back to the defective measurement and superposition of several impact parameters (section 3.3.2). Conclusively, the PV-step tests can replace laborious tribological testing and therefore can be regarded as highly vital method to characterize sealing materials' PV-dependency.

To summarize, in Figure 4.4-13 the PV-dependency of contact pressure and sliding velocity is outlined based on the data presented in Table 4.4-5.

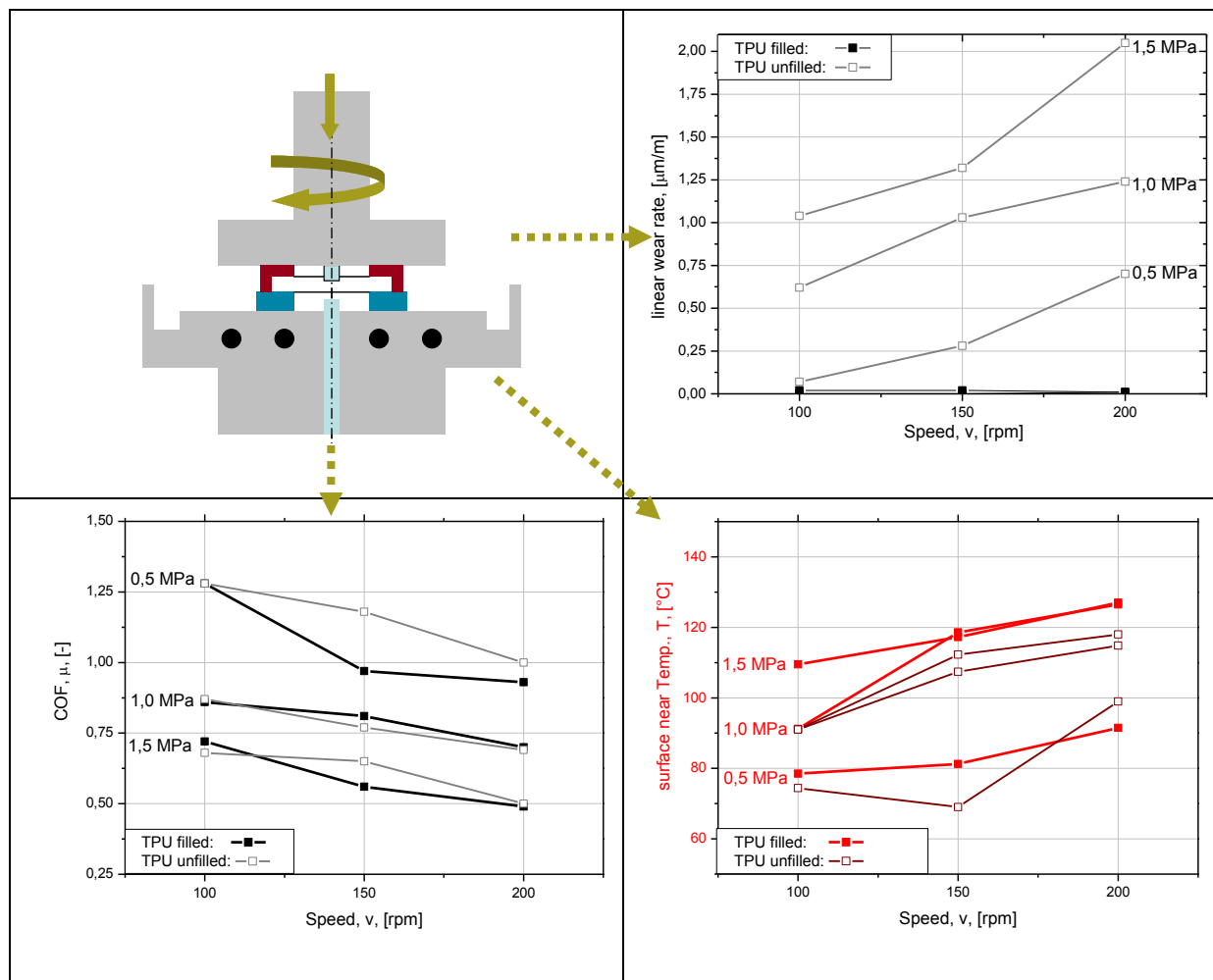


Figure 4.4-13: Overall review on PV-dependency based on step tests

Significantly, the frictional force and the resulting COF decrease with increasing PV-conditions, mainly due to changes in the contact geometry of the tribological pairing (Uetz and Wiedmeyer, 1985). The temperature at the rubbing contact rises with higher loadings in accordance with hysteretic heat-up of elastomeric materials and energy dissipation (Müller et al, 2002). The filled material shows few lower COF values. The lower frictional forces result from the dissected filler network, which particularly carries load and has a lubricating function. Considering the wear aspects, the filled material shows scarce wear, whereas the unfilled material is characterized by an increasing wear rate with increasing PV-settings. Failure cannot be deflected for the filled material over the tested range, whereas the applied PV-settings generally compel instabilities and failure for the unfilled TPU.

The frictional heat-build up, characterized by the temperatures measured in the counterpart, increases with the PV-setting. Contrasting both materials by heat-up, is not accurate, due to stable operational conditions with the filled material compared with instabilities/high wear and failure with the unfilled one. Furthermore, the temperature measurements at the testing device at hand are rather defective, in accordance with imprecise positioning of the thermo-couples and differences in counterpart heights due to polishing.

The effect of the testing speed on the tribological performance is typically less pronounced than the impact of contact pressure variations, since the contact surface is highly affected by variation of the contact pressure. This effect is already described for rubbing TPU-metal contacts (Elleuch et al, 2007). As a result the assessment of speed step tests can be reduced to the PV-settings, and the effect of altering contact geometry can be neglected.

Conclusively, both testing methodologies generate data appropriate for benchmarking, on account of the significant and reproducible conditions at the particular steps nearly independent from the pre-running and the testing procedure (varying p or v). Which methodology at which testing range has to be used, depends on the application.

4.4.4 Impact of varying contact pressure or sliding speed on the Surface Formation-Approach to define a phenomenological wear model

In the following section the influence of PV-parameters on the surface mutations of the rubbing TPU surface are assessed. Therefore, initially the surface in its manufacturing condition is investigated via light microscopy and SEM. Afterwards, the surface mutations after a tribological operation at moderate PV-settings (gradually performed speed step test at 1MPa, 1st step at 100rpm) is examined. Furthermore, the impact of increasing the contact pressure and accordingly sliding velocity is separately analysed. Consequently, the rubbing surfaces after a test with advanced contact pressure at moderate sliding velocity and reversed are configured.

Friction and wear phenomena of the unfilled material

In Figure 4.4-14 the manufacturing condition of the surface is depicted. It is dominated by processing traces of the fine turning process. The surface asperities are at their initial stage.

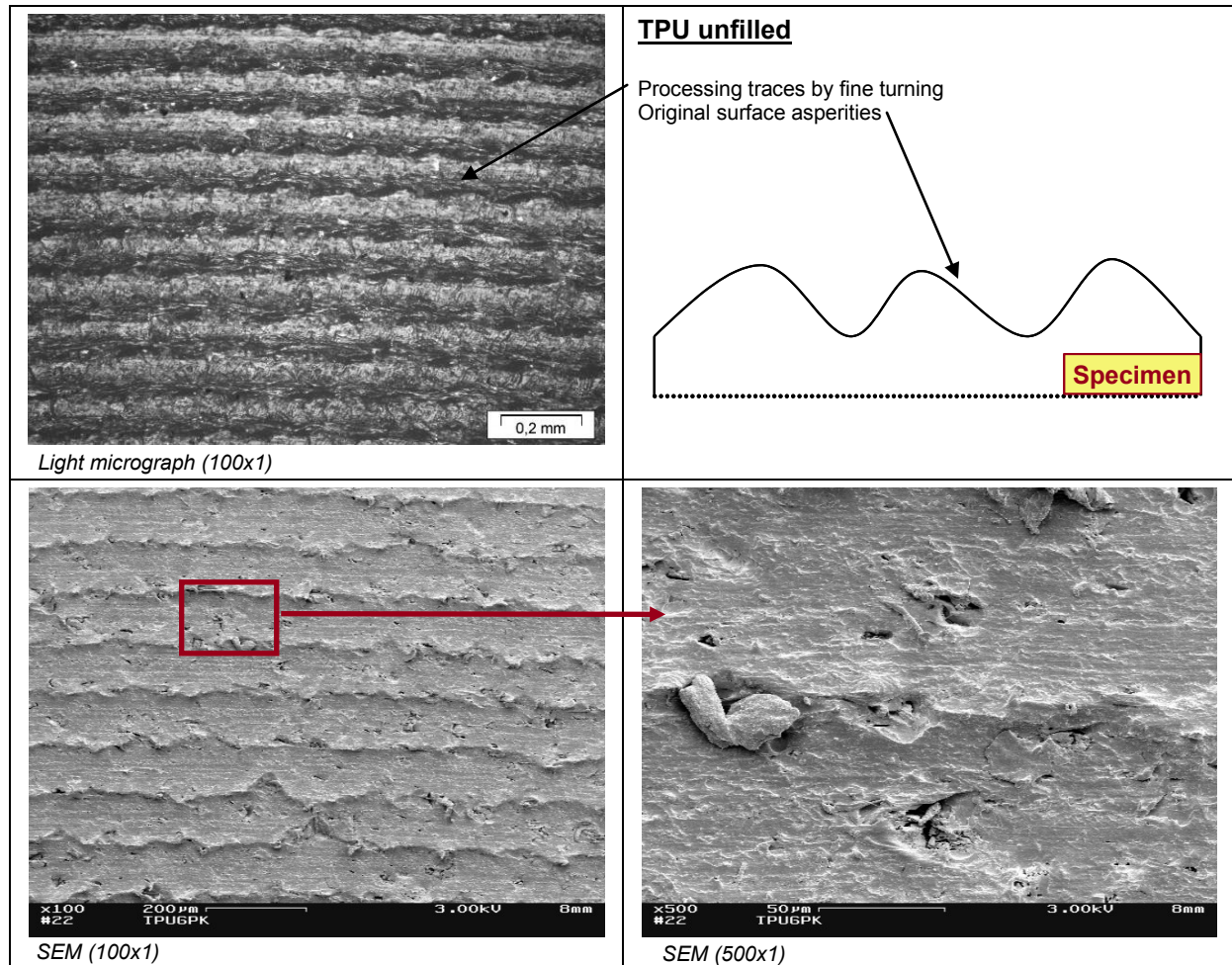


Figure 4.4-14: Surface in manufacturing conditions (turning grooves); TPU unfilled

Figure 4.4-15 depicts the surface mutations of a tribological operation at moderate PV-settings. The soft matrix asperities adhere to the roughness peaks of the counterpart and are deformed. They are stretched due to sliding processes and shear forces. Frictional heat accumulation enforces this effect. The highly oriented matrix sections are described as “stretched membranes”.

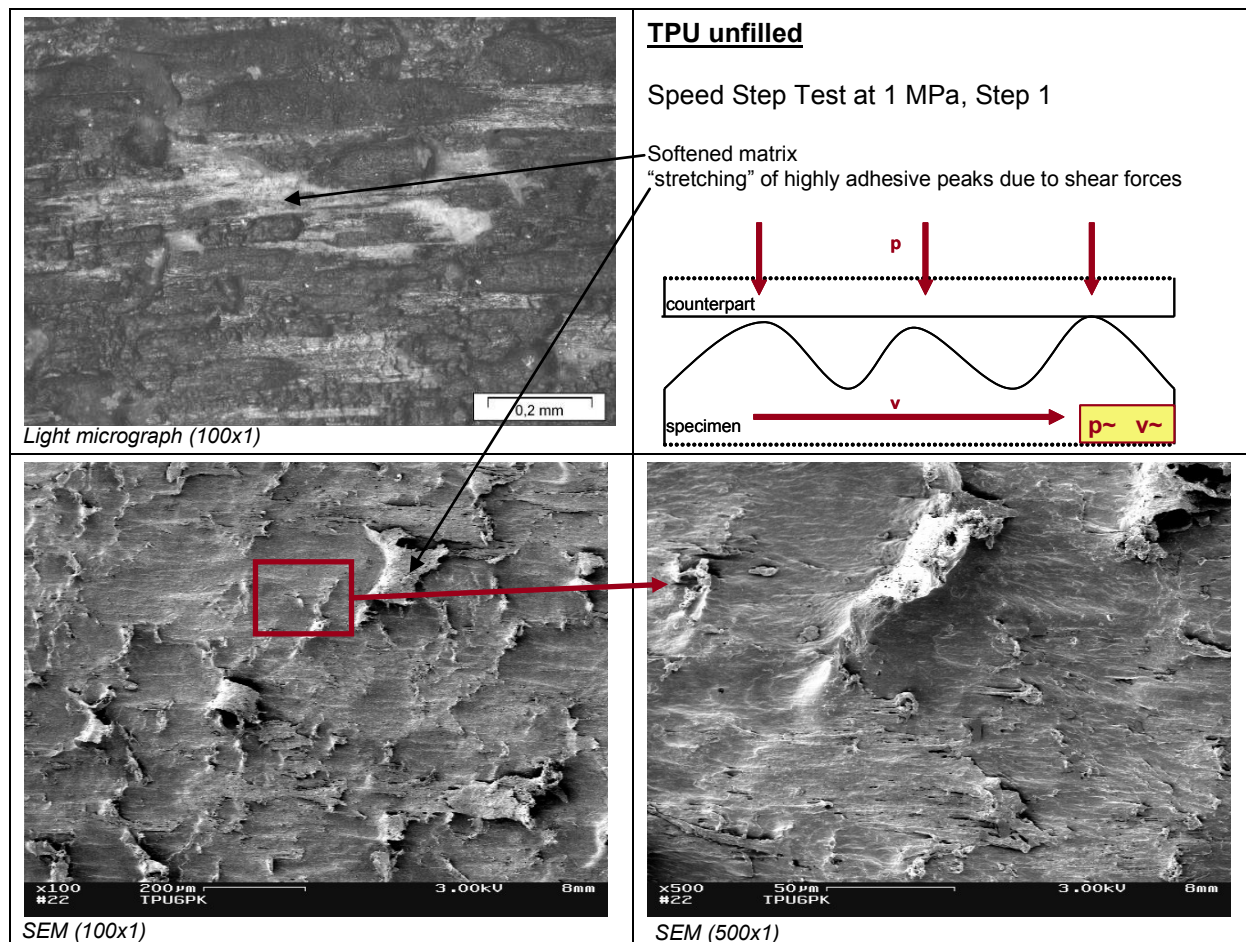


Figure 4.4-15: Mutations of surface layers at moderate PV-conditions; TPU unfilled

The effect of enlarging the contact pressure at moderate speed levels is investigated by the micrographs of the standard load step test at 100 rpm with five load steps up to 1,5 MPa. Wear and failure already occurs at these PV-settings (evaluation of results can be seen in the appendix, section 8.4.5.1). Higher contact pressures result in a more severe structured surface. The rubbing contact area enlarges and a lubricating film is formed on the counterpart (see section 0). The oriented membranes are ruptured and accordingly parts of the softened matrix strongly adhere to the counterpart (formation of severe wear pits). Wear particles are scraped off. The wear particles possibly consist of the ruptured foils and respectively the lubricating material scaling on the counterpart. Regarding the evaluation of wear rate and frictional heat accumulation these phenomena indicate failure and damage mechanisms (section 0). The light micrographs in Figure 4.4-16 depict a coarse surface formation. The SEM graphs represent the formation of a wear pit on account of the rupture of a stretched membrane.

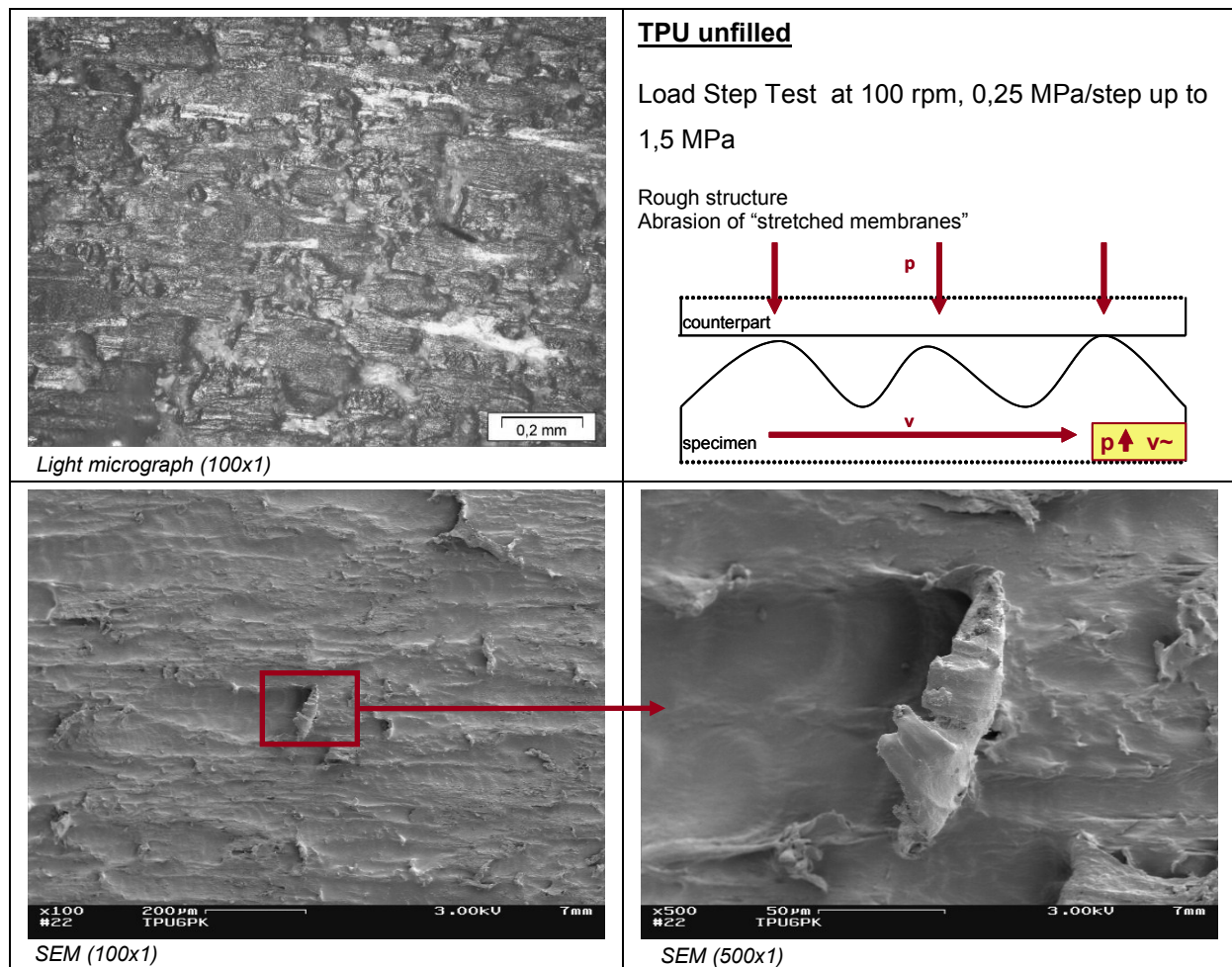


Figure 4.4-16: Mutations of surface layers at increased contact pressure conditions; TPU unfilled

A standard speed step test at a contact pressure of 1 MPa with four speed steps up to 250 rpm is also exemplarily outlined to analyze the impact of advanced sliding speeds in contrast with contact pressure variations. A detailed evaluation of the results can be seen in the appendix (chapter 8.4.6.1 & 2). Higher testing rates generally result in bulk stiffening (Birley, 1992) due to the viscoelastic character of TPU. The rubbing surface stiffens at higher sliding velocities (Uetz and Wiedmeyer, 1985).

Significantly, the tribological operation is dominated by instabilities and failure mechanisms over the tested range for the unfilled material. The failure mechanism, depicted in Figure 4.4-17, is similar to the failure mechanisms occurring at higher loading conditions. The stretched foils rupture and form wear particles. The wear pits are structured wavy. A wavy textured rubbing surface is typically for rubber friction sliding in contact with hard counterparts and are commonly denoted "Schallamach waves" (Schallamach, 1971). The waves originate from deformation processes (shelving of the soft elastomeric surface layers) (Schallamach, 1971). The presence of small

waves at higher velocities in tribological testing of elastomer-steel-pairings has also been described by Fukahori (Fukahori et al, 2010). Due to the more rigid surface layer of the TPU in the rubbing contact, the wear pits are less profound, and the surface is textured finer as the one depicted at high contact pressure conditions. In Figure 4.4-17 the process of the foil detachment and the resulting wear pits are presented in greater detail.

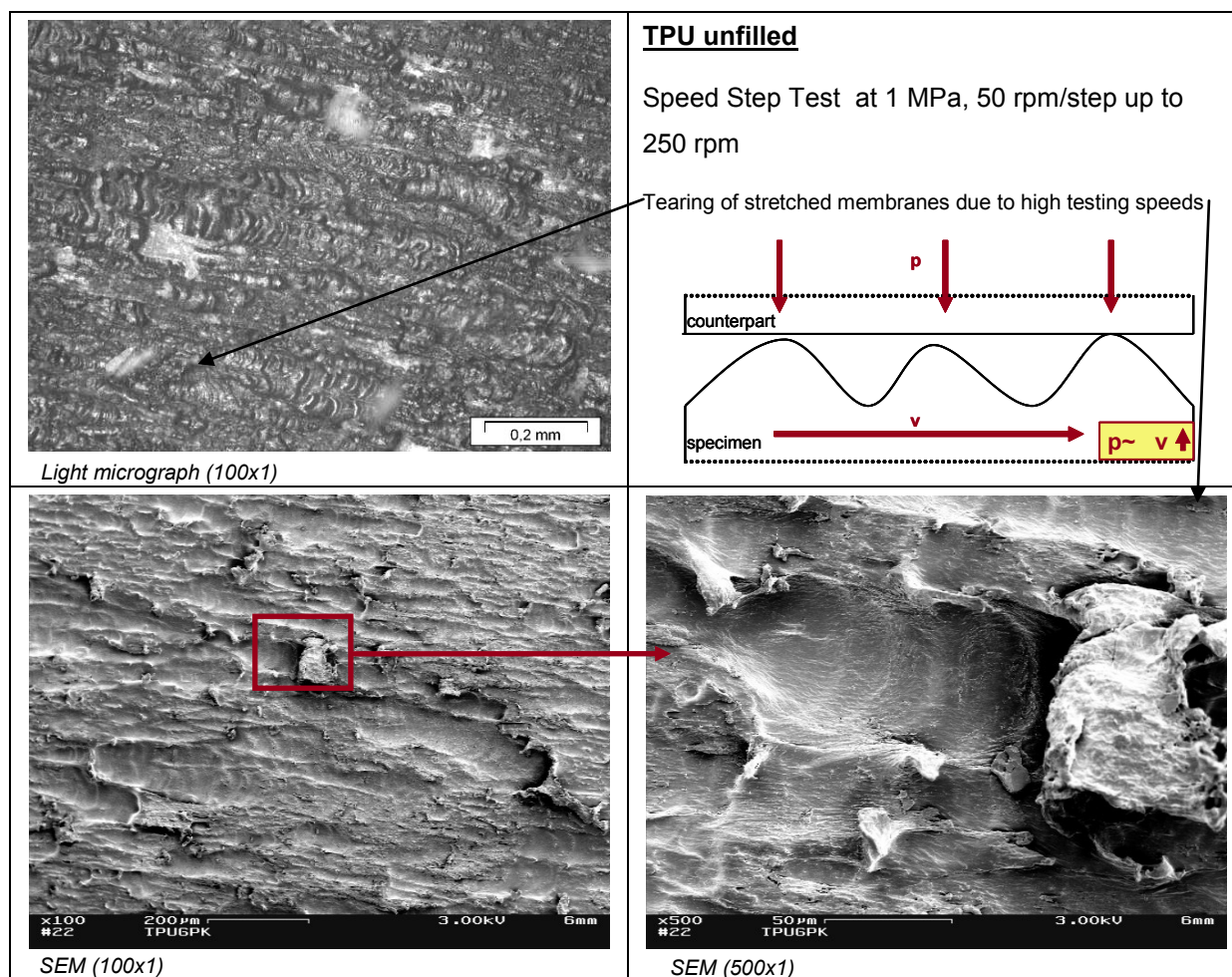


Figure 4.4-17: Mutations of surface layers at increased sliding velocity conditions; TPU unfilled

Conclusively, the wear phenomena are similar to wear mechanisms described for adhesion of rubbers (Zhang, 2004), by means of stretching strongly adhering regions and thus roll-like wear particle formation, and the fatigue processes can possibly be regarded as delamination processes, as described by Suh (Suh, 1973).

A phenomenological description and exposition of the wear model of the unfilled TPU system is illustrated in Figure 4.4-18.

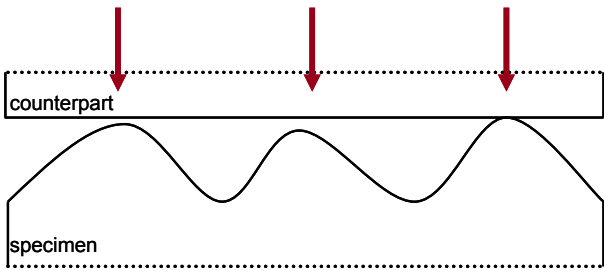
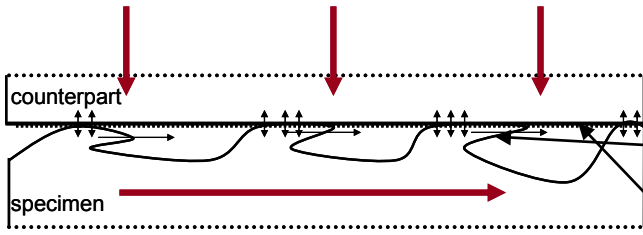
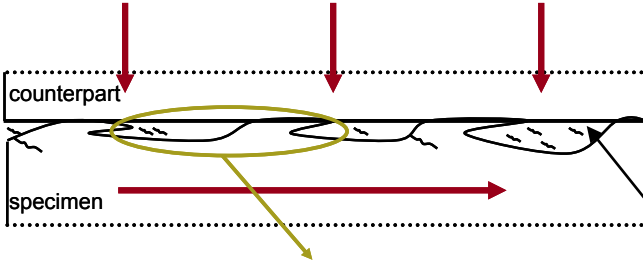
Initial stage	
	<p>Processing traces depicted on surface</p> <p>Surface asperities in their original state</p>
Surface mutation	
	<p>Adhesion between counterfaces</p> <p>Deformation of the TPU</p> <p>Softening due to frictional heat accumulation</p> <p>Stretching of highly adhesive sections, formation of highly oriented membranes</p> <p>Formation of a lubricating film on the counterpart</p>
Stable operation	
	Cannot be detected over the tested range
Wear/Failure mechanisms	
	<p>Severe heat accumulation</p> <p>Detachment of highly oriented foils out of the bulk, "racking of membranes"</p> <p>Formation of wear particles (stretched foils) and wear pits</p> <p>Failure due to thermal and mechanical overloads</p>

Figure 4.4-18: Schematical demonstration of wear mechanisms investigated at tribological operation of TPU unfilled

Friction and wear phenomena of the filled material

Similar to the unfilled TPU, processing traces from the fine turning process are pictured at the surface of the filled material (see Figure 4.4-14).

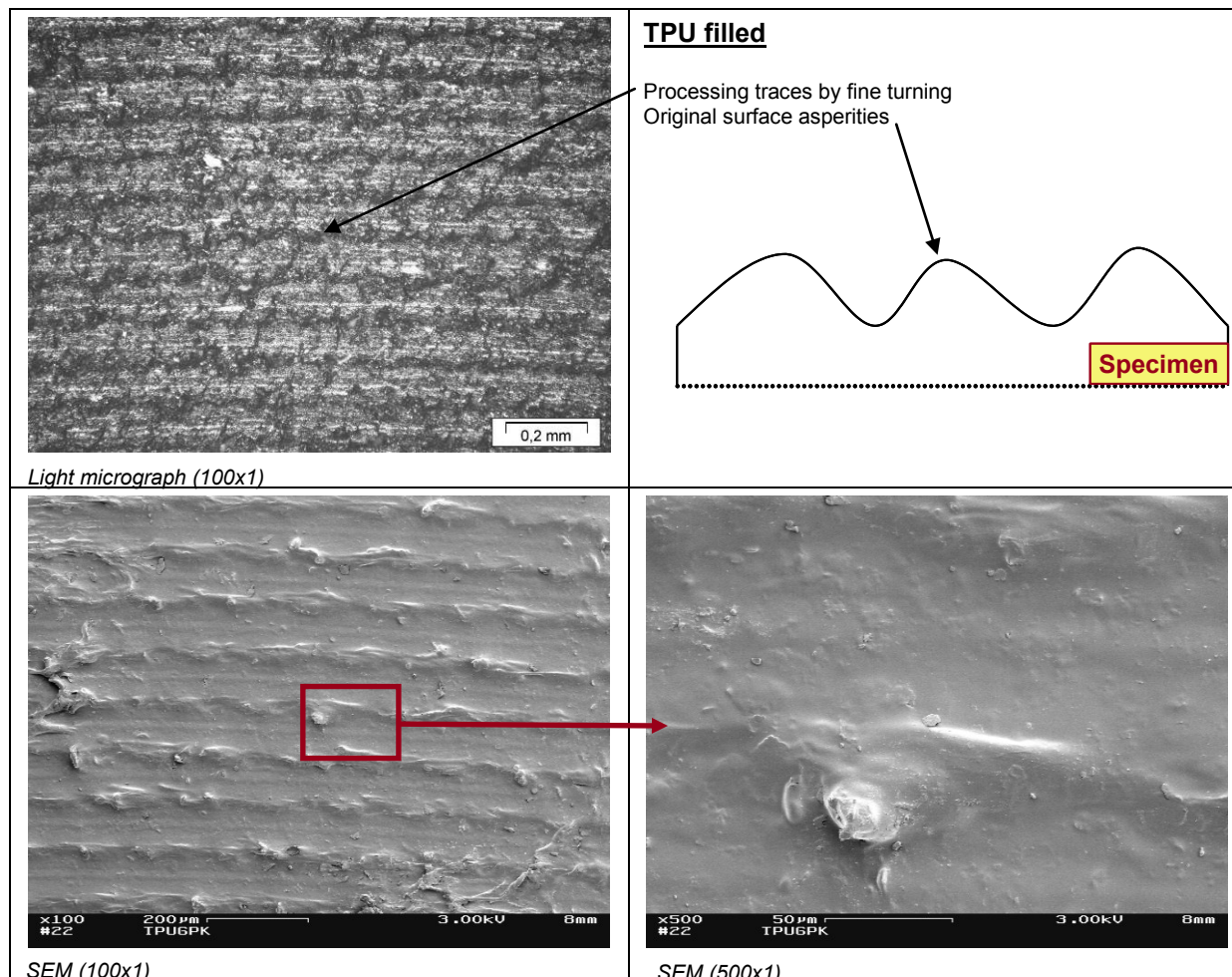


Figure 4.4-19: Surface in manufacturing condition (turning grooves); TPU filled

The filled system is characterized by marginal surface mutations and reactions to the tribological loading at moderate PV-settings. The processing traces are slightly deformed and ablated, but are still present on the surface (Figure 4.4-20). The asperities of specimen and counterpart get into contact and form adhesive bondings. As a result, a transfer layer is formed on the counterpart (see section 0). High frictional forces can be detected at this stage (further results are demonstrated in the appendix, chapter 8.4.6), which is related to the unfinished surface formation, denoted as “run-in stage “.

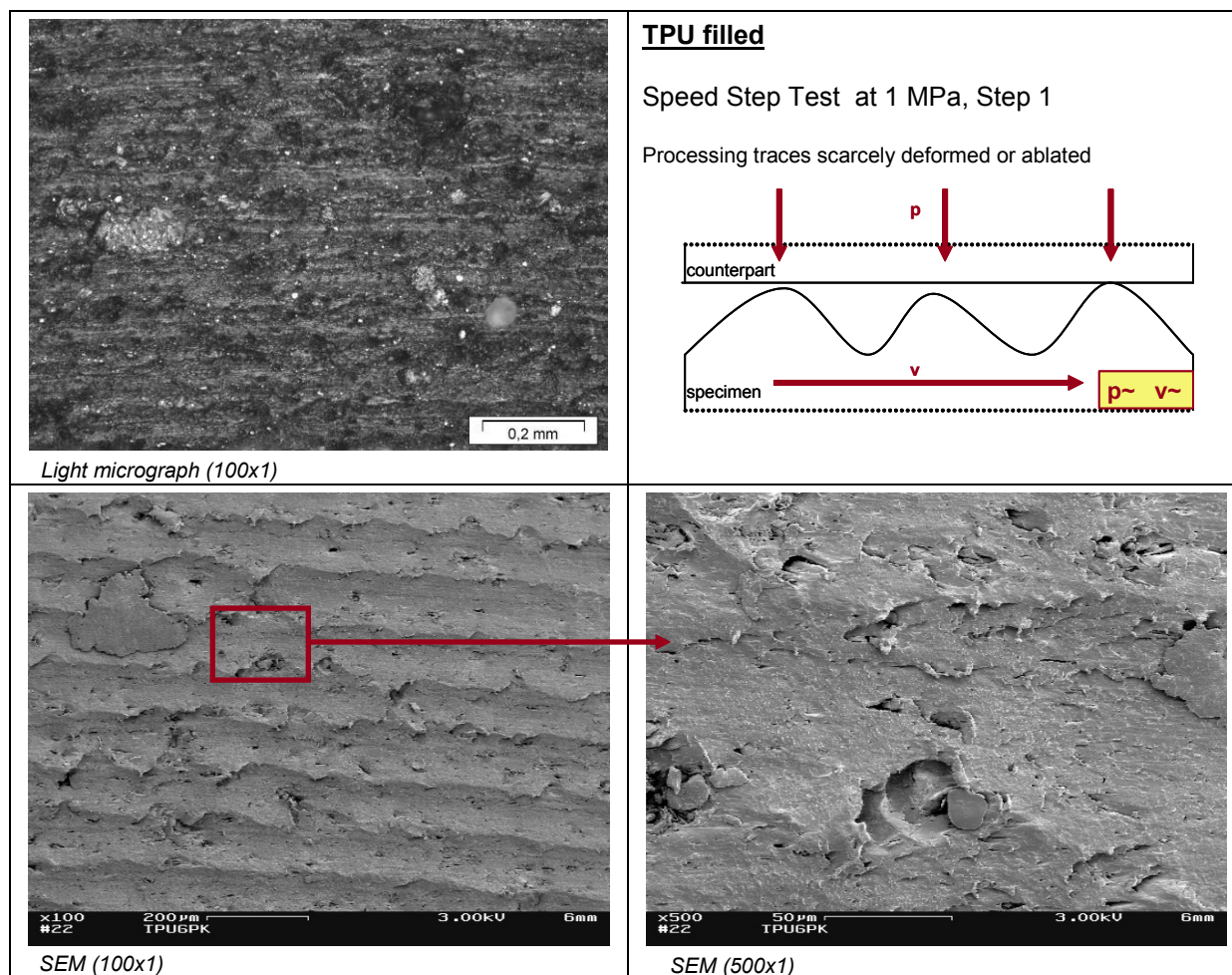


Figure 4.4-20: Mutations of surface layers at moderate PV-conditions; TPU filled

The filled material typically shows scarce reactions to the tribological PV-loadings over the tested range of the PV-step tests in terms of wear and failure mechanisms. Stable conditions are achieved at all tested PV-steps. The surface formation is conventionally dominated by the formation of a dissected filler network with a particularly bearing or lubricating function. The step tests are hence performed at higher loading conditions (“advanced PV-step tests”, results demonstrated in the appendix, section 8.4.7) to highlight the surface mutations due to higher testing PV-settings.

Figure 4.4-21 depicts the surface mutations of the filled TPU system after an advanced load step test at a testing speed of 100 rpm and up to a load step of 2,75 MPa. The performance is again characterized by stable operation during the particular steps. Wear and failure mechanisms cannot be deflected. On the rubbing surface, a more distinctive filler network is developed. Furthermore, ruptures in the matrix are demonstrated in the SEM micrographs.

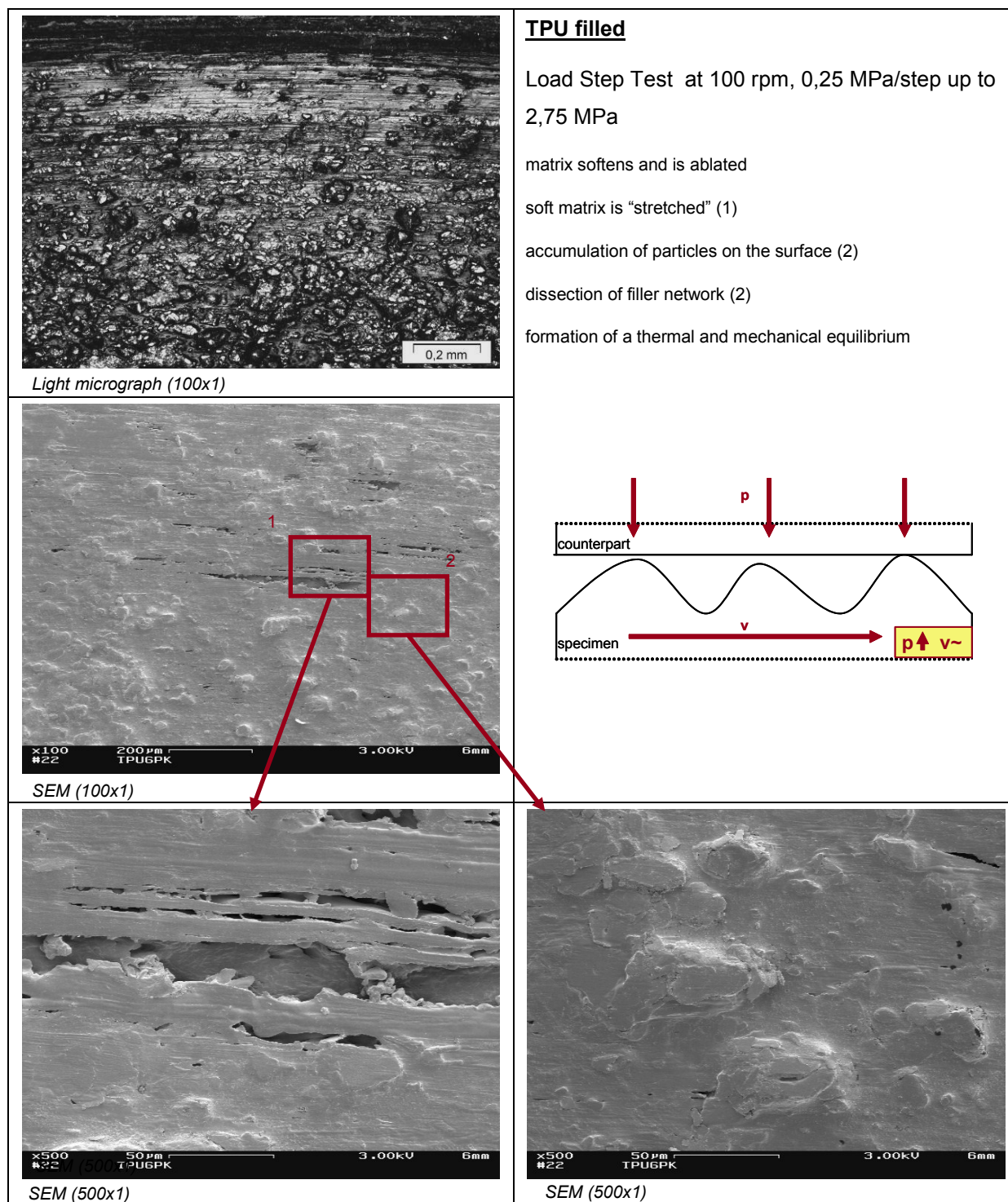


Figure 4.4-21: Mutations of surface layers at increased contact pressure conditions; TPU filled

A speed step test at a contact pressure of 1 MPa at sliding velocities up to 400 rpm is performed to investigate the surface formations due to higher rates. Similar to other performed tests for the filled material, stable conditions are achieved over the tested range and wear and failure mechanisms do not occur (appendix, section 8.4.7). During operation, a filler network is developed (Figure 4.4-22) as already described in

previous declarations of the tribological phenomena of the filled material. Furthermore, brittle ruptures of the matrix can be depicted on the SEM micrographs on account of stiffening mechanisms at higher testing rates.

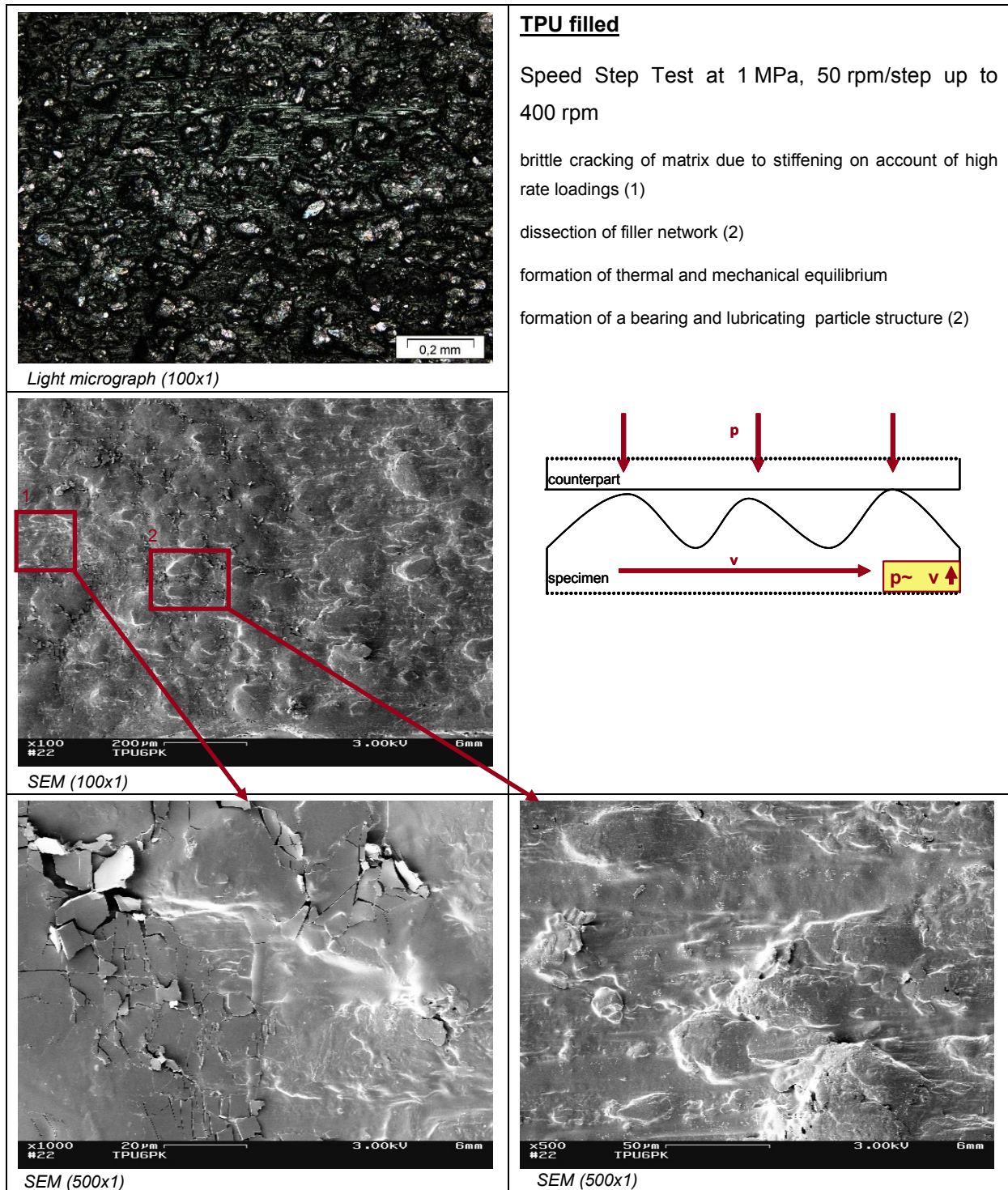


Figure 4.4-22: Mutations of surface layers at increased contact pressure conditions; TPU filled

Figure 4.4-23 summarizes the frictional phenomenons depicted from the PV-step tests of the filled TPU system.

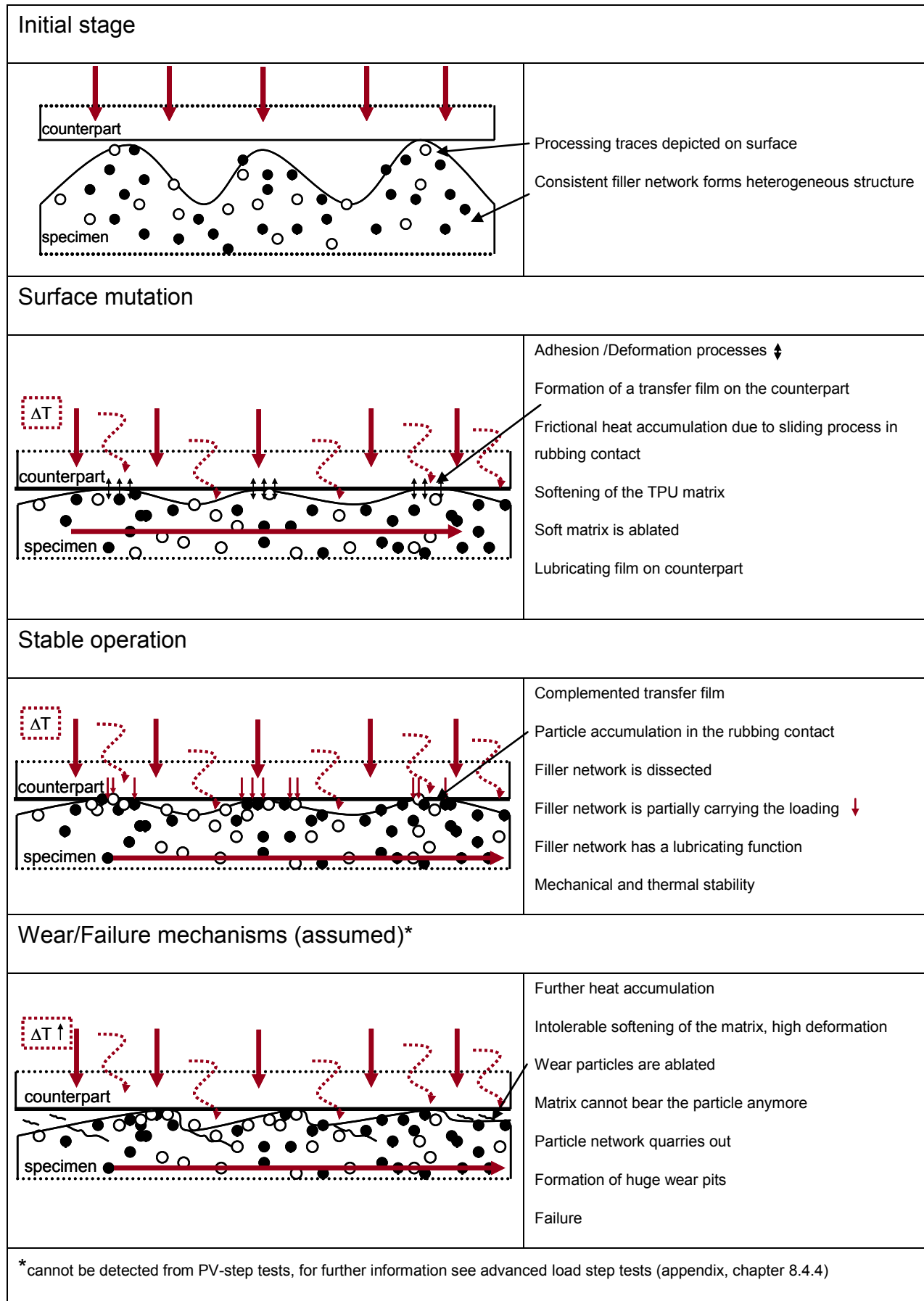


Figure 4.4-23: Schematical demonstration of wear mechanisms investigated at tribological operation of TPU filled

4.5 PV-Rating and Definition of a PV-limiting value

4.5.1 PV-Rating based on Results from PV-Step tests

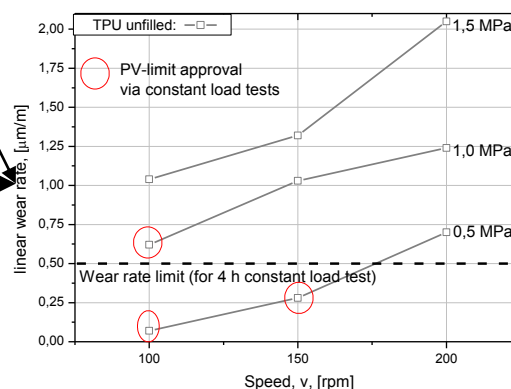
Assessment of Tolerable Wear for the unfilled TPU system

Table 4.5-1 demonstrates the average wear rates for certain PV-settings (evaluated from the PV-step tests). At contact pressures of 0,5 MPa, they are rather moderate. Additionally, the wear rate of the standard settings (1 MPa, 100 rpm) are close to the critical value of 0,5 $\mu\text{m}/\text{m}$. At those PV-settings, the unfilled material operates efficient and nearly stable. The wear course depicts moderate slopes regarding the plots of the PV-step tests (appendix, chapter 8.4.5 and 8.4.6).

Within the scope of the above described PV-impact on the tribological performance, a PV application limit is assumed to be at levels of 0,5 to 1,0 MPa contact pressure and about 100 to 150 rpm sliding speed.

Table 4.5-1: Averaged results of PV-step tests of TPU unfilled

		TPU unfilled			
p	v		COF	T	wear rate
[MPa]	[rpm]		[-]	[°C]	[$\mu\text{m}/\text{m}$]
0,5	100	avg	1,28	74,38	0,07
		dev	0,1	6,09	0,07
0,5	150	avg	1,18	69	0,28
		dev	0,09	38,8	0,17
0,5	200	avg	1	99	0,7
		dev	0,06	8,02	0,17
1	100	avg	0,87	91	0,62
		dev	0,06	7,83	0,46
1	150	avg	0,77	107,43	1,03
		dev	0,03	3,31	0,35
1	200	avg	0,69	114,83	1,24
		dev	0,06	3,19	0,19
1,5	100	avg	0,68	91	1,04
		dev	0,04	1,41	0,24
1,5	150	avg	0,65	112,25	1,32
		dev	0,04	5,85	0,64
1,5	200	avg	0,5	118	2,05
		dev	0,01	1,41	0,78



Constant load tests at the selected PV-limit-settings (0,5 MPa at 100 rpm, 0,5 MPa at 150 rpm, 1,0 MPa at 100 rpm) are further carried out (at least two reproducible re-

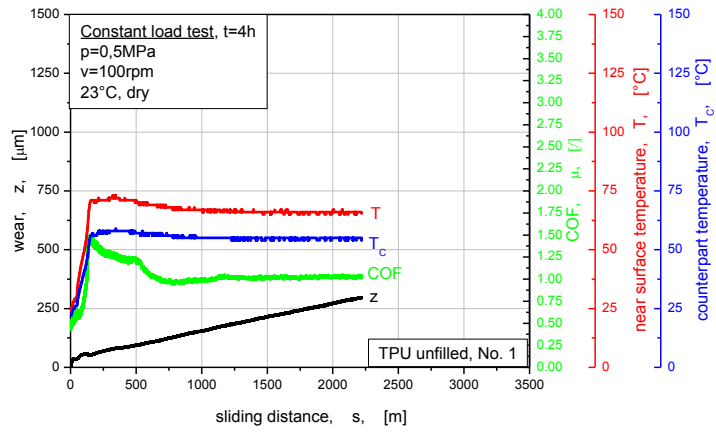
sults to approve the repeatability of the PV-step tests). A detailed evaluation of the results is shown in the appendix (chapter 8.4.4). Figure 4.5-1 exemplarily depicts some results and highlights the arising wear rates. Additionally, the wear rates are compared in Table 4.5-2. Significantly, the linear wear rate is higher for the constant load tests than for the step tests. This occurs, since at the PV-step tests the specimen at every step performs a maximum of 6000 revisions, whereas the constant load tests stresses the sample for four hours. The test at 0,5 MPa and 100 rpm depicts a moderate wear, the near surface temperature is approximately 70 °C and the COF levels out at values of approximately 1. Relatively stable operational conditions can be achieved for those settings, and the PV-application limit is not overrun for those settings. In comparison, both other tests conventionally are aborted due to excess of the testing machine's tolerable wear. The near surface temperatures flatten out at about 100 °C. The wear rate is above the previously denoted critical value. Regarding the wear plots, instable conditions are demonstrated, which can be described as failure. Albeit, the test at 0,5 MPa and 150 rpm just slightly exceeds the tolerable wear rate limit and can therefore be regarded as less critical.

Table 4.5-2: Comparison of wear rate of TPU unfilled at critical PV-settings evaluated from different testing procedures

p	v	linear wear rate			
		overall	speed step test	load step test	4 h constant load test
[MPa]	[rpm]	[$\mu\text{m}/\text{m}$]	[$\mu\text{m}/\text{m}$]	[$\mu\text{m}/\text{m}$]	[$\mu\text{m}/\text{m}$]
0,50	100,00	0,07	0,02	0,04	0,17
0,50	150,00	0,28	0,04	0,14	0,65
1,00	100,00	0,62	0,26	0,84	1,18

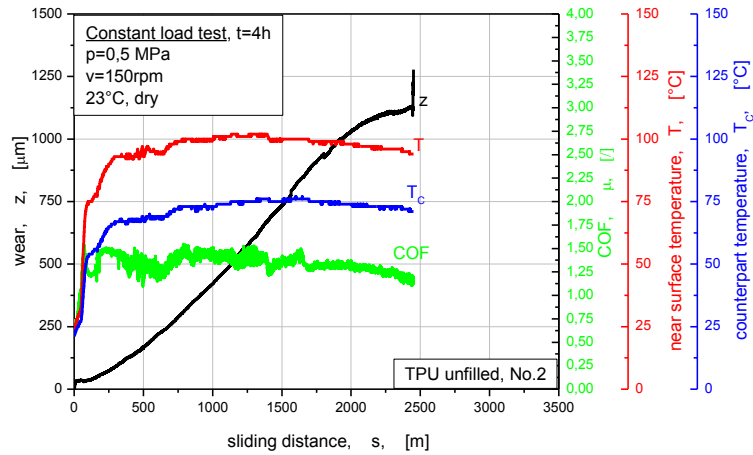
Conclusively, the wear rate values of the PV-step tests are exceeded at the constant load tests. As a result, the critical values have to be adapted to a lower value of 0,25 $\mu\text{m}/\text{m}$ to assure the assignability from the step tests to the constant load tests and ultimately the final seal application. A PV-setting of $p=0,5$ MPa and $v=100$ rpm is overall identified as PV-application limit over the tested range for the unfilled material.

Constant load test (4 h, 0,5 MPa, 100 rpm)



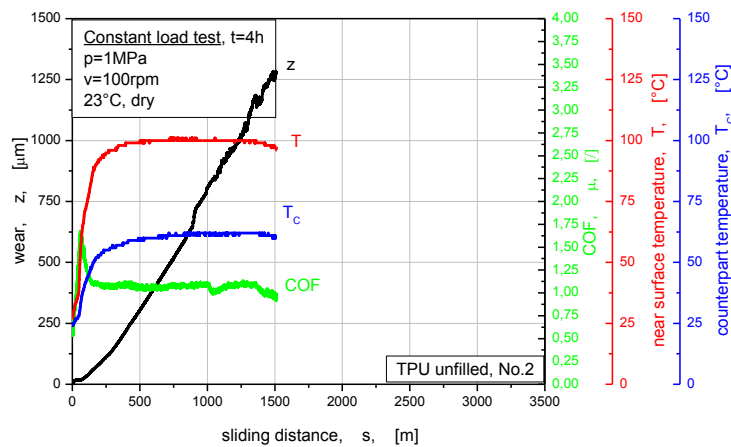
wear rate=0,17 $\mu\text{m}/\text{m}$

Constant load test (4 h, 0,5 MPa, 150 rpm)



wear rate=0,65 $\mu\text{m}/\text{m}$

Constant load test (4 h, 1,0 MPa, 100 rpm)



wear rate=1,18 $\mu\text{m}/\text{m}$

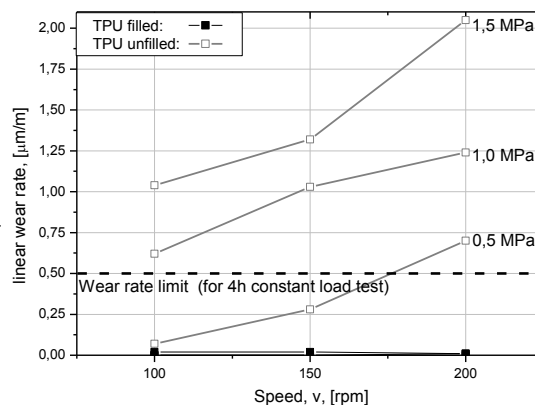
Figure 4.5-1: Comparison of constant load tests at critical PV-settings

Assessment of Tolerable Wear for the filled TPU system

A similar procedure as is performed to rate the unfilled systems PV-dependency, is adopted to assess the filled TPU. The averaged results of the PV-step tests at certain settings are presented in Table 4.5-3.

Table 4.5-3: Averaged results of PV-step tests of TPU filled

		TPU filled			
p	v		COF	T	wear rate
[MPa]	[rpm]		[-]	[°C]	[$\mu\text{m}/\text{m}$]
0,5	100	avg	1,28	78,5	0,00
		dev	0,05	5,32	0,00
0,5	150	avg	0,97	81,25	0,00
		dev	0,06	5,85	0,00
0,5	200	avg	0,93	91,5	0,00
		dev	0,09	6,36	0,00
1	100	avg	0,86	91,18	0,00
		dev	0,1	4,81	0,01
1	150	avg	0,81	117,57	0,00
		dev	0,03	5,35	0,01
1	200	avg	0,7	126,5	0,01
		dev	0,06	8,31	0,01
1,5	100	avg	0,72	109,5	0,02
		dev	0,09	8,02	0,01
1,5	150	avg	0,56	117,25	0,02
		dev	0,03	6,55	0,01
1,5	200	avg	0,49	127	0,01
		dev	0,02	4,97	0,00



The filled material is characterized by low wear (the wear rate barely reaches values greater than $0,01 \mu\text{m}/\text{m}$). Failure and critical operational stages can not be achieved over the tested range

Step tests at advanced PV-settings are performed in this manner to rate the PV-dependency. Consequently a speed step tests at $1,0 \text{ MPa}$ is carried out up to sliding speeds of 400 rpm in addition to a load step test at 100 rpm up to contact pressures of $2,75 \text{ MPa}$. Table 4.5-4 and Table 4.5-5 present the averaged results. Figure 4.5-2 and Figure 4.5-3 exemplarily depict the testing procedure. A more detailed evaluation of the results can be found in the appendix (section 8.4.7).

Table 4.5-4: Averaged results of advanced load step tests of TPU filled

Advanced load step test, TPU filled												
100 rpm			0,5 MPa	0,75 MPa	1,00 MPa	1,25 MPa	1,50 MPa	1,75 MPa	2,00 MPa	2,25 MPa	2,50 MPa	2,75 MPa
COF	[-]	avg	1,15	0,74	0,60	0,69	0,68	0,65	0,59	0,55	0,51	0,47
		dev	0,01	0,03	0,01	0,01	0,04	0,01	0,00	0,02	0,03	0,00
near surface temperature	[°C]	avg	72,00	66,00	69,50	94,50	104,50	108,50	110,50	112,50	114,00	116,00
		dev	0,00	0,00	0,71	0,71	3,54	0,71	2,12	0,71	1,41	0,00
counterpart temperature	[°C]	avg	53,50	50,50	57,00	68,50	75,00	78,50	80,00	82,50	83,50	83,50
		dev	4,95	4,95	11,31	9,19	5,66	9,19	7,07	7,78	7,78	9,19
linear wear rate	[μm/m]	avg	0,01	0,03	0,01	0,02	0,02	0,03	0,02	0,02	0,03	0,03
		dev	0,01	0,01	0,02	0,01	0,00	0,00	0,00	0,01	0,01	0,00

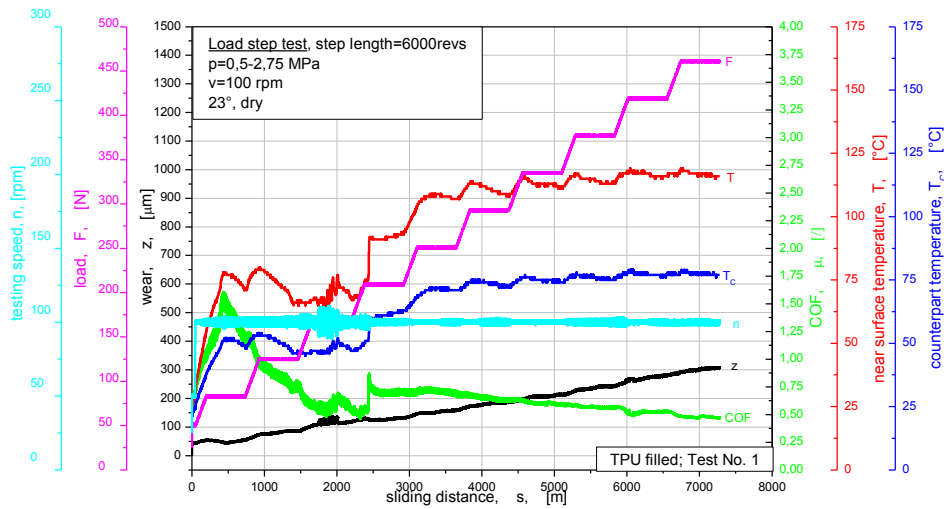


Figure 4.5-2: Advanced load step test of TPU filled, Test No. 1

Table 4.5-5: Averaged results of advanced speed step tests of TPU filled

Advanced speed step test, TPU unfilled									
1,0 MPa			100 rpm	150 rpm	200 rpm	250 rpm	300 rpm	350 rpm	400 rpm
COF	[-]	avg	0,80	0,80	0,66	0,56	0,56	0,51	0,47
		dev	0,00	0,05	0,01	0,01	0,02	0,01	0,01
near surface temperature	[°C]	avg	84,50	112,00	121,00	124,50	135,00	143,50	155,50
		dev	4,95	8,49	2,83	2,12	1,41	2,12	2,12
counterpart temperature	[°C]	avg	60,50	78,00	83,00	87,00	91,50	96,00	100,50
		dev	10,61	15,56	12,73	11,31	12,02	12,73	16,26
linear wear rate	[μm/m]	avg	0,04	0,01	0,02	0,00	0,01	0,01	0,02
		dev	0,02	0,01	0,00	0,01	0,00	0,00	0,00

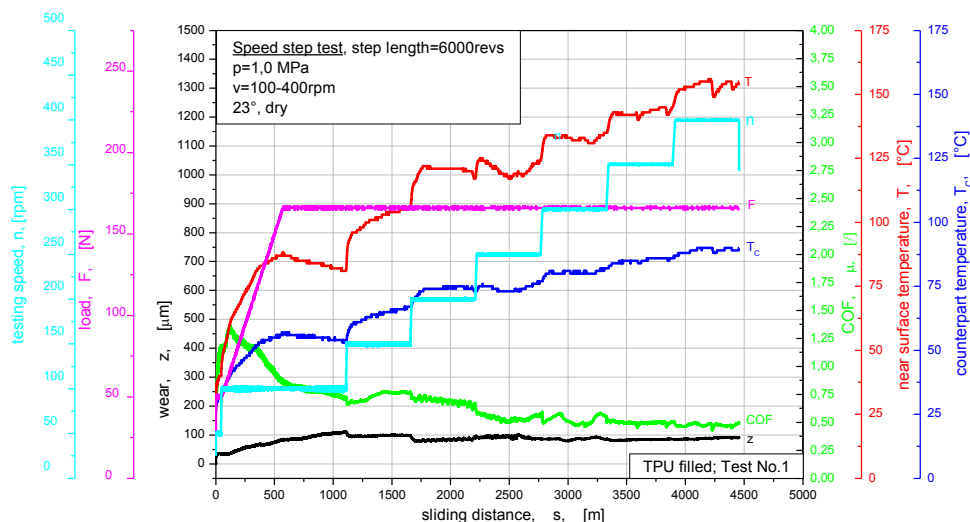


Figure 4.5-3: Advanced speed step test of TPU filled, Test No. 1

The filled material generally shows the same phenomena at the advanced PV-settings than at the standard ones. In passing, the abrupt reaction to an increase of either p or v is relieved, since the contact conditions of the tribological pairing are more favourably developed. All in all, the filled material delivers a stable performance and shows high resistance to the higher loadings. No critical PV-stage could thus be identified regarding the results, following no PV-application limit. For verification, a constant load test at the maximum PV-levels ($p=2,75$ MPa, $v=400$ rpm) is implemented (detailed evaluation demonstrated in appendix, section 8.4.4). An exemplarily plot of the test results is shown in Figure 4.5-4.

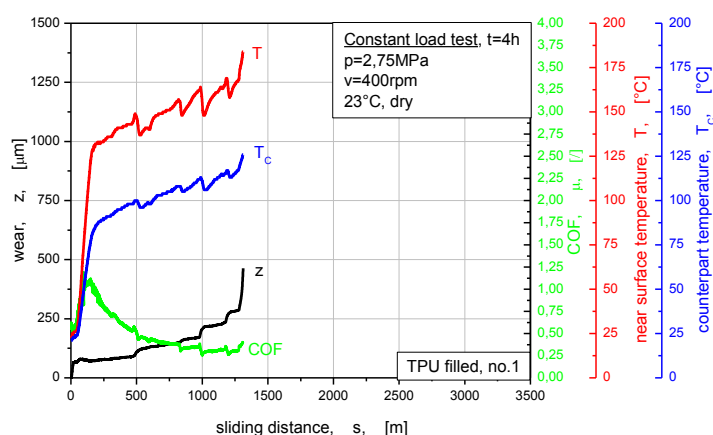


Figure 4.5-4: Constant load test at extreme PV-settings, Test No. 1

Unexpectedly, the test is aborted in accordance with an intolerable high wear rates. The frictional force, represented by the COF, rapidly drops down after a severe run-in

peak. During the first 500 m sliding distance instabilities already occur (COF and temperature oscillate to a high degree). Furthermore, temperatures rise quickly. The sample suffers from a severe softening due to the rapid and extreme heat accumulation. The wear escalates as the specimen is too pliant to sustain the compressive loading and the test is aborted. At first, it is assumed that the PV-loadings exceed the bearing capacity of the material, which is contrary to the performance depicted from the step tests. Precisely, the main difference between those tests is, that at the step test the extreme loading are applied unless the material has performed a kind of “run-in” at the previous milder PV-settings and the bearing surface mutations are fully developed. At the constant load test the high stresses are indeed applied ramp-wise at the beginning of the test, but the scarcely developed surface is not able to bear and stabilize them. The typical bearing filler structure is not yet dissected, but the high loadings already enforce heat accumulation. Conjointly, the bulk softens and fails. A longer run-in phase has to be set to accurately perform a constant load test at elevated PV-settings. Compellingly, no PV-application limit can be derived for the filled material by focussing on the wear rates.

4.5.2 PV-limit based on Investigations of worn Surfaces

Assessment of the unfilled TPUs PV-application limit

The unfilled TPU's tribological performance is mainly operated by wear mechanisms. Wear particles are steadily accumulated and form a lubricating debris on the counterpart, which is permanently building up and breaking down. Conventionally, highly adhering regions are developed, which are deformed. At more crucial PV-settings the so-called “membranes” are overstretched and detached from the surface. The more severe the loadings, the more profound the wear pits originated from the membrane tearing. A more detailed demonstration of the above described wear mechanism is shown in chapter 4.4.4.1. In Figure 4.5-5 the main wear mechanism based on the rupture of highly stretched adhering membranes and the formation of wavy textured wear pits is shown.

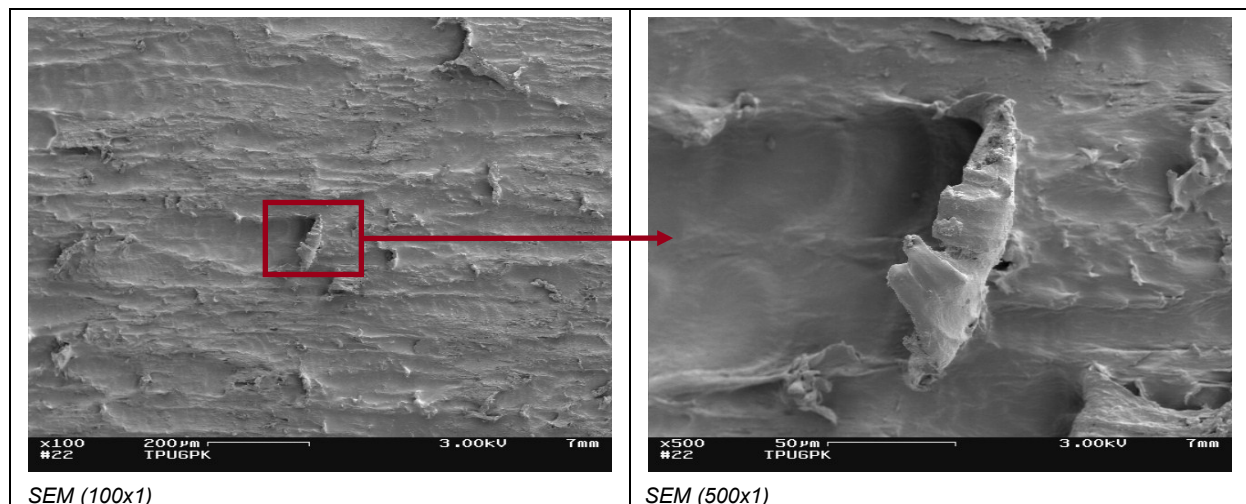
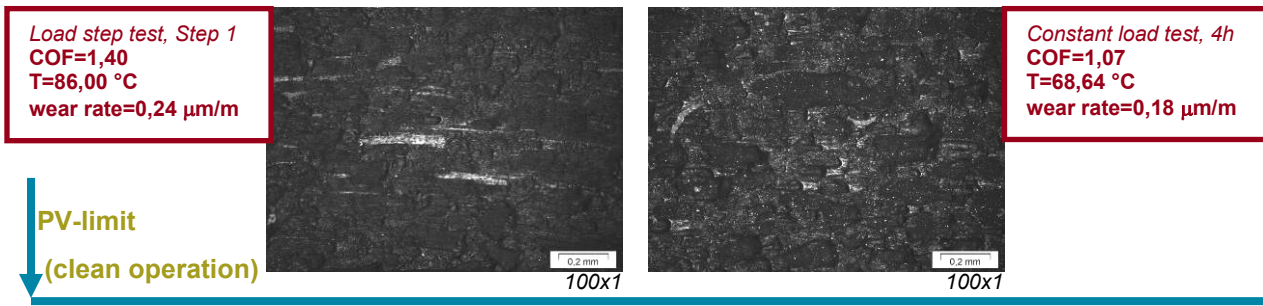


Figure 4.5-5: „Membrane tearing“ as typical wear mechanism of TPU unfilled

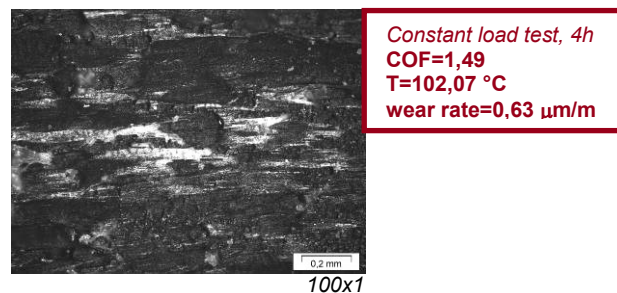
The following scheme presents surface formations of the unfilled TPUs specimen in dependency of the critical PV-settings (determined in accordance with an evaluation of the linear wear rates in section 4.5.2). A representative micrograph from an exemplary constant load test and one from either a gradually performed load or speed step test, at which the critical PV-settings are run through, and the corresponding parameters like COF, near surface temperature and linear wear rate, are demonstrated. The assignability between step tests and constant load tests, which is generally approved for the performed tests in section 4.4.3. Deviations of parameter values result from the different testing procedures and the different testing durations, but do not influence the main conclusions.

At the lowest PV-settings ($p=0,5$ MPa, $v=100$ rpm) the surface mutations are moderate. A typical wavy surface with shelved peaks is formed on account of deformation processes (also described at Schallamach, 1971). The lighter regions on the micrographs indicate adhesion processes. The less rigid TPU asperities adhere to the steel roughness peaks and are thus deformed by them due to the sliding process. At PV-settings of $p=0,5$ MPa with $v=150$ rpm and respectively at $p=1,0$ MPa with $v=100$ rpm more severe adhesion regions are deformed and stretched. In section 4.4.4.1 they are denoted “stretched membranes”. These phenomena indicate failure mechanisms, since those membranes are torn as a result of increasing the PV-settings or simply due to further operation. Their rupture forms wear pits on the surface. The detached foils itself are ablated on the counterpart as a lubricating film or removed from the rubbing contact as wear particles.

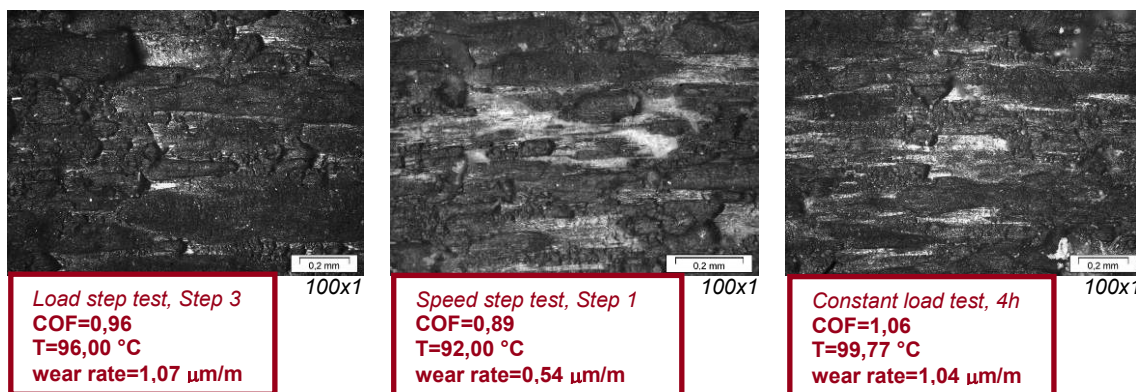
$p=0,5$ MPa; $v=100$ rpm



$p=0,5$ MPa; $v=150$ rpm



$p=1,0$ MPa; $v=100$ rpm



$p=1,0$ MPa; $v=250$ rpm

$p=1,5$ MPa; $v=100$ rpm

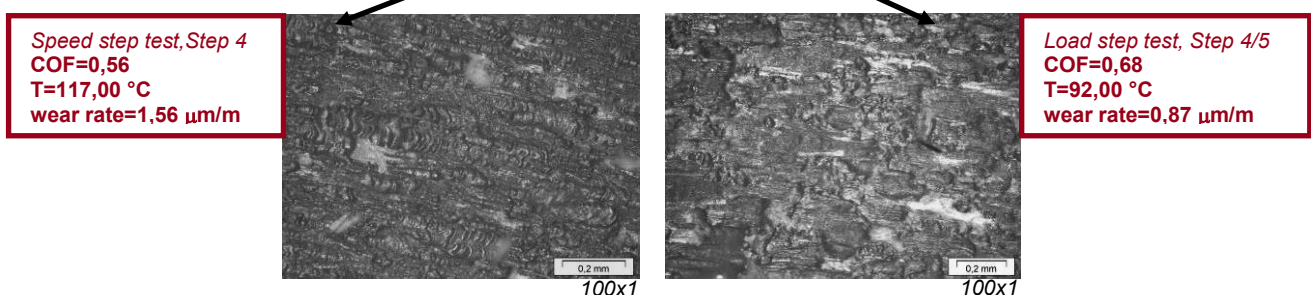


Figure 4.5-6: PV-dependency of the surface formations for TPU unfilled

During operation increased PV-levels result in more severe wear pits and traces, which possibly indicate a change in the wear mechanism from adhesion to a kind of ploughing.

Conclusively, the appearance of enlarged adhering regions signals failure initiation and the material fails as a result of the combination of thermal overloading and mechanical fatigue, which is possibly signalled by the wavy structure of wear pits (Bartenev and Lavrentev, 1981). The mechanism itself is similar to failure mechanisms described with regards to delamination processes (Suh, 1973; Da Silva et al, 2007).

PV-settings of 0,5 MPa and 100 rpm are conclusively defined as application limit for the unfilled material.

Assessment of the filled TPUs PV-application limit

Conventionally, colossal resistance to tribological loadings distinguishes the filled material. Wear mechanisms could scarcely be detected at both the standard PV-tests and the advanced PV-tests (see section 4.5.1). The dominating surface mutations result from the detachment of the softened matrix and the dissection of a possibly partially bearing or lubricating filler network (see Figure 4.5-7). A more detailed assessment of the above described phenomena can be found in 4.4.4.

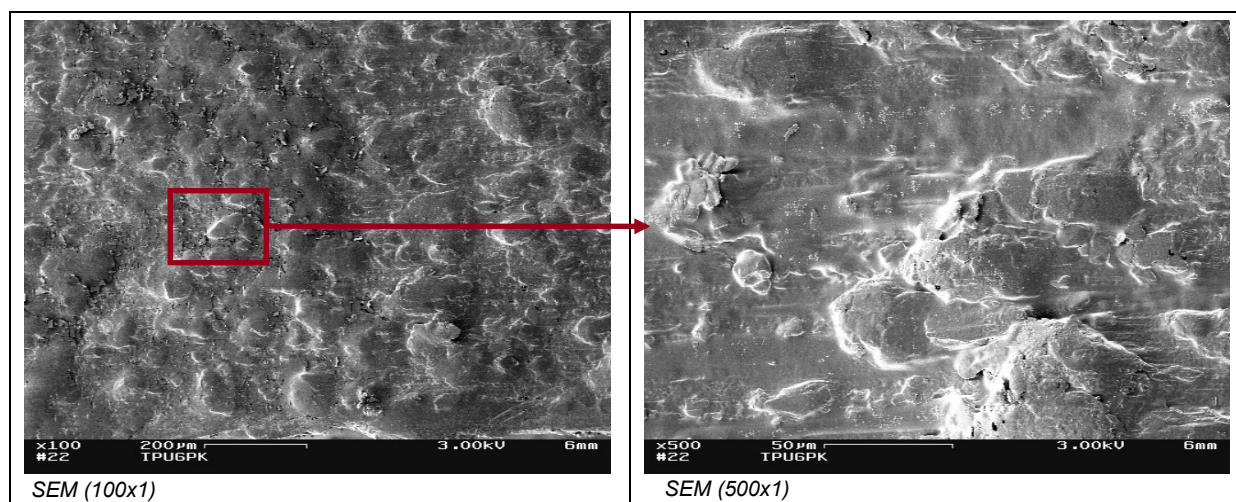


Figure 4.5-7: Dissection of a partially bearing or lubricating filler network during tribological performance of TPU filled

Figure 4.5-8 demonstrates the surface mutations after the advanced speed step test. The filler network structure is fully developed. The micrographs of the advanced load step test show similar formations (Figure 4.5-9).

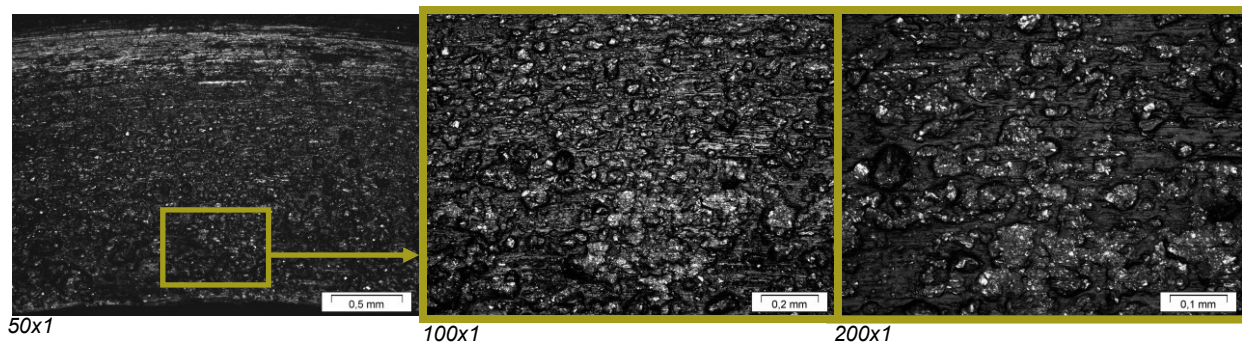


Figure 4.5-8: Advanced speed step test of TPU filled, Test No. 1

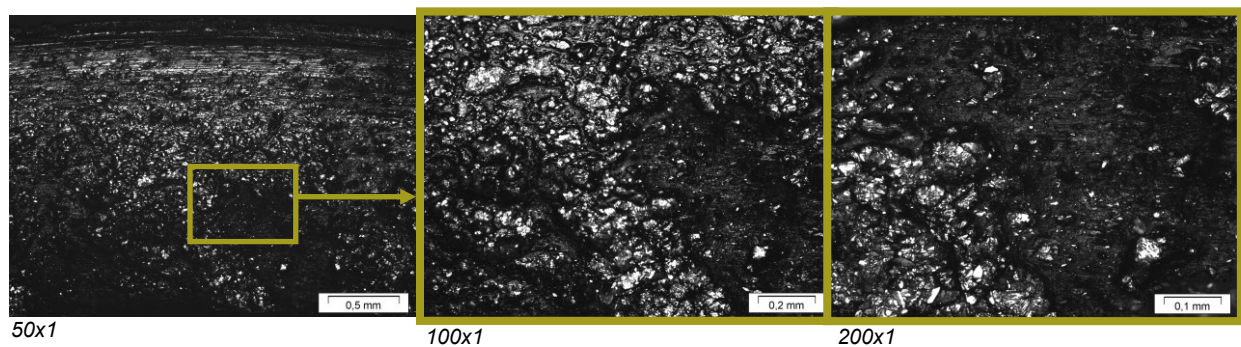


Figure 4.5-9: Advanced load step test of TPU filled, Test No. 1

Additionally, it has to be highlighted that the formations developed during the load step test show severe pits. The filler network structure is probably detached on account of elevated contact pressure. This results in a reduction of the real contact area, which explains the rather “moderate” frictional heat build-up of about 116°C. The depicted phenomenon is related with material fatigue henceforth. Moreover, the loss of contact spots and the severe pits on the surface can indicate failure mechanisms not correlated with wear, but with a possible malfunction of the seal in case that leak tightness cannot be provided anymore. Those PV-settings ($p=2,75$ MPa and $v=100$ rpm) have thus to be connoted as critical.

4.5.3 Correlations with Thermo-Mechanical Material Characteristics

Both materials conventionally show a similar thermo-mechanical response, since there are scarcely differences in the matrix composition of both materials and the thermo-mechanical response is roughly not affected by the filler network or matrix-filler-interactions (Röthemeyer and Sommer, 2006).

Figure 4.5-10 exemplarily shows a DSC-plot of the unfilled material representing the thermal response of the tested sealing materials. The first heating run is relevant for correlations with tribological operational characteristics, since cooling and reheating

is not expected during clean tribological operation due to continuous heat generation from the deformation of material at the actual contact spots (Myshkin, 2005). The seal materials conventionally depict a roughly bimodal melting peak at an onset temperature of approximately 175 to 180 °C, resulting from crystallite melting of paracrystalline and crystalline structures of higher order (chapter 4.1.2).

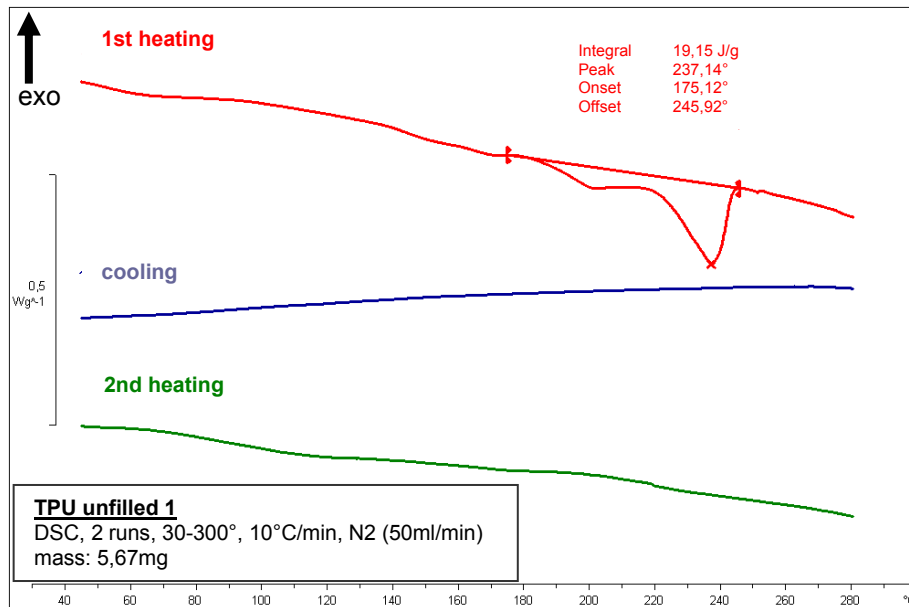


Figure 4.5-10: exemplary thermal response of TPU unfilled (DSC-plot)

DMA-results (described in chapter 4.1.1 in greater detail) show a significant softening at approximately temperatures of 150 °C for both matrix systems (Figure 4.5-11).

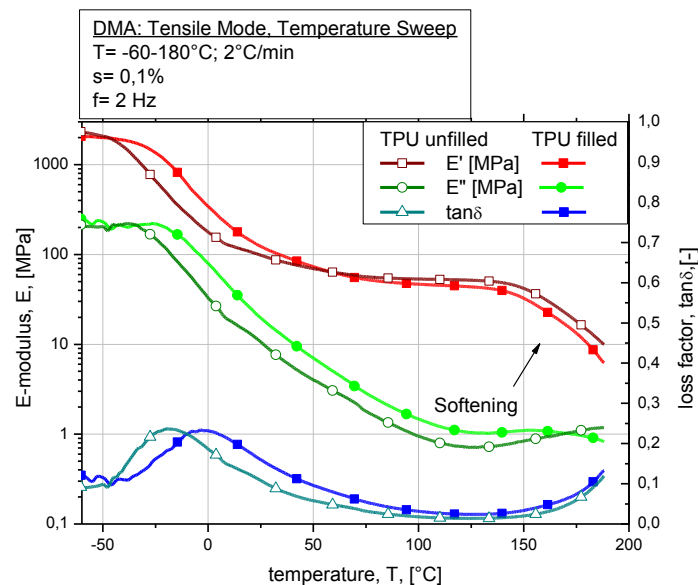


Figure 4.5-11: Review on DMA-Temperature Sweeps of TPU filled/unfilled at a testing frequency of 2 Hz

For those morphological phenomena mainly hard domains are concerned (Schwarz, 1993), which are of considerable importance for the TPUs performance at thermo-mechanical loadings. The melting state thus characterizes the thermal stability of the material. Even partial melting can cause a severe loss in mechanical properties. During tribological performance an extreme heat build-up is assumed to develop at the real contact spots. Melting occurs and conjointly the bearing stability of the surface layer is lost. In Figure 4.5-12 the average results of the measured near surface temperatures are opposed to the PV-settings for both materials and a critical temperature limit is marked.

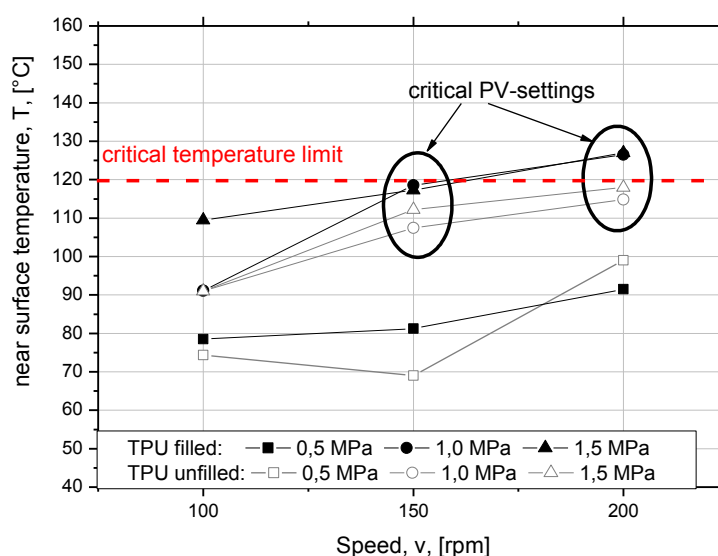


Figure 4.5-12: Review of near surface temperatures for TPU filled /unfilled, averaged values from PV-step tests

Above the critical temperature partial melting and bulk softening processes are expected, which prevail instable operation and introduce failure in addition to damage mechanisms. The level of the critical temperature limit is related to the results from Grün (2007) Gódor et al (2009), determining a rubbing contact temperature of about 30 °C higher than the measured near surface temperatures. Significantly, PV settings of $p=1,0$ MPa and 1,5 MPa at $v=150$ rpm and 200 rpm lead to critical temperature accumulations of about 120 °C near surface, thus 150 °C or more in the rubbing contact. It has been indubitably noted, that the temperatures of the unfilled material subdue at lower values than those for the filled material. This phenomenon can be described as an effect of the wear dominated tribological performance of the unfilled TPU. Surface layers are permanently detached and the wear particles are removed

from the rubbing groove. New surface layers thus are continuously tribologically stressed, which disclose lower hysteretic heat-up due to the rather low heat conductivity of the TPU. A review of the near surface temperature build-up, occurring at the advanced step tests for the filled material, is shown in Figure 4.5-13.

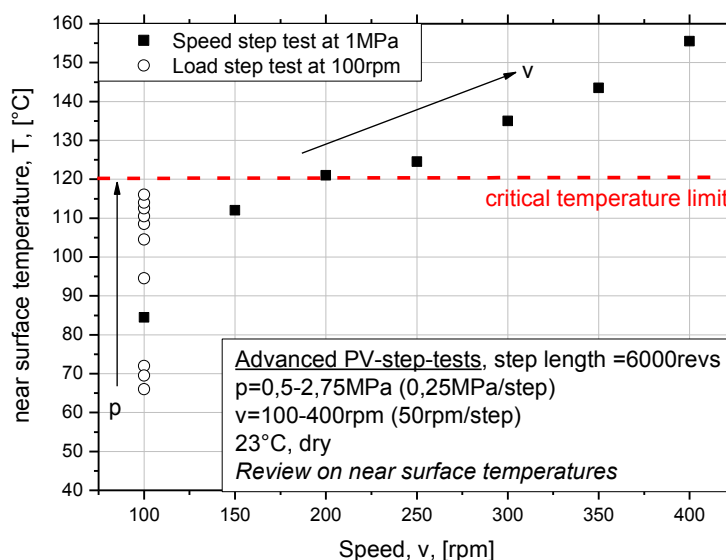


Figure 4.5-13: Review of near surface temperatures for TPU filled, advanced PV-step tests

At speed levels of greater than 200 rpm at a contact pressure of 1 MPa the critical temperature limit is overrun, which has been expected with regard to the previously performed standard PV-step tests. It has been further expected, that an increase of the contact pressure would also result in extreme heat accumulation, which actually doesn't occur. This phenomenon is explained by the loss of contact area due to severe surface mutations (section 4.5.3.2).

Conclusively, sliding velocities greater than 150/200 rpm at 1,0 MPa pressure and contact pressures greater than 2,5 MPa at testing speeds of 100 rpm are set as critical values/PV-limits with regards on the heat accumulation.

4.5.4 Approach to define a PV- application limit

Conclusively, the three investigated parameters (linear wear rate, surface mutations and frictional heat accumulation) are at first solely evaluated and then correlated to each other to define a PV-application limit. In Table 4.5-6 the results are summarized.

Table 4.5-6: PV-application limit with regards on linear wear rate, frictional heat accumulation and surface mutations

p [MPa]	v [rpm]	TPU unfilled			TPU filled		
		linear wear rate	heat accumulation	critical surface mutations	linear wear rate	heat accumulation	critical surface mutations
0,50	100,00	instable operation, failure	instable operation, failure	instable operation, failure	clean operation	clean operation	clean operation
	150,00	instable operation, failure	instable operation, failure	instable operation, failure	clean operation	clean operation	clean operation
	200,00	instable operation, failure	instable operation, failure	instable operation, failure	clean operation	clean operation	clean operation
1,00	100,00	instable operation, failure	instable operation, failure	instable operation, failure	clean operation	clean operation	clean operation
	150,00	instable operation, failure	instable operation, failure	instable operation, failure	clean operation	instable operation, failure	clean operation
	200,00	instable operation, failure	instable operation, failure	instable operation, failure	clean operation	instable operation, failure	clean operation
	250,00	instable operation, failure	instable operation, failure	instable operation, failure	clean operation	instable operation, failure	clean operation
	300,00	instable operation, failure	instable operation, failure	instable operation, failure	clean operation	instable operation, failure	clean operation
	350,00	instable operation, failure	instable operation, failure	instable operation, failure	clean operation	instable operation, failure	clean operation
1,50	400,00	instable operation, failure	instable operation, failure	instable operation, failure	clean operation	instable operation, failure	clean operation
	100,00	instable operation, failure	instable operation, failure	instable operation, failure	clean operation	instable operation, failure	clean operation
	150,00	instable operation, failure	instable operation, failure	instable operation, failure	clean operation	instable operation, failure	clean operation
	200,00	instable operation, failure	instable operation, failure	instable operation, failure	clean operation	instable operation, failure	clean operation
1,75	100,00	instable operation, failure	instable operation, failure	instable operation, failure	clean operation	clean operation	
2,00	100,00	instable operation, failure	instable operation, failure	instable operation, failure	clean operation	clean operation	
2,25	100,00	instable operation, failure	instable operation, failure	instable operation, failure	clean operation	clean operation	
2,50	100,00	instable operation, failure	instable operation, failure	instable operation, failure	clean operation	clean operation	
2,75	100,00	instable operation, failure	instable operation, failure	instable operation, failure	clean operation	clean operation	instable operation, failure

	clean operation
	PV-limit
	instable operation, failure

For the unfilled TPU material the three parameters correlate appropriately to each other. The calculated linear wear rate precisely reflects the same phenomena as the investigations of the surface formations. The observed surface mutations are an appropriate approach to declare the wear mechanisms of the unfilled material henceforth. The limit examined focussing on the heat accumulation slightly falls out of line, as a result of the wear dominated detachment of tribologically stressed surface layers and the further rubbing of thermally less stressed surfaces with the counterpart (further descriptions in chapter 4.5.4.3).

The PV-application limit for the unfilled TPU in tribological operation at the testing configuration at hand is finally set at $p=0,5$ MPa and $v=100$ rpm.

The definition of a PV-application limit for the filled material is of greater complexity. Regarding the wear rate, no limit can be set due to the absence of wear mechanisms during tribological operation. This phenomenon is also reflected by the surface mutations, except for outburst of stressed material in terms of mechanical fatigue due to elevated contact pressures observed at $p=2,75$ MPa and $v=100$ rpm (see section 4.5.3.2). The evaluation of the frictional heat build-up and the resulting softening and melting of the matrix is affected by crucial difficulties: Bulk softening generally introduces failure, because the thermal stability of the matrix is exceeded. The filler network partially inherits a bearing function, but in case that a sufficient embedding ability in the matrix cannot be sustained anymore (e.g. due to melting), the materials' tribological capacity breaks down. Additionally, the filler network structure is not able to avoid morphological mechanisms in terms of melting. During the performed PV-tests of the filled material certain temperature levels are reached, at which melting processes are expected conjointly with tribological instabilities, concluding in the materials' break down. Failure mechanisms barely could be detected though. Notwithstanding, the materials breakdown simply is a matter of time. A more durable tribological performance at those stage is assumed to result in collapse of the materials bearing capability to withstand the applied stresses. The PV-application limit hence should incorporate such phenomena.

Subsuming, settings of $p=1,0$ MPa at $v=200$ rpm, $p=1,5$ MPa at $v=150$ rpm and respectively $p=2,75$ MPa at $v=100$ rpm are defined as PV-application limit for the filled material performing at the present test configuration.

4.5.5 Characterization of operational range by composing PV-diagrams

A PV-diagram for the filled TPU-system, as is described by Mäurer (2002), is shown in Figure 4.5-14. The points are determined with regards to the results of the PV-step tests and are linear fitted and extrapolated. The ranges of the pressure and thermal limits are assumed based on the findings on tribological performance of the material. The linear slope divides the tribological performance of TPU filled into two main parts: Below the line, clean tribological operation is assumed and this area roughly remarks the possible operating range. None of the three above described critical parameters

are eclipsed. Beyond the limit critical stages regarding the three parameters are expected, which definitely doesn't result in abrupt failure, but can introduce failure mechanisms. During more durable operations a breakdown of the material is expected above the PV-limit.

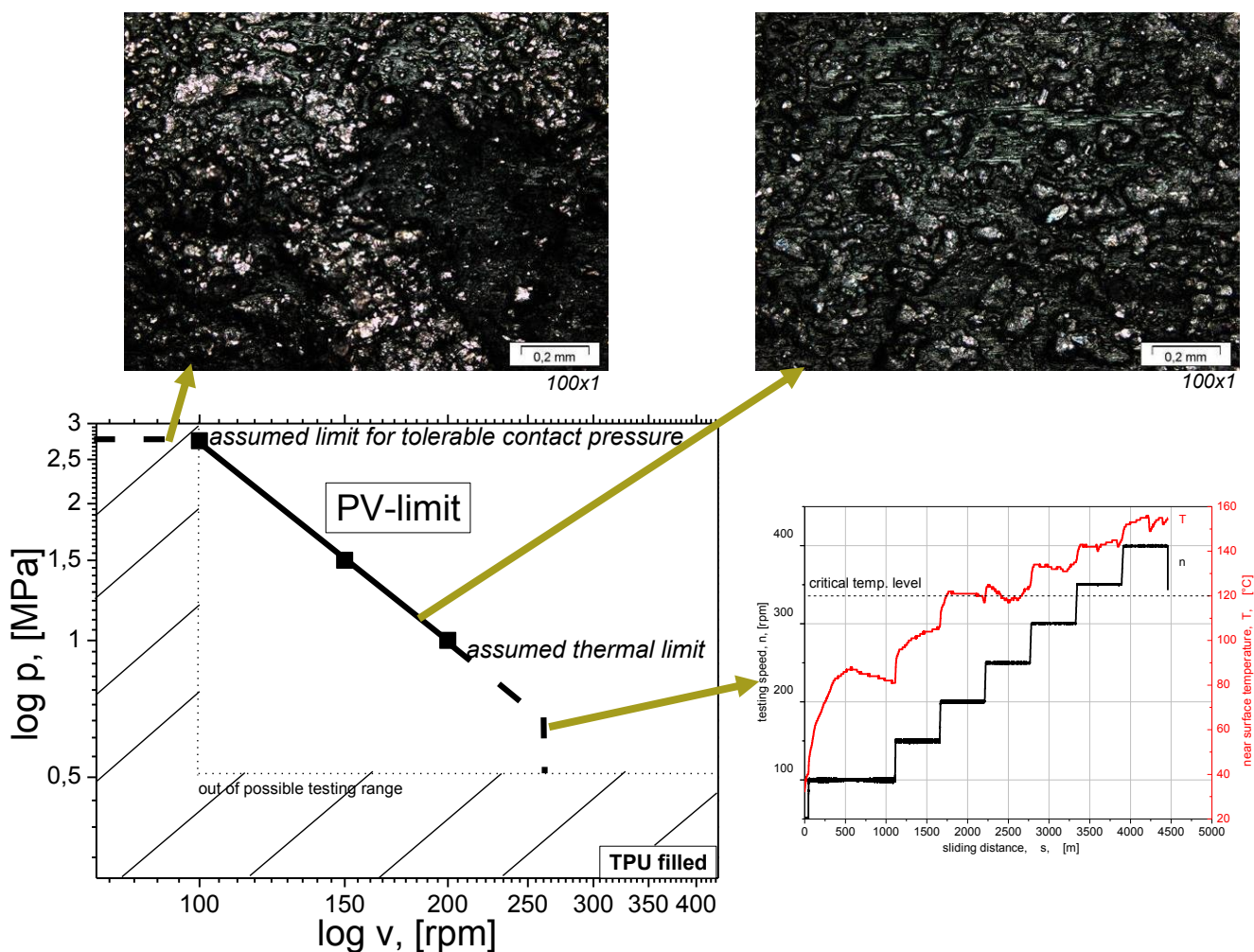


Figure 4.5-14: PV-diagram of TPU filled

The drawing of a PV-diagram for the unfilled TPU-system entails greater difficulties. In fact, the determination of a meaningful ignition map is not feasible, as a result from an inappropriate combination of the testing machine's testing range and the material's bad tribological performance. Ultimately, at PV-settings of $p=0,5$ MPa and $v=100$ rpm clean operation is depicted (see approval of assumptions in section 4.5.2.1. regarding the 4 h-constant load tests). At a slight rise of the PV-settings ($p=0,75$ MPa and $v=100$ rpm (Project IV 3.07, PCCL GmbH, Austria, 2011) and respectively $p=0,5$ MPa and $v=150$ rpm) nearly stable conditions can be achieved. A further increase of the PV-settings rapidly results in intolerable wear rates and ex-

treme heat accumulation in accordance with melting (severe wear phenomena depicted on the rubbing surface). Further tests at lower PV-settings have to be performed to mark the feasible operating range more reliably. However, those tests cannot be performed on the current testing rig.

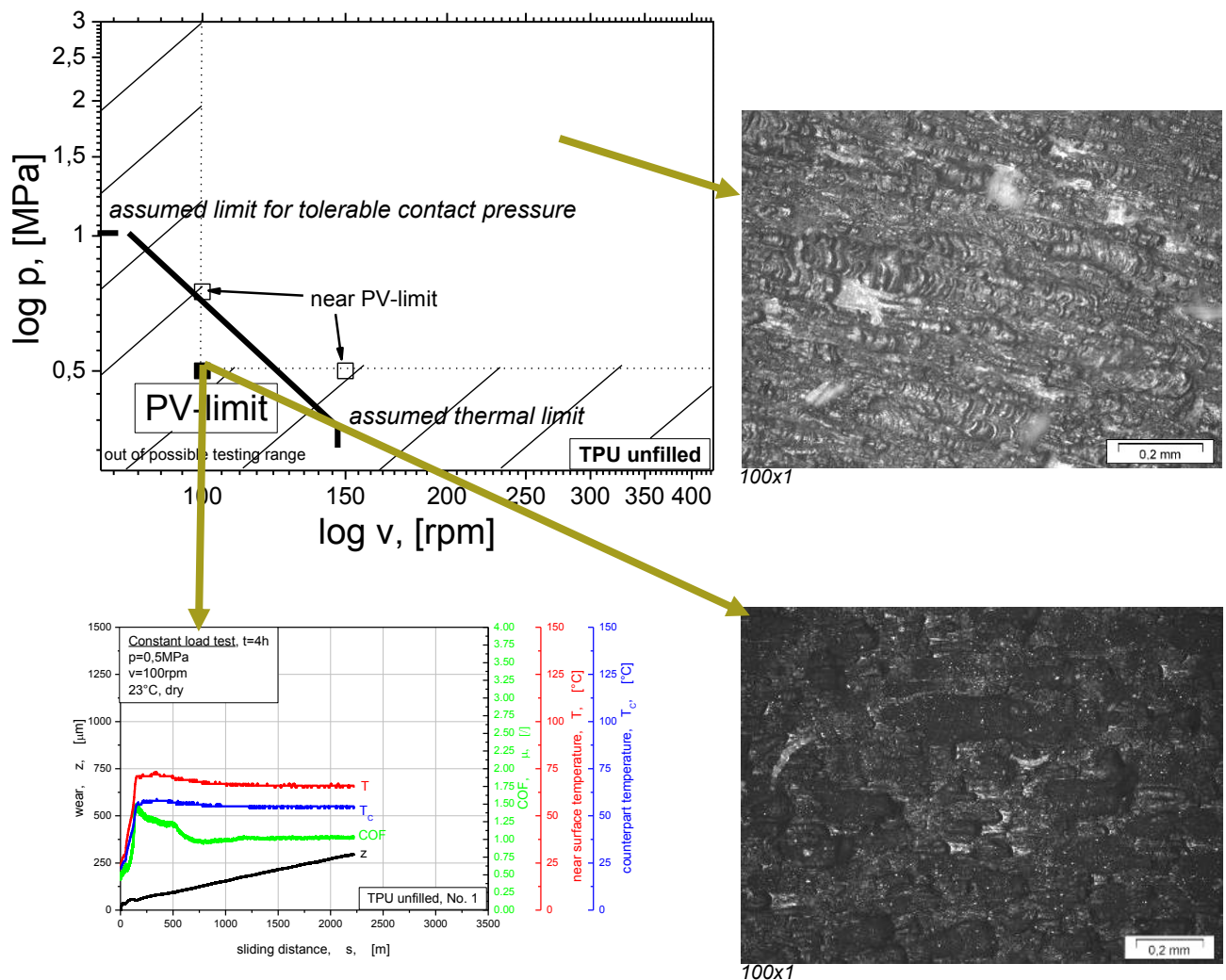


Figure 4.5-15: PV-diagram of TPU unfilled

The PV-diagram (Figure 4.5-15) is composed by correlating settings resulting in assured stable operation and critical settings, based on test results from the PV-step tests and for further verification from current research work (Project IV 3.07, PCCL GmbH, Austria, 2011).

Lastly, Figure 4.5-16 contrasts the PV-diagrams of the filled and unfilled system with each other. The materials differ significantly in their tribological performance, although their thermo-mechanical properties are roughly similar (regarding melting and softening regions of hard domains evaluated from DSC- and DMA-measurements,

chapter 4.1). The filler system hence mainly affects the tribological bearing capacity. Conclusively, the PV-diagrams compellingly summarize the application limits for the materials and can be used with restrictions to predict the seals application limit.

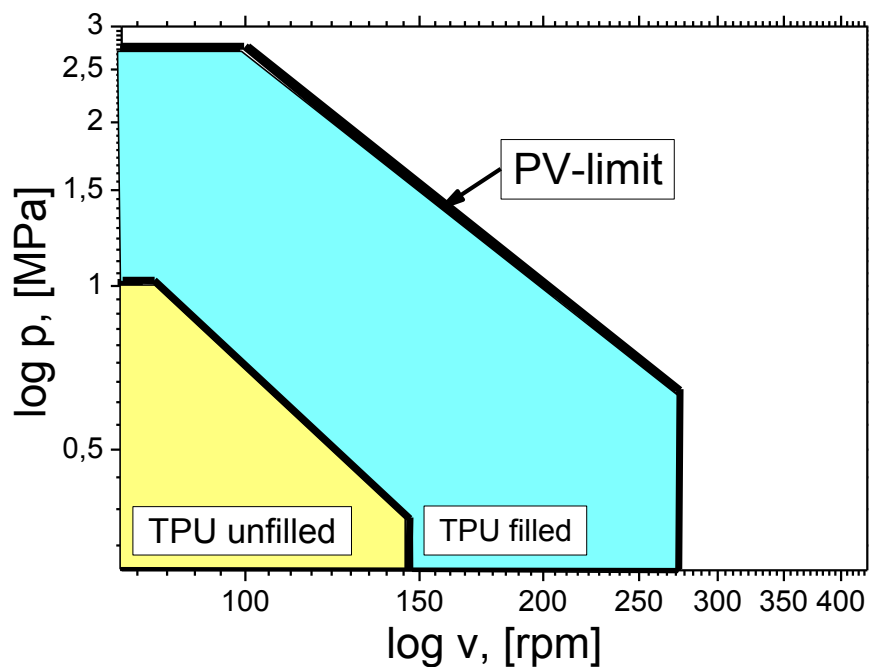


Figure 4.5-16: Review: PV-diagrams of TPU unfilled/ filled

5. Conclusion

The compelling objective of the current research is the development and finalization of a comprehensive testing methodology to rate the tribological performance of TPU seal materials with regards on the PV-dependency. The methodology in its initial stage is based on the standard ASTM D3702 (ASTM International Standard D3702-94, 1999) for thrust washer testing of materials in unlubricated rubbing contacts and has already been adapted to TPU seal materials in former research tasks (Gódor et al, 2009). Further modifications in the RoD-testing set-up are performed to precisely carry out the tribological tests at the applied rotary tribometer. Entirely, the developed methodology covers the tasks shown in Figure 4.5-1.

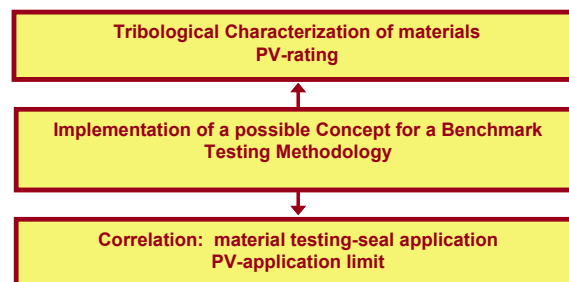


Figure 4.5-1: Requirements for the testing methodology for tribological characterization of TPU seal materials

Conclusively, a concept is elaborated combining tribological material characterization with seals applied performance and implemented in a benchmark testing methodology.

The improved RoD-testing set-up facilitates a general tribological characterization of TPU materials. In dynamical seal applications the applied contact pressure and the performed sliding velocity affect the seal's function and operating life to a high degree (Flitney, 2007). A more detailed assessment on the PV-dependency is integrated in the testing procedure henceforth (development of PV-step tests). Precisely, the PV-step tests are approved to accurately rate the materials PV-dependency. First, a thermo-mechanical equilibrium can be achieved for every performed PV-step, which then enables a comprehensive PV-rating based on the frictional and wear characteristics depicted during the single steps instead of carrying out a multitude of tests. Moreover, it could be demonstrated, that the PV-settings mainly dominate the tribology.

logical performance of the tested materials. The frictional phenomena depend to a high degree on the PV-settings and are nearly independent from the test duration by means of the already covered sliding distance. The results from load and speed step tests thus can be summarized (section 4.4.3).

Detailed optical investigations of the worn surfaces are carried out to relate PV-setting with surface mutations for an improved comprehension of frictional and wear mechanisms. Gradually performed PV-step tests, combined with microscopy of the tribologically stressed surfaces for every step, afford a specified analysis of the surface mutations evolving with variations in loadings/PV-settings.

Furthermore, the thermo-mechanical material characteristics of both TPU seal materials are analyzed via DMA- and DSC- measurements. Viscoelastic effects and morphological alterations highly affect the tribological performance due by means of time-temperature-dependency of materials capacity. The melting range of the hard domains at elevated temperatures signals a critical temperature limit for the developed temperatures in the rubbing contacts. Frictional heat accumulation up to those critical temperatures affects partial melting of surface structures or layers, which crucially leads to wear and damage mechanisms. The bearing stability of the material is lost and fillers cannot influence this loss in mechanical properties, since melting solely is a morphological change. At critical PV-settings the critical temperature level for melting processes is surpassed and can result in instable operation, failure initiation until overall material breakdown (section 4.5.4).

Summing up, the elaborated benchmark testing methodology combines and correlates PV-step tests with precise optical surface investigations and thermo-mechanical bulk properties, which enable a compelling PV-rating of TPU-seal materials.

Based on the collected data, the friction and wear mechanisms, occurring at the worn surfaces of the tested materials, are phenomenological described to identify feasible failure mechanisms.

Subsequently, the PV-rating acts as a basis to define a PV-application limit. Within the scope of the finalized benchmark testing methodology failure and failure initiation has been investigated by means of three specified influencing parameters: The failure limit thus is related to a limit for linear wear rate, unfavourable surface mutations and a critical temperature range, where the material suffers from morphological alter-

ations. The linear wear rate is proven to strongly depend on the PV-settings and is used to confine the tolerable wear. The thermal limit by means of partial melting of TPU asperities is further consulted and the near surface temperature, evolved in the rubbing contact, is set as critical parameter. Furthermore, detailed surface investigations and the assumed occurring wear mechanisms allegorize the third crucial parameter for the definition of a PV-application limit. A combination of several critical parameters is certified as of considerable importance (Stachowiak and Batchelor, 2001), since the three parameters do not result in precisely the same PV-limits. If one parameter indeed exceeds a critical level, further clean operation has been no prospect anymore, consequently failure is initialized. The finally set PV-application limit is then used to compose a PV-diagram (chapter 2.1.2.3). The PV-diagram schematically plots the operating range of the material and acts as connector between material characteristics and seal application. The outlined results of the PV-diagrams demonstrate a first approach to correlate model testing with end-use application. It should mainly depict the difficulty to establish such correlation by means of the limited validity of the results in order to achieve equivalent damage mechanisms. Finally, the main results of this thesis are summarized in Figure 4.5-2.

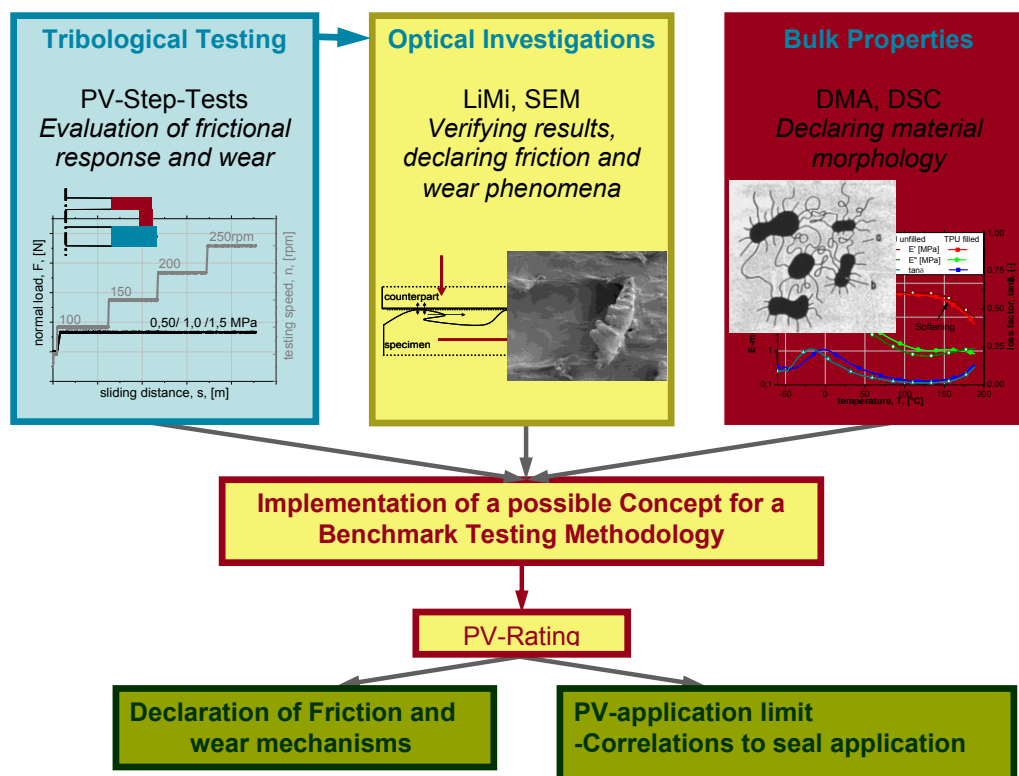


Figure 4.5-2: Overview of the developed benchmark testing methodology and application examples

6. Perspectives

Developing a benchmark testing methodology to rate the PV-dependency of TPU seal materials allegorizes a suitable access for a comprehensive tribological characterization of TPU seal materials. Moreover, this methodology, combining PV-step tests with optical investigations of surface mutations and thermo-mechanical bulk properties, implements a procedure to roughly characterize, for once friction and wear mechanisms, and on the other assignments to seal operation in practice. Summing up, one feasible research “path” goes into depth with a detailed assessment of the materials’ bulk properties, its morphology and as far as its chemical composition. The second “path” focuses on assignments for seal application in practice. Further research should focus on supplementary correlations of mechanical properties with tribological operation as is already approved in literature (Friedrich et al, 1999; Rymuza, 1981; Viswanath and Bellow, 1995).

Cyclic or dynamical compression and shear tests present a feasible methodology to approximate tribological stresses, because the surface asperities of the TPU sample are cyclically deformed by the counterpart. Furthermore, mechanical testing should be performed on micro-level (indentation tests, micro-thermo mechanical analysis via AFM) to differentiate between surface and bulk properties. Contrasting the surface and bulk properties is of outermost significance, since the samples are processed by fine turning, which results in an already stressed surface at the beginning of the loading. Furthermore the surface evenly suffers from higher stresses during tribological testing. The evolution of surface hardness during tribological testing could further explain wear mechanisms. Additionally, the morphology of the surface regions, both of the turned and tribologically stressed surface, differentiates from the bulk material by means of crystallization degree, crystallite structure and hard domain configurations, which can possibly be analyzed by DSC-analysis or SAXS/WAXS-investigations.

Supposing that the wear mechanism of the TPU seal material is mainly dominated by adhesion and deformation, the above cited testing methods could explain the deformation and hysteresis part. Contact angle measurements and a specific assessment on the surface energies could declare adhesion mechanisms in greater detail.

A fracture mechanical analysis of the materials is critically important with regards on the wear mechanisms. It has to be declared how wear particles are formed. The already described model for the filled and unfilled TPU do not elucidate, whether the wear particles are torn by brittle subsurface cracks (“delamination” as described et Suh, 1973) or rather ductile tearing. Additionally, the role of the filler, influencing the fracture toughness of the material, is not declared. The impact of a material’s fatigue on the tribological operation has to be analyzed by long-term cyclic and creep and fatigue analysis, since the wavy structured surface mutation of the unfilled system indicate fatigue wear due to cyclic pass of asperities (Bartenev and Lavrentev, 1981). The analysis can be continued in greater detail via assessment of molecular structure, molecular mass and chemical composition.

On the other hand, the tribological testing set-up has to be improved, to better correlate with seal’s performance in practice. To compose compelling PV-diagrams statistical test series should be performed. Furthermore, a more extensive range of influencing parameters should be assessed. Testing under lubricated conditions or higher system temperatures, as example, would approximate seal application in practice to a greater detail. The use of other tribological testing devices can complement the testing range by means of inappropriate material-tribometer-combinations and can expand the feasible materials range. A simulation approach concerning the contact conditions would be of further significance. Finally, correlations between the materials constitution and the final application should be implemented in seals engineering and design (Figure 4.5-1).

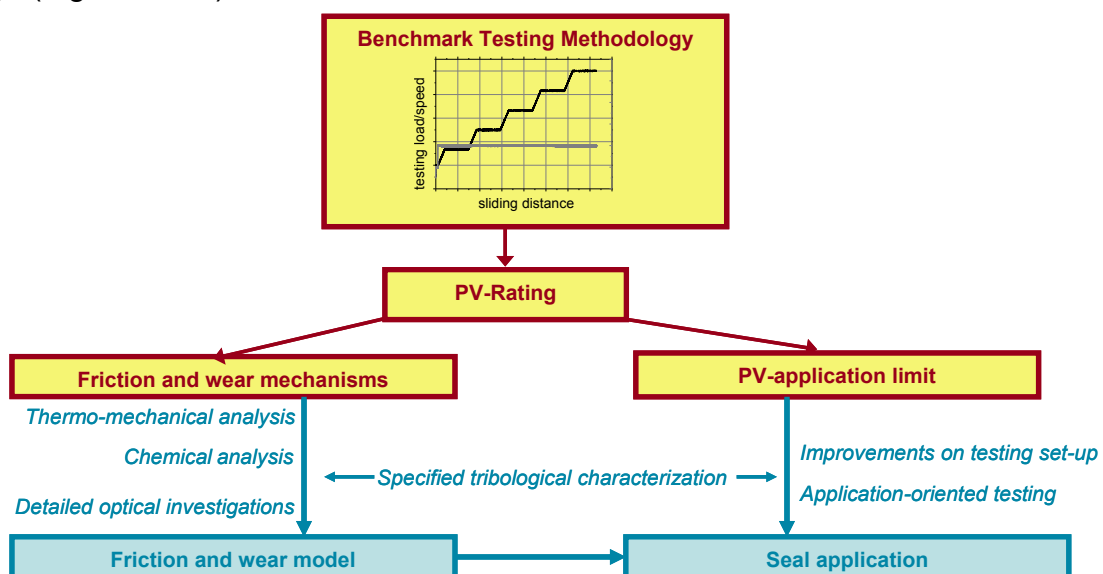


Figure 4.5-1: Further feasible research based on benchmark testing methodology

7. References

- Archard (1953)*, Contact and rubbing of flat surfaces, *Applied Physics* 24, p.981-988.
- Ashby and Jones (1995)*, *Engineering materials: An Introduction to Microstructure, Processing and Design*, Vol. 2, Pergamon Press, p.495.
- ASM Handbook (1992)*, Vol 18, Friction lubrication and wear technology.
- ASTM International Standard D 3702-94 (1999)*, Standard Test Method for Wear Rate and Coefficient of Friction of Materials in Self Lubricated Rubbing Contact Using a Thrust Washer Testing Machine, Beuth Verlag GmbH, Berlin, Germany.
- Bartenev and Lavrentev (1981)*, Friction and Wear of Polymers, Tribology Series, No.6, Elsevier Scientific Publishing Company, p. 10-260.
- Baur et al (2007)*, Saechtling Kunststoff Taschenbuch, 30th edition, Carl Hanser Verlag, Munich, Germany.
- Beck and Truss (1998)*, Effect of chemical structure on the wear behaviour of polyurethane-urea elastomer, *Wear* 218, p. 145-152.
- Birley (1992)*, *Physics of Plastics, Processing Properties and Materials Engineering*, Carl Hanser Verlag, Munich, Germany.
- Bode (1996)*, *Konstruktionsatlas*, 6th edition, Friedr. Vieweg & Sohn Verlag, Braunschweig/Wiesbaden, Germany.
- Boyce et al (2006)*, Large deformation rate-dependent stress-strain behaviour of polyurea and polyurethanes, *Polymer* 47, p. 319-329.
- Cahn et al (1993)*, *Materials Science and Technology- A Comprehensive Treatment, Structure and Properties of Polymers*, 12th edition, VCH Verlagsgesellschaft mbH, Weinheim, Germany.
- Crawford, Bass, Haas (1998)*, Strain effects on thermal transitions and mechanical properties of thermoplastic polyurethane elastomers, *Thermochimica Acta* 323, p. 53-63.
- Czichos and Habig (2003)*, *Tribologie-Handbuch*, Second Edition, Friedr. Vieweg & Sohn Verlag, Wiesbaden, Germany.

Da Silva and Sinatora (2007), Development of severity parameters for wear study of thermoplastics, *Wear* 263, p.957-964.

Da Silva et al (2007), Is there delamination wear in polyurethane?, *Wear* 263, p. 974-983.

Debler (2005), Bestimmung und Vorhersage des Verschleißes für die Auslegung von Dichtungen, Dissertation, Faculty of Mechanical Engineering, University of Hannover, Germany.

Decker (2007), Maschinenelemente- Funktion, Gestaltung und Berechnung, 16th edition, Carl Hanser Verlag, Munich, Germany.

Decker (2007), Maschinenelemente- Tabellen und Diagramme, 16th edition, Carl Hanser Verlag, Munich, Germany.

DIN 4768 (1990), Ermittlung der Rauheitskenngößen R_a R_z R_{max} mit elektrischen Tastschnittgeräten, Beuth Verlag GmbH, Berlin, Germany.

Dominghaus (1993), Plastics for engineers- Materials, Properties, Applications, Carl Hanser Verlag, Munich, Germany.

Dominghaus (2004), Die Kunststoffe und ihre Eigenschaften, 6th edition, VDI Springer Verlag, Berlin, Germany.

Drobny (2007), Handbook of Thermoplastic Elastomers, William Andrew Inc., New York.

Ehrenstein, Riedel, Trawiel (2003), Praxis der thermischen Analyse von Kunststoffen, Carl Hanser Verlag, Munich, Germany.

Elleuch et al (2007), Tribological behaviour of thermoplastic polyurethane elastomers, *Materials and Design* 28, p. 824-830.

Fleischer (1973), Energetische Methode der Bestimmung des Verschleißes, *Schmierungstechnik* 4, No.9, p. 269-274.

Flitney (2007), Seals and Sealing Handbook, Fifth Edition, Butterworth-Heinemann (imprint of Elsevier Ltd.), Great Britain.

Frick, Mikoszek, Michler, Henning (2010), Segmented Thermoplastic Polyurethanes- Dependence of Viscoelastic Properties on Thermal History, 14th International Scientific Conference on Polymeric Materials, Halle, Germany.

Friedrich et al (1999), Numerical and finite element contact and thermal analysis of real composite-steel surfaces in sliding contact, *Wear* 225-229, p. 368-379.

Fukahori et al (2010), How does rubber truly slide between Schallamach waves and stick-slip motion?, *Wear* 269, p. 854-866.

GfT Arbeitsblatt 7 (2002), Tribologie, Verschleiß Reibung, Definitionen Begriffe Prüfung, Aachen, Germany.

Gódor et al (2006), Development of a tribological functional and failure model for PTFE-Bz compounds, *Advanced Problems in Mechanics*, Russian Academy of Sciences, St. Petersburg, p. 181-192.

Gódor, Grün, Eichlseder (2009), Characterization of the tribological properties of polymer basis compounds in respect to component application. Final report Nr. WPR-S.17, Polymer Competence Center Leoben, Austria.

Gódor, Strohhäussl et al (2009), Tribologische Eigenschaften von TPU-Modellmaterialien und ihre anwendungsorientierte Charakterisierung, ÖTG-Symposium, p-245-258.

Grellmann and Seidler (2007), *Polymer Testing*, Carl Hanser Verlag, Munich, Germany.

Grote and Feldhusen (2007), *Doppel Taschenbuch für den Maschinenbau*, 22nd edition, Springer Verlag, Berlin Heidelberg New York.

Grün (2007), Entwicklung von Prüfmethoden für die Charakterisierung von zweiphasigen Tribomaterialien, Dissertation, Chair of Mechanical Engineering, Montanuniversitaet Leoben, Austria.

Grün et al (2008), Test methods to characterise differently designed tribomaterials, *Tribotest* 14, p.159-176.

Hausberger (2008), Development and implementation of novel tribological test methods on UMT and characterization of TPU, Bachelor's Thesis, Chair of Materials Science and Testing of Plastics, Montanuniversitaet Leoben, Austria.

Hausberger (2009), Methodenentwicklung zur Charakterisierung des Stick.Slip-Verhaltens von TPU-Materialien, Master's thesis, Chair of Materials Science and Testing of Plastics, Montanuniversitaet Leoben, Austria.

Hepburn (1992), Polyurethane Elastomers, Second Edition, Elsevier Science Publishers Ltd, England.

Hofmann (1989), Rubber Technology Handbook, Carl Hanser Verlag, Munich, Germany.

Holden, Kricheldorf, Quirk (2004), Thermoplastic Elastomers, 3rd edition, Carl Hanser Verlag, Munich, Germany.

Holden, Legge, Quirk, Schroeder (1996), Thermoplastic Elastomers, 2nd edition, Carl Hanser Verlag, Munich, Germany.

Igus GmbH (2010), polymer.gleitlager 7.2010, catalogue 7/2010, Köln, Germany.

Johnson et al (1971), Surface energy and the contact of elastic solids, Proceedings of the Royal society London, A324, p. 301.

Jones(2004), On the tribological behaviour of mechanical seal face materials in dry line contact, Wear 256 (415-432).

Kaden (2008), Beitrag zum Reibungs- und Verschleißverhalten von Zahnriemenförderern, Dissertation, Faculty of Mechanical Engineering, Technical University of Chemnitz, Germany.

Kämpf (1986), Characterization of Plastics by Physical Methods- Experimental Techniques and Practical Application, Carl Hanser Verlag, Munich, Germany.

Kornprobst (2007), CATIA V5 Volumenmodellierung, Carl Hanser Verlag, Munich, Germany.

Kornprobst (2008), CATIA V5 Baugruppen und technische Zeichnungen, Carl Hanser Verlag, Munich, Germany.

Kragelski et al (1982), Grundlagen der Berechnung von Reibung und Verschleiß, VEB Verlag Technik, Berlin, Germany.

Martínez et al (2010), Relationship between wear rate and mechanical fatigue in sliding TPU-metal contacts, Wear 268, p. 388-398.

Marx and Junghans (1996), Friction and wear of highly stressed thermoplastic bearings under dry sliding conditions, Wear 193, p. 253-260.

Mäurer (2002), Tribologische Untersuchung an Radialgleitlagern aus Kunststoffen, Dissertation, Faculty of Mechanical Engineering, Technical University of Chemnitz, Germany.

Menges et al (2002), Werkstoffkunde Kunststoffe, 5th edition, Carl Hanser Verlag, Munich, Germany.

Mennig and Lake (2008), Verschleißminimierung in der Kunststoffverarbeitung- Phänomene und Schutzmaßnahmen, Carl Hanser Verlag, Munich, Germany.

Muhs et al (2007), Roloff/Matek Maschinenelemente-Normung Berechnung Gestaltung, 18th edition, Friedr. Vieweg & Sohn Verlag, Wiesbaden, Germany.

Muhs et al (2007), Roloff/Matek Maschinenelemente-Tabellen, 18th edition, Friedr. Vieweg & Sohn Verlag, Wiesbaden, Germany.

Müller et al (2002), Ein neues Modell der Hysteresereibung von Elastomeren auf fraktalen Oberflächen, KGK Kautschuk Gummi Kunststoffe, 55. Jahrgang, Nr. 9/2002.

Müller, Deters (2004), Friction and wear behaviour of dry rubbing polymer steel/ matings, Mat.-wiss. u. Werkstofftech., 35, No 10/11.

Myshkin et al (2005), Tribology of polymers, Adhesion, friction, wear and mass transfer, Tribology international 38, p. 910-921.

Persson (1998), On the theory of rubber friction, Surface Science 401, p.445-454.

Phoenix Tribology Ltd Homepage, PLINT Tribology Products, www.phoenix-tribology.com, Newbury, England, 2011-04-27.

Qi and Boyce (2005), Stress-strain behaviour of thermoplastic polyurethanes, Mechanics of Materials 37, p. 817-839.

Retting (1992), Mechanik der Kunststoffe, Carl Hanser Verlag, Munich, Germany.

Retting and Laun (1991), Kunststoff-Physik, Carl Hanser Verlag, Munich, Germany.

Ronsin et al (2001), State, rate and temperature dependent sliding friction of elastomers, Proceedings of the Royal Society London A457, p.1277-1294.

Röthemeyer and Sommer (2006), Kautschuktechnologie, 2nd edition, Carl Hanser Verlag, Munich, Germany.

Rymuza (1981), Wear in Polymer micro-pairs, Proceedings of the, 3rd International Conference on Wear of Materials, p.125-132.

Sarva et al (2007), Stress-strain behaviour of a polyurea and a polyurethane from low to high strain rates, Polymer 48, p. 2208-2213.

Sarva, Hsieh (2009), The effect of microstructure on the rate dependent stress-strain behaviour of poly(urethane)urea elastomers, Polymer 50, p. 3007-3015.

Schallamach (1971), How does rubber slide?, Wear 17, p. 301.

Schmiedel (1992), Kunststoffprüfung, Carl Hanser Verlag, Munich, Germany.

Schneider (1998), Zum Aussagepotential praxisrelevanter tribotechnischer Kenngrößen für maschinentechnische Reibpaarungen bei Trocken-, Grenz- und Mischreibung, Internationale Tribologie Fachtagung "Reibung, Schmierung und Verschleiß", 28th-30th September 1998, Göttingen, Germany.

Schwarz (1993), Development of thermoplastic polyurethane-elastomers for sealing applications -Structure/property-relationships and aging behaviour, Dissertation, Chair of Materials Science and Testing of Plastics, Montanuniversitaet Leoben, Austria.

Schwarzl (1990), Polymermechanik, Springer Verlag, Berlin, Germany.

SKF Group (2004), SKF spherical plain bearings and rod ends, publication 4407/II E, Göteborg, Sweden.

SKF Group Homepage, Hydraulic Seals, www.skf.com, Göteborg, Sweden; 2011-04-26.

SKF Group (1990), SKF Gleitlager, catalogue 3500 T/VI, Göteborg, Sweden.

Stachowiak and Batchelor (2001), Engineering Tribology, 2nd edition, Butterworth-Heinemann, p. 743.

Strobl (1996), The Physics of Polymers-Concepts for Understanding their Structure and Behavior, Springer Verlag, Berlin, Germany.

Suh (1973), The delamination theory of wear, Wear 25, p.111-124.

Thomine et al (2007), Study of relations between viscoelasticity and tribological behaviour of filled elastomer for lip seal application, Tribology International 40, p.405-411.

Trepte (2002), Tribology parameters for friction materials, *Mat.-wiss. u. Werkstofftech.*, 33, p. 142-154.

Uetz and Wiedmeyer (1985), *Tribologie der Polymere*, Carl Hanser Verlag, Munich, Germany.

Viswanath and Bellow (1995), Development of an equation for the wear of polymers, *Wear* 181-183, p. 42-49.

Walker, Rader (1988), *Handbook of Thermoplastic Elastomers*, Van Nostrand Reinhold Company Inc., USA.

Yi et al (2006), Large deformation rate-dependent stress-strain behavior of polyurea and polyurethanes, *Polymer* 47, p.319-329.

Zhang (2004), *Tribology of elastomers- Tribology and Interface Engineering Series*, 47, Elsevier Ltd., Amsterdam.

8. Appendix

8.1 List of Figures

Figure 2.1-1: Schematical demonstration of the Tribological System (Czichos and Habig, 2003).....	9
Figure 2.1-2: Acknowledged tribological model testing configurations and equivalent application examples (Copyright © 2009 Phoenix Tribology Ltd, PLINT Tribology Products, www.phoenix-tribology.com, Newbury, England, 2011-04-27).....	10
Figure 2.1-3: Schematical PV-diagram as reported at Mäurer (2002)	11
Figure 2.1-4: Adhesion and deformation part of friction of elastomers (Müller, 2002).....	13
Figure 2.1-5: Common wear mechanisms of elastomers in dry sliding contact (Uetz and Wiedmeyer, 1985; Myshkin et al, 2005)	13
Figure 2.2-1: Diphenylmethane-4,4'-diisocyanate (MDI)	15
Figure 2.2-2: Multiblock structure of phase-separated TPU system	16
Figure 2.2-3: Examples for reciprocating seals/O-rings of TPU materials (SKF Group Homepage, Hydraulic seals, www.skf.com, Göteborg, Sweden, 2011-04-26).....	18
Figure 2.2-4: Adhesive/Frictional wear of Rubber (Zhang, 2004)	19
Figure 2.2-5: Wear mechanisms described for TPU materials (Martínez et al, 2010).....	20
Figure 3.2-1: a) Mettler Toledo DMA 861 SDTA, b) Tensile Device for DMA 861 SDTA.....	22
Figure 3.2-2: Testing procedure of DMA-analysis	23
Figure 3.2-3: Mettler Toledo DSC 822 ^e ; b) Testing Methodology for TPU analysis ..	24
Figure 3.3-1: a) Tribometer TE93, b) Test configuration TE 93 (schematically)	25
Figure 3.3-2: TE 93; Scheme of a) Frictional torque measuring at RoD-device, b) Temperature measuring	26

Figure 3.3-3: Geometrical optimization of RoD- specimen (schematically).....	27
Figure 3.3-4: Derived parameters from TE93 testing.....	28
Figure 3.3-5: Schematical demonstration of adjustment of specimen micrographs..	29
Figure 3.3-6: Schematical demonstration of adjustment of counterpart micrographs	30
Figure 3.3-7: Turning grooves at the filled TPU specimen.....	31
Figure 3.3-8: Turning grooves at the unfilled TPU specimen.....	31
Figure 3.3-9: Constant load test at 1 MPa and 100 rpm for TPU sealing materials ..	32
Figure 3.3-10: Schematical representation of a) load step tests, b) speed step tests	33
Figure 3.3-11: Schematical representation of gradual performance of a) load step tests, b) speed step tests.....	33
Figure 3.3-12: Review of tribological loading conditions on the TPU-sample in a RoD-testing configuration and their effect on failure	36
Figure 3.3-13: Assumptions made on the frictional heat accumulation in the rubbing contact for the tribological system at hand	39
Figure 3.3-14: Schematical PV-diagram for TPU seal materials.....	40
Figure 4.1-1: Frequency Sweeps at different temperatures for the a) filled b) unfilled TPU	42
Figure 4.1-2: Comparison of frequency sweeps of filled and unfilled TPU performed at room temperature	42
Figure 4.1-3: Temperature Sweeps for the filled and unfilled TPU performed at 2Hz	43
Figure 4.1-4: Temperature sweeps in dependency of the testing frequency for the a) filled, b) unfilled TPU system	44
Figure 4.1-5: DSC- measurement for TPU unfilled	46
Figure 4.1-6: DSC- measurement for TPU filled	46
Figure 4.2-1: Impact of geometrical improvements of the testing disc on the tribological profile of TPU unfilled; a) specimen RoD standard, b) specimen RoD BB	47

Figure 4.2-2: Impact of the improved upper bracket on the tribological profile at a speed step test of a) TPU unfilled and b) TPU filled	48
Figure 4.3-1: Constant load test ($p=1$ MPa, $v=100$ rpm, $t=4$ h) for a) TPU unfilled; b) TPU filled	49
Figure 4.3-2: Micrographs of unfilled specimen's wear track (Constant load test, $p=1$ MPa, $v=100$ rpm, $t=4$ h, Test No. 1)	50
Figure 4.3-3: Micrographs of counterpart's wear track (Constant load test, $p=1$ MPa, $v=100$ rpm, $t=4$ h, Test No. 1).....	50
Figure 4.3-4: Micrographs of filled specimen's wear track (Constant load test, $p=1$ MPa, $v=100$ rpm, $t=4$ h, Test No. 1)	51
Figure 4.3-5: Micrographs of counterpart's wear track (Constant load test, $p=1$ MPa, $v=100$ rpm, $t=4$ h, Test No. 1).....	51
Figure 4.4-1: a) exemplary load step test; b) assessment of contact pressure dependency for the unfilled TPU	53
Figure 4.4-2: Wear traces on counterpart of load step test at 200 rpm of TPU unfilled (Test No.1)	55
Figure 4.4-3: Gradually performed load step test of TPU unfilled at a testing speed of 100 rpm	56
Figure 4.4-4:a) exemplary load step test; b) assessment of contact pressure dependency for the filled TPU	56
Figure 4.4-5: Wear traces on counterpart of load step test at 100 rpm of TPU filled (Test No.1)	58
Figure 4.4-6: Gradually performed load step test of TPU filled at 100 rpm	58
Figure 4.4-7: a) exemplary speed step test; b) assessment of testing speed dependency for the unfilled TPU	60
Figure 4.4-8: Wear traces on counterpart of speed step test at 0,5 MPa of TPU unfilled (Test No. 2)	61
Figure 4.4-9: Gradually performed speed step test of TPU unfilled at a testing load of 1,0 MPa	62

Figure 4.4-10: a) exemplary speed step test; b) assessment of testing speed dependency for the filled TPU	62
Figure 4.4-11: Wear traces on counterpart of speed step test at 0,5 MPa of TPU filled (Test No.2)	64
Figure 4.4-12: Gradually performed speed step test of TPU filled at a testing load of 1,0 MPa	64
Figure 4.4-13: Overall review on PV-dependency based on step tests	66
Figure 4.4-14: Surface in manufacturing conditions (turning grooves); TPU unfilled	68
Figure 4.4-15: Mutations of surface layers at moderate PV-conditions; TPU unfilled	69
Figure 4.4-16: Mutations of surface layers at increased contact pressure conditions; TPU unfilled.....	70
Figure 4.4-17: Mutations of surface layers at increased sliding velocity conditions; TPU unfilled.....	71
Figure 4.4-18: Schematical demonstration of wear mechanisms investigated at tribological operation of TPU unfilled	72
Figure 4.4-19: Surface in manufacturing condition (turning grooves); TPU filled.....	73
Figure 4.4-20: Mutations of surface layers at moderate PV-conditions; TPU filled ...	74
Figure 4.4-21: Mutations of surface layers at increased contact pressure conditions; TPU filled.....	75
Figure 4.4-22: Mutations of surface layers at increased contact pressure conditions; TPU filled.....	76
Figure 4.4-23: Schematical demonstration of wear mechanisms investigated at tribological operation of TPU filled	77
Figure 4.5-1: Comparison of constant load tests at critical PV-settings.....	80
Figure 4.5-2: Advanced load step test of TPU filled, Test No. 1	82
Figure 4.5-3: Advanced speed step test of TPU filled, Test No. 1	83
Figure 4.5-4: Constant load test at extreme PV-settings, Test No. 1	83
Figure 4.5-5: „Membrane tearing“ as typical wear mechanism of TPU unfilled.....	85

Figure 4.5-6: PV-dependency of the surface formations for TPU unfilled	86
Figure 4.5-7: Dissection of a partially bearing or lubricating filler network during tribological performance of TPU filled.....	87
Figure 4.5-8: Advanced speed step test of TPU filled, Test No. 1	88
Figure 4.5-9: Advanced load step test of TPU filled, Test No. 1	88
Figure 4.5-10: exemplary thermal response of TPU unfilled (DSC-plot).....	89
Figure 4.5-11: Review on DMA-Temperature Sweeps of TPU filled/unfilled at a testing frequency of 2 Hz.....	89
Figure 4.5-12: Review of near surface temperatures for TPU filled /unfilled, averaged values from PV-step tests.....	90
Figure 4.5-13: Review of near surface temperatures for TPU filled, advanced PV-step tests.....	91
Figure 4.5-14: PV-diagram of TPU filled	94
Figure 4.5-15: PV-diagram of TPU unfilled	95
Figure 4.5-16: Review: PV-diagrams of TPU unfilled/ filled	96
Figure 4.5-1: Requirements for the testing methodology for tribological characterization of TPU seal materials	97
Figure 4.5-2: Overview of the developed benchmark testing methodology and application examples.....	99
Figure 4.5-1: Further feasible research based on benchmark testing methodology	101
Figure 8.4-1: Amplitude Sweeps of TPU filled and unfilled; a) at 2 and 100 Hz up to $s=30\ \mu\text{m}$, b) at 10 Hz up to $300\ \mu\text{m}$	122
Figure 8.4-2: Frequency Sweeps at different temperatures for the a) filled b) unfilled TPU	122
Figure 8.4-3: Temperature Sweeps for the unfilled TPU at a) 2 Hz, b) 20 Hz.....	123
Figure 8.4-4: Temperature Sweeps for the filled TPU at a) 2 Hz, b) 20 Hz	123
Figure 8.4-5: DSC- measurement for TPU unfilled (sample 1)	124
Figure 8.4-6: DSC- measurement for TPU unfilled (sample 2)	124

Figure 8.4-7: DSC- measurement for TPU filled (sample 1)	125
Figure 8.4-8: DSC- measurement for TPU filled (sample 2)	125
Figure 8.4-9: Constant load test (0,75 MPa, 100 rpm, 4 h), TPU unfilled, RoD standard, No.1	128
Figure 8.4-10: Constant load test (0,75 MPa, 100 rpm, 4 h), TPU unfilled, RoD standard, No.2	128
Figure 8.4-11: Constant load test (0,75 MPa, 100 rpm, 4h), TPU unfilled, RoD standard, No.3	129
Figure 8.4-12: Constant load test (0,75 MPa, 100 rpm, 4h), TPU unfilled, RoD standard, No.4	129
Figure 8.4-13: Constant load test (0,75 MPa, 100 rpm, 4h), TPU unfilled, RoD standard, No.5	130
Figure 8.4-14: Constant load test (0,75 MPa, 100 rpm, 4 h), TPU unfilled, RoD BB, No.1	130
Figure 8.4-15: Constant load test (0,75 MPa, 100 rpm, 4 h), TPU unfilled, RoD BB, No.2	131
Figure 8.4-16: Constant load test (0,75 MPa, 100 rpm, 4 h), TPU unfilled, RoD BB, No.3	131
Figure 8.4-17: RoD BB specimen	132
Figure 8.4-18: Socket flange of new specimen bracket	132
Figure 8.4-19: Upper specimen holder of new specimen bracket	133
Figure 8.4-20: Constant load test ($p=0,5$ MPa, $v=100$ rpm, $t=4$ h) for TPU unfilled, Test No. 1	135
Figure 8.4-21: Constant load test ($p=0,5$ MPa, $v=100$ rpm, $t=4$ h) for TPU unfilled, Test No. 2	135
Figure 8.4-22: Constant load test ($p=0,5$ MPa, $v=150$ rpm, $t=4$ h) for TPU unfilled, Test No. 1	136
Figure 8.4-23: Constant load test ($p=0,5$ MPa, $v=150$ rpm, $t=4$ h) for TPU unfilled, Test No. 2	136

Figure 8.4-24: Constant load test ($p=1,0$ MPa, $v=100$ rpm, $t=4$ h) for TPU unfilled, Test No. 1.....	137
Figure 8.4-25: Constant load test ($p=1,0$ MPa, $v=100$ rpm, $t=4$ h) for TPU unfilled, Test No. 2.....	137
Figure 8.4-26: Constant load test ($p=1$ MPa, $v=100$ rpm, $t=4$ h) for TPU filled, Test No. 1.....	139
Figure 8.4-27: Constant load test ($p=1$ MPa, $v=100$ rpm, $t=4$ h) for TPU filled, Test No. 2.....	139
Figure 8.4-28: Constant load test ($p=2,75$ MPa, $v=400$ rpm, $t=4$ h) for TPU filled, Test No. 1.....	140
Figure 8.4-29: Constant load test ($p=2,75$ MPa, $v=400$ rpm, $t=4$ h) for TPU filled, Test No. 2.....	140
Figure 8.4-30: Load Step test at 100 rpm of TPU unfilled, Test No.1	143
Figure 8.4-31: Load Step test at 100 rpm of TPU unfilled, Test No.2	143
Figure 8.4-32: Load Step test at 150 rpm of TPU unfilled, Test No.1	144
Figure 8.4-33: Load Step test at 150 rpm of TPU unfilled, Test No.2	144
Figure 8.4-34: Load Step test at 200 rpm of TPU unfilled, Test No.1	145
Figure 8.4-35: Load Step test at 200 rpm of TPU unfilled, Test No.2	145
Figure 8.4-36: Gradually performed load step test at 100 rpm of TPU unfilled, Step 1	147
Figure 8.4-37: Gradually performed load step test at 100 rpm of TPU unfilled, Step 2	147
Figure 8.4-38: Gradually performed load step test at 100 rpm of TPU unfilled, Step 3	148
Figure 8.4-39: Gradually performed load step test at 100 rpm of TPU unfilled, Step 4	148
Figure 8.4-40: Gradually performed load step test at 100 rpm of TPU unfilled, Step 5	149
Figure 8.4-41: Load Step test at 100 rpm of TPU filled, Test No.1	151

Figure 8.4-42: Load Step test at 100 rpm of TPU filled, Test No.2	152
Figure 8.4-43: Load Step test at 150 rpm of TPU filled, Test No.1	152
Figure 8.4-44: Load Step test at 150 rpm of TPU filled, Test No.2	153
Figure 8.4-45: Load Step test at 200 rpm of TPU filled, Test No.1	153
Figure 8.4-46: Load Step test at 200 rpm of TPU filled, Test No.2	154
Figure 8.4-47: Gradually performed load step test at 100 rpm of TPU filled, Step 1	156
Figure 8.4-48: Gradually performed load step test at 100 rpm of TPU filled, Step 2	156
Figure 8.4-49: Gradually performed load step test at 100 rpm of TPU filled, Step 3	157
Figure 8.4-50: Gradually performed load step test at 100 rpm of TPU filled, Step 4	157
Figure 8.4-51: Gradually performed load step test at 100 rpm of TPU filled, Step 5	158
Figure 8.4-52: Speed Step test at 0,5 MPa of TPU unfilled, Test No.1.....	161
Figure 8.4-53: Speed Step test at 0,5 MPa of TPU unfilled, Test No.2.....	161
Figure 8.4-54: Speed Step test at 1,0 MPa of TPU unfilled, Test No.1.....	162
Figure 8.4-55: Speed Step test at 1,0 MPa of TPU unfilled, Test No.2.....	162
Figure 8.4-56: Speed Step test at 1,5 MPa of TPU unfilled, Test No.1.....	163
Figure 8.4-57: Speed Step test at 1,5 MPa of TPU unfilled, Test No.2.....	163
Figure 8.4-58: Gradually performed speed step test at 1 MPa of TPU unfilled, Step 1	165
Figure 8.4-59: Gradually performed speed step test at 1 MPa of TPU unfilled, Step 2	165
Figure 8.4-60: Gradually performed speed step test at 1 MPa of TPU unfilled, Step 3	166
Figure 8.4-61: Gradually performed speed step test at 1 MPa of TPU unfilled, Step 4	166
Figure 8.4-62: Gradually performed speed step test at 1 MPa of TPU unfilled, Step 4 (old specimen bracket)	167
Figure 8.4-63: Speed Step test at 0,5 MPa of TPU filled, Test No.1.....	169

Figure 8.4-64: Speed Step test at 0,5 MPa of TPU filled, Test No.2.....	169
Figure 8.4-65: Speed Step test at 1,0 MPa of TPU filled, Test No.1.....	170
Figure 8.4-66: Speed Step test at 1,0 MPa of TPU filled, Test No.2.....	170
Figure 8.4-67: Speed Step test at 1,5 MPa of TPU filled, Test No.1.....	171
Figure 8.4-68: Speed Step test at 1,5 MPa of TPU filled, Test No.2.....	171
Figure 8.4-69: Gradually performed speed step test at 1 MPa of TPU filled, Step 1173	
Figure 8.4-70: Gradually performed speed step test at 1 MPa of TPU filled, Step 2173	
Figure 8.4-71: Gradually performed speed step test at 1 MPa of TPU filled, Step 3174	
Figure 8.4-72: Gradually performed speed step test at 1 MPa of TPU filled, Step 4174	
Figure 8.4-73: Gradually performed speed step test at 1 MPa of TPU filled, Step 4 (old specimen bracket)	175
Figure 8.4-74: Advanced Load Step test at 100 rpm of TPU filled, Test No.1	177
Figure 8.4-75: Advanced Load Step test at 100 rpm of TPU filled, Test No.2	177
Figure 8.4-76: Advanced Speed Step test at 1,0 MPa of TPU filled, Test No.1	179
Figure 8.4-77: Advanced Speed Step test at 1,0 MPa of TPU filled, Test No.2.....	179

8.2 List of Tables

Table 3.1-1: Overview of TPU unfilled and filled	21
Table 4.1-1: Comparison of the Results from Temperature Sweeps	44
Table 4.3-1: Evaluation of constant load ($p=1$ MPa, $v=100$ rpm) tests of TPU filled and unfilled	52
Table 4.4-1: Evaluation and exemplary contact surface micrographs of load step tests of TPU unfilled	54
Table 4.4-2: Evaluation and exemplary contact surface micrographs of load step tests of TPU filled	57
Table 4.4-3: Evaluation and exemplary contact surface micrographs of speed step tests of TPU unfilled	60
Table 4.4-4: Evaluation and exemplary contact surface micrographs of speed step tests of TPU filled	63
Table 4.4-5: Evaluation of COF, T and linear wear rate for selected PV-levels for TPU filled and unfilled	65
Table 4.5-1: Averaged results of PV-step tests of TPU unfilled	78
Table 4.5-2: Comparison of wear rate of TPU unfilled at critical PV-settings evaluated from different testing procedures	79
Table 4.5-3: Averaged results of PV-step tests of TPU filled	81
Table 4.5-4: Averaged results of advanced load step tests of TPU filled	82
Table 4.5-5: Averaged results of advanced speed step tests of TPU filled	82
Table 4.5-6: PV-application limit with regards on linear wear rate, frictional heat accumulation and surface mutations	92
Table 8.4-1: Comparison of the Results from Frequency Sweeps	123
Table 8.4-2: Comparison of Peak-Temperatures and Areas of DSC Measurements	126
Table 8.4-3: Evaluation of tribological performance of RoD standard and BB specimens	127

Table 8.4-4: Review of constant load tests of TPU unfilled	134
Table 8.4-5: Review of constant load tests of TPU filled	138
Table 8.4-6: Overview of the testing procedure of the load step test.....	141
Table 8.4-7: Summary of load step tests for the unfilled material	141
Table 8.4-8: Summary of gradually performed load step tests for the unfilled material	146
Table 8.4-9: Summary of load step tests for the filled material	150
Table 8.4-10: Summary of gradually performed load step tests for the filled material	155
Table 8.4-11: Overview of the testing procedure of the speed step test.....	159
Table 8.4-12: Summary of speed step tests for the unfilled material	159
Table 8.4-13: Summary of gradually performed speed step tests for the unfilled TPU	164
Table 8.4-14: Summary of speed step tests for the filled material	167
Table 8.4-15: Summary of gradually performed speed step tests for the filled material	172
Table 8.4-16: Overview of the testing procedure of the advanced load step test ...	176
Table 8.4-17: Summary of advanced load step tests for the filled material	176
Table 8.4-18: Overview of the testing procedure of the advanced speed step test	178
Table 8.4-19: Summary of advanced speed step tests for the filled material	178

8.3 List of Abbreviations

avg.....	average value
COF.....	coefficient of friction
dev.....	standard deviation
DMA.....	dynamical mechanical analysis
DSC.....	differential scanning calorimetry
E^*	complex E-modulus [MPa]
E'	storage modulus [MPa]
E''	loss modulus [MPa]
e_F^*	apparent frictional energy density [J/mm ³]
F.....	normal load [N]
f.....	testing frequency [Hz]
F_F, F_R	frictional force [N]
FKM.....	Fluoro-elastomer
HNBR.....	Hydrated Nitrile-Butadien-Rubber
i.d.....	inner diameter
K.....	wear rate [cm ³ /(Nm)]
lve.....	linear viscoelastic
M.....	frictional torque[N]
MVQ.....	Methyl-Vinyl-Silicone rubber
NBR.....	Nitrile-Butadien-Rubber
o.d.....	outer diameter
P,p.....	contact pressure at tribological tests [MPa]
PoD.....	Pin on Disc-Configuration
R_a	center line average roughness [μm]
revs.....	revisions [-]

RoD	Ring on Disc- Configuration
s.....	amplitude at DMA analysis [%, μm]
s.....	sliding distance at tribological tests [m]
T	testing temperature [$^{\circ}\text{C}$]
$\tan\delta$	loss factor
TPU	thermoplastic polyurethane elastomer
V, v	sliding velocity at tribological tests [rpm]
W_F	frictional work [J]
W_h	linear wear [μm]
W_m	gravimetric wear [mg]
W_v	volumetric wear [mm^3]
Z.....	linear wear [μm]
τ_F	frictional shear stress [MPa]

8.4 Table of Context

8.4.1 DMA-Analysis

Amplitude Sweeps

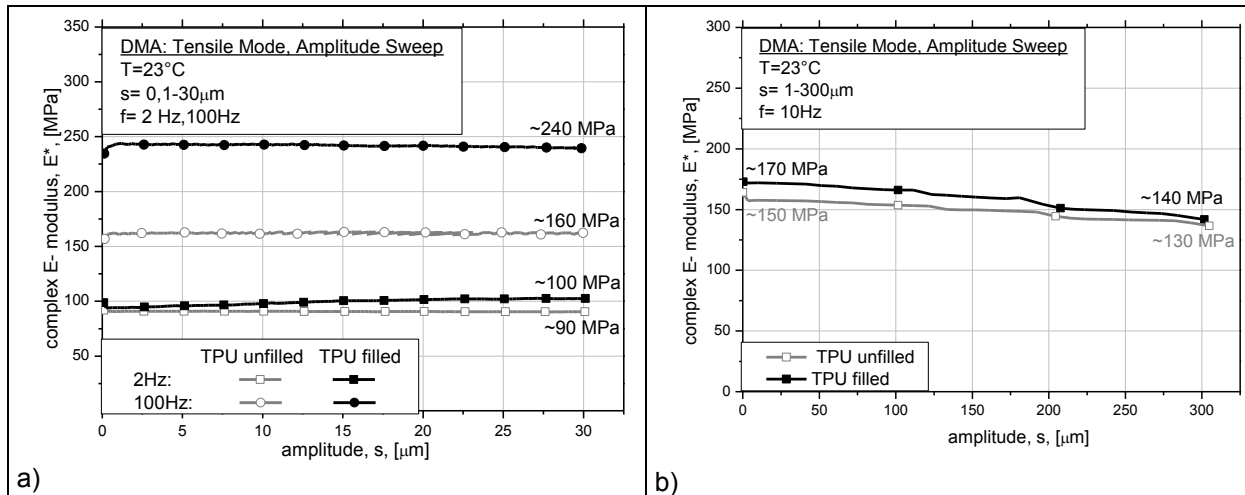


Figure 8.4-1: Amplitude Sweeps of TPU filled and unfilled; a) at 2 and 100 Hz up to $s=30 \mu\text{m}$, b) at 10 Hz up to $300 \mu\text{m}$

Frequency Sweeps

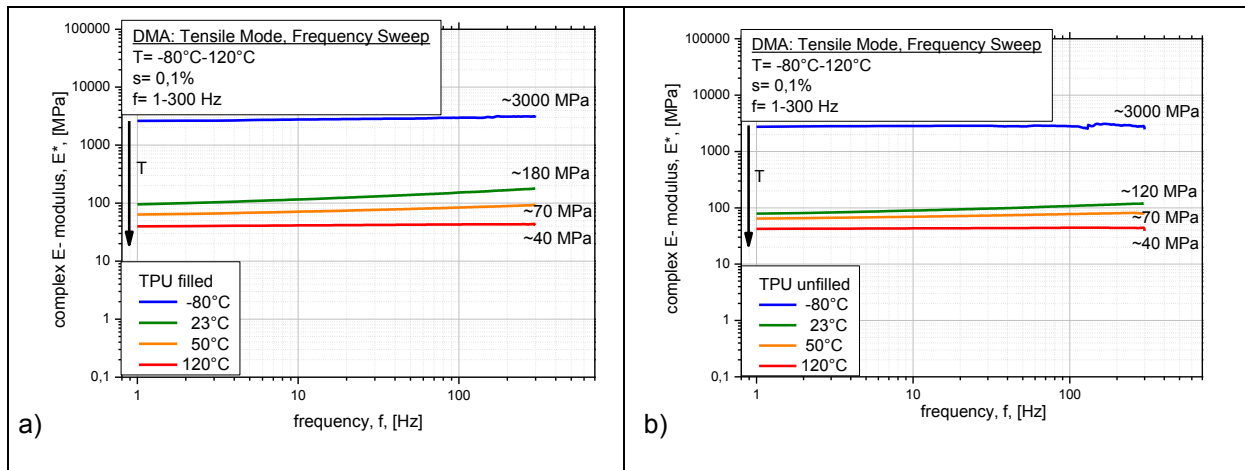


Figure 8.4-2: Frequency Sweeps at different temperatures for the a) filled b) unfilled TPU

Temperature Sweeps

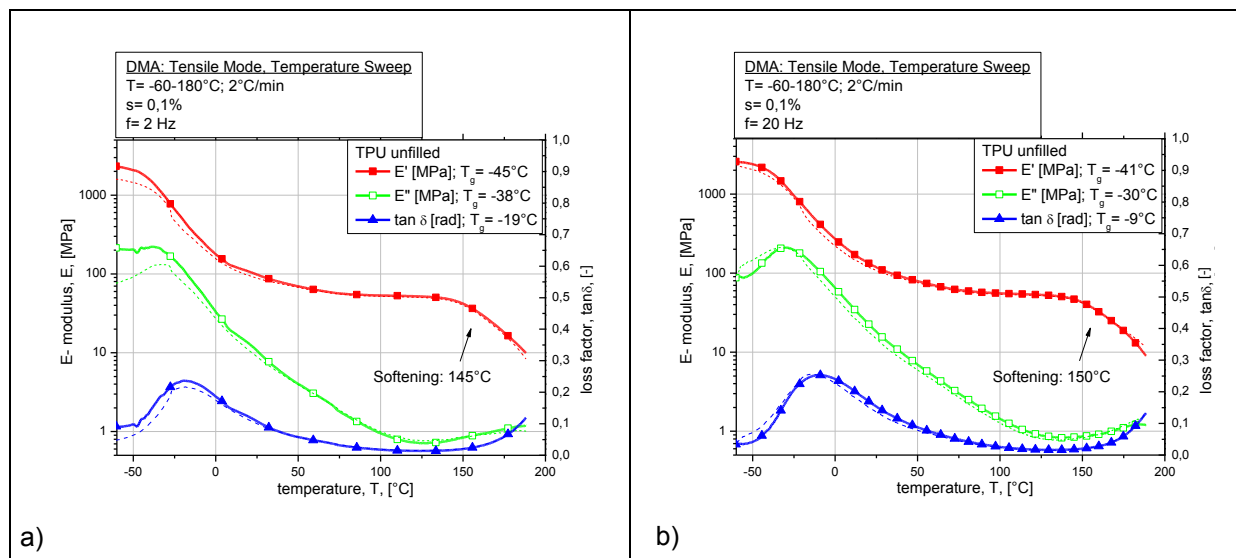


Figure 8.4-3: Temperature Sweeps for the unfilled TPU at a) 2 Hz, b) 20 Hz

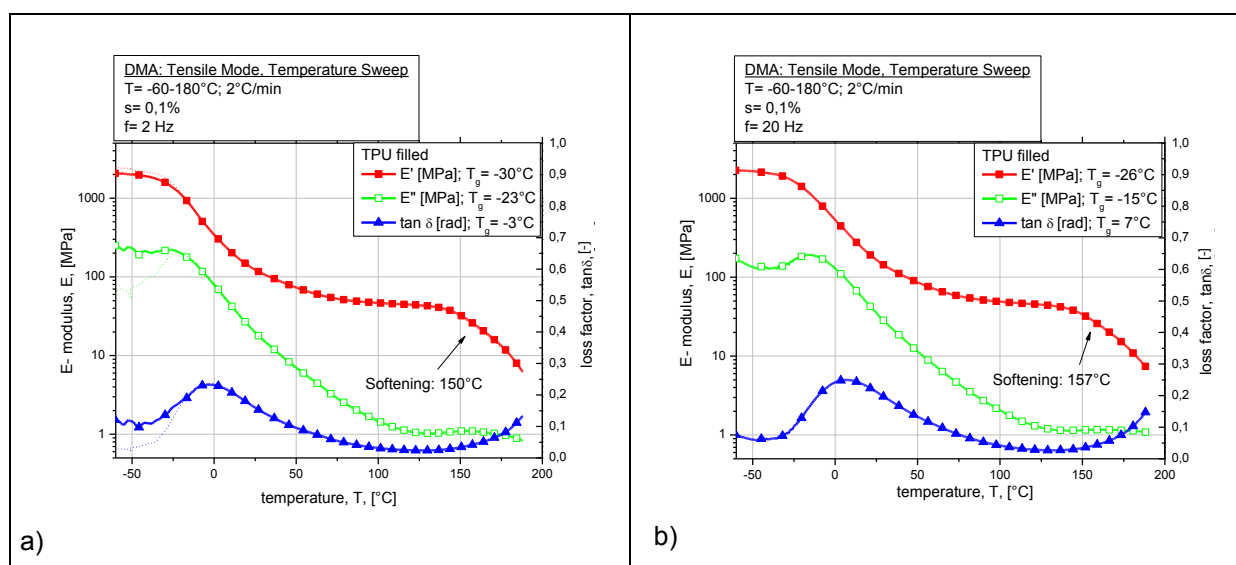


Figure 8.4-4: Temperature Sweeps for the filled TPU at a) 2 Hz, b) 20 Hz

Table 8.4-1: Comparison of the Results from Frequency Sweeps

Material		TPU unfilled		TPU filled	
		2 Hz	20 Hz	2 Hz	20 Hz
Glass Transition (E')	[°C]	-45	-41	-30	-26
Glass Transition (E'')	[°C]	-38	-30	-22	-15
E'_{\max}	[MPa]	210	207	200	190
Glass Transition ($\tan \delta$)	[°C]	-19	-9	-3	7
$\tan \delta_{\max}$	[-]	0,25	0,25	0,24	0,25
Softening	[°C]	145	150	151	157

8.4.2 DSC-measurements

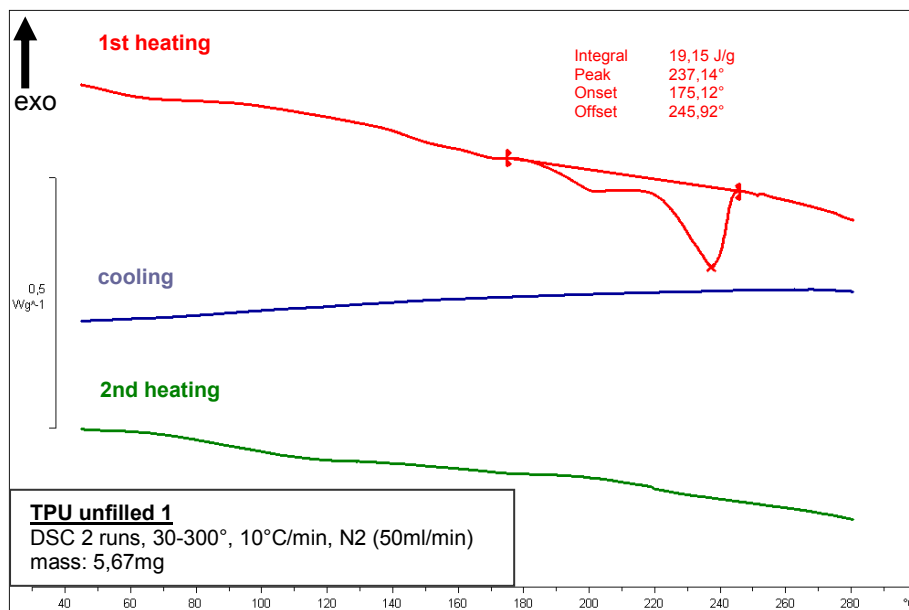


Figure 8.4-5: DSC- measurement for TPU unfilled (sample 1)

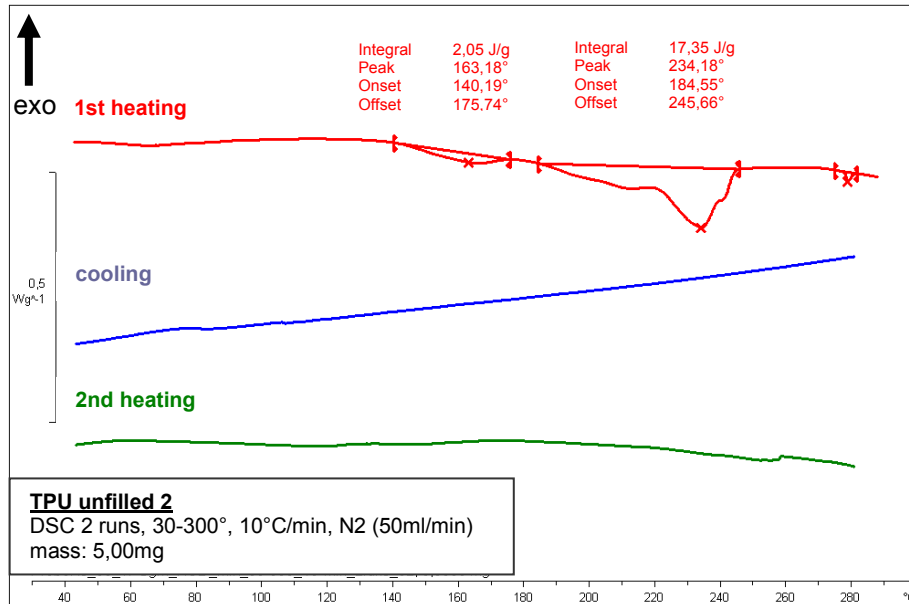


Figure 8.4-6: DSC- measurement for TPU unfilled (sample 2)

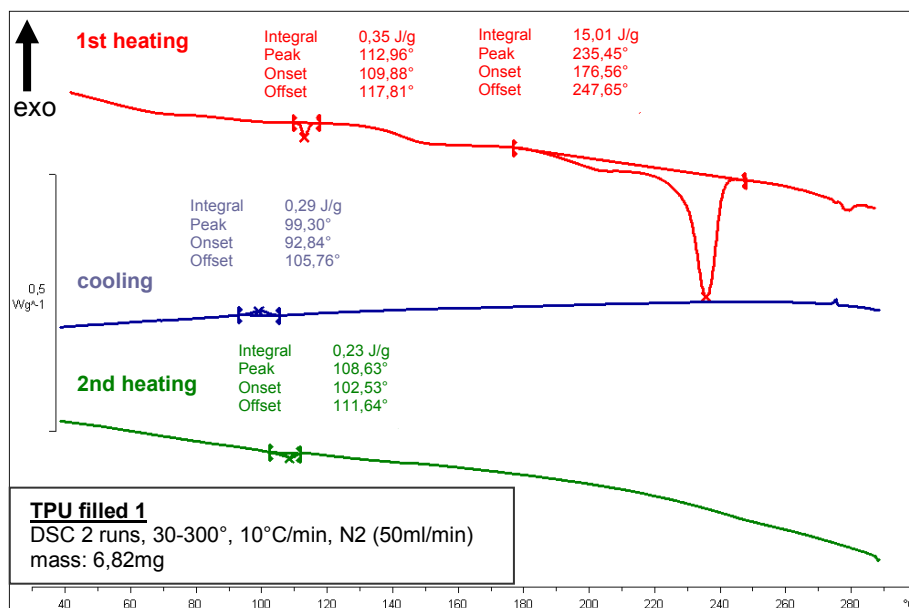


Figure 8.4-7: DSC- measurement for TPU filled (sample 1)

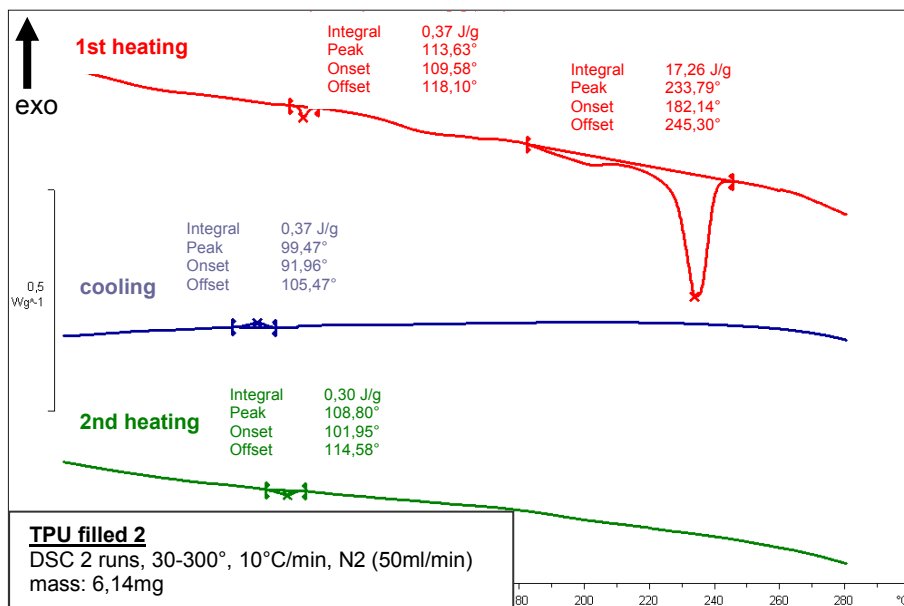


Figure 8.4-8: DSC- measurement for TPU filled (sample 2)

Table 8.4-2: Comparison of Peak-Temperatures and Areas of DSC Measurements

Material	No	Mass [mg]			1st heating		1st cooling	2nd heating	Notes
					~100 °C	~240 °C	~100 °C	~100 °C	
TPU filled	1	6,82	Peak-temp.	[°C]	112,96	235,45	99,30	108,63	
			Peak-area	[J/g]	0,35	15,01	0,29	0,23	
			Process	-	paracrystalline melting	crystalline melting	recrystallization	paracrystalline melting	
TPU filled	2	6,14	Peak-temp.	[°C]	113,63	233,79	99,47	108,80	
			Peak-area	[J/g]	0,37	17,26	0,37	0,30	
			Process	-	paracrystalline melting	crystalline melting	recrystallization	paracrystalline melting	
TPU unfilled	1	5,67	Peak-temp.	[°C]		237,14			
			Peak-area	[J/g]		19,15			
			Process	-		crystalline melting			
TPU unfilled	2	5,00	Peak-temp.	[°C]		234,18			further paracrystalline melting
			Peak-area	[J/g]		17,35			
			Process	-		crystalline melting			

8.4.3 Development and Adaptation of the ASTM D3702 Testing methodology for TPU materials

Tribological Assessment of the geometrical optimization of the specimen

Table 8.4-3: Evaluation of tribological performance of RoD standard and BB specimens

TPU unfilled		RoD standard specimen					RoD BB specimen		
		I	II	III	IV	V	I	II	III
Material Parameters									
Density	[g/cm ³]	1,20							
Test parameters									
Run in track	[m]	53,87							
Run in time	[s]	360,00							
Run in load	[N]	100,00	100,00	100,00	100,00	100,00	125,00	125,00	125,00
Run in speed	[rpm]	100,00							
Testing sliding distance	[m]	2155,00							
Testing time	[h]	4,00							
Testing force	[N]	100,00	100,00	100,00	100,00	100,00	125,00	125,00	125,00
Contact pressure	[MPa]	0,75							
Testing speed	[rpm]	100,00							
Testing temperature	[°C]	23,00							
Lubrication		dry							
Wear parameters									
Actual sliding distance	[m]	2155,00	2155,00	2155,00	2155,00	2155,00	2155,00	2155,00	2155,00
Mass loss	[mg]	101,55	101,33	298,22	290,32	199,91	207,45	193,02	249,44
Worn specimen height	[µm]	509,07	626,34	1843,34	1794,51	1235,67	1014,58	944,01	1219,94
Worn volume	[mm ³]	84,63	84,44	248,52	241,93	166,59	168,66	156,93	202,80
Wear rate K	[cm ³ /Nm]	3,93E-07	3,92E-07	1,15E-06	1,12E-06	7,73E-07	6,42E-07	5,97E-07	7,72E-07
Wear resistance	[Nm/cm ³]	2,55E+06	2,55E+06	8,67E+05	8,91E+05	1,29E+06	1,56E+06	1,67E+06	1,30E+06
Wear intensity	[mm ³ /m]	3,93E-02	3,92E-02	1,15E-01	1,12E-01	7,73E-02	7,83E-02	7,28E-02	9,41E-02
Linear wear intensity	[mm/m]	2,36E-04	2,91E-04	8,55E-04	8,33E-04	5,73E-04	4,71E-04	4,38E-04	5,66E-04
Friction Parameters									
COF	[-]	1,33	1,38	1,35	1,40	1,50	1,27	1,23	1,24
Frictional work	[J]	285793,37	297032,41	297780,43	299368,38	327031,34	325227,94	314009,76	306357,05
Near surface temperature	[°C]	not measured	not measured	not measured	not measured	not measured	not measured	not measured	not measured
Counterpart temperature	[°C]	not measured	not measured	not measured	not measured	not measured	not measured	not measured	not measured
Combined Parameters									
Frictional energy density	[J/mm ³]	3377,17	3517,60	1198,23	1237,40	1963,07	1928,32	2000,99	1510,66
Frictional shear stress	[N/mm ²]	0,80	1,02	1,02	1,03	1,13	0,91	0,88	0,86

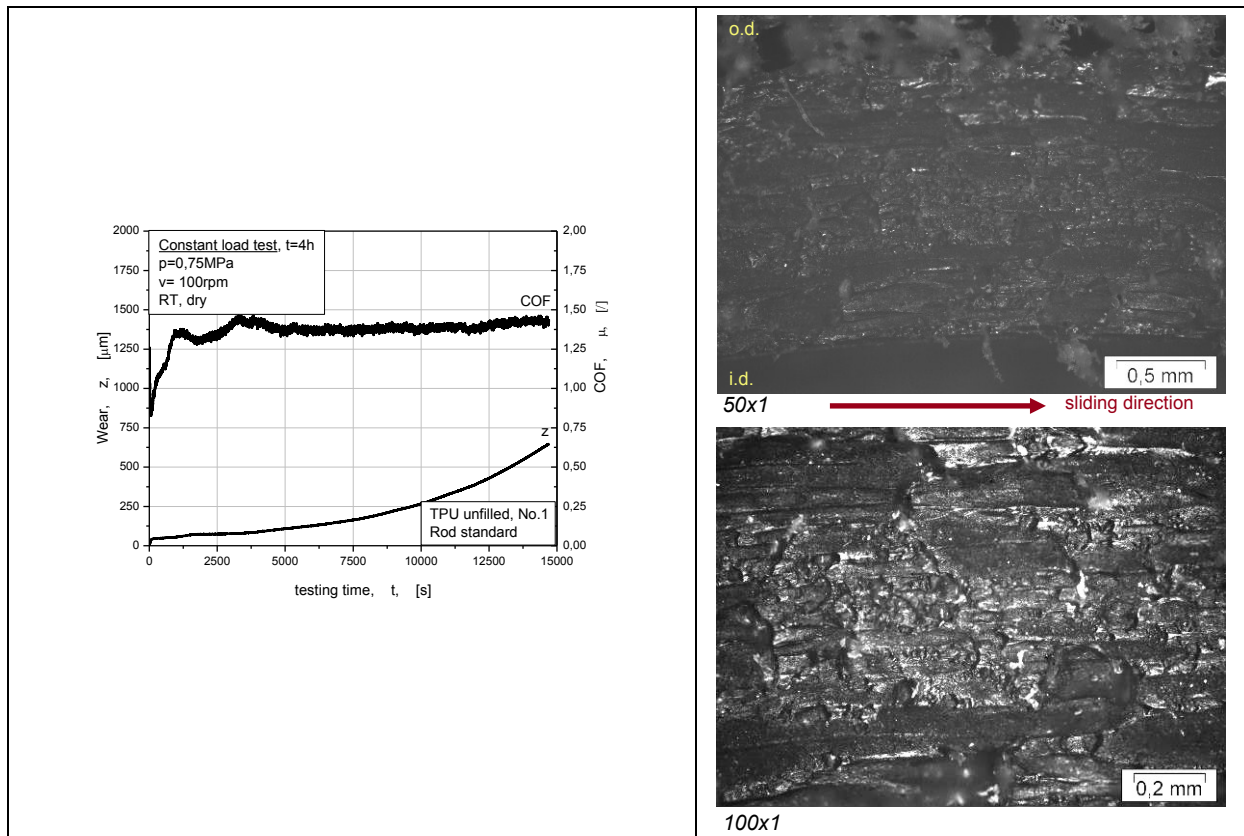


Figure 8.4-9: Constant load test (0,75 MPa, 100 rpm, 4 h), TPU unfilled, RoD standard, No.1

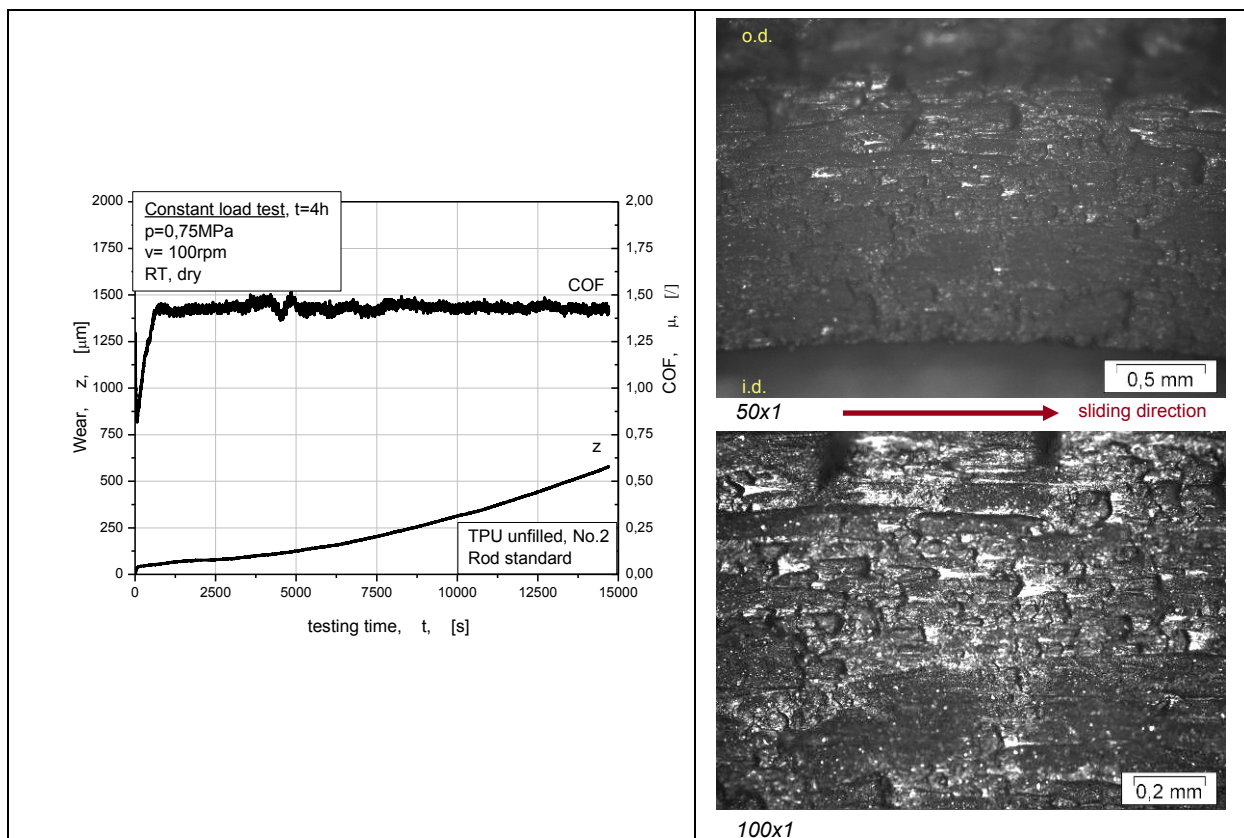


Figure 8.4-10: Constant load test (0,75 MPa, 100 rpm, 4 h), TPU unfilled, RoD standard, No.2

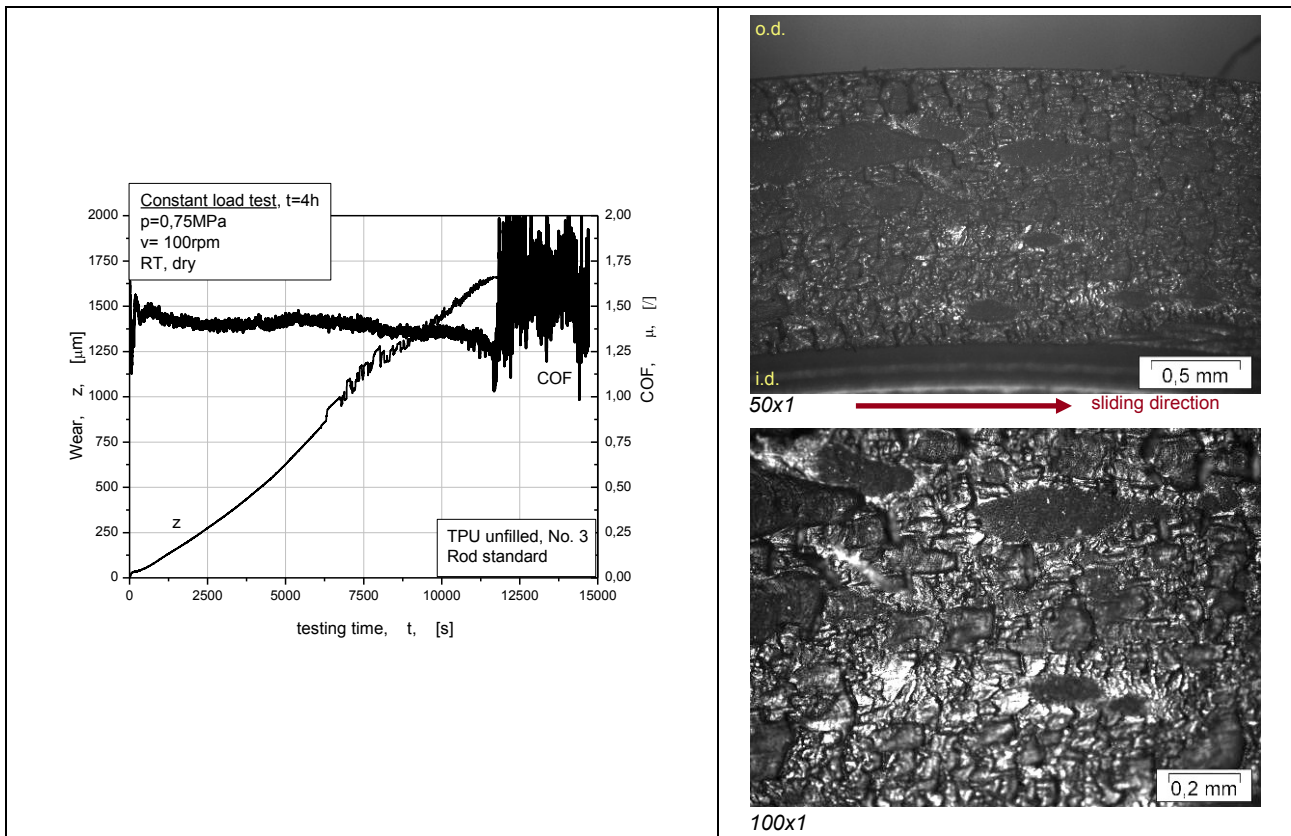


Figure 8.4-11: Constant load test (0,75 MPa, 100 rpm, 4h), TPU unfilled, RoD standard, No.3

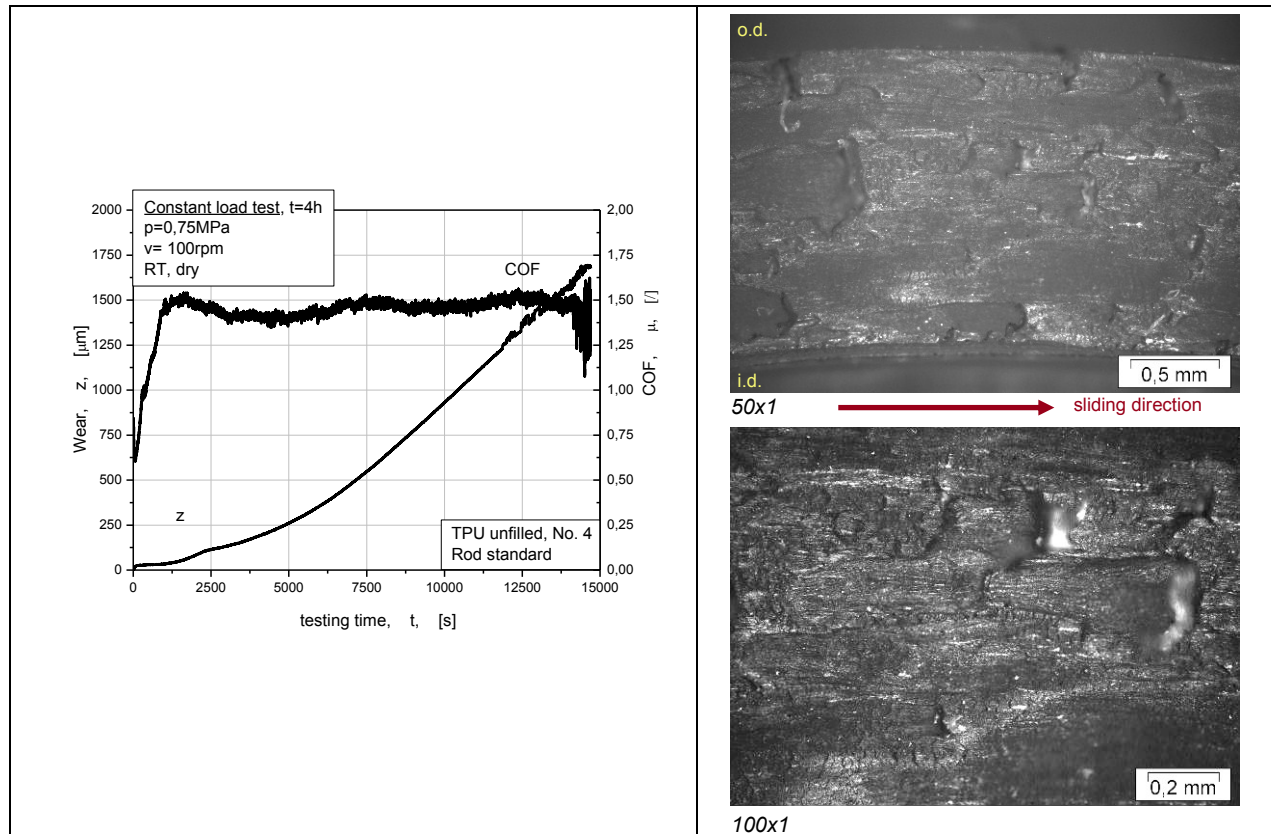


Figure 8.4-12: Constant load test (0,75 MPa, 100 rpm, 4h), TPU unfilled, RoD standard, No.4

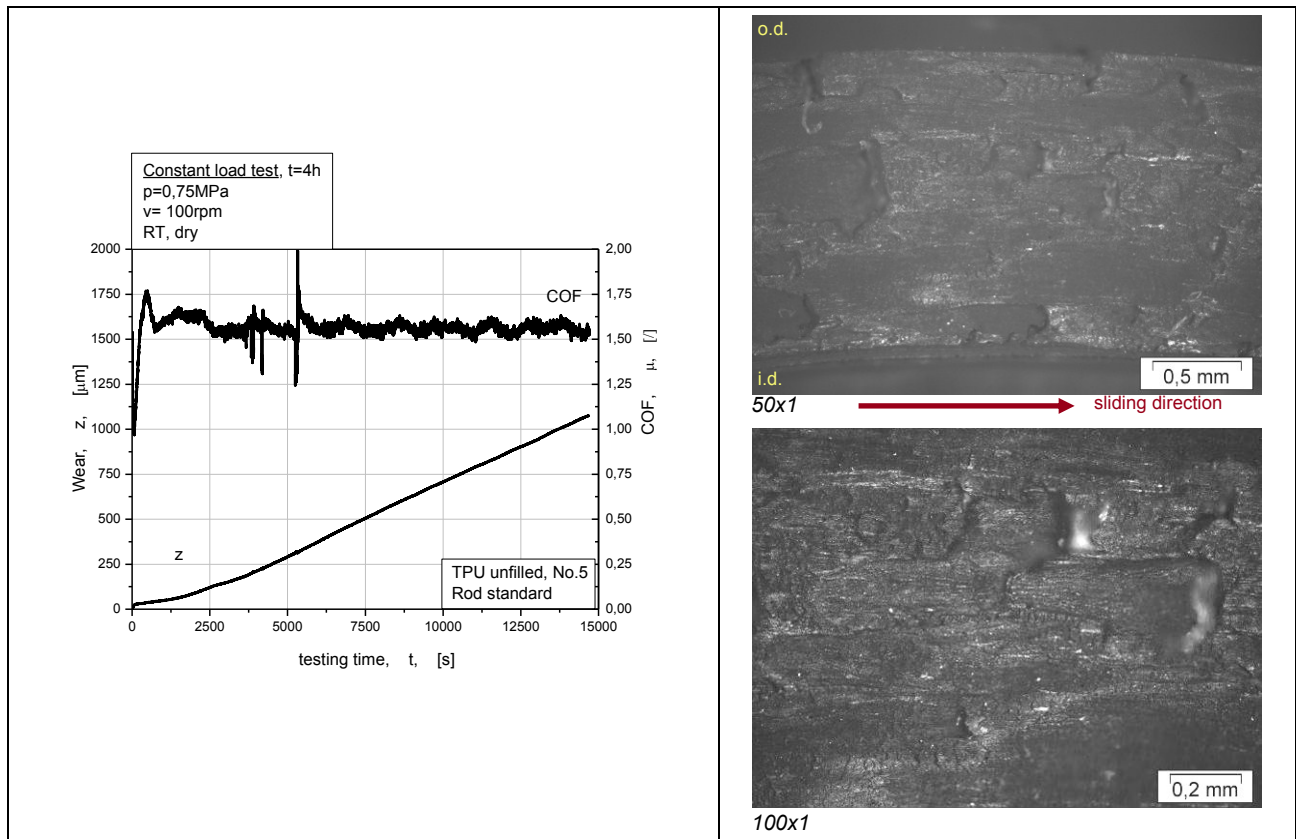


Figure 8.4-13: Constant load test (0,75 MPa, 100 rpm, 4h), TPU unfilled, RoD standard, No.5

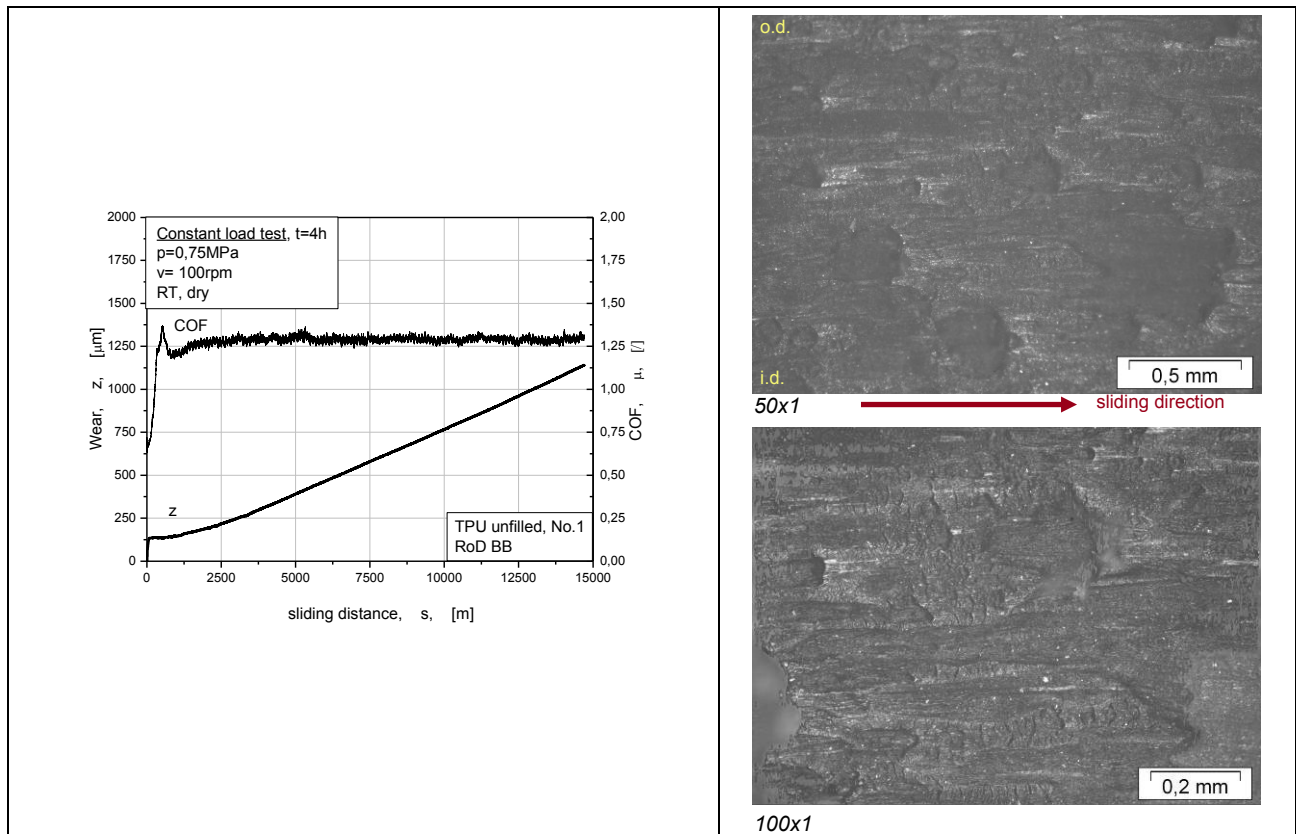


Figure 8.4-14: Constant load test (0,75 MPa, 100 rpm, 4 h), TPU unfilled, RoD BB, No.1

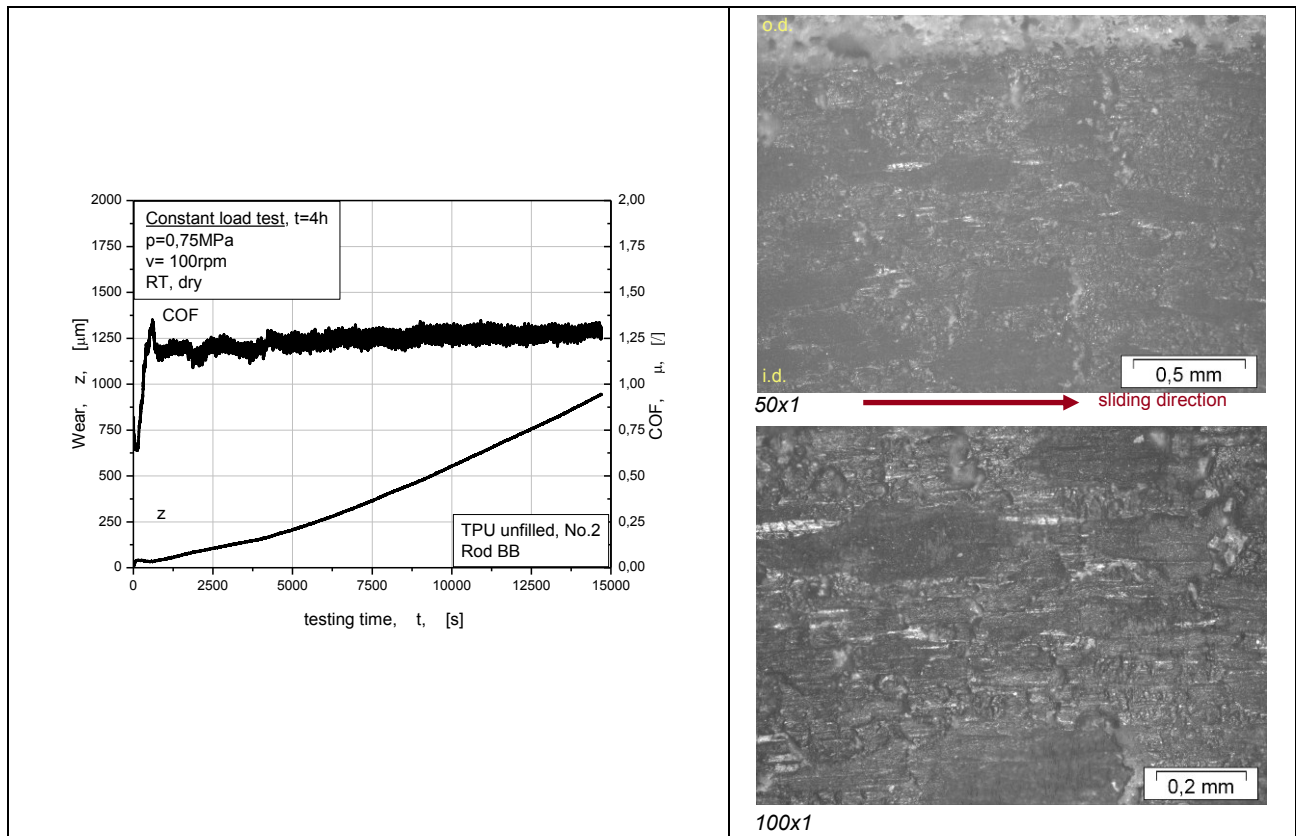


Figure 8.4-15: Constant load test (0,75 MPa, 100 rpm, 4 h), TPU unfilled, RoD BB, No.2

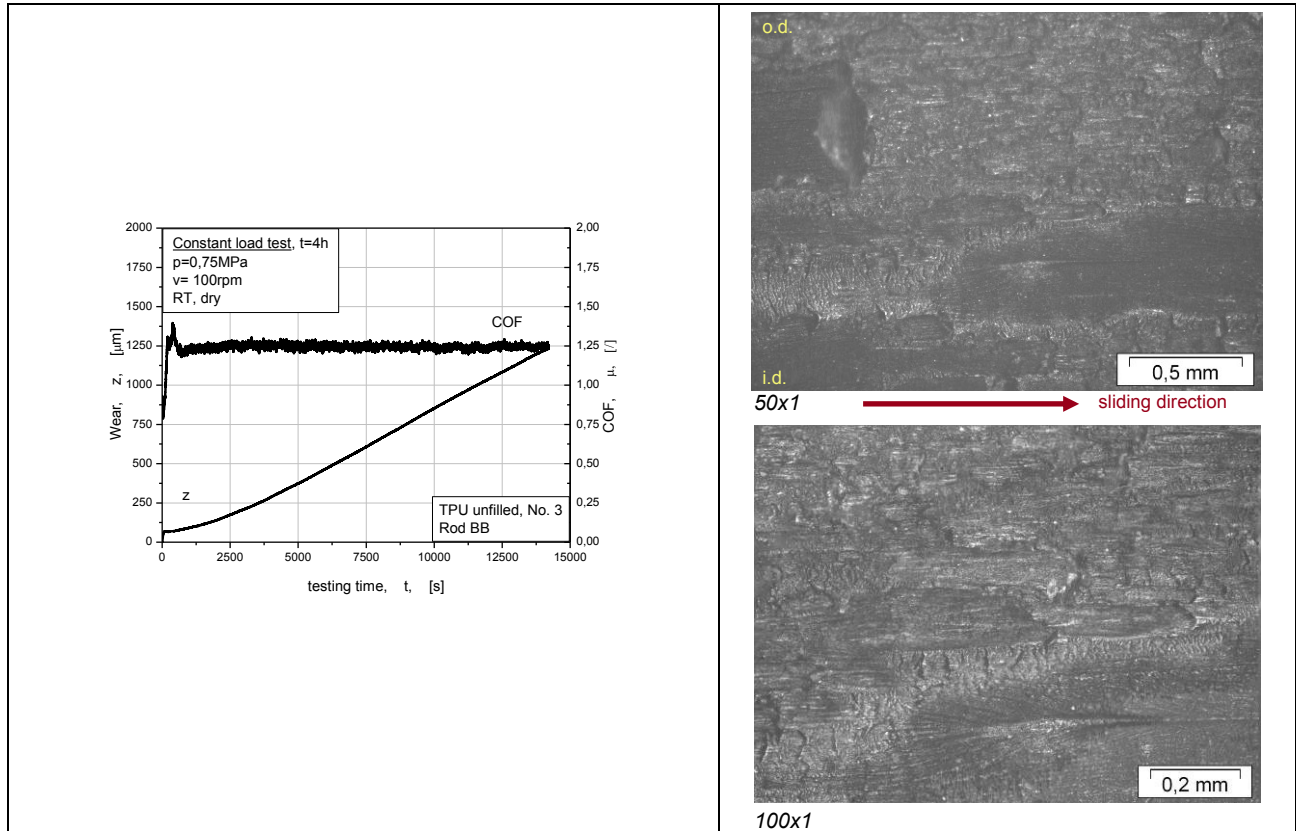


Figure 8.4-16: Constant load test (0,75 MPa, 100 rpm, 4 h), TPU unfilled, RoD BB, No.3

Engineering drawing of the optimized specimen

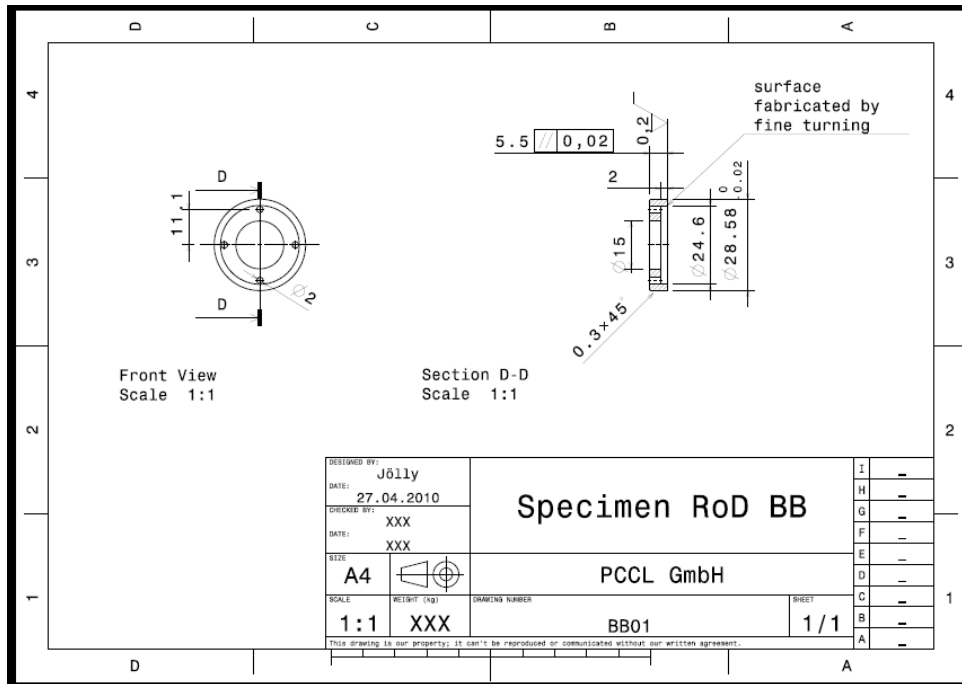


Figure 8.4-17: RoD BB specimen

Engineering drawings of improved specimen holder

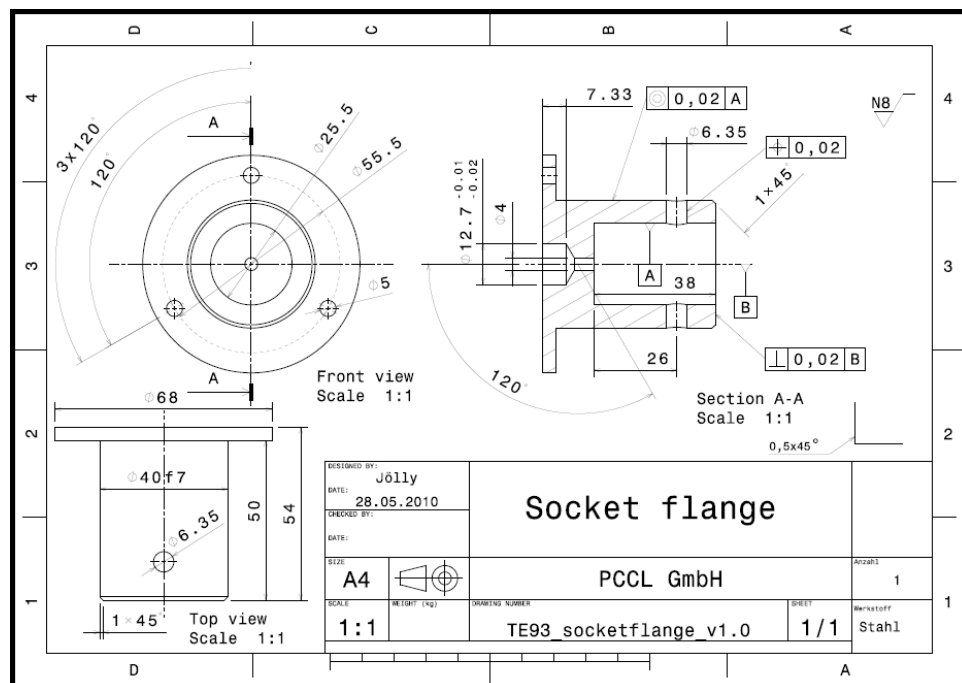


Figure 8.4-18: Socket flange of new specimen bracket

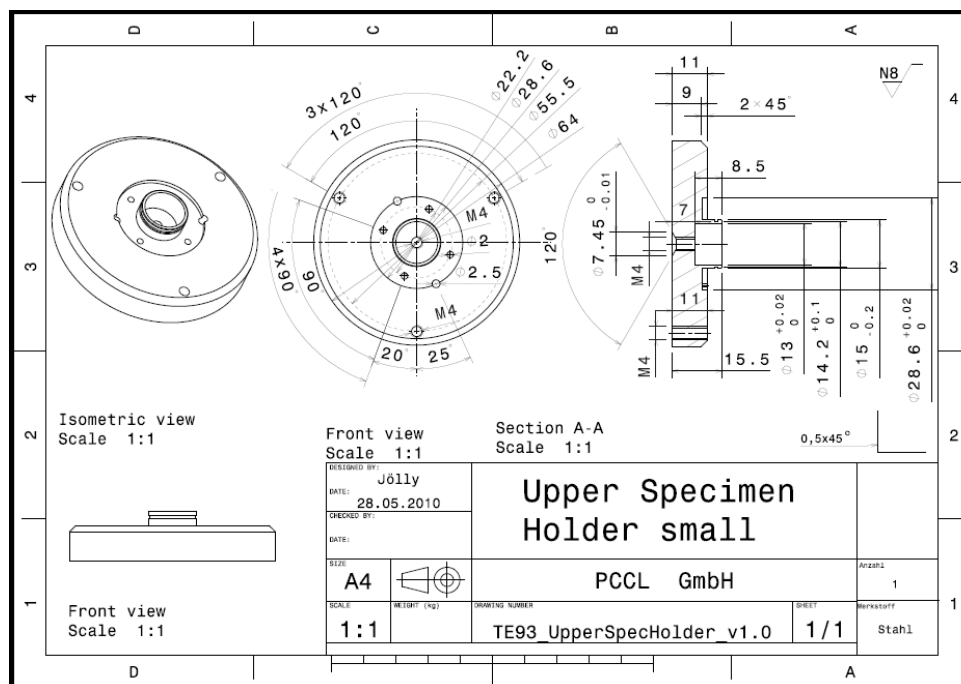


Figure 8.4-19: Upper specimen holder of new specimen bracket

Impact of improved test configuration on materials' tribological performance

The speed step tests to assess the impact of the new specimen holder are shown in 8.4.6. within the framework of a more detailed evaluation of those tests.

8.4.4 Standard tribological characterization- Constant load tests

Constant load tests of TPU unfilled

Table 8.4-4: Review of constant load tests of TPU unfilled

Constant load test TPU unfilled		p=0,5 MPa, v=100 rpm		p=0,5 MPa, v=150 rpm		p=1,0 MPa, v=100 rpm	
		I	II	I	II	I	II
Material Parameters							
Density	[g/cm ³]	1,20	1,20	1,20	1,20	1,20	1,20
Test parameters							
Run in track	[m]	45,00		45,00		45,00	
Run in time	[s]	600,00		600,00		600,00	
Run in load	[N]	50,00		50,00		50,00	
Run in speed	[rpm]	50,00		50,00		50,00	
Testing sliding distance	[m]	2155,00	2155,00	3232,32	3232,32	2155,00	2155,00
Testing time	[h]	4,00		4,00		4,00	
Testing force	[N]	83,00	83,00	83,00	83,00	166,00	166,00
Contact pressure	[MPa]	0,50	0,50	0,50	0,50	1,00	1,00
Testing speed	[rpm]	100,00	100,00	150,00	150,00	100,00	100,00
Testing temperature	[°C]	23,00		23,00		23,00	
Lubrication		dry		dry		dry	
Wear parameters							
Actual sliding distance	[m]	2219,10	2220,20	2333,60	2450,70	1091,60	1513,20
Mass loss	[mg]	69,36	83,29	290,33	330,00	288,41	313,94
Worn specimen height	[µm]	347,70	417,53	1455,42	1654,29	1445,80	1573,78
Worn volume	[mm ³]	57,80	69,41	241,94	275,00	240,34	261,62
Wear rate K	[cm ³ /Nm]	3,14E-07	3,77E-07	1,25E-06	1,35E-06	1,33E-06	1,04E-06
Wear resistance	[Nm/cm ³]	3,19E+06	2,65E+06	8,01E+05	7,40E+05	7,54E+05	9,60E+05
Wear intensity	[mm ³ /m]	2,60E-02	3,13E-02	1,04E-01	1,12E-01	2,20E-01	1,73E-01
Linear wear intensity	[mm/m]	1,57E-04	1,88E-04	6,24E-04	6,75E-04	1,32E-03	1,04E-03
Friction Parameters							
COF	[-]	1,01	1,07	1,49	1,34	1,12	1,06
Frictional work	[J]	190651,01	202449,11	276407,42	268333,31	181122,28	257323,61
Near surface temperature	[°C]	66,23	68,64	102,07	98,58	100,39	99,77
Counterpart temperature	[°C]	54,91	50,42	66,53	73,46	75,09	61,28
Combined Parameters							
Frictional energy density	[J/mm ³]	3298,46	2916,78	1142,45	975,76	753,60	983,59
Frictional shear stress	[N/mm ²]	0,52	0,55	0,71	0,66	1,00	1,02

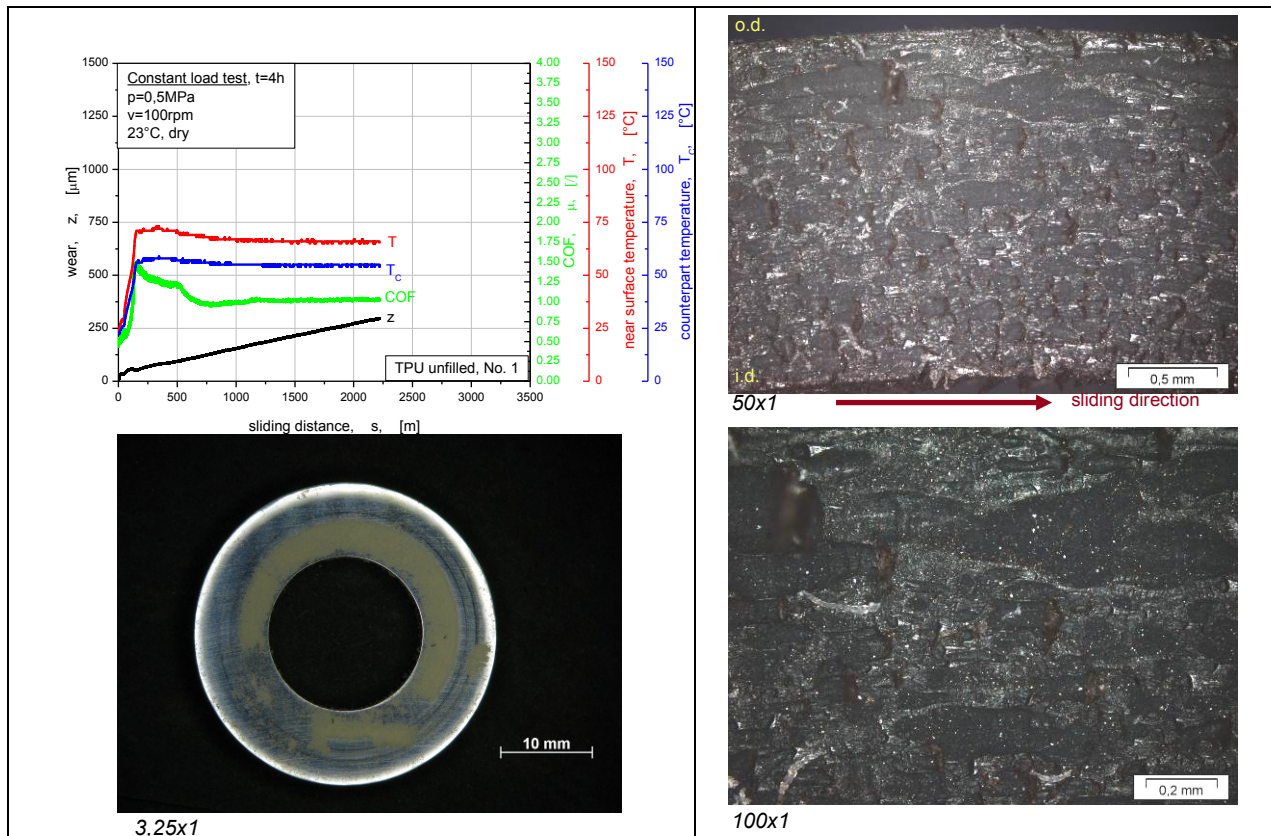


Figure 8.4-20: Constant load test ($p=0,5\text{ MPa}$, $v=100\text{ rpm}$, $t=4\text{ h}$) for TPU unfilled, Test No. 1

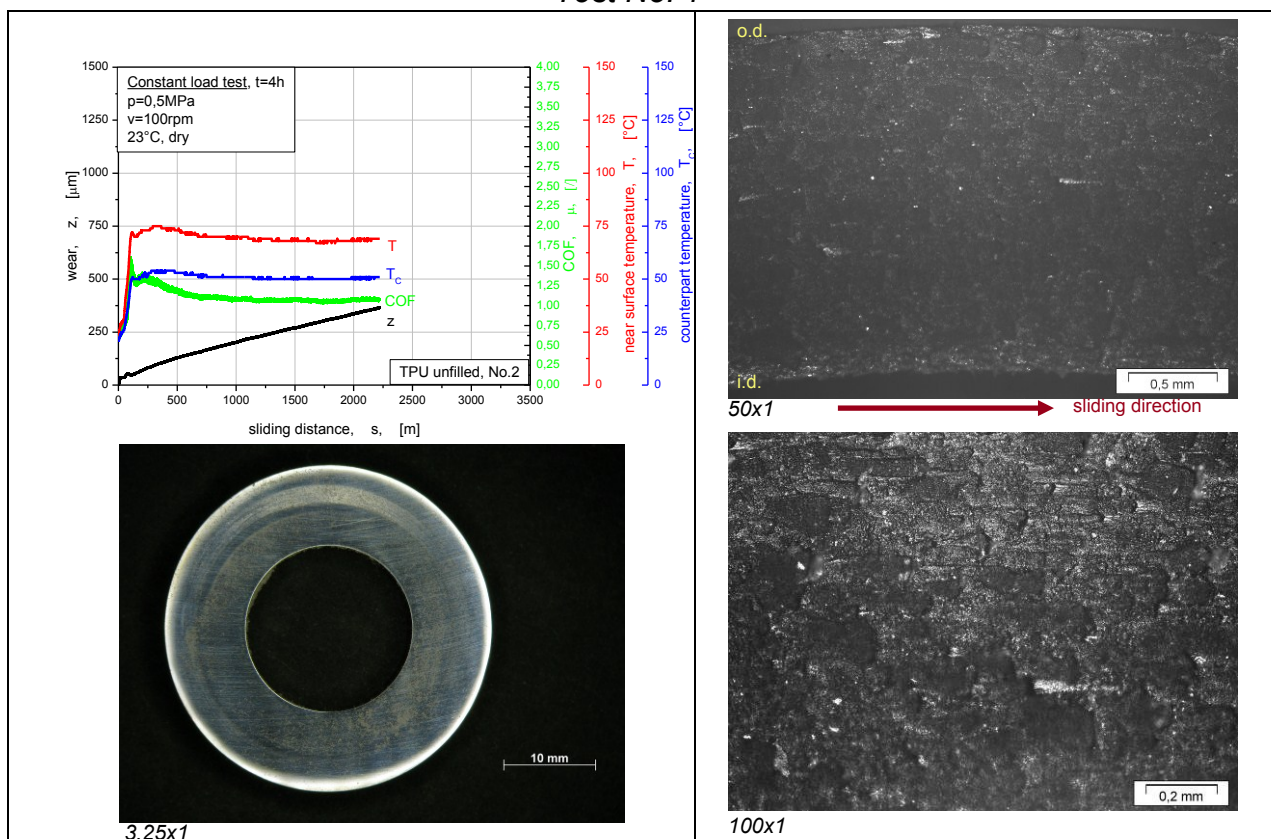


Figure 8.4-21: Constant load test ($p=0,5\text{ MPa}$, $v=100\text{ rpm}$, $t=4\text{ h}$) for TPU unfilled, Test No. 2

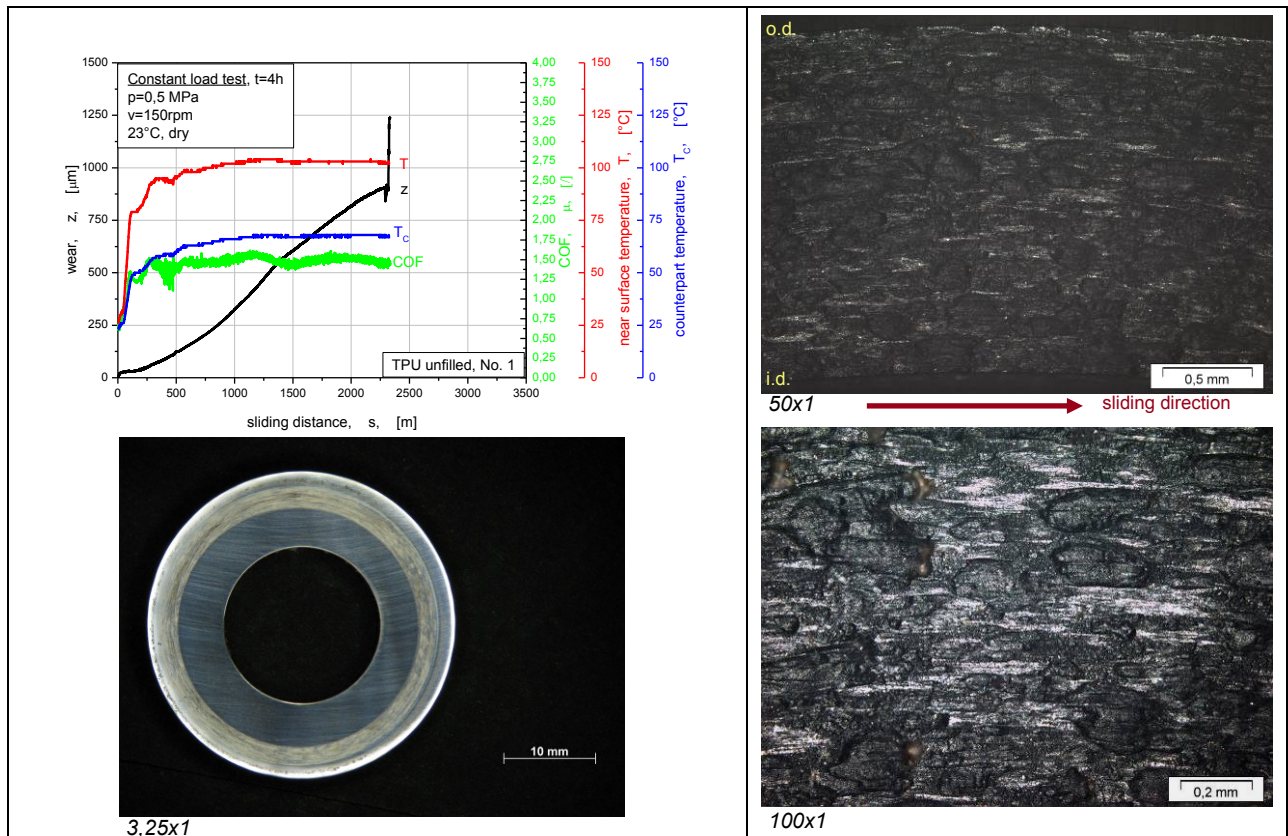


Figure 8.4-22: Constant load test ($p=0,5\text{ MPa}$, $v=150\text{ rpm}$, $t=4\text{ h}$) for TPU unfilled, Test No. 1

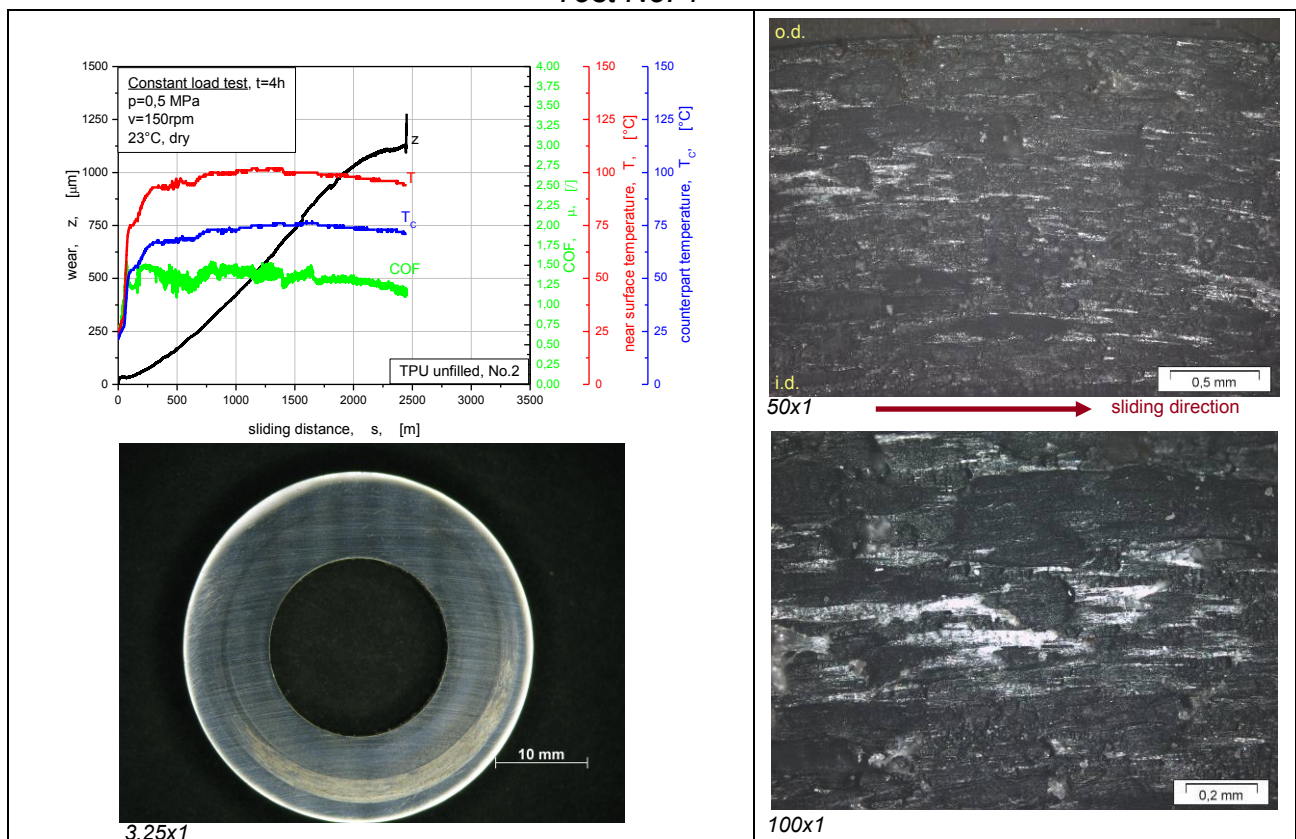


Figure 8.4-23: Constant load test ($p=0,5\text{ MPa}$, $v=150\text{ rpm}$, $t=4\text{ h}$) for TPU unfilled, Test No. 2

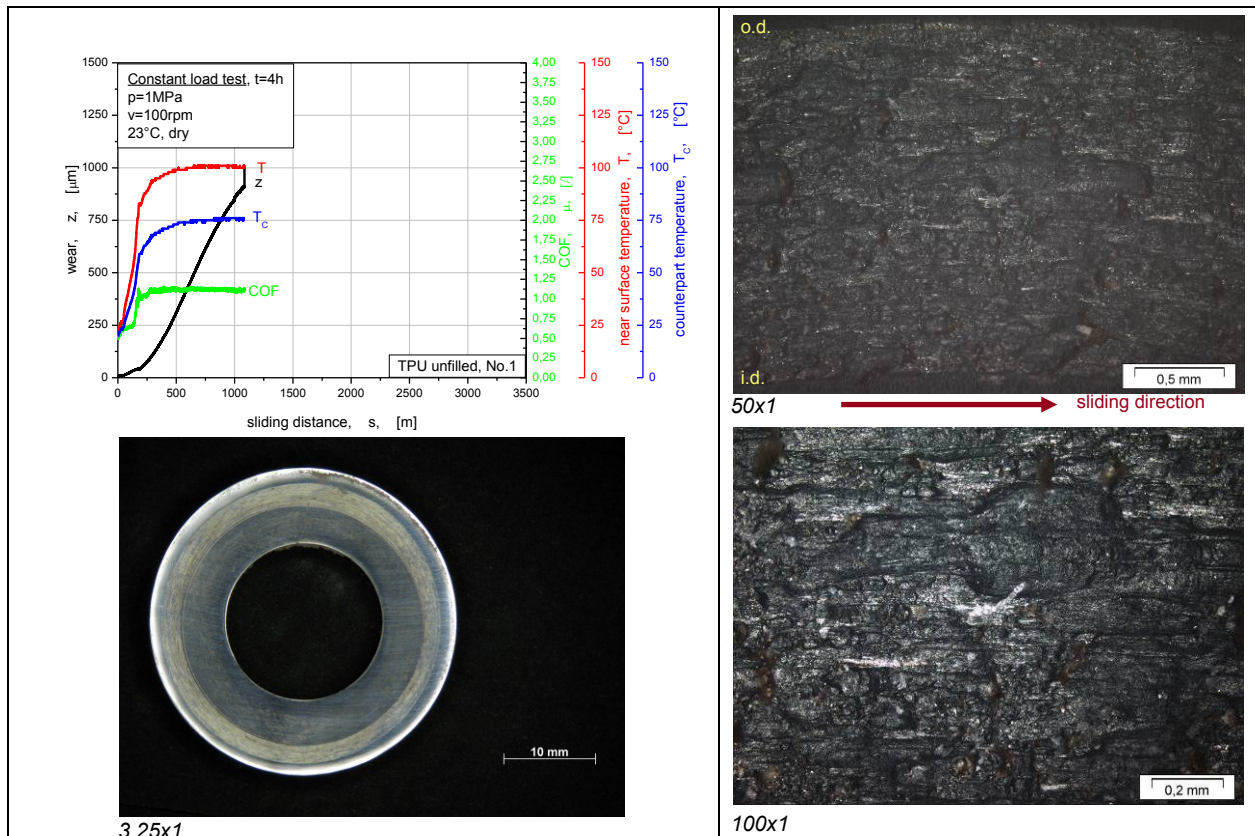


Figure 8.4-24: Constant load test ($p=1,0\text{ MPa}$, $v=100\text{ rpm}$, $t=4\text{ h}$) for TPU unfilled, Test No. 1

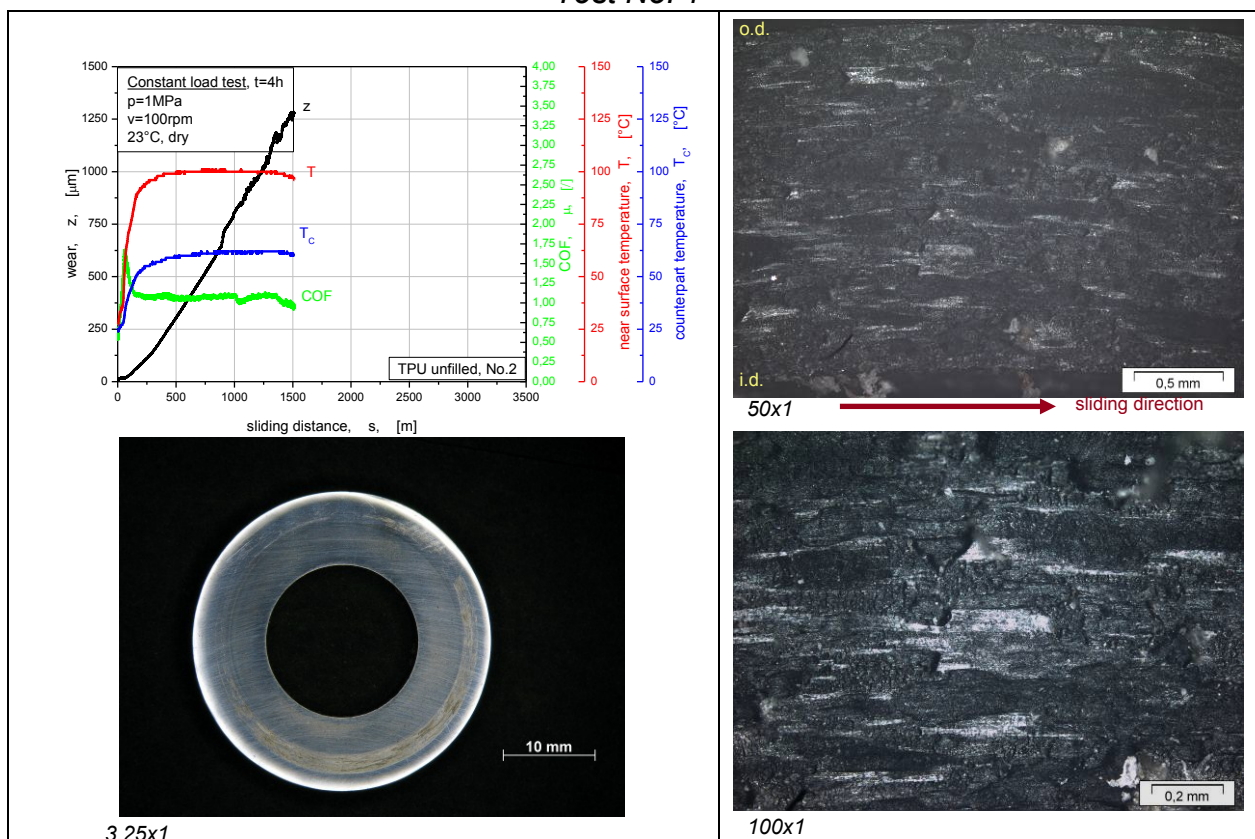


Figure 8.4-25: Constant load test ($p=1,0\text{ MPa}$, $v=100\text{ rpm}$, $t=4\text{ h}$) for TPU unfilled, Test No. 2

Constant load tests of TPU filled

Table 8.4-5: Review of constant load tests of TPU filled

Constant load test TPU filled		p=1MPa, v=100rpm		p=2,75MPa, v=400rpm	
		I	II	I	II
Material Parameters					
Density	[g/cm ³]	1,23	1,23	1,23	1,23
Test parameters					
Run in track	[m]	45,00		45,00	
Run in time	[s]	600,00		600,00	
Run in load	[N]	50,00		50,00	
Run in speed	[rpm]	50,00		50,00	
Testing sliding distance	[m]	2155,00		2155,00	
Testing time	[h]	4,00		4,00	
Testing force	[N]	166,00	166,00	461,00	461,00
Contact pressure	[MPa]	1,00		1,00	
Testing speed	[rpm]	100,00		400,00	
Testing temperature	[°C]	23,00		23,00	
Lubrication		dry		dry	
Wear parameters					
Actual sliding distance	[m]	2293,00	2295,00	1311,00	568,00
Mass loss	[mg]	2,61	3,49	179,77	196,52
Worn specimen height	[µm]	12,76	17,07	879,21	961,13
Worn volume	[mm ³]	2,12	2,84	146,15	159,77
Wear rate K	[cm ³ /Nm]	5,57E-09	7,45E-09	2,42E-07	6,10E-07
Wear resistance	[Nm/cm ³]	1,79E+08	1,34E+08	4,14E+06	1,64E+06
Wear intensity	[mm ³ /m]	9,25E-04	1,24E-03	1,11E-01	2,81E-01
Linear wear intensity	[mm/m]	5,57E-06	7,44E-06	6,71E-04	1,69E-03
Friction Parameters					
COF	[-]	0,90	0,90	0,36	0,32
Frictional work	[J]	339870,11	343868,61	111657,84	94310,14
Near surface temperature	[°C]	93,57	88,62	155,00	162,00
Counterpart temperature	[°C]	73,83	71,13	108,00	108,00
Combined Parameters					
Frictional energy density	[J/mm ³]	160168,67	121191,51	763,97	590,28
Frictional shear stress	[N/mm ²]	0,89	0,90	0,51	1,00

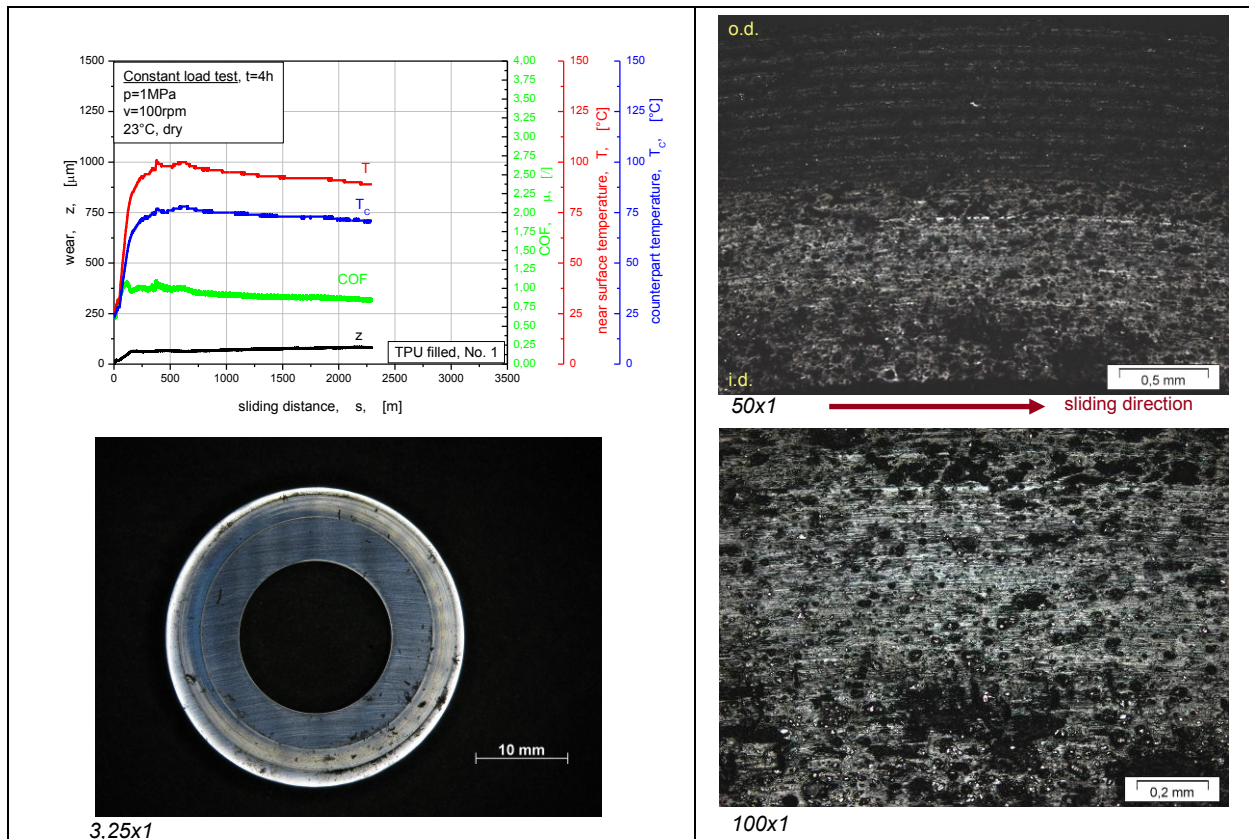


Figure 8.4-26: Constant load test ($p=1\text{ MPa}$, $v=100\text{ rpm}$, $t=4\text{ h}$) for TPU filled, Test No. 1

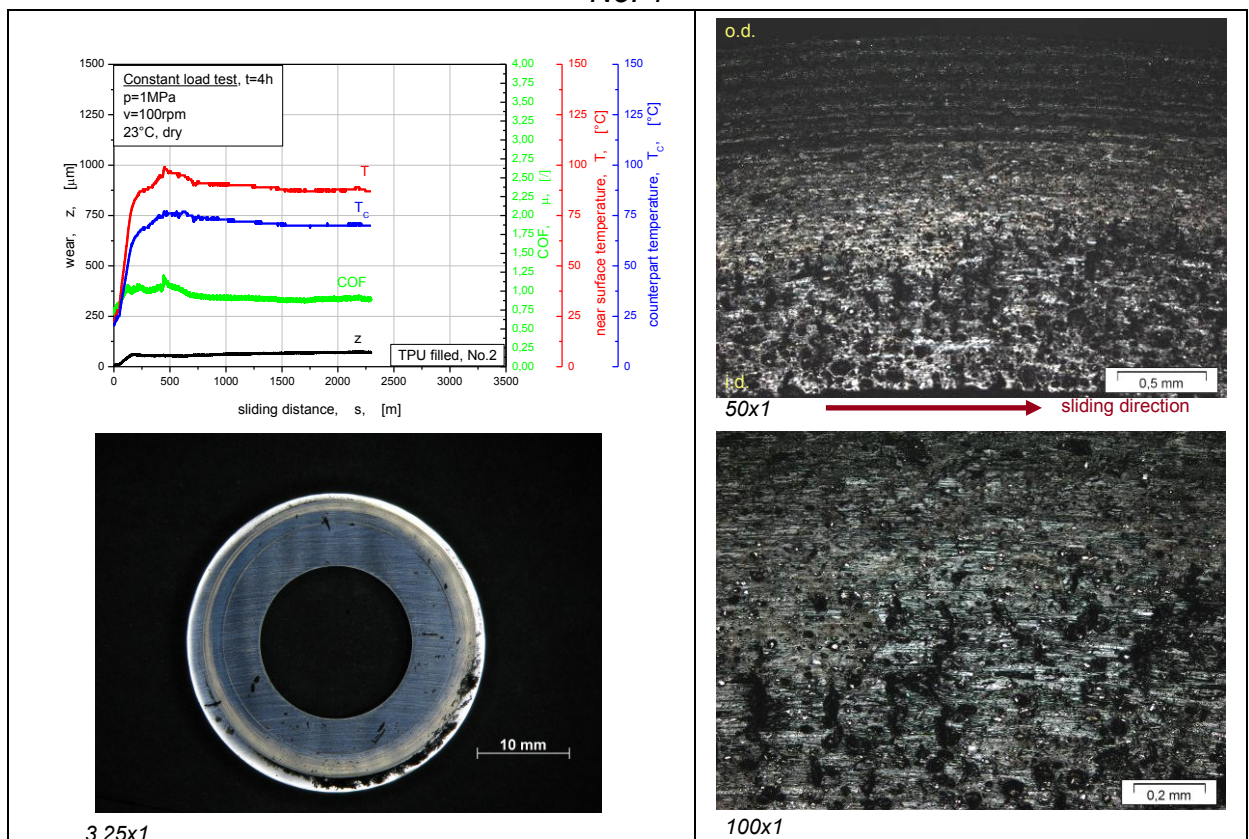


Figure 8.4-27: Constant load test ($p=1\text{ MPa}$, $v=100\text{ rpm}$, $t=4\text{ h}$) for TPU filled, Test No. 2

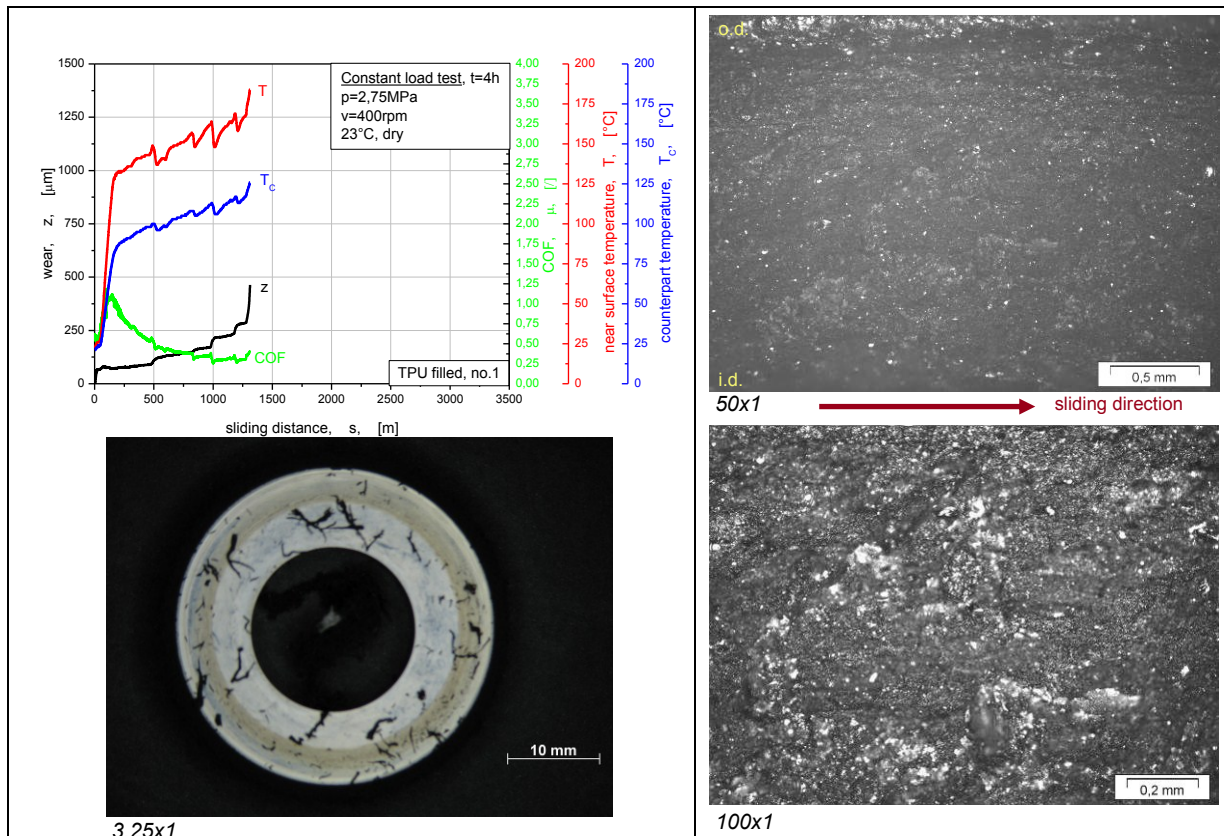


Figure 8.4-28: Constant load test ($p=2,75\text{MPa}$, $v=400\text{rpm}$, $t=4\text{h}$) for TPU filled, Test No. 1

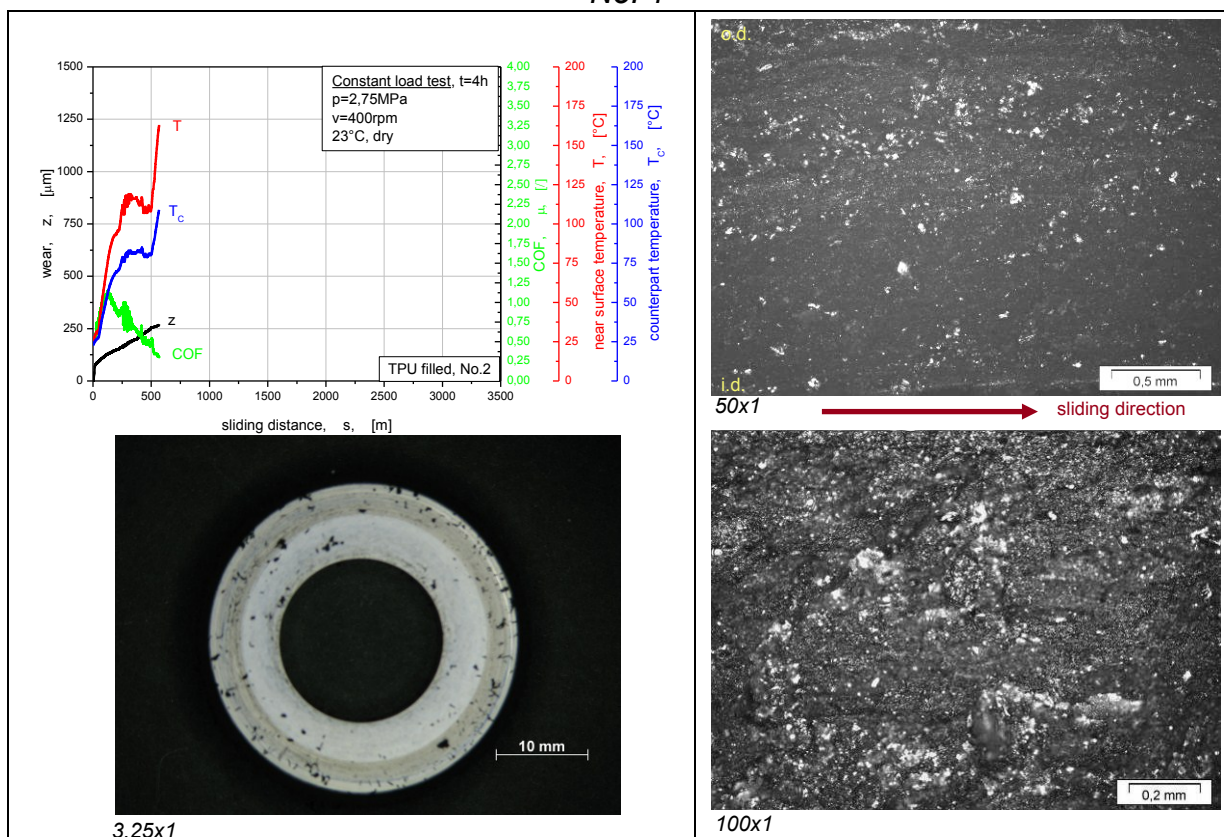


Figure 8.4-29: Constant load test ($p=2,75\text{MPa}$, $v=400\text{rpm}$, $t=4\text{h}$) for TPU filled, Test No. 2

8.4.5 Load step tests

Table 8.4-6: Overview of the testing procedure of the load step test

Load step test TPU unfilled/filled							
Test Parameters							
Step		Run in	1	2	3	4	5
Ramp time	[s]	x	1030,00	1260,00	1260,00	1260,00	1260,00
Ramp distance	[m]	x	154,10	188,30	188,30	188,30	188,30
Testing force	[N]	50,00	83,00	125,00	166,00	208,00	250,00
Contact pressure	[MPa]	0,30	0,50	0,75	1,00	1,25	1,50
Testing speed	[rpm]	50,00	100/150/200				
Step length	[Revs]	x	6000,00				
Step distance	[m]	44,50	539,00	539,00	539,00	539,00	539,00
Testing temperature	[°C]	23,00					
Lubrication		dry					

Load step tests of the unfilled material

Table 8.4-7: Summary of load step tests for the unfilled material

Load Step Test TPU unfilled, 100 rpm, No. 1		0,5 MPa	0,75 MPa	1,00 MPa	1,25 MPa	1,50 MPa
Wear Parameters						
mass loss	[mg]	325,00				
overall wear rate K	[cm ³ /Nm]	7,22E-07				
linear wear rate	[µm/m]	0,00	0,16	0,80	1,04	1,04
Friction Parameters						
COF	[-]	1,31	1,00	0,88	0,79	0,71
near surface temperature	[°C]	65,04	74,94	83,12	88,45	89,95
counterpart temperature	[°C]	56,56	65,32	72,10	77,04	77,04
Load Step Test TPU unfilled, 100 rpm, No. 2		0,5 MPa	0,75 MPa	1,00 MPa	1,25 MPa	1,50 MPa
Wear Parameters						
mass loss	[mg]	332,00				
overall wear rate K	[cm ³ /Nm]	7,76E-07				
linear wear rate	[µm/m]	0,08	0,25	0,88	0,88	0,88
Friction Parameters						
COF	[-]	1,31	0,96	0,87	0,74	0,65
near surface temperature	[°C]	70,76	76,25	86,32	90,41	91,54
counterpart temperature	[°C]	63,29	68,72	76,63	80,23	81,77
Load Step Test TPU unfilled, 150 rpm, No. 1		0,5 MPa	0,75 MPa	1,00 MPa	1,25 MPa	1,50 MPa
Wear Parameters						
mass loss	[mg]	325,00				
overall wear rate K	[cm ³ /Nm]	8,62E-07				
linear wear rate	[µm/m]	0,17	0,70	0,82	1,32	1,32
Friction Parameters						
COF	[-]	1,19	0,90	0,81	0,70	0,65
near surface temperature	[°C]	87,22	99,80	106,59	112,79	113,93
counterpart temperature	[°C]	72,36	80,89	85,00	87,92	89,90

Load Step Test TPU unfilled, 150 rpm, No. 2		0,5 MPa	0,75 MPa	1,00 MPa	1,25 MPa	1,50 MPa
Wear Parameters						
mass loss	[mg]	316,00				
overall wear rate K	[cm ³ /Nm]	7,99E-07				
linear wear rate	[μm/m]	0,11	0,51	0,80	0,80	0,80
Friction Parameters						
COF	[-]	1,29	0,92	0,76	0,73	0,70
near surface temperature	[°C]	93,01	98,45	105,66	109,03	110,96
counterpart temperature	[°C]	74,32	79,14	82,85	85,08	85,08
Load Step Test TPU unfilled, 200 rpm, No. 1		0,5 MPa	0,75 MPa	1,00 MPa	1,25 MPa	1,50 MPa
Wear Parameters						
mass loss	[mg]	310,00				
overall wear rate K	[cm ³ /Nm]	1,43E-06				
linear wear rate	[μm/m]	0,54	1,15	1,15	1,15	x
Friction Parameters						
COF	[-]	1,01	0,69	0,69	0,69	X
near surface temperature	[°C]	97,11	113,10	113,10	113,10	X
counterpart temperature	[°C]	77,54	88,09	88,09	88,09	X
Load Step Test TPU unfilled, 200 rpm, No. 2		0,5 MPa	0,75 MPa	1,00 MPa	1,25 MPa	1,50 MPa
Wear Parameters						
mass loss	[mg]	317,00				
overall wear rate K	[cm ³ /Nm]	1,61E-06				
linear wear rate	[μm/m]	0,72	1,07	0,93	0,93	x
Friction Parameters						
COF	[-]	1,07	0,94	0,81	0,68	X
near surface temperature	[°C]	93,14	107,58	112,40	115,57	X
counterpart temperature	[°C]	78,11	83,86	89,52	92,61	X

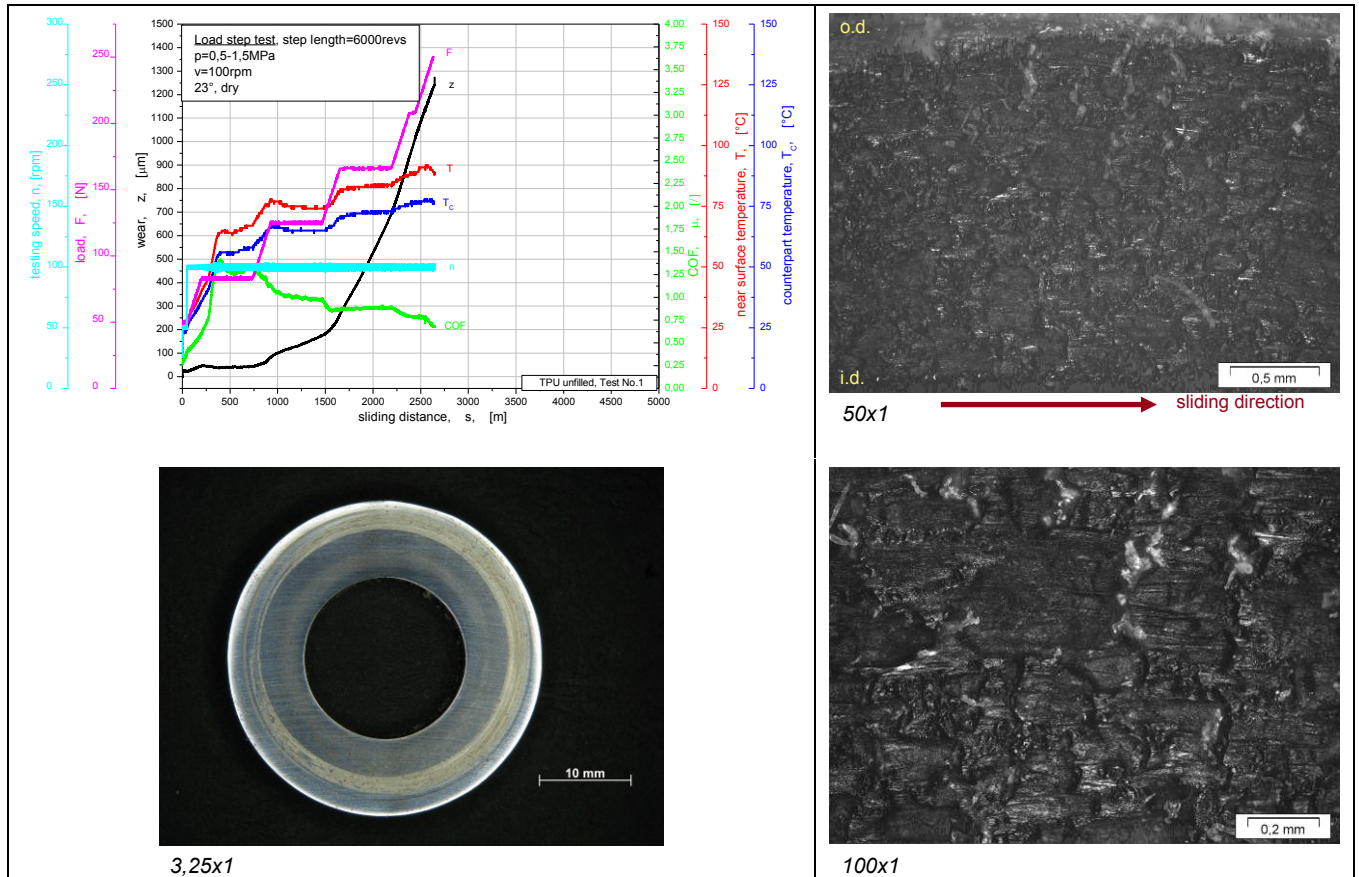


Figure 8.4-30: Load Step test at 100 rpm of TPU unfilled, Test No.1

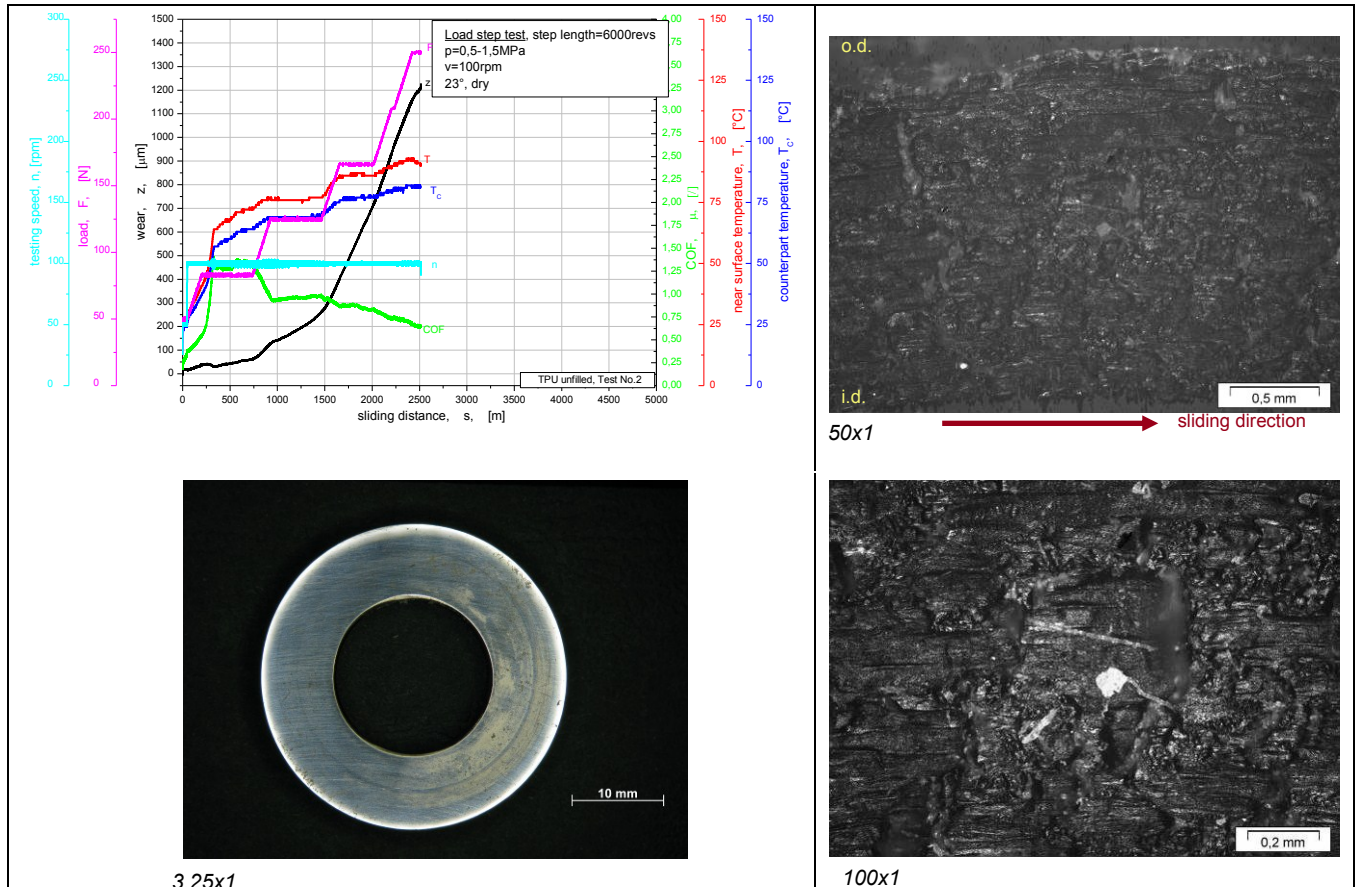


Figure 8.4-31: Load Step test at 100 rpm of TPU unfilled, Test No.2

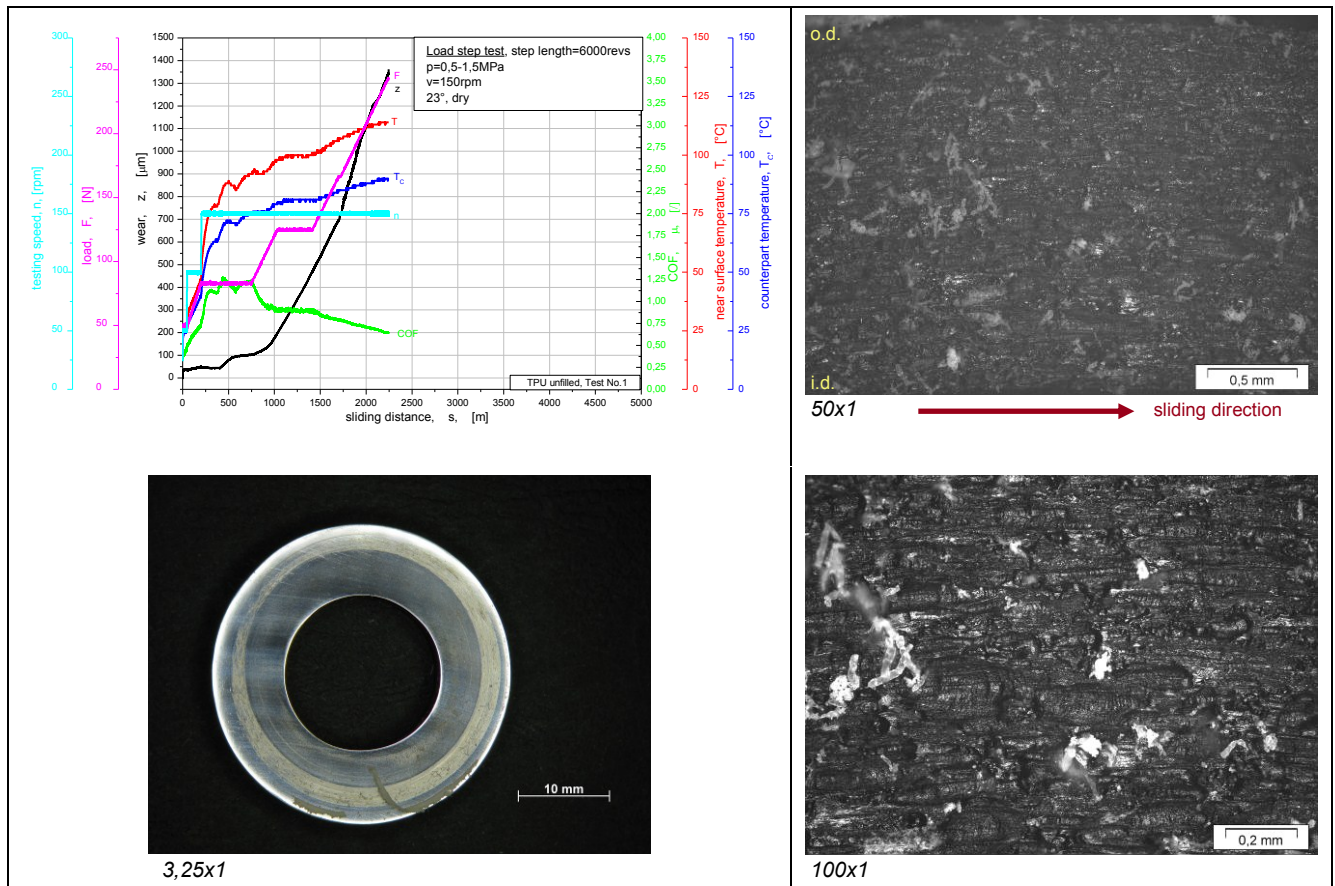


Figure 8.4-32: Load Step test at 150 rpm of TPU unfilled, Test No.1

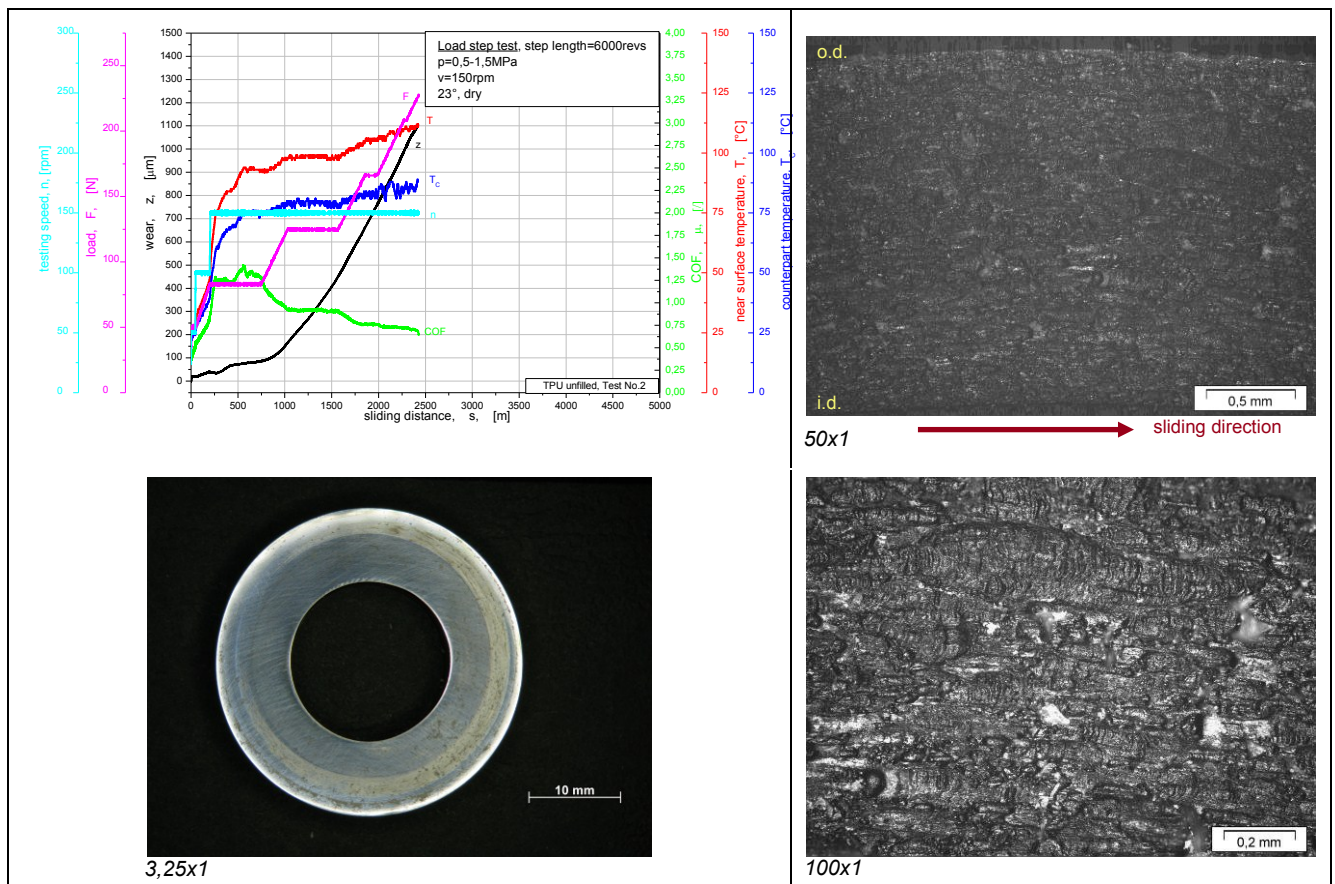


Figure 8.4-33: Load Step test at 150 rpm of TPU unfilled, Test No.2

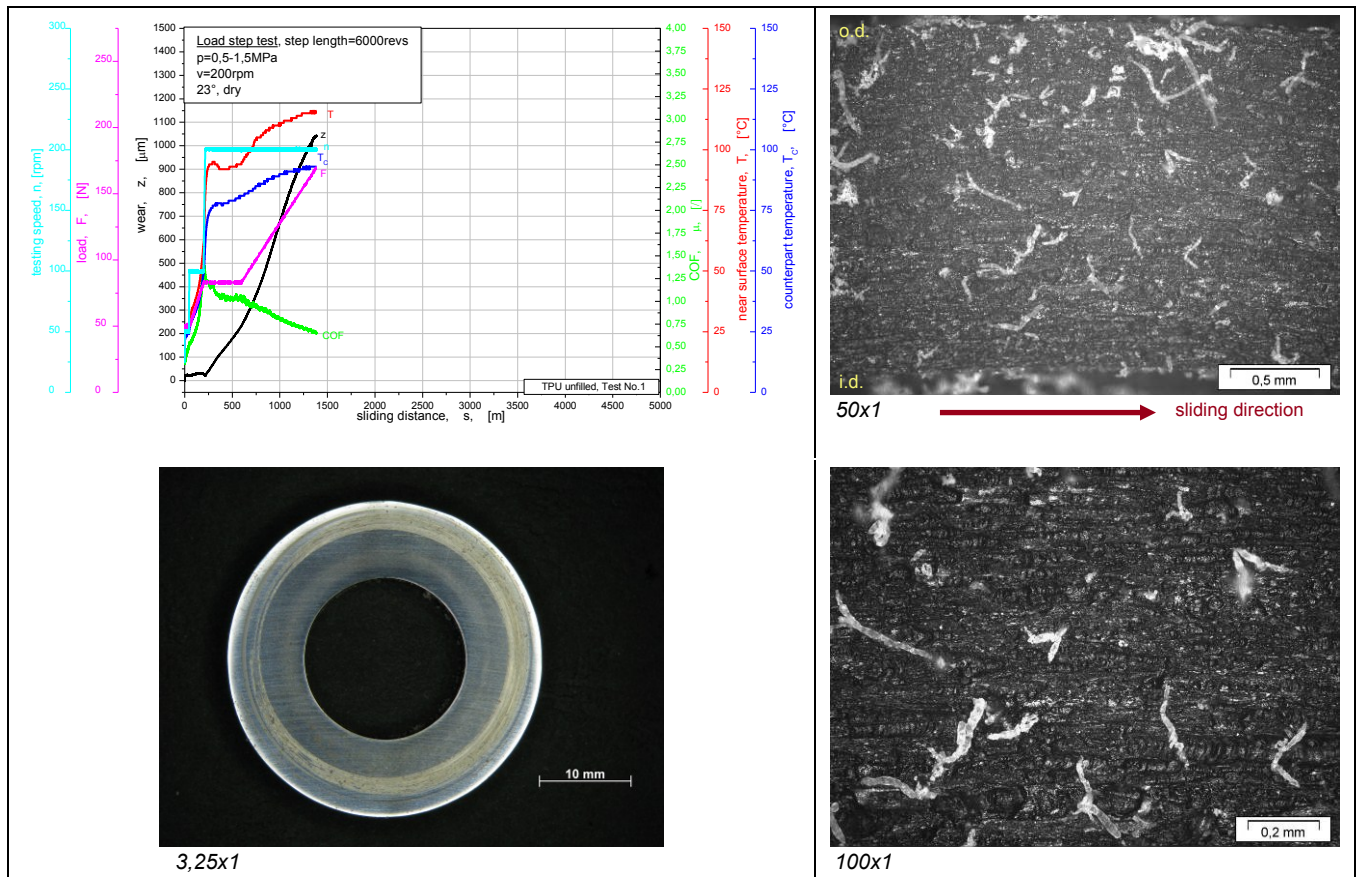


Figure 8.4-34: Load Step test at 200 rpm of TPU unfilled, Test No.1

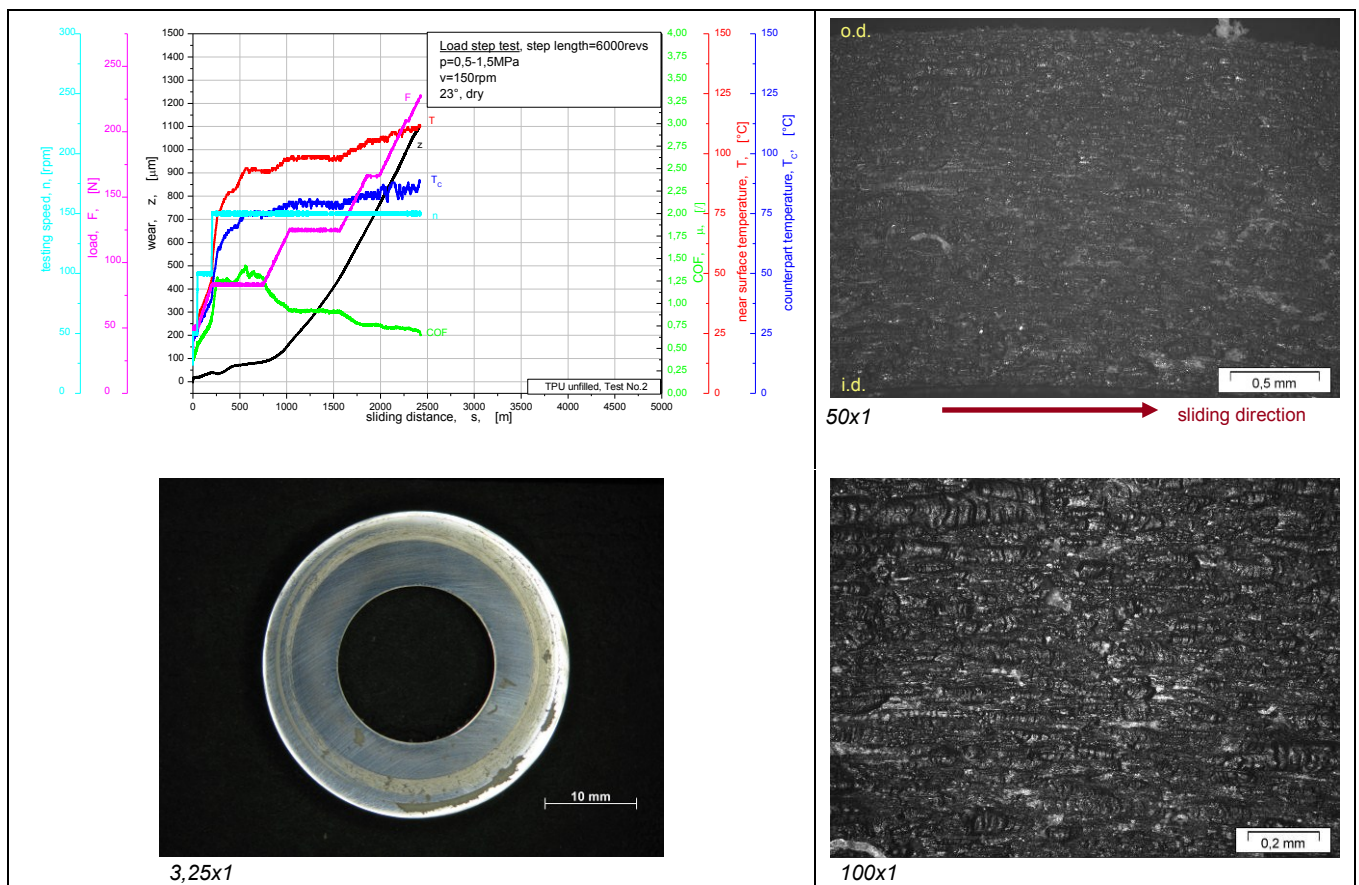


Figure 8.4-35: Load Step test at 200 rpm of TPU unfilled, Test No.2

Gradually performed load step tests of TPU unfilled

Table 8.4-8: Summary of gradually performed load step tests for the unfilled material

Load Step Test TPU unfilled,100 rpm, Step 1		0,5 MPa	0,75 MPa	1,00 MPa	1,25 MPa	1,50 MPa
Wear Parameters						
mass loss	[mg]	41,43				
overall wear rate K	[cm ³ /Nm]	5,78E-07				
linear wear rate	[µm/m]	0,24	x	x	x	x
Friction Parameters						
COF	[-]	1,40	x	x	x	x
near surface temperature	[°C]	86,00	x	x	x	x
counterpart temperature	[°C]	58,00	x	x	x	x
Load Step Test TPU unfilled,100 rpm, Step 2		0,5 MPa	0,75 MPa	1,00 MPa	1,25 MPa	1,50 MPa
Wear Parameters						
mass loss	[mg]	80,22				
overall wear rate K	[cm ³ /Nm]	4,68E-07				
linear wear rate	[µm/m]	0,04	0,51	x	x	x
Friction Parameters						
COF	[-]	1,30	1,15	x	x	x
near surface temperature	[°C]	76,00	91,00	x	x	x
counterpart temperature	[°C]	59,00	71,00	x	x	x
Load Step Test TPU unfilled,100 rpm, Step 3		0,5 MPa	0,75 MPa	1,00 MPa	1,25 MPa	1,50 MPa
Wear Parameters						
mass loss	[mg]	210,58				
overall wear rate K	[cm ³ /Nm]	8,30E-07				
linear wear rate	[µm/m]	0,06	0,67	1,07	x	x
Friction Parameters						
COF	[-]	1,35	1,20	0,96	x	x
near surface temperature	[°C]	76,00	92,00	96,00	x	x
counterpart temperature	[°C]	49,00	57,00	61,00	x	x
Load Step Test TPU unfilled,100 rpm, Step 4		0,5 MPa	0,75 MPa	1,00 MPa	1,25 MPa	1,50 MPa
Wear Parameters						
mass loss	[mg]	292,49				
overall wear rate K	[cm ³ /Nm]	6,30E-07				
linear wear rate	[µm/m]	0,04	0,22	0,54	0,87	x
Friction Parameters						
COF	[-]	0,89	0,85	0,75	0,68	X
near surface temperature	[°C]	75,00	77,00	87,00	92,00	X
counterpart temperature	[°C]	52,00	53,00	60,00	64,00	X
Load Step Test TPU unfilled,100 rpm, Step 5		0,5 MPa	0,75 MPa	1,00 MPa	1,25 MPa	1,50 MPa
Wear Parameters						
mass loss	[mg]	305,36				
overall wear rate K	[cm ³ /Nm]	9,31E-07				
linear wear rate	[µm/m]	0,09	0,37	1,66	1,28	x
Friction Parameters						
COF	[-]	1,10	0,90	0,83	0,77	x
near surface temperature	[°C]	73,00	82,00	91,00	97,00	x
counterpart temperature	[°C]	50,00	54,00	62,00	66,00	x

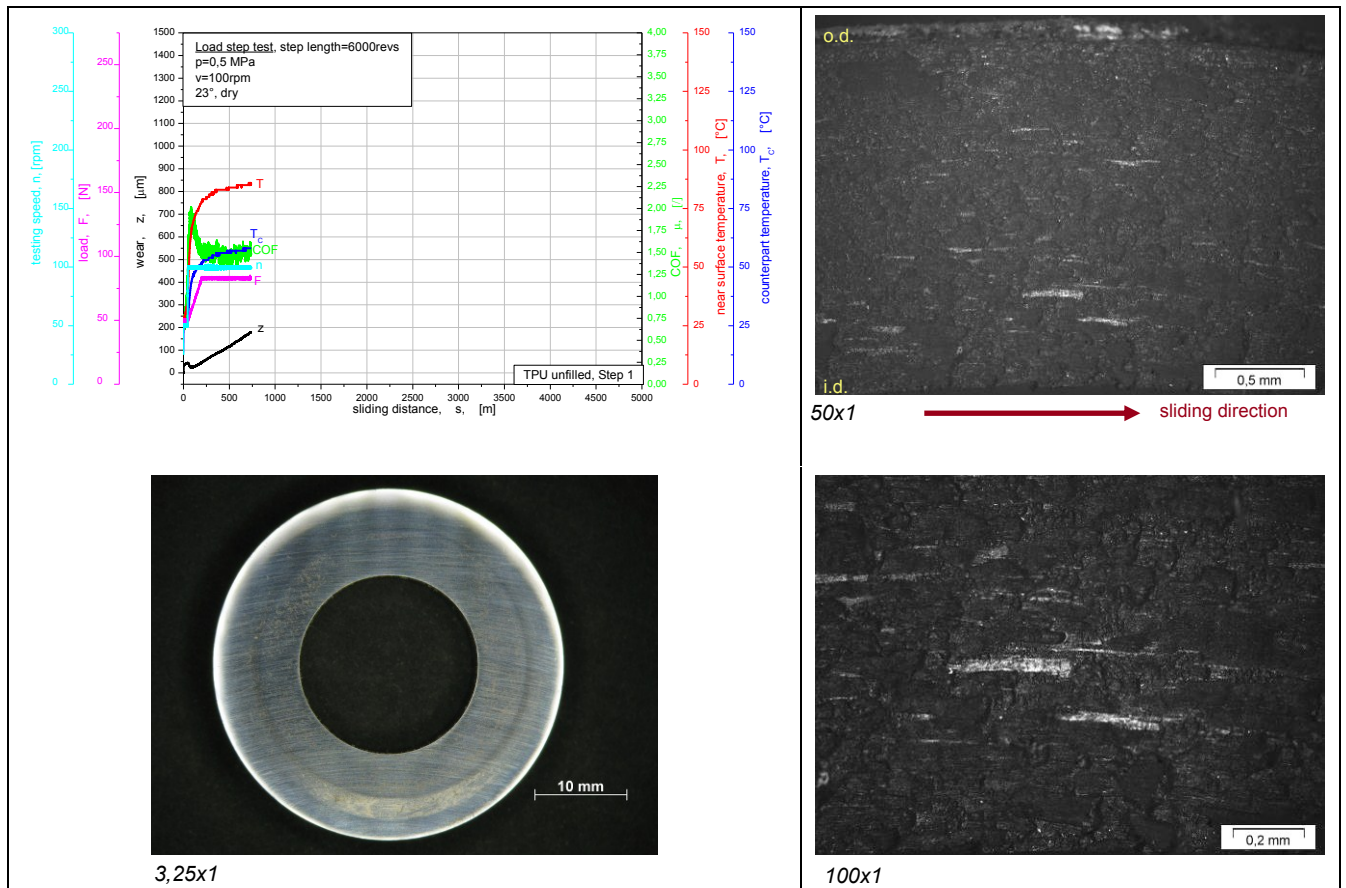


Figure 8.4-36: Gradually performed load step test at 100 rpm of TPU unfilled, Step 1

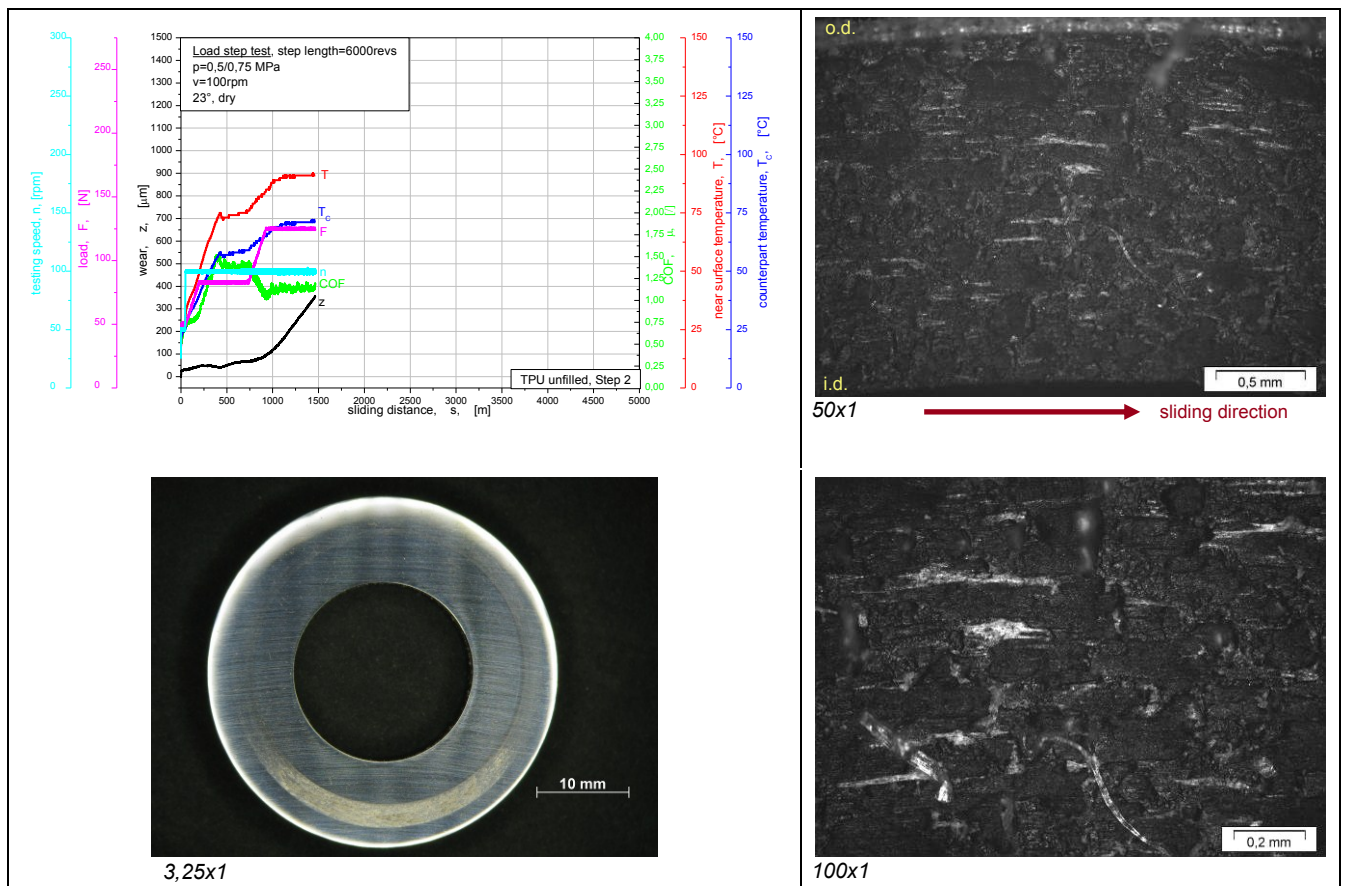


Figure 8.4-37: Gradually performed load step test at 100 rpm of TPU unfilled, Step 2

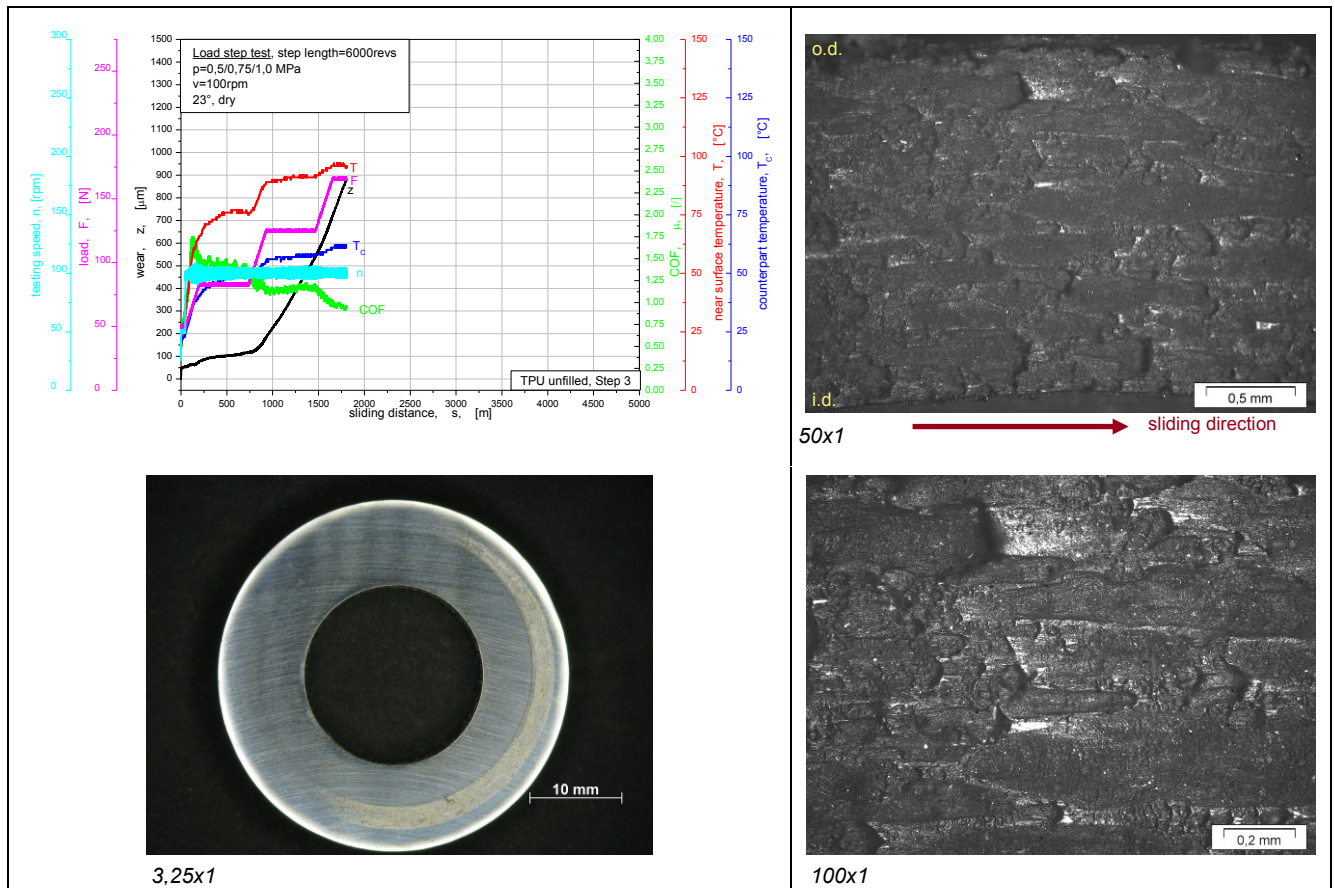


Figure 8.4-38: Gradually performed load step test at 100 rpm of TPU unfilled, Step 3

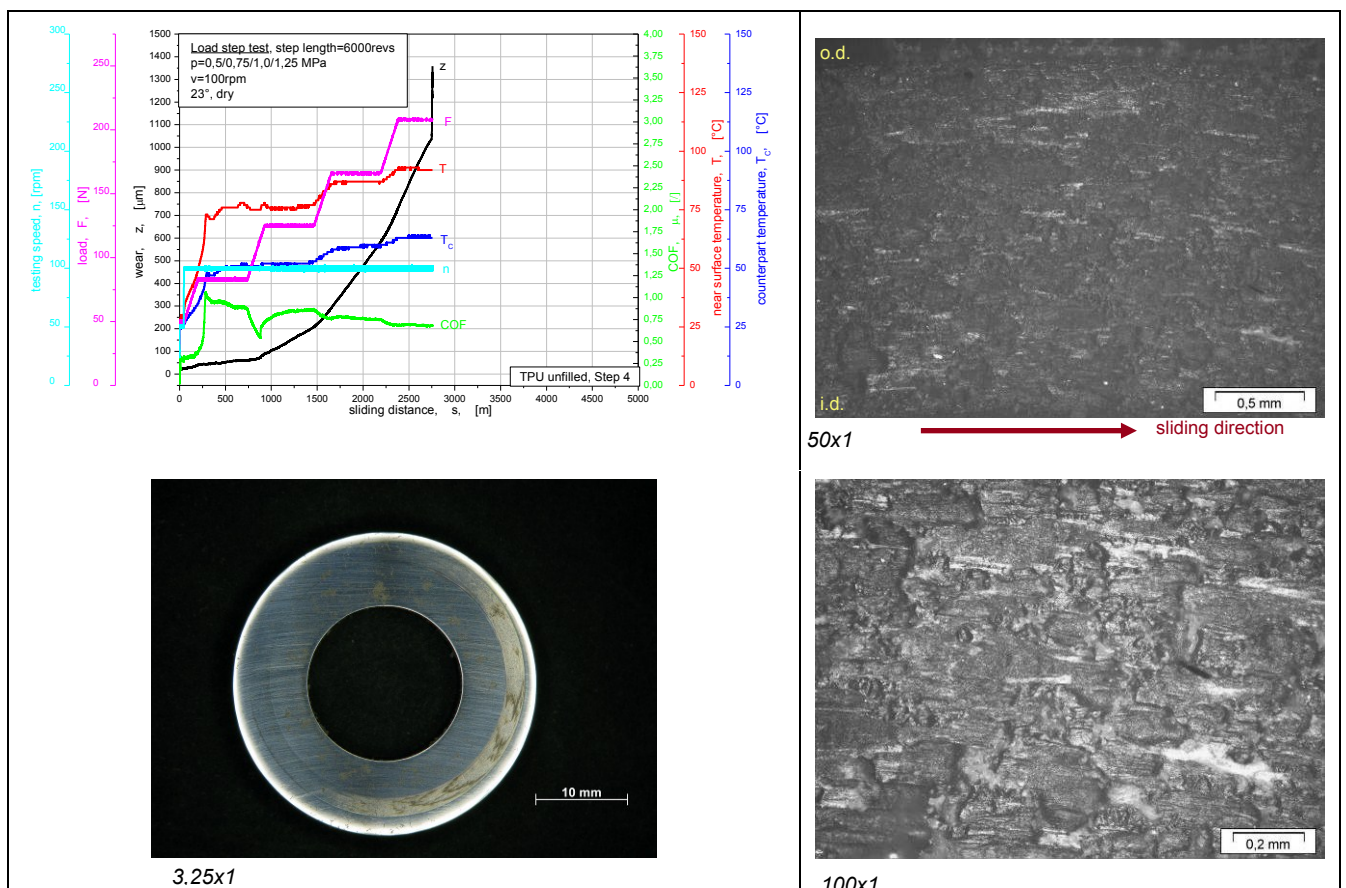


Figure 8.4-39: Gradually performed load step test at 100 rpm of TPU unfilled, Step 4

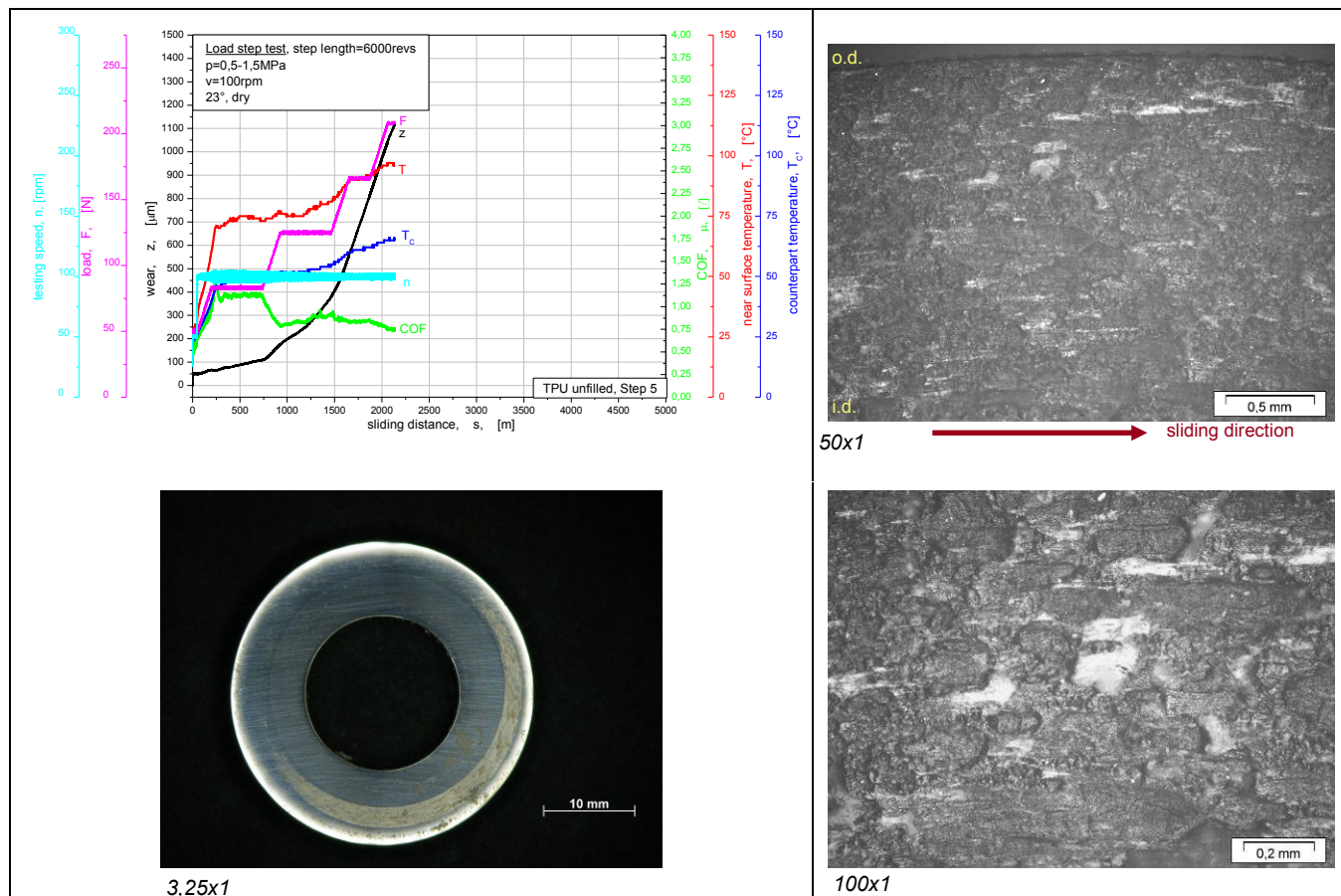


Figure 8.4-40: Gradually performed load step test at 100 rpm of TPU unfilled, Step 5

Load step tests of the filled material

Table 8.4-9: Summary of load step tests for the filled material

Load Step Test TPU filled,100 rpm, No. 1		0,5 MPa	0,75 MPa	1,00 MPa	1,25 MPa	1,50 MPa
Wear Parameters						
mass loss	[mg]	3,00				
overall wear rate K	[cm ³ /Nm]	5,81E-09				
linear wear rate	[μm/m]	0,00	0,01	0,01	0,00	X
Friction Parameters						
COF	[-]	X	1,12	0,92	0,91	X
near surface temperature	[°C]	X	85,63	89,73	103,75	X
counterpart temperature	[°C]	X	64,68	68,35	77,91	X
Load Step Test TPU filled,100 rpm, No. 2		0,5 MPa	0,75 MPa	1,00 MPa	1,25 MPa	1,50 MPa
Wear Parameters						
mass loss	[mg]	4,00				
overall wear rate K	[cm ³ /Nm]	5,39E-09				
linear wear rate	[μm/m]	0,00	0,01	0,01	0,02	0,02
Friction Parameters						
COF	[-]	1,33	1,07	0,94	0,92	0,81
near surface temperature	[°C]	77,43	87,06	98,35	114,73	118,55
counterpart temperature	[°C]	56,82	63,32	69,93	80,24	83,28
Load Step Test TPU filled,150 rpm, No. 1		0,5 MPa	0,75 MPa	1,00 MPa	1,25 MPa	1,50 MPa
Wear Parameters						
mass loss	[mg]	7,00				
overall wear rate K	[cm ³ /Nm]	8,42E-09				
linear wear rate	[μm/m]	0,00	0,00	0,02	0,03	0,01
Friction Parameters						
COF	[-]	0,92	0,96	0,79	0,65	0,57
near surface temperature	[°C]	77,62	111,01	117,88	122,13	126,35
counterpart temperature	[°C]	64,53	85,65	92,37	97,47	99,40
Load Step Test TPU filled,150 rpm, No. 2		0,5 MPa	0,75 MPa	1,00 MPa	1,25 MPa	1,50 MPa
Wear Parameters						
mass loss	[mg]	10,00				
overall wear rate K	[cm ³ /Nm]	1,20E-08				
linear wear rate	[μm/m]	0,00	0,00	0,01	0,02	0,02
Friction Parameters						
COF	[-]	1,04	0,87	0,77	0,59	0,52
near surface temperature	[°C]	82,98	99,99	112,45	108,51	113,16
counterpart temperature	[°C]	63,14	72,67	80,58	77,52	80,29
Load Step Test TPU filled,200 rpm, No. 1		0,5 MPa	0,75 MPa	1,00 MPa	1,25 MPa	1,50 MPa
Wear Parameters						
mass loss	[mg]	12,00				
overall wear rate K	[cm ³ /Nm]	1,30E-08				
linear wear rate	[μm/m]	0,00	0,03	0,01	0,01	0,02
Friction Parameters						
COF	[-]	0,89	0,75	0,64	0,53	0,47
near surface temperature	[°C]	83,85	101,30	116,56	118,59	123,38
counterpart temperature	[°C]	72,91	86,61	98,40	99,20	102,11

Load Step Test TPU filled, 200 rpm, No. 2		0,5 MPa	0,75 MPa	1,00 MPa	1,25 MPa	1,50 MPa
Wear Parameters						
mass loss	[mg]	6,00				
overall wear rate K	[cm ³ /Nm]	6,53E-09				
linear wear rate	[μm/m]	0,00	0,02	0,02	0,02	0,02
Friction Parameters						
COF	[-]	1,06	0,81	0,69	0,57	0,51
near surface temperature	[°C]	100,32	113,80	124,29	127,71	133,69
counterpart temperature	[°C]	79,03	90,77	97,48	100,00	102,02

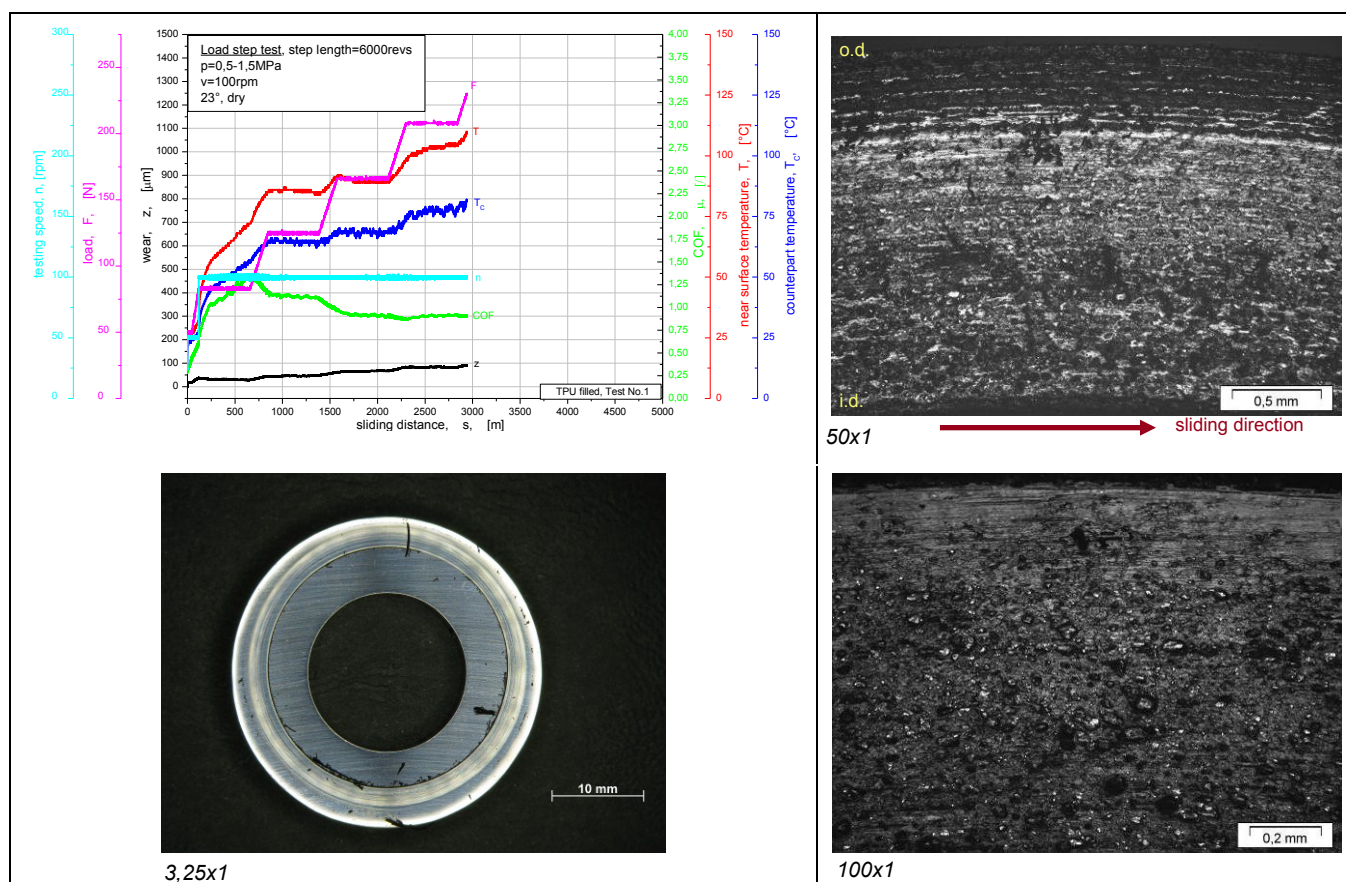


Figure 8.4-41: Load Step test at 100 rpm of TPU filled, Test No.1

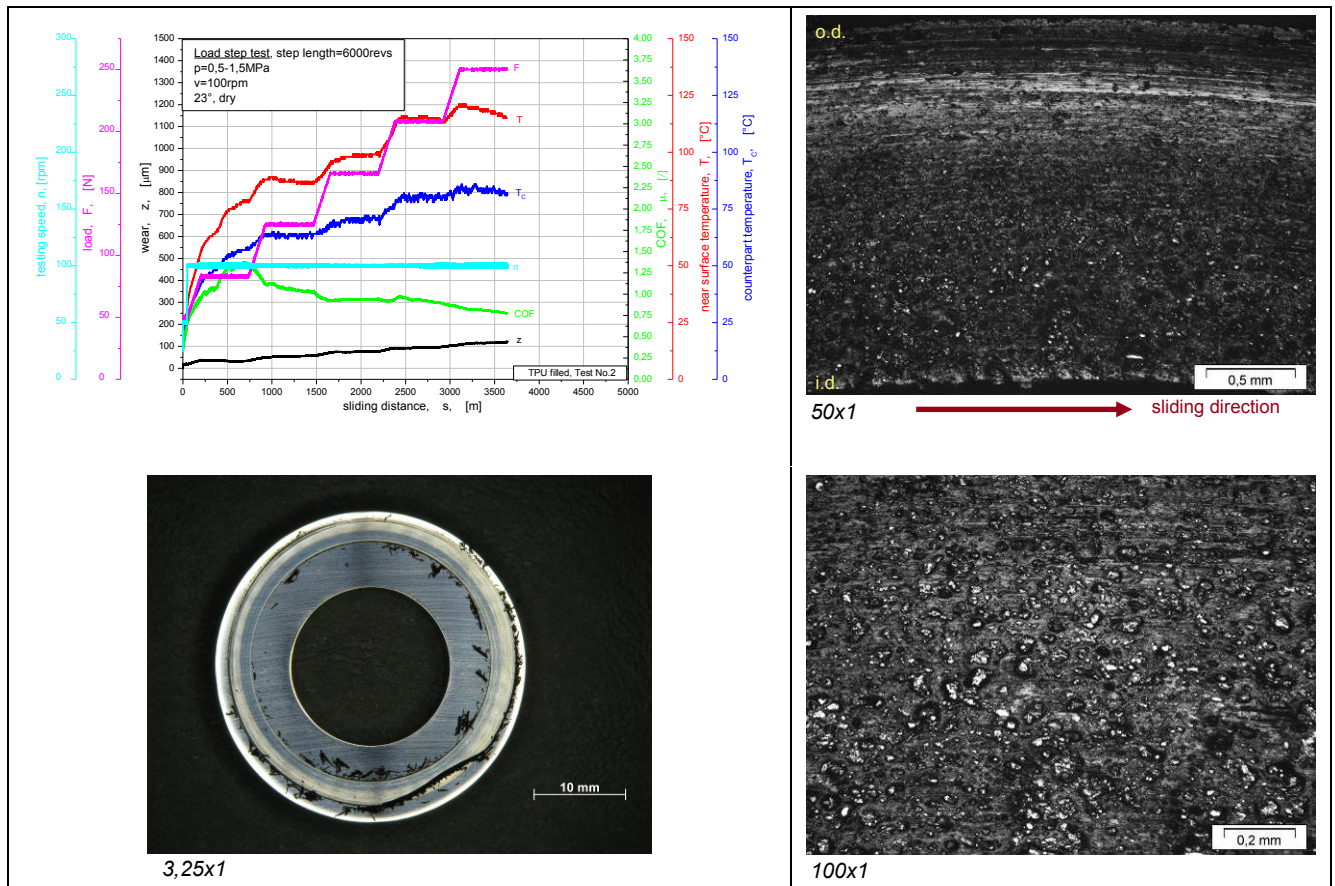


Figure 8.4-42: Load Step test at 100 rpm of TPU filled, Test No.2

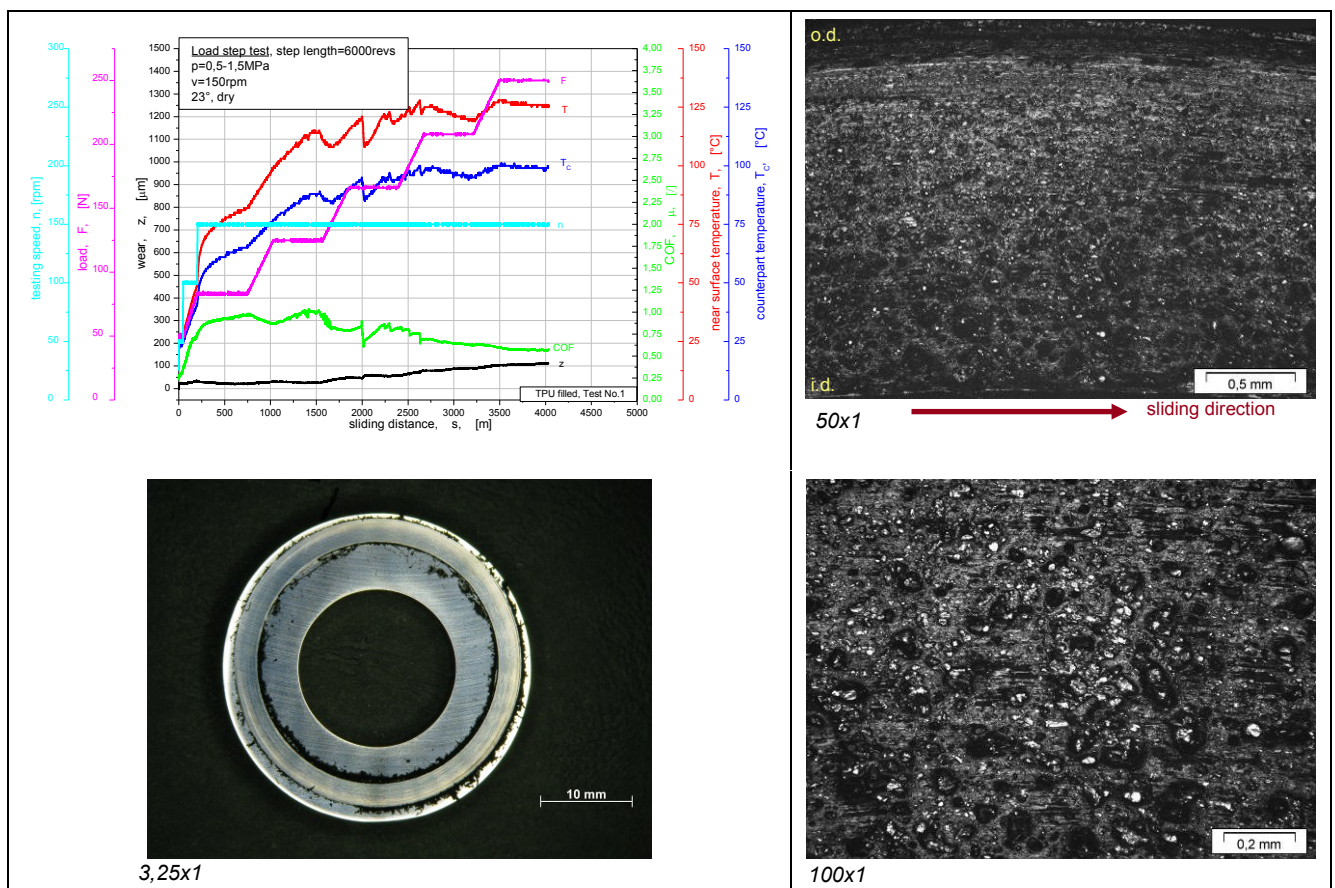


Figure 8.4-43: Load Step test at 150 rpm of TPU filled, Test No.1

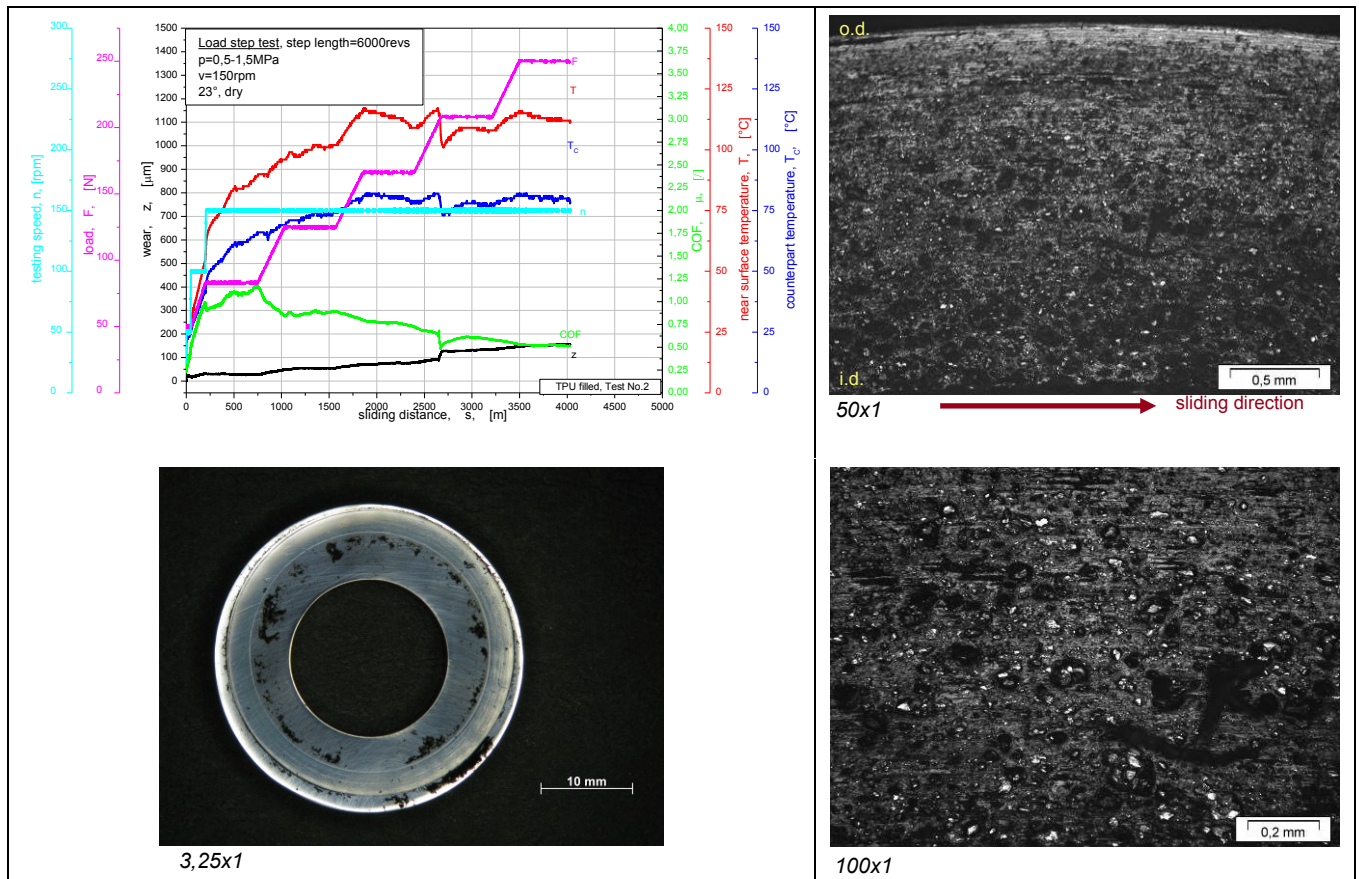


Figure 8.4-44: Load Step test at 150 rpm of TPU filled, Test No.2

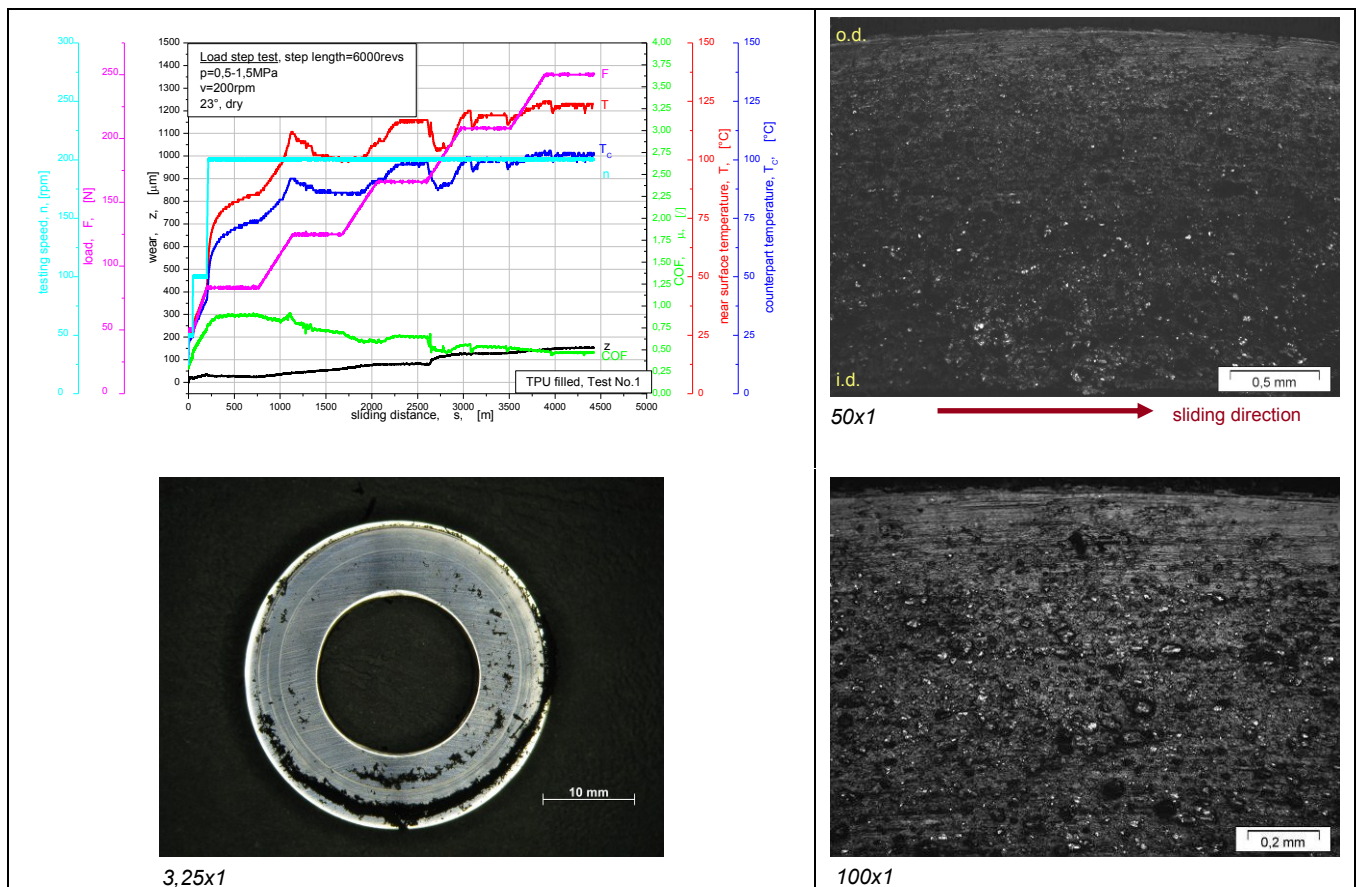


Figure 8.4-45: Load Step test at 200 rpm of TPU filled, Test No.1

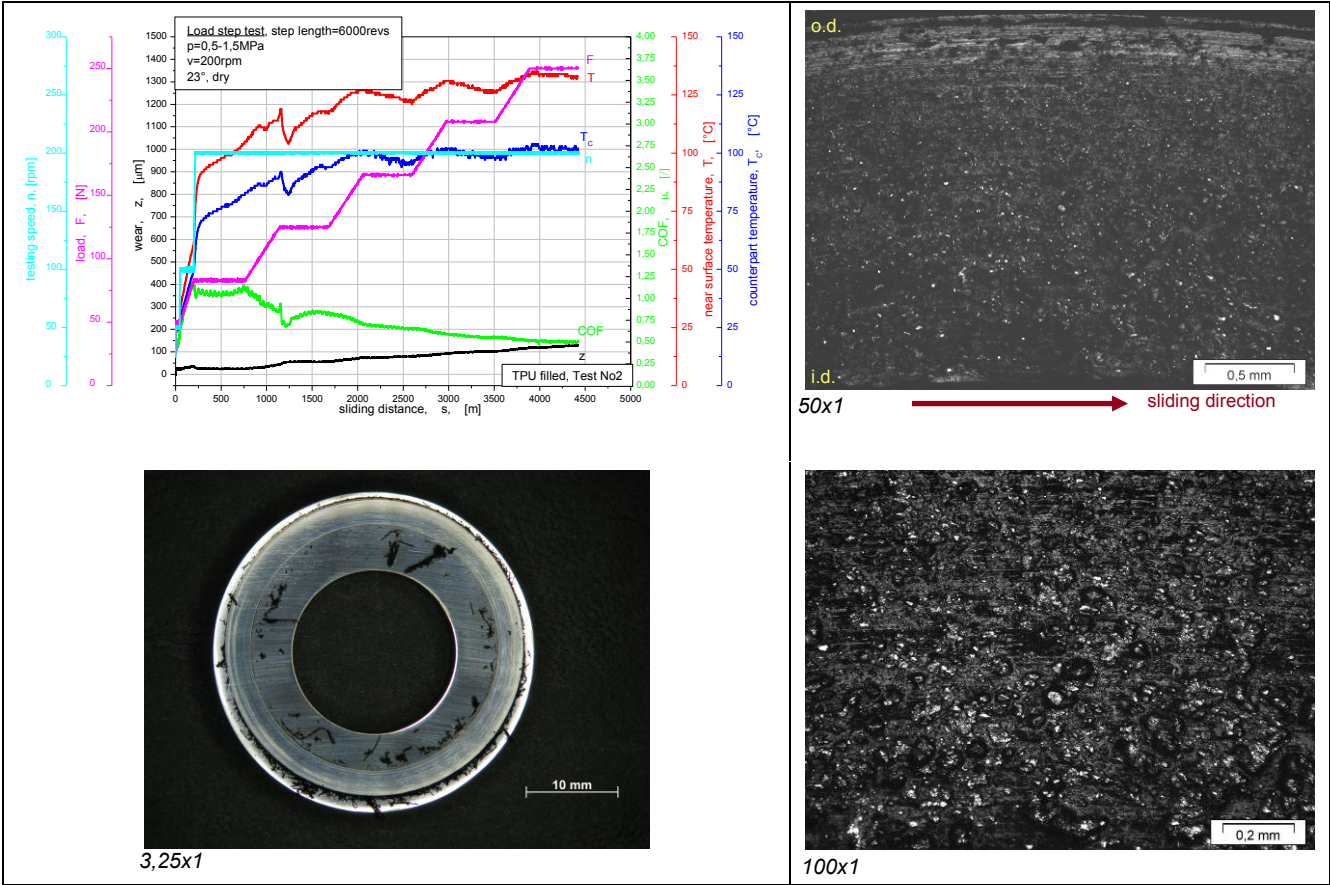


Figure 8.4-46: Load Step test at 200 rpm of TPU filled, Test No.2

Gradually performed load step tests of TPU filled

Table 8.4-10: Summary of gradually performed load step tests for the filled material

Load Step Test TPU filled,100 rpm, Step 1		0,5 MPa	0,75 MPa	1,00 MPa	1,25 MPa	1,50 MPa
Wear Parameters						
mass loss	[mg]	0,92				
overall wear rate K	[cm ³ /Nm]	1,25E-08				
linear wear rate	[µm/m]	0,00	x	x	x	x
Friction Parameters						
COF	[-]	1,33	x	x	x	x
near surface temperature	[°C]	82,00	x	x	x	x
counterpart temperature	[°C]	57,00	x	x	x	x
Load Step Test TPU filled,100 rpm, Step 2		0,5 MPa	0,75 MPa	1,00 MPa	1,25 MPa	1,50 MPa
Wear Parameters						
mass loss	[mg]	1,24				
overall wear rate K	[cm ³ /Nm]	6,74E-09				
linear wear rate	[µm/m]	0,00	0,00	x	x	x
Friction Parameters						
COF	[-]	1,20	0,97	x	x	x
near surface temperature	[°C]	79,00	87,00	x	x	x
counterpart temperature	[°C]	64,00	70,00	x	x	x
Load Step Test TPU filled,100 rpm, Step 3		0,5 MPa	0,75 MPa	1,00 MPa	1,25 MPa	1,50 MPa
Wear Parameters						
mass loss	[mg]	1,72				
overall wear rate K	[cm ³ /Nm]	5,18E-09				
linear wear rate	[µm/m]	0,00	0,00	0,01	x	x
Friction Parameters						
COF	[-]	1,24	0,73	0,71	X	X
near surface temperature	[°C]	85,00	81,00	84,00	X	X
counterpart temperature	[°C]	55,00	53,00	59,00	X	X
Load Step Test TPU filled,100 rpm, Step 4		0,5 MPa	0,75 MPa	1,00 MPa	1,25 MPa	1,50 MPa
Wear Parameters						
mass loss	[mg]	3,50				
overall wear rate K	[cm ³ /Nm]	6,75E-09				
linear wear rate	[µm/m]	0,00	0,00	0,01	0,01	x
Friction Parameters						
COF	[-]	1,32	0,88	0,80	0,70	X
near surface temperature	[°C]	74,00	76,00	86,00	94,00	X
counterpart temperature	[°C]	64,00	65,00	72,00	78,00	X
Load Step Test TPU filled,100 rpm, Step 5		0,5 MPa	0,75 MPa	1,00 MPa	1,25 MPa	1,50 MPa
Wear Parameters						
mass loss	[mg]	3,44				
overall wear rate K	[cm ³ /Nm]	4,64E-09				
linear wear rate	[µm/m]	0,00	0,00	0,01	0,01	0,02
Friction Parameters						
COF	[-]	1,22	0,70	0,64	0,64	0,60
near surface temperature	[°C]	85,00	80,00	90,00	99,00	112,00
counterpart temperature	[°C]	65,00	64,00	71,00	78,00	86,00

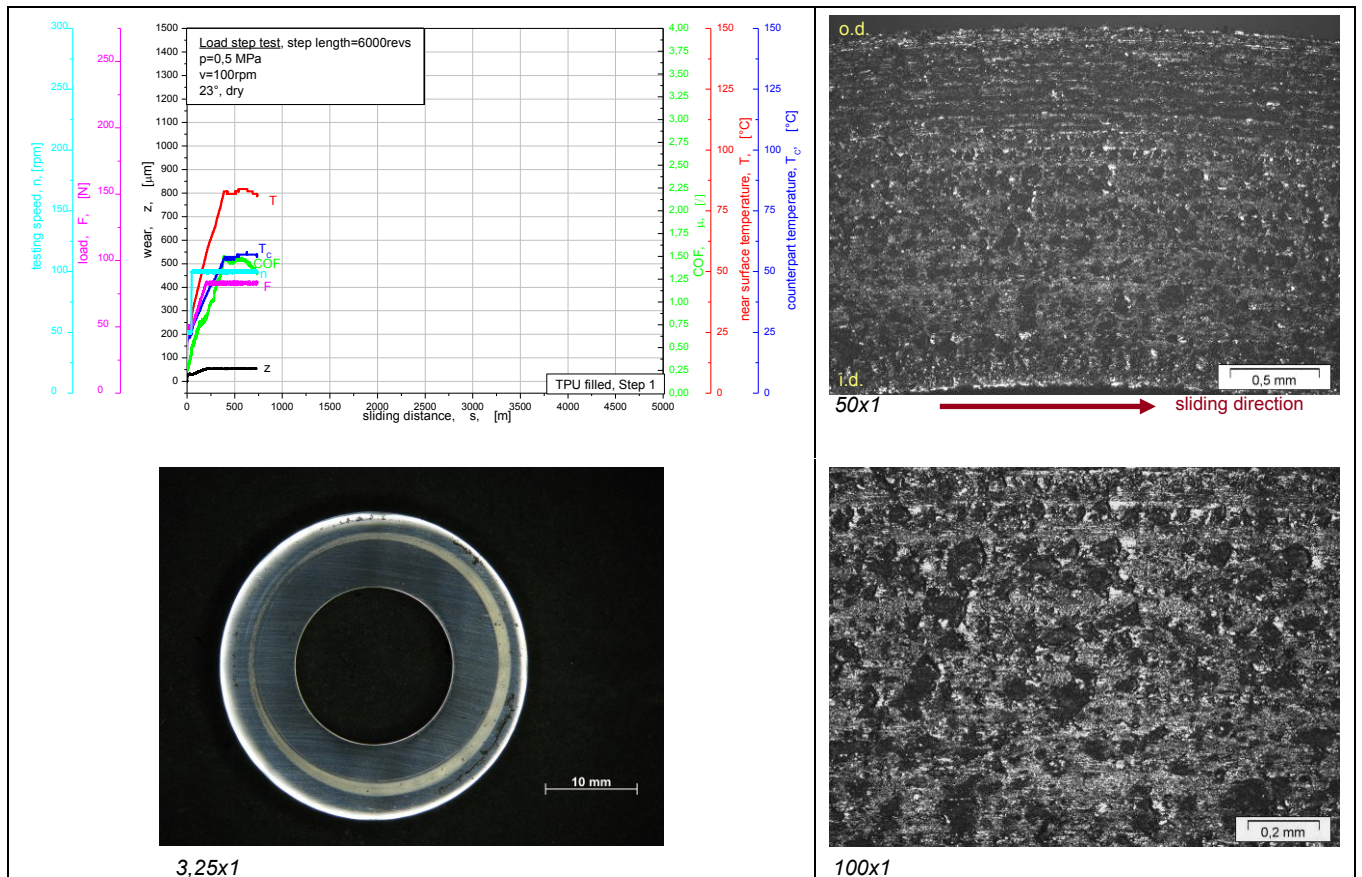


Figure 8.4-47: Gradually performed load step test at 100 rpm of TPU filled, Step 1

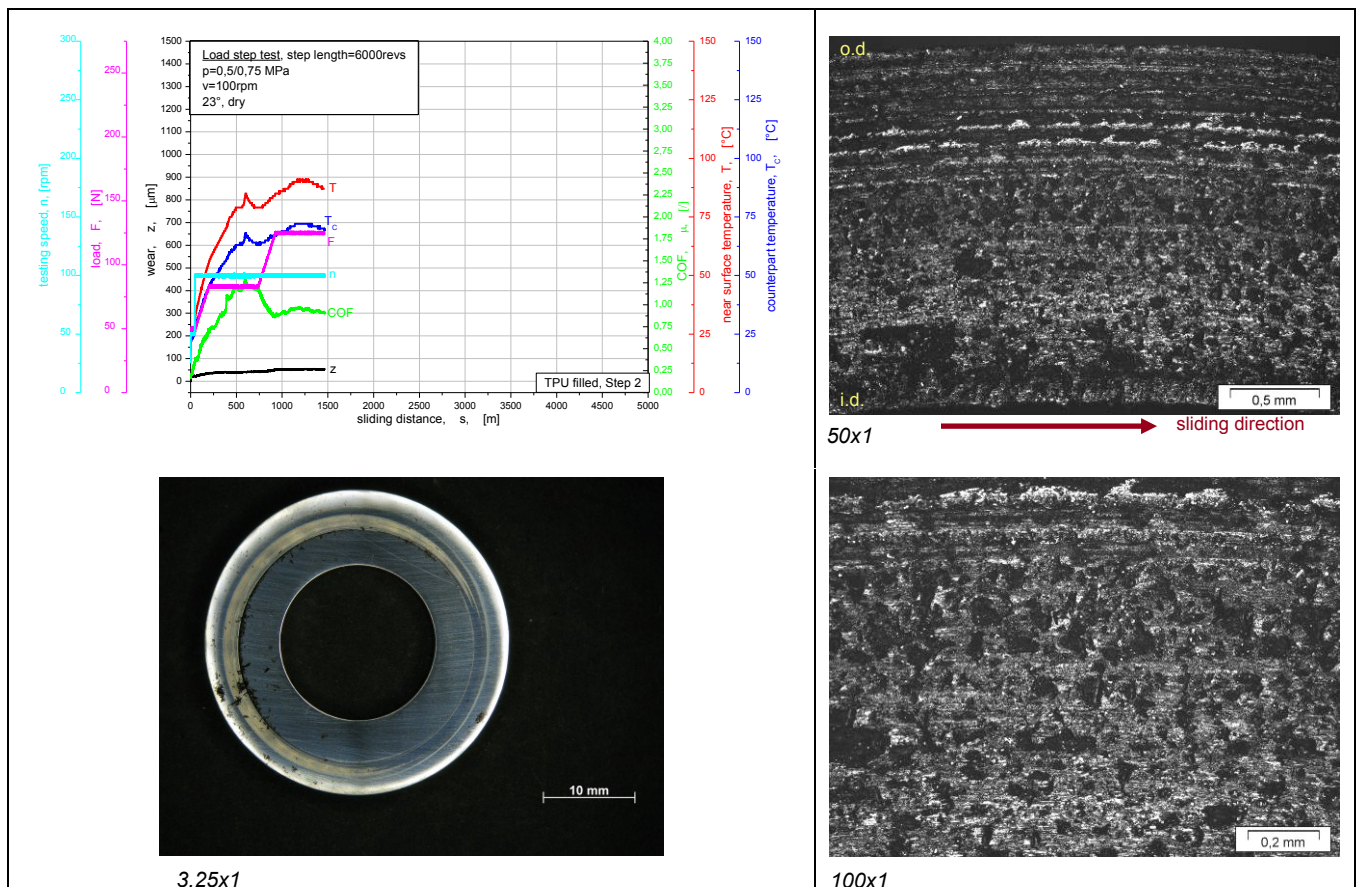


Figure 8.4-48: Gradually performed load step test at 100 rpm of TPU filled, Step 2

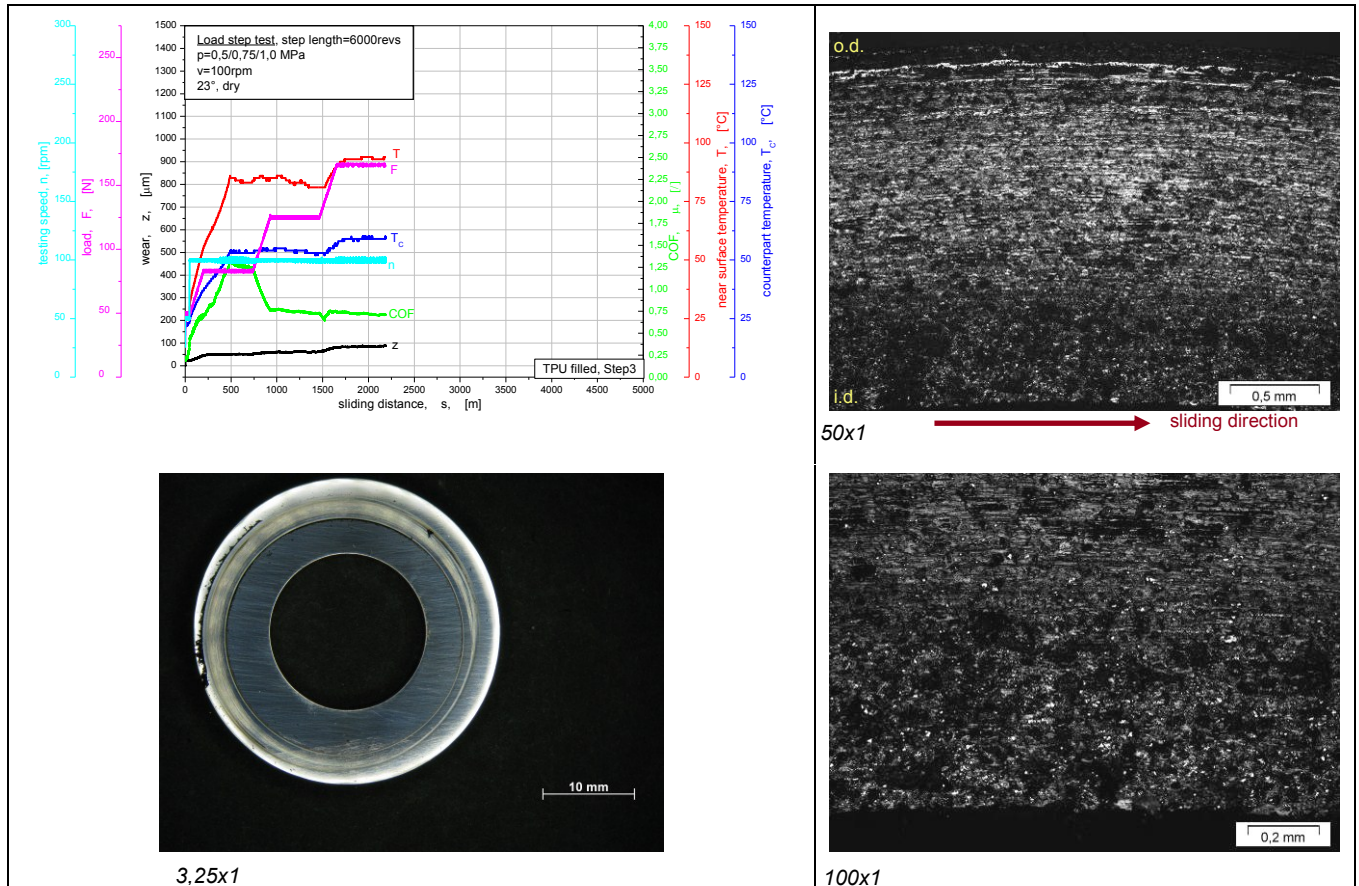


Figure 8.4-49: Gradually performed load step test at 100 rpm of TPU filled, Step 3

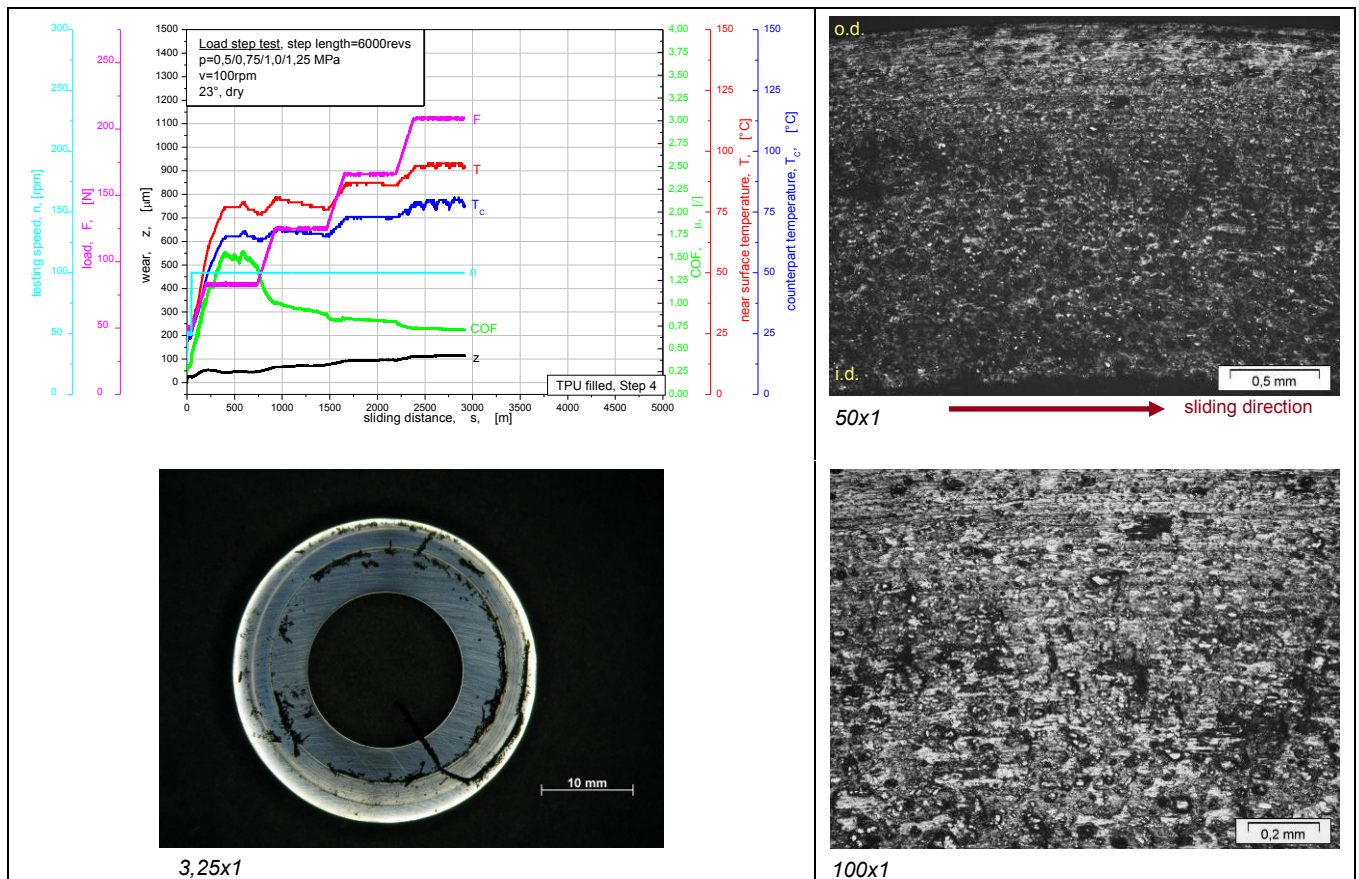


Figure 8.4-50: Gradually performed load step test at 100 rpm of TPU filled, Step 4

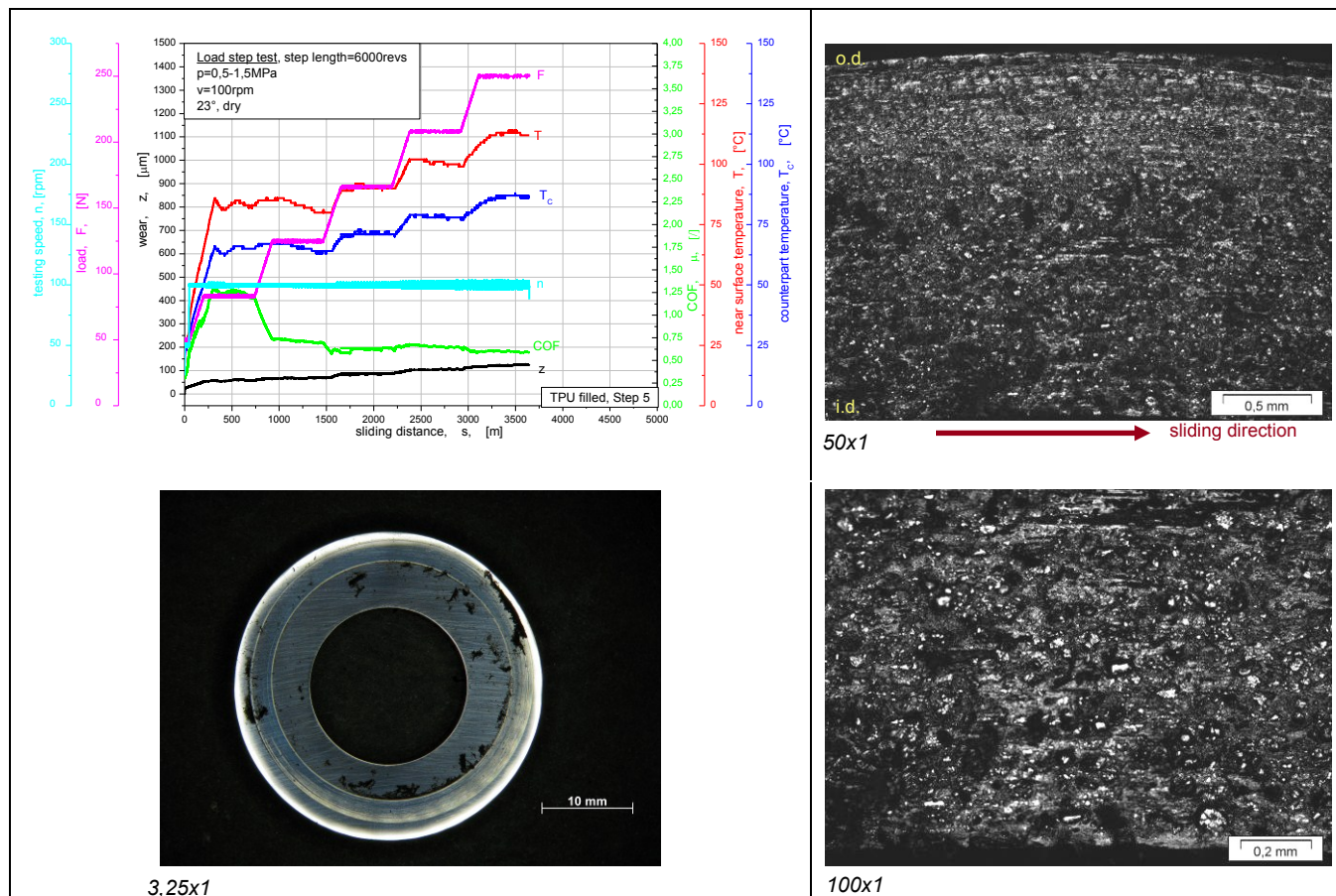


Figure 8.4-51: Gradually performed load step test at 100 rpm of TPU filled, Step 5

8.4.6 Speed step tests

Table 8.4-11: Overview of the testing procedure of the speed step test

Speed step test TPU unfilled/filled						
Test Parameters						
Step		Run in	1	2	3	4
Ramp time	[s]	x	237,90	43,21	44,77	45,71
Ramp distance	[m]	x	35,60	9,70	13,40	17,10
Testing force	[N]	50,00	83/166/250			
Contact pressure	[MPa]	0,30	0,50/1,00/1,50			
Testing speed	[rpm]	50,00	100,00	150,00	200,00	250,00
Step length	[Revs]	x	6000,00			
Step distance	[m]	44,50	539,00	539,00	539,00	539,00
Testing temperature	[°C]	23,00				
Lubrication		dry				

Speed step tests of the unfilled material

Table 8.4-12: Summary of speed step tests for the unfilled material

Speed Step Test TPU unfilled,0,5 MPa, No. 1		100rpm	150rpm	200rpm	250rpm
Wear Parameters					
mass loss	[mg]	302,00			
overall wear rate K	[cm ³ /Nm]	1,34E-06			
linear wear rate	[µm/m]	0,00	0,35	0,62	0,94
Friction Parameters					
COF	[-]	1,14	1,09	0,92	0,83
near surface temperature	[°C]	76,51	100,14	110,83	119,89
counterpart temperature	[°C]	48,85	60,68	65,96	71,14
Speed Step Test TPU unfilled,0,5 MPa, No. 2		100rpm	150rpm	200rpm	250rpm
Wear Parameters					
mass loss	[mg]	310,00			
overall wear rate K	[cm ³ /Nm]	1,57E-06			
linear wear rate	[µm/m]	0,04	0,48	0,93	0,80
Friction Parameters					
COF	[-]	1,34	1,13	0,99	0,87
near surface temperature	[°C]	70,81	85,13	95,61	101,38
counterpart temperature	[°C]	58,58	73,60	81,48	86,00
Speed Step Test TPU unfilled,1,0 MPa, No. 1		100rpm	150rpm	200rpm	250rpm
Wear Parameters					
mass loss	[mg]	307,00			
overall wear rate K	[cm ³ /Nm]	9,74E-07			
linear wear rate	[µm/m]	0,11	0,93	1,30	1,36
Friction Parameters					
COF	[-]	0,85	0,73	0,64	0,56
near surface temperature	[°C]	87,77	106,85	114,46	119,81
counterpart temperature	[°C]	70,94	83,99	88,76	94,86

Speed Step Test TPU unfilled, 1,0 MPa, No. 2		100rpm	150rpm	200rpm	250rpm
Wear Parameters					
mass loss	[mg]	315,00			
overall wear rate K	[cm ³ /Nm]	1,32E-06			
linear wear rate	[μm/m]	0,40	0,73	1,31	1,92
Friction Parameters					
COF	[-]	X	0,81	0,68	0,58
near surface temperature	[°C]	X	106,37	117,23	121,65
counterpart temperature	[°C]	X	75,46	82,76	85,44
Speed Step Test TPU unfilled, 1,5 MPa, No. 1		100rpm	150rpm	200rpm	250rpm
Wear Parameters					
mass loss	[mg]	335,00			
overall wear rate K	[cm ³ /Nm]	1,15E-06			
linear wear rate	[μm/m]	1,14	0,93	1,49	1,42
Friction Parameters					
COF	[-]	X	0,62	0,49	0,40
near surface temperature	[°C]	X	104,21	116,52	117,73
counterpart temperature	[°C]	X	86,52	92,64	93,49
Speed Step Test TPU unfilled, 1,5 MPa, No. 2		100rpm	150rpm	200rpm	250rpm
Wear Parameters					
mass loss	[mg]	303,00			
overall wear rate K	[cm ³ /Nm]	1,60E-06			
linear wear rate	[mm/m]	1,27	2,21	2,60	1,76
Friction Parameters					
COF	[-]	X	0,61	0,51	0,43
near surface temperature	[°C]	X	118,52	118,87	118,99
counterpart temperature	[°C]	X	72,01	75,57	77,18

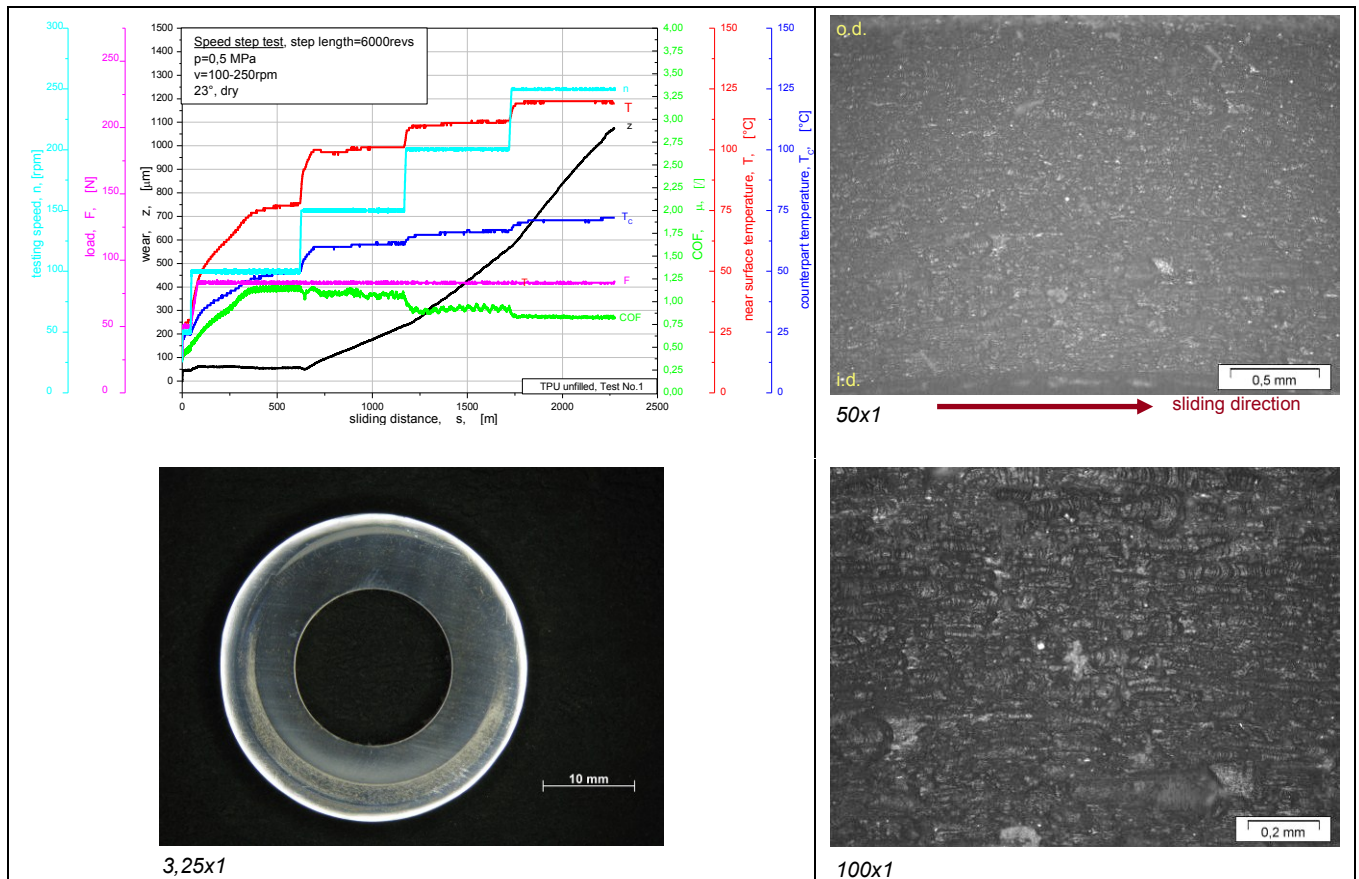


Figure 8.4-52: Speed Step test at 0,5 MPa of TPU unfilled, Test No.1

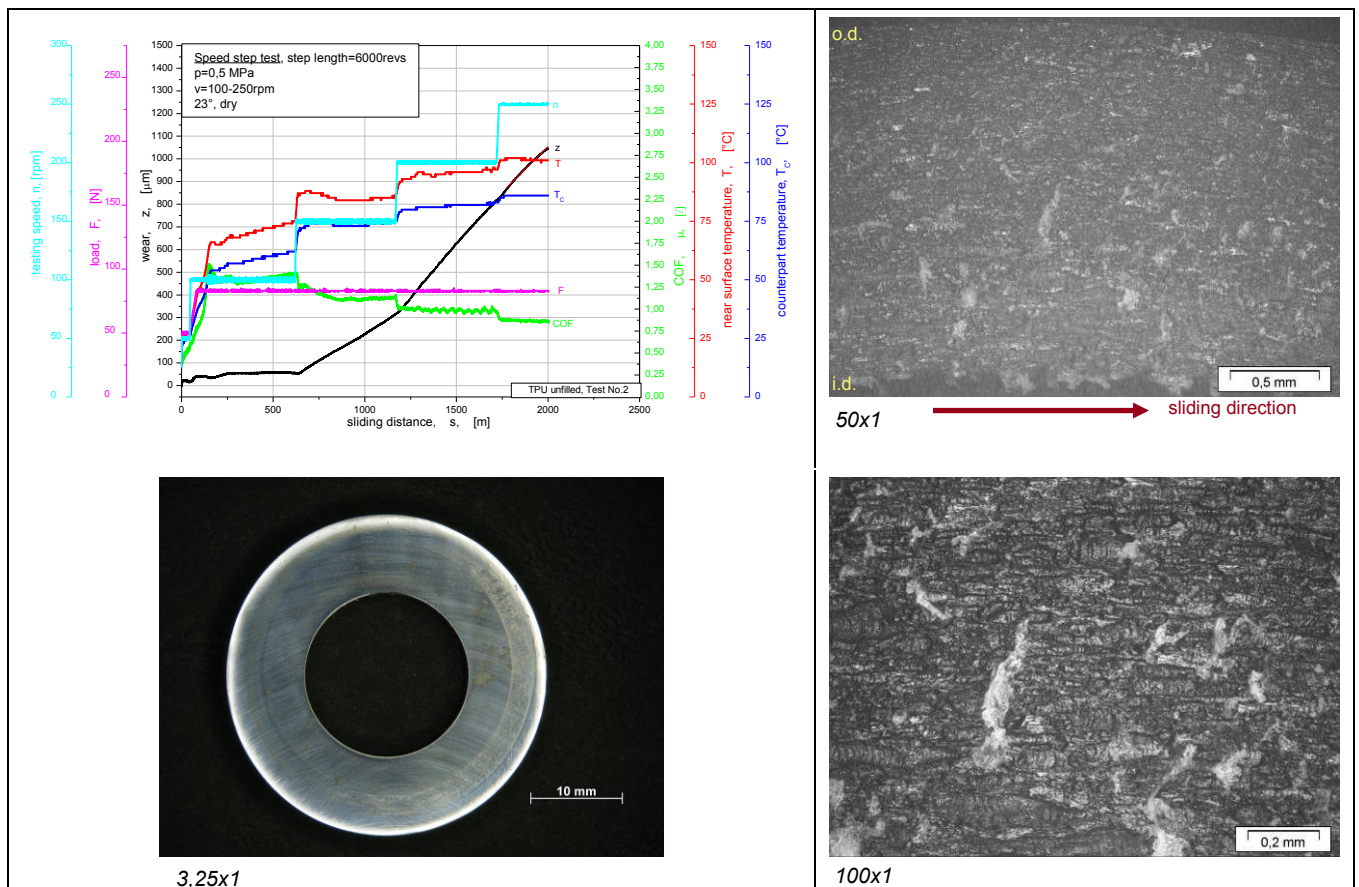


Figure 8.4-53: Speed Step test at 0,5 MPa of TPU unfilled, Test No.2

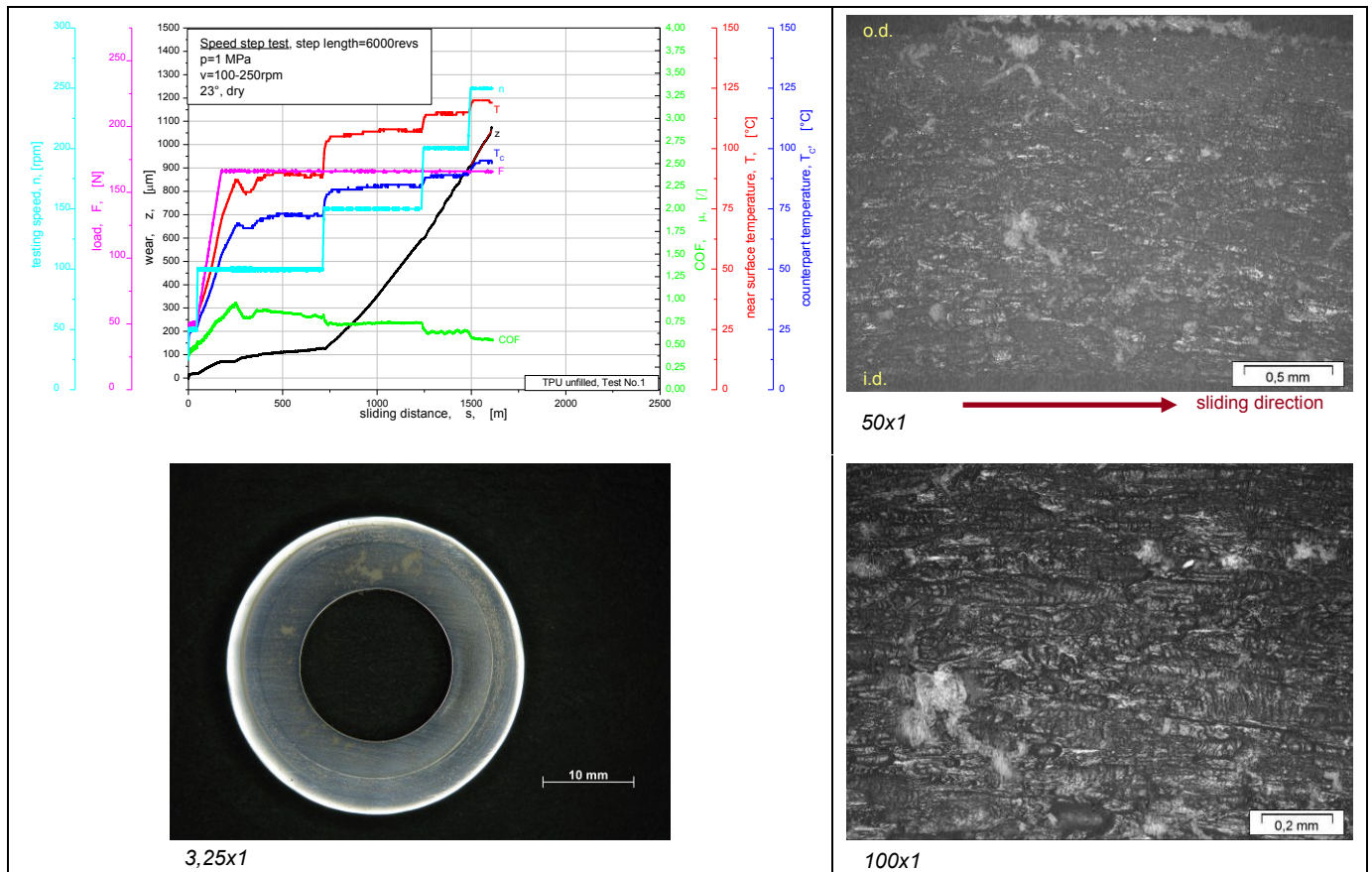


Figure 8.4-54: Speed Step test at 1,0 MPa of TPU unfilled, Test No.1

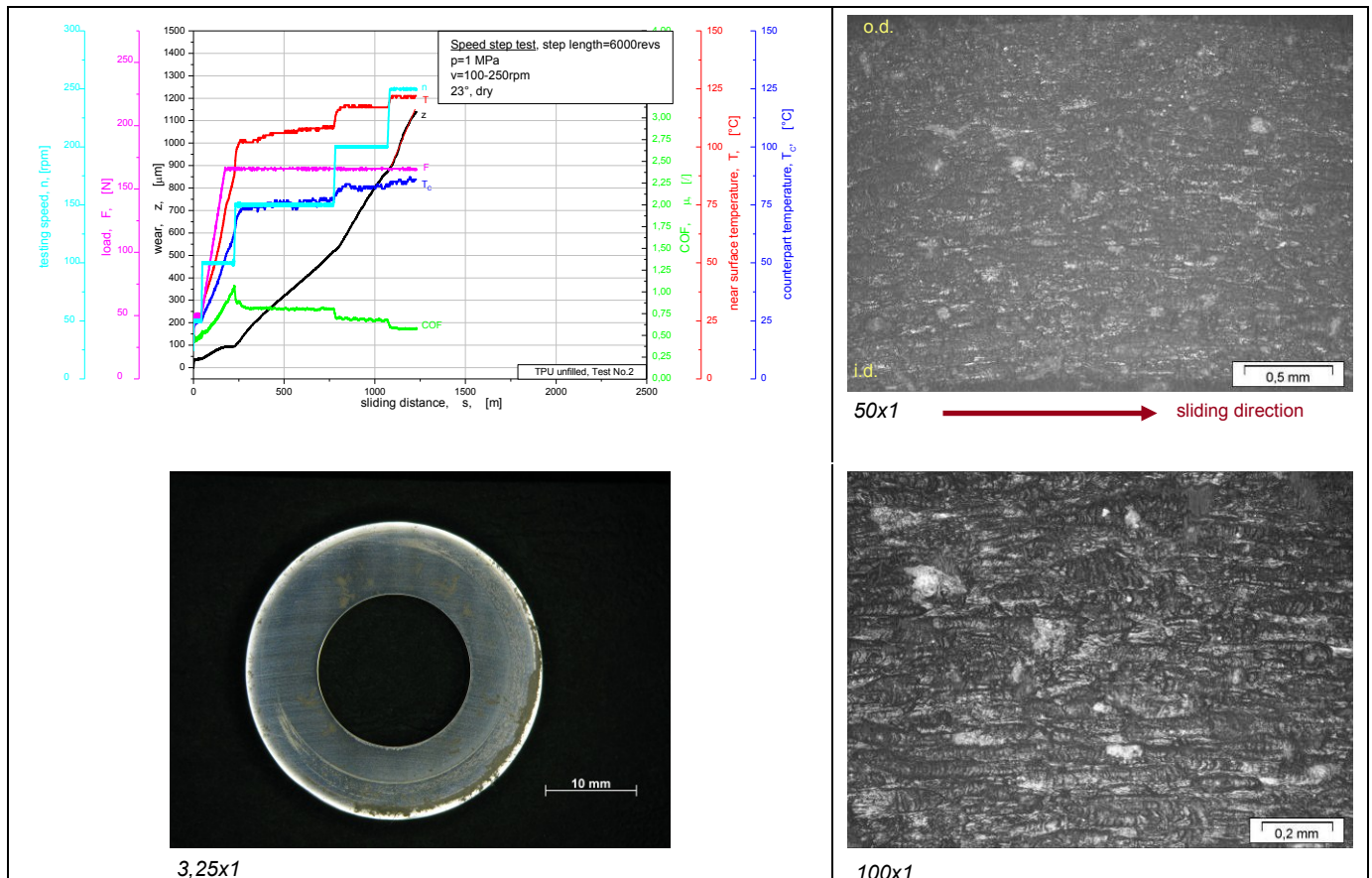


Figure 8.4-55: Speed Step test at 1,0 MPa of TPU unfilled, Test No.2

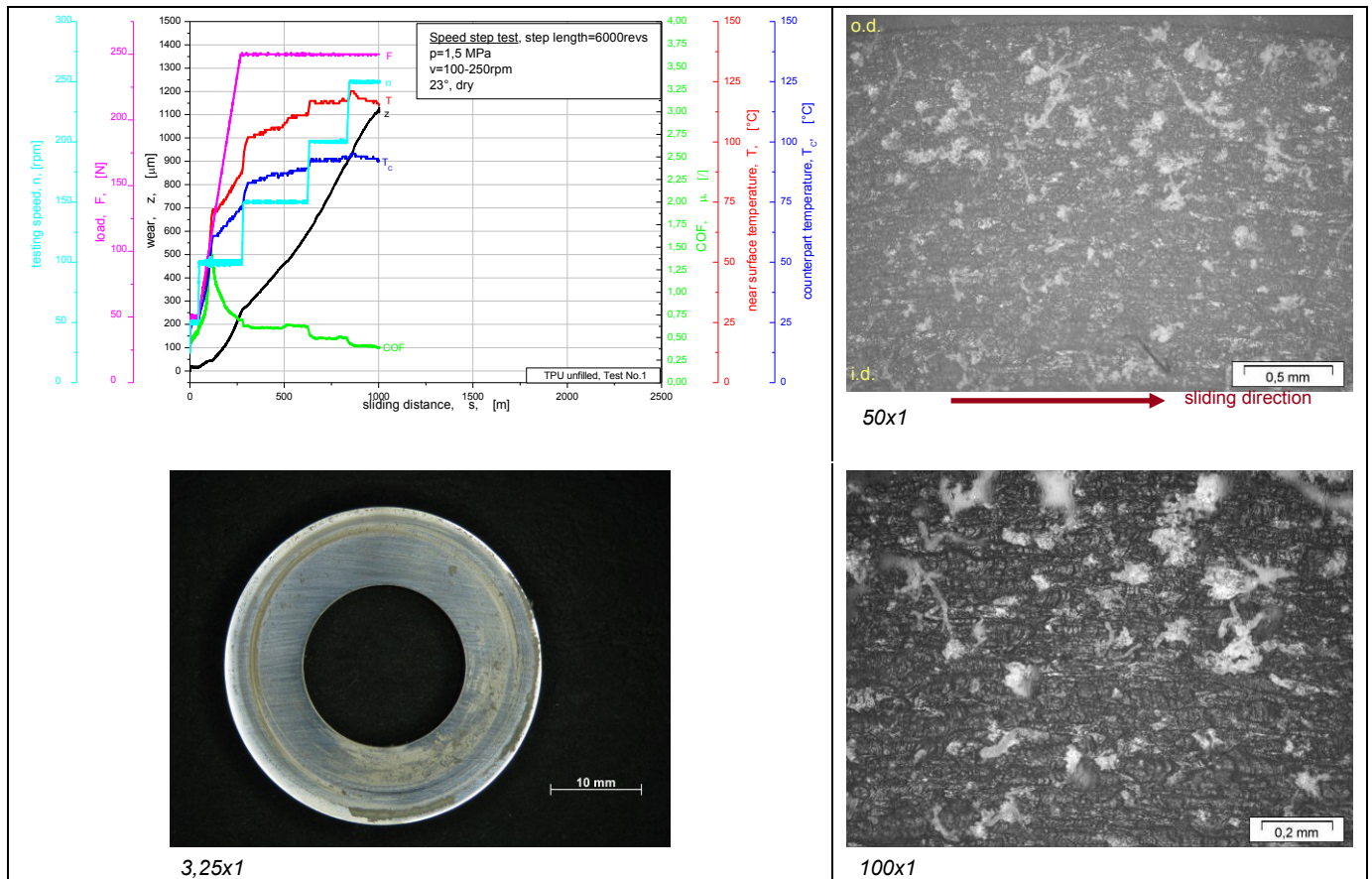


Figure 8.4-56: Speed Step test at 1,5 MPa of TPU unfilled, Test No.1

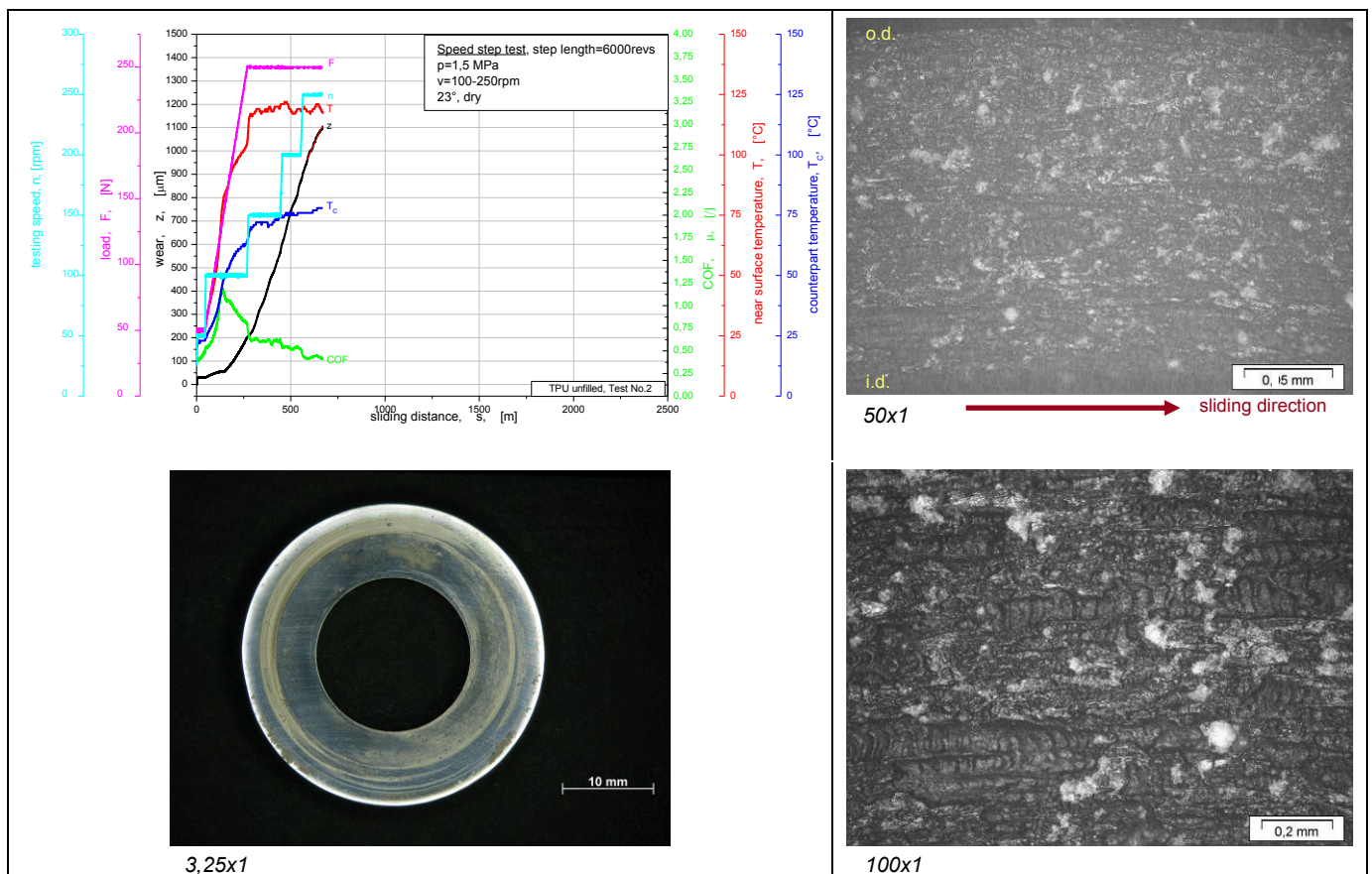


Figure 8.4-57: Speed Step test at 1,5 MPa of TPU unfilled, Test No.2

Gradually performed speed step tests of TPU unfilled

Table 8.4-13: Summary of gradually performed speed step tests for the unfilled TPU

Speed Step Test TPU unfilled, 1MPa, Step 1		100rpm	150rpm	200rpm	250rpm
Wear Parameters					
mass loss	[mg]	81,78			
overall wear rate K	[cm ³ /Nm]	6,03E-07			
linear wear rate	[µm/m]	0,54	x	x	x
Friction Parameters					
COF	[-]	0,89	x	x	x
near surface temperature	[°C]	91,74	x	x	x
counterpart temperature	[°C]	69,26	x	x	x
Speed Step Test TPU unfilled, 1MPa, Step 2		100rpm	150rpm	200rpm	250rpm
Wear Parameters					
mass loss	[mg]	222,66			
overall wear rate K	[cm ³ /Nm]	9,09E-07			
linear wear rate	[µm/m]	0,48	1,12	x	x
Friction Parameters					
COF	[-]	0,95	0,75	x	x
near surface temperature	[°C]	98,37	110,49	x	x
counterpart temperature	[°C]	72,81	83,19	x	x
Speed Step Test TPU unfilled, 1MPa, Step 3		100rpm	150rpm	200rpm	250rpm
Wear Parameters					
mass loss	[mg]	325,92			
overall wear rate K	[cm ³ /Nm]	1,78E-06			
linear wear rate	[µm/m]	0,22	1,75	1,48	x
Friction Parameters					
COF	[-]	0,87	0,79	0,67	x
near surface temperature	[°C]	104,85	111,80	120,02	x
counterpart temperature	[°C]	74,97	84,10	90,57	x
Speed Step Test TPU unfilled, 1MPa, Step 4		100rpm	150rpm	200rpm	250rpm
Wear Parameters					
mass loss	[mg]	322,33			
overall wear rate K	[cm ³ /Nm]	1,05E-06			
linear wear rate	[µm/m]	0,16	1,07	1,27	1,56
Friction Parameters					
COF	[-]	0,77	0,74	0,66	0,56
near surface temperature	[°C]	80,61	101,84	112,22	117,02
counterpart temperature	[°C]	70,23	85,35	90,99	96,21
Speed Step Test TPU unfilled, 1MPa, Step 4 old, specimen bracket		100rpm	150rpm	200rpm	250rpm
Wear Parameters					
mass loss	[mg]	272,53			
overall wear rate K	[cm ³ /Nm]	2,01E-06			
linear wear rate	[µm/m]	0,58	1,76	2,32	3,67
Friction Parameters					
COF	[-]	1,17	0,74	0,66	0,62
near surface temperature	[°C]	88,41	108,35	118,28	123,08
counterpart temperature	[°C]	61,54	81,03	89,26	91,47

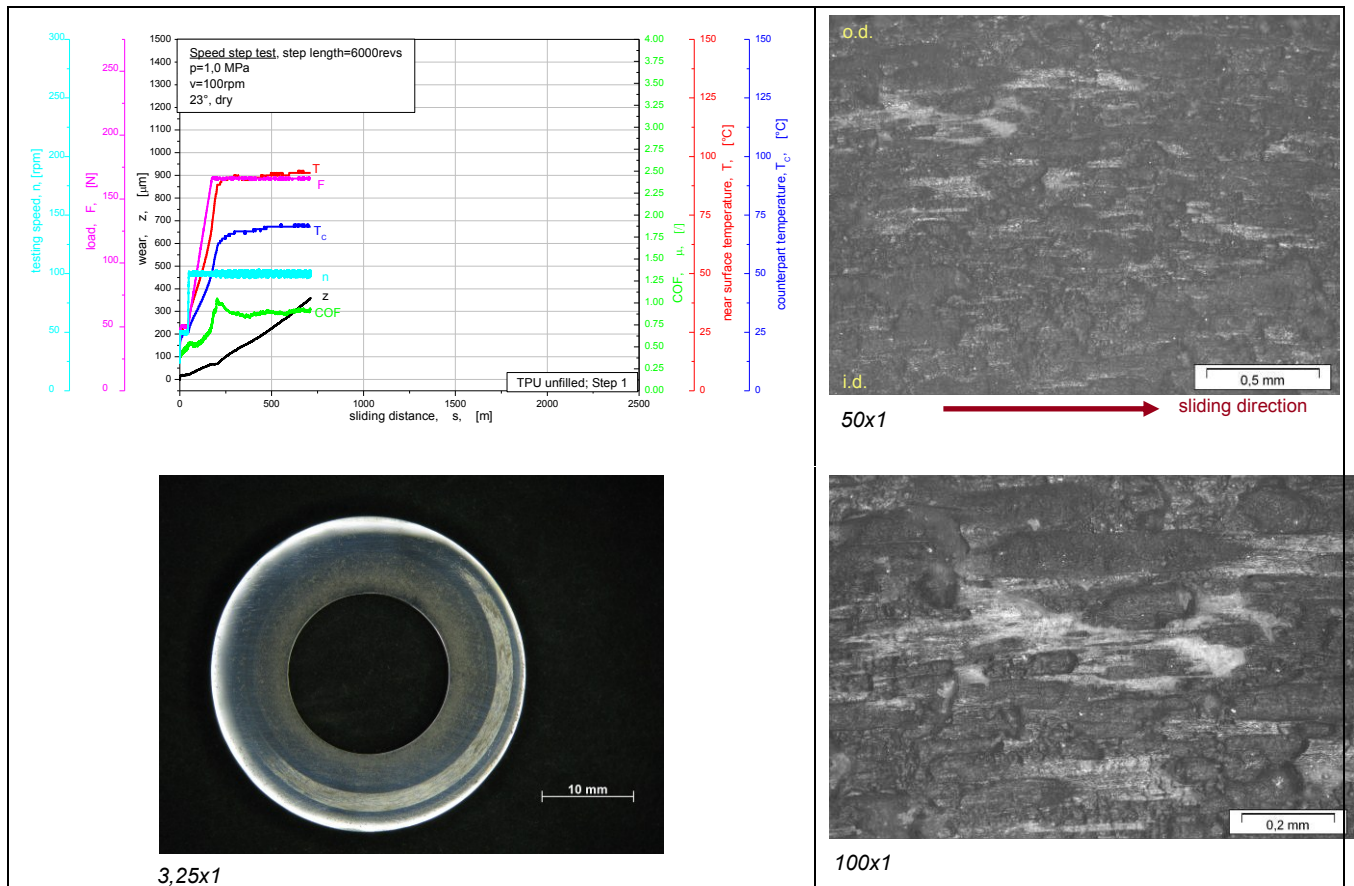


Figure 8.4-58: Gradually performed speed step test at 1 MPa of TPU unfilled, Step 1

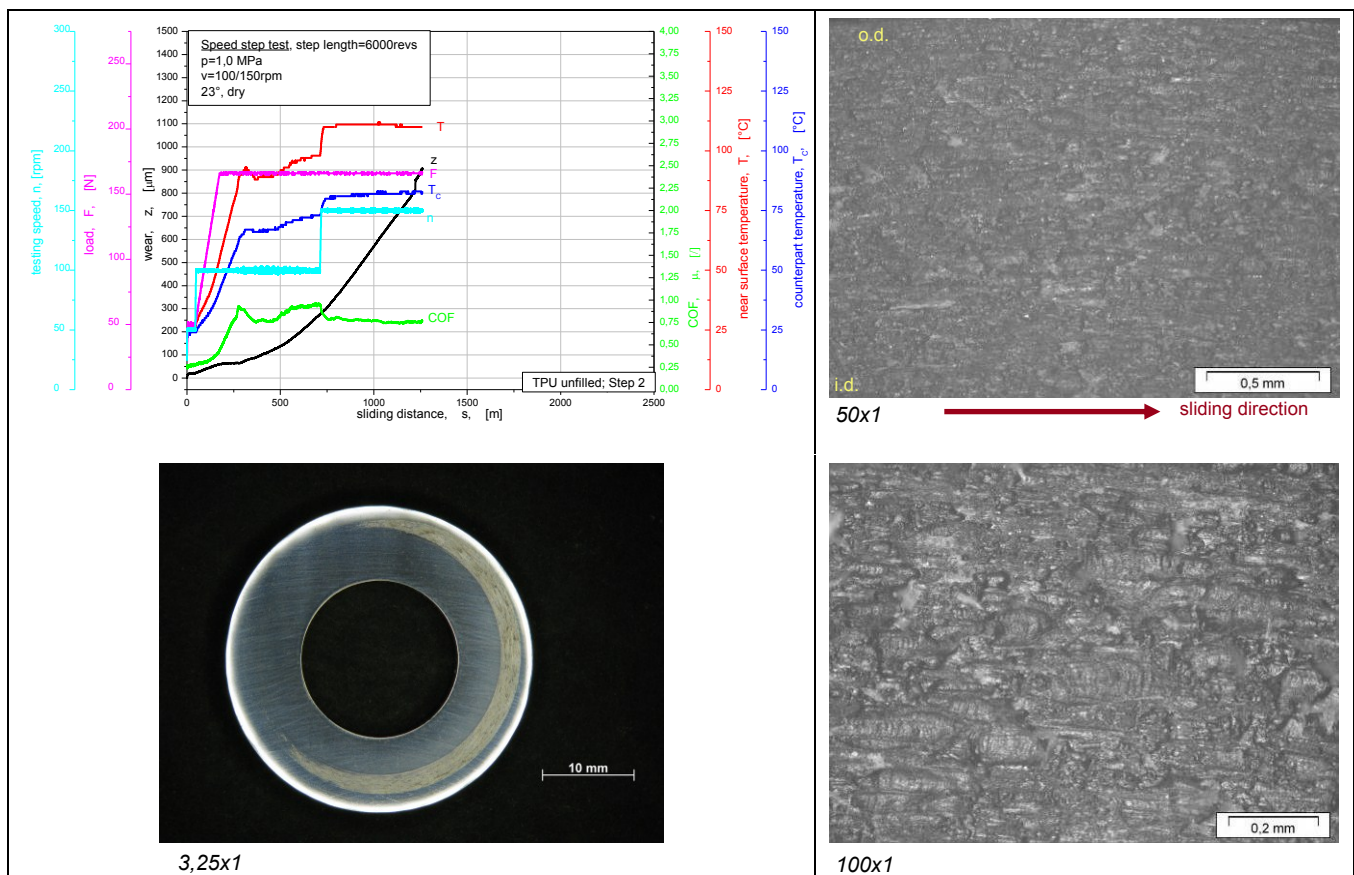


Figure 8.4-59: Gradually performed speed step test at 1 MPa of TPU unfilled, Step 2

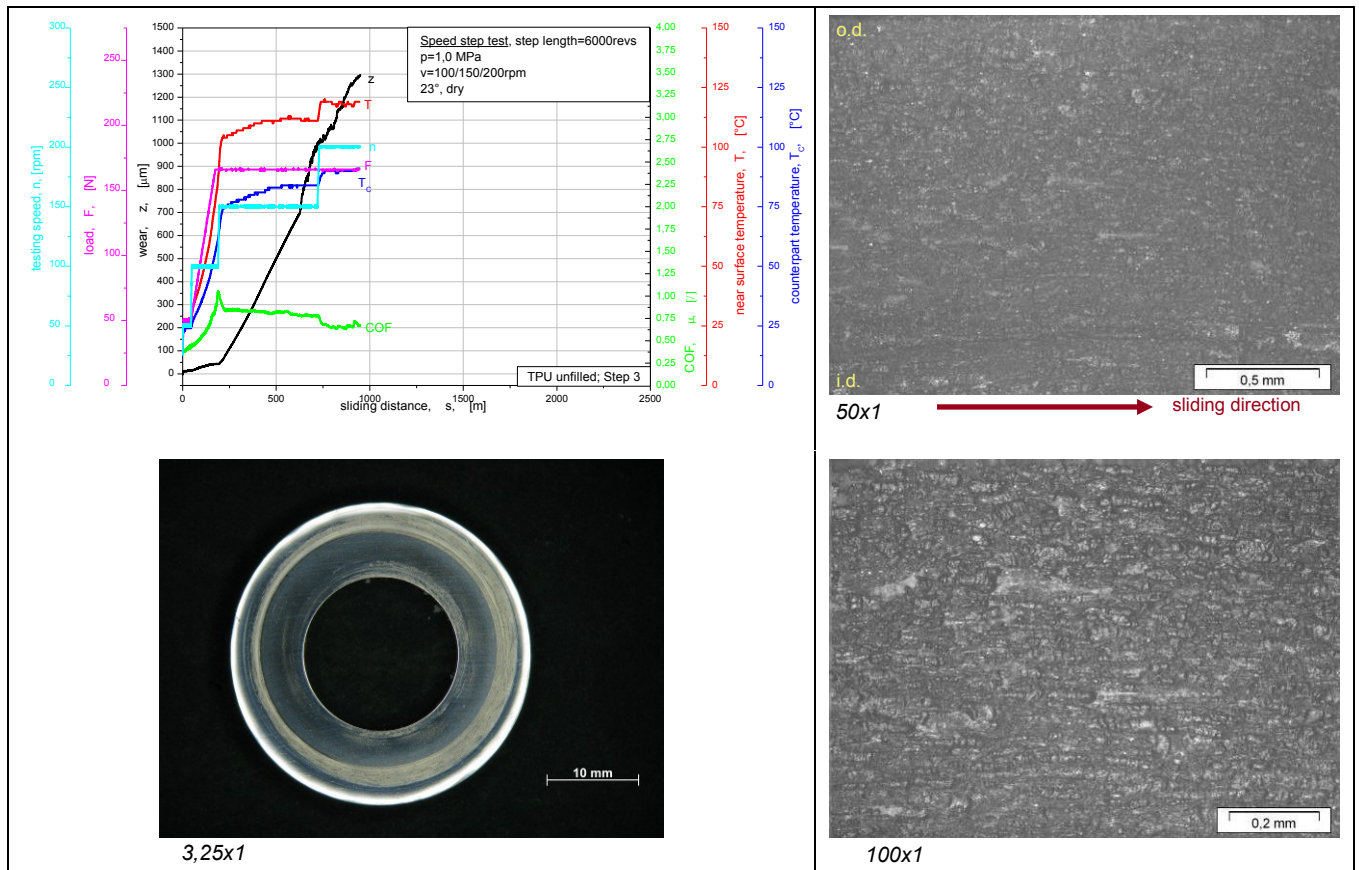


Figure 8.4-60: Gradually performed speed step test at 1 MPa of TPU unfilled, Step 3

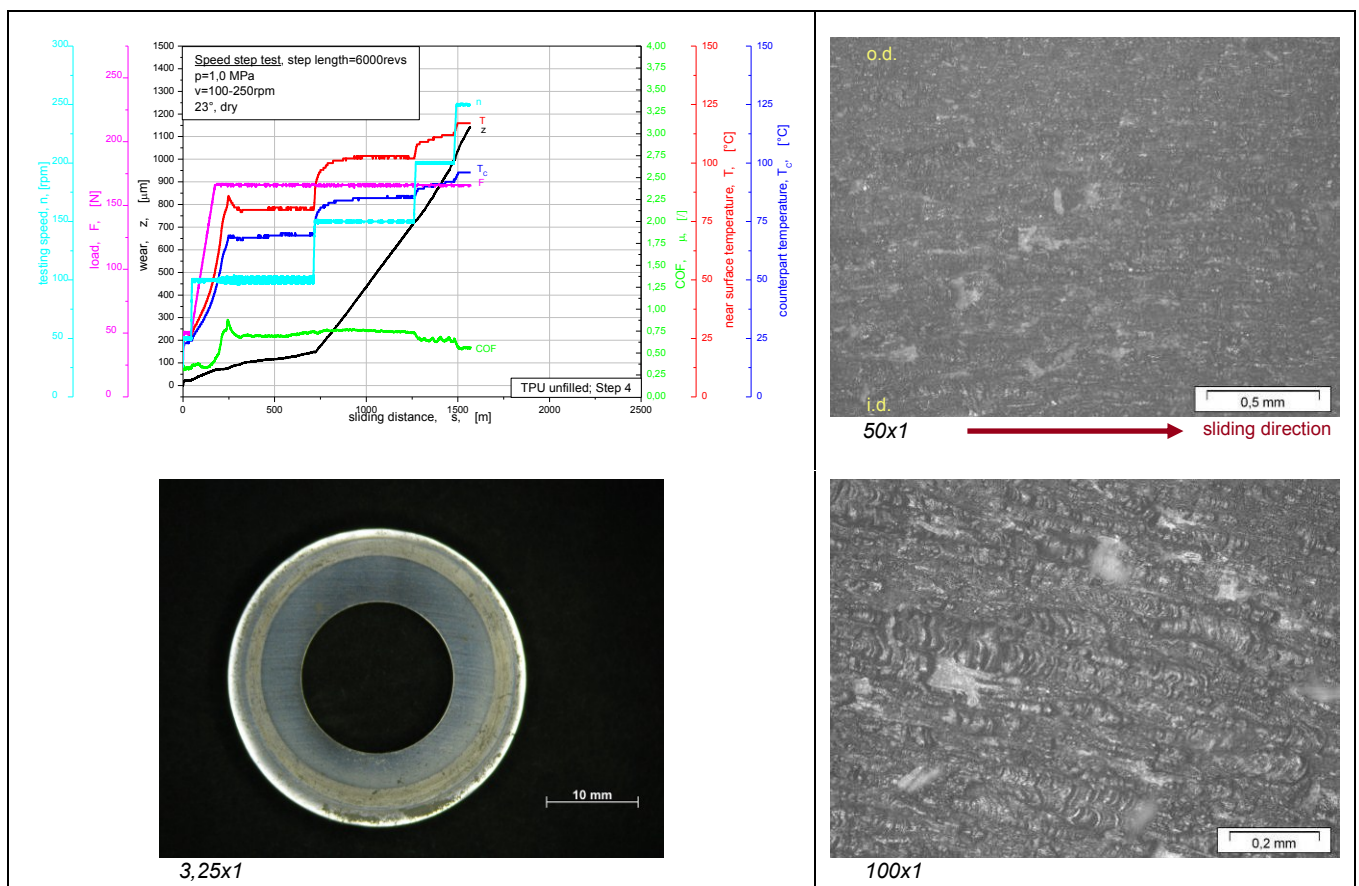


Figure 8.4-61: Gradually performed speed step test at 1 MPa of TPU unfilled, Step 4

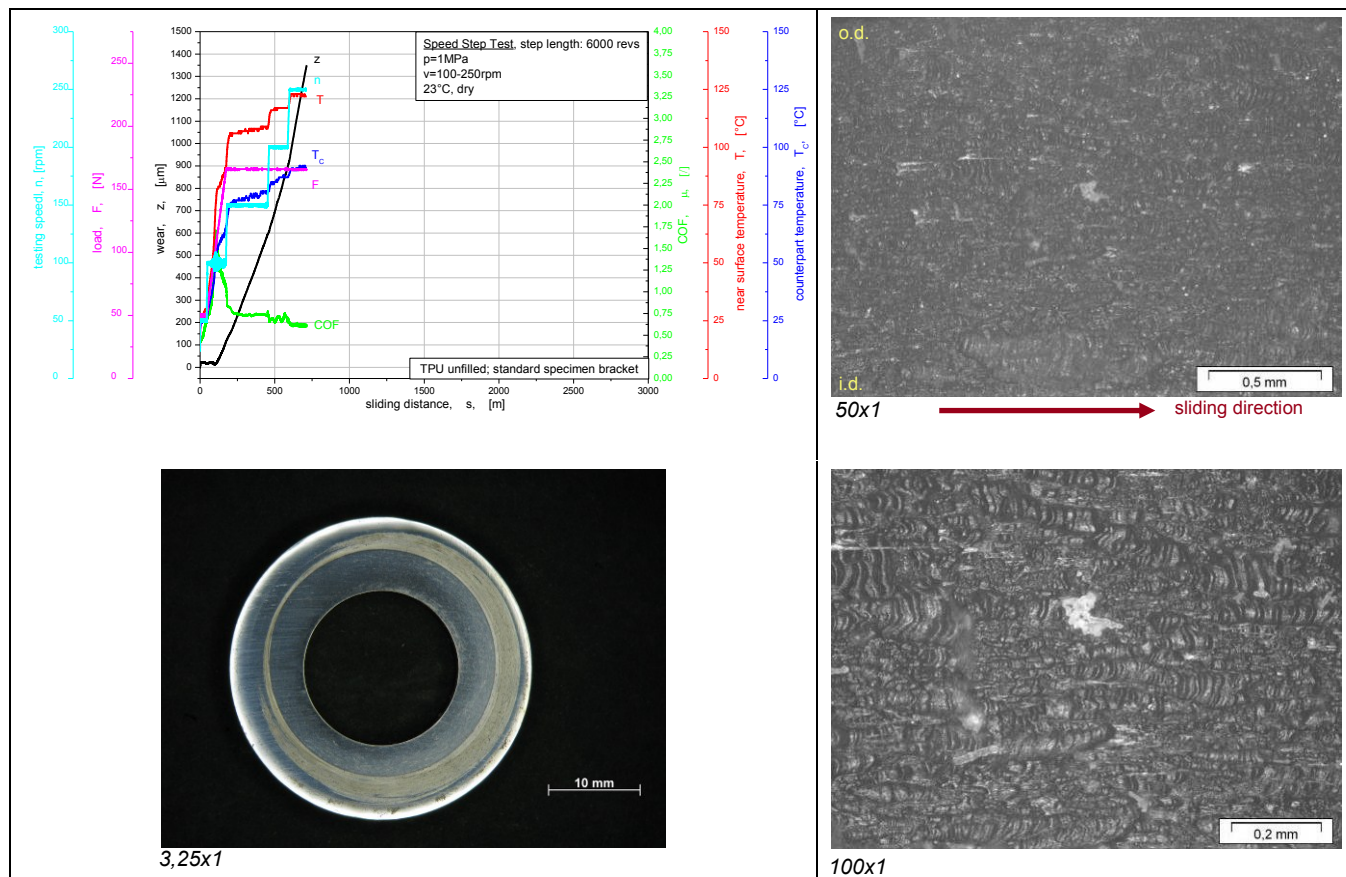


Figure 8.4-62: Gradually performed speed step test at 1 MPa of TPU unfilled, Step 4 (old specimen bracket)

Speed step tests of the filled material

Table 8.4-14: Summary of speed step tests for the filled material

Speed Step Test TPU filled, 0,5 MPa, No. 1		100 rpm	150 rpm	200 rpm	250 rpm
Wear Parameters					
mass loss	[mg]	2,00			
overall wear rate K	[cm^3/Nm]	8,68E-09			
linear wear rate	[$\mu\text{m}/\text{m}$]	0,00	0,00	0,00	0,00
Friction Parameters					
COF	[-]	1,31	1,04	0,88	0,79
near surface temperature	[$^{\circ}\text{C}$]	76,20	88,54	95,94	105,38
counterpart temperature	[$^{\circ}\text{C}$]	64,18	73,67	80,20	87,85
Speed Step Test TPU filled, 0,5 MPa, No. 2		100 rpm	150 rpm	200 rpm	250 rpm
Wear Parameters					
mass loss	[mg]	2,00			
overall wear rate K	[cm^3/Nm]	8,68E-09			
linear wear rate	[$\mu\text{m}/\text{m}$]	0,00	0,00	0,00	0,00
Friction Parameters					
COF	[-]	1,30	0,92	0,87	0,83
near surface temperature	[$^{\circ}\text{C}$]	69,52	74,93	86,89	98,53
counterpart temperature	[$^{\circ}\text{C}$]	55,24	58,85	66,68	74,17
Speed Step Test TPU filled, 1,0MPa, No. 1		100 rpm	150 rpm	200 rpm	250 rpm

Wear Parameters					
mass loss	[mg]	5,00			
overall wear rate K	[cm ³ /Nm]	1,05E-08			
linear wear rate	[μm/m]	0,00	0,00	0,00	0,00
Friction Parameters					
COF	[-]	0,88	0,81	0,69	0,57
near surface temperature	[°C]	93,94	119,75	132,73	136,87
counterpart temperature	[°C]	73,13	92,09	102,47	104,84
Speed Step Test TPU filled,1,0MPa, No. 2		100 rpm	150 rpm	200 rpm	250 rpm
Wear Parameters					
mass loss	[mg]	2,00			
overall wear rate K	[cm ³ /Nm]	3,86E-09			
linear wear rate	[μm/m]	0,00	0,00	0,00	0,00
Friction Parameters					
COF	[-]	0,86	0,84	0,78	0,66
near surface temperature	[°C]	87,58	116,13	138,49	145,96
counterpart temperature	[°C]	65,58	84,85	100,59	105,36
Speed Step Test TPU filled,1,5MPa, No. 1		100 rpm	150 rpm	200 rpm	250 rpm
Wear Parameters					
mass loss	[mg]	9,00			
overall wear rate K	[cm ³ /Nm]	1,21E-08			
linear wear rate	[μm/m]	0,00	0,01	0,01	0,01
Friction Parameters					
COF	[-]	0,74	0,56	0,49	0,41
near surface temperature	[°C]	106,09	114,58	126,67	132,28
counterpart temperature	[°C]	83,10	90,14	99,89	103,37
Speed Step Test TPU filled,1,5MPa, No. 2		100 rpm	150 rpm	200 rpm	250 rpm
Wear Parameters					
mass loss	[mg]	8,00			
overall wear rate K	[cm ³ /Nm]	1,07E-08			
linear wear rate	[μm/m]	0,03	0,03	0,01	0,02
Friction Parameters					
COF	[-]	0,74	0,59	0,50	0,42
near surface temperature	[°C]	99,57	113,84	123,80	129,44
counterpart temperature	[°C]	82,83	95,33	102,79	106,03

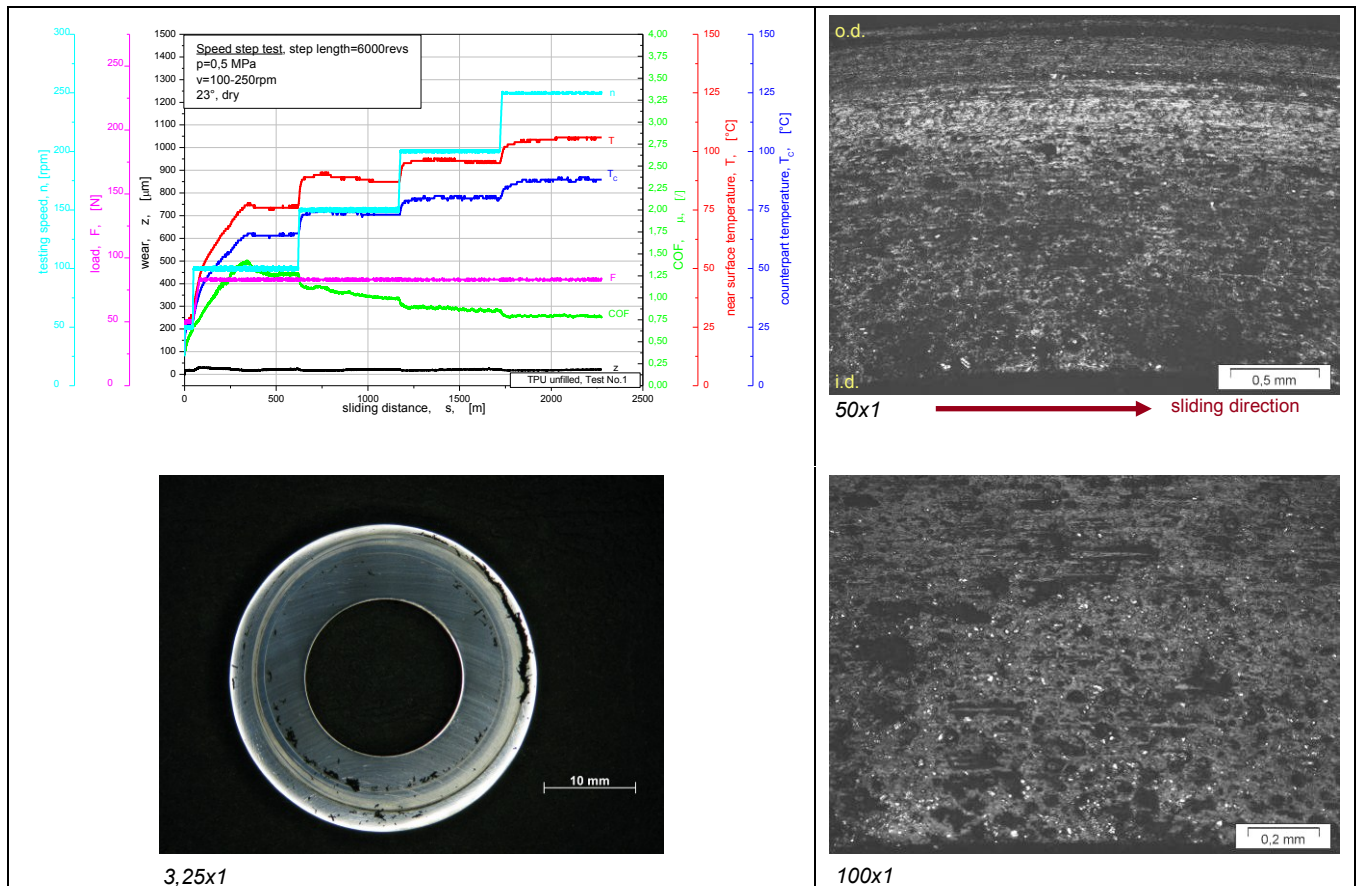


Figure 8.4-63: Speed Step test at 0,5 MPa of TPU filled, Test No.1

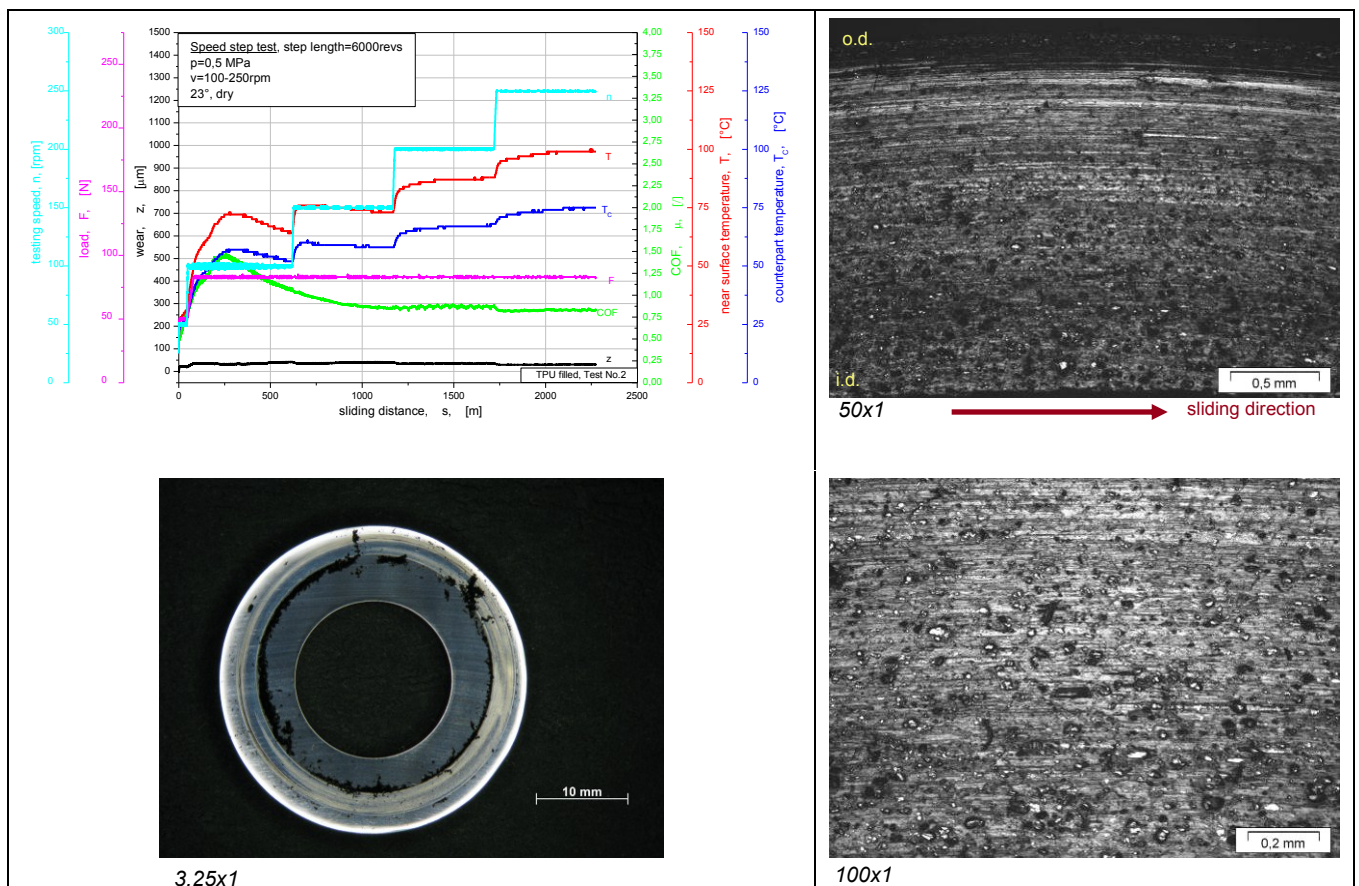


Figure 8.4-64: Speed Step test at 0,5 MPa of TPU filled, Test No.2

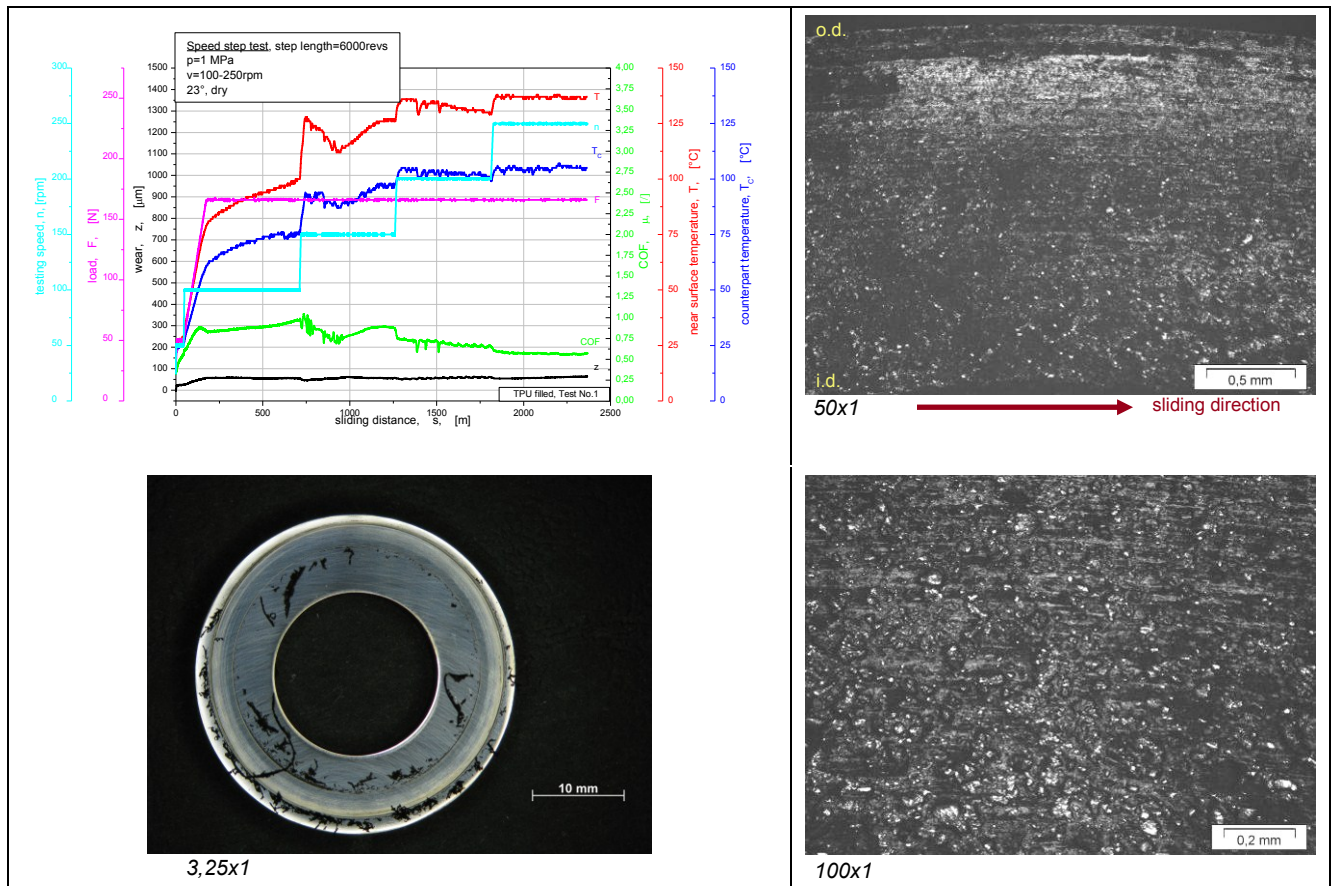


Figure 8.4-65: Speed Step test at 1,0 MPa of TPU filled, Test No.1

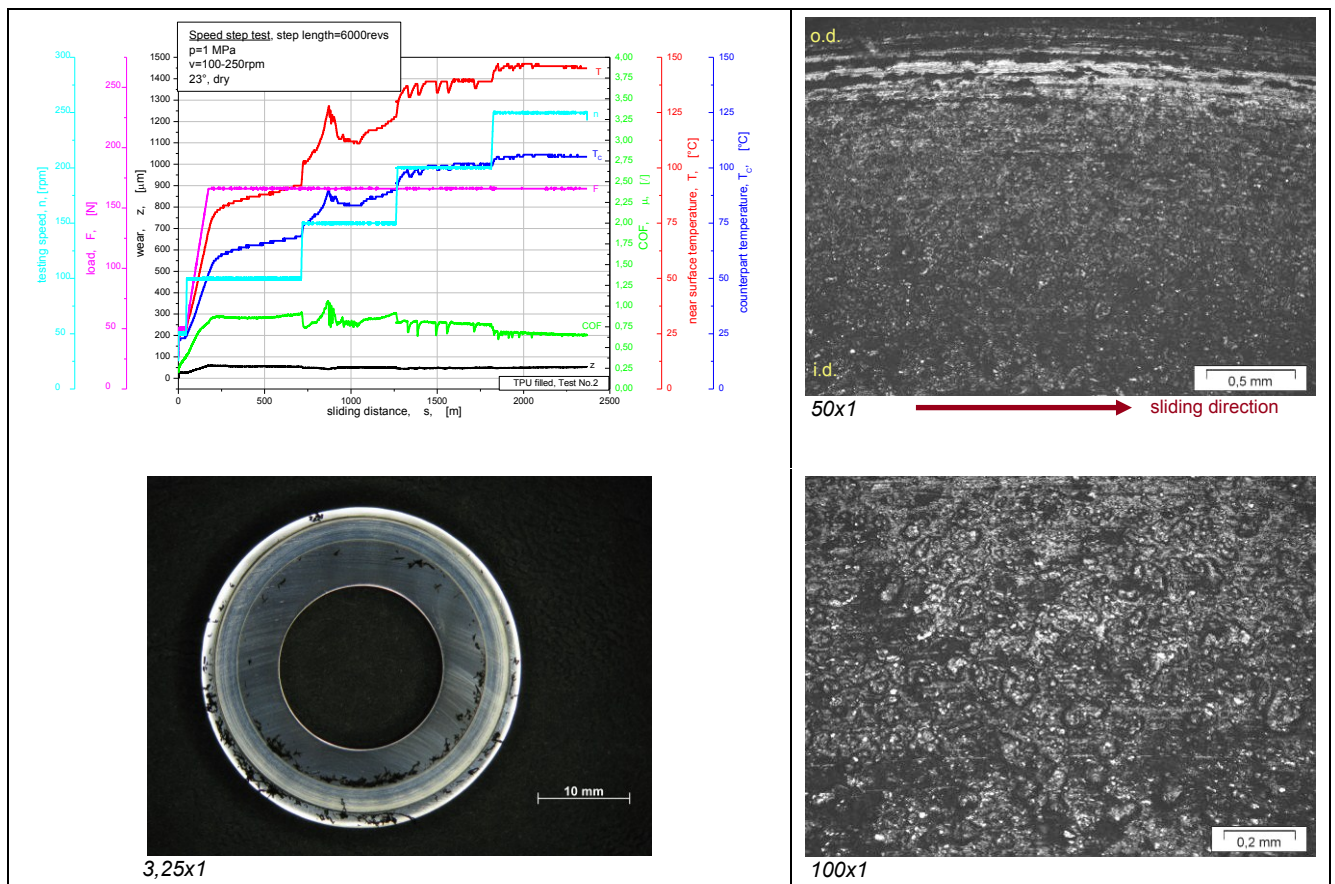


Figure 8.4-66: Speed Step test at 1,0 MPa of TPU filled, Test No.2

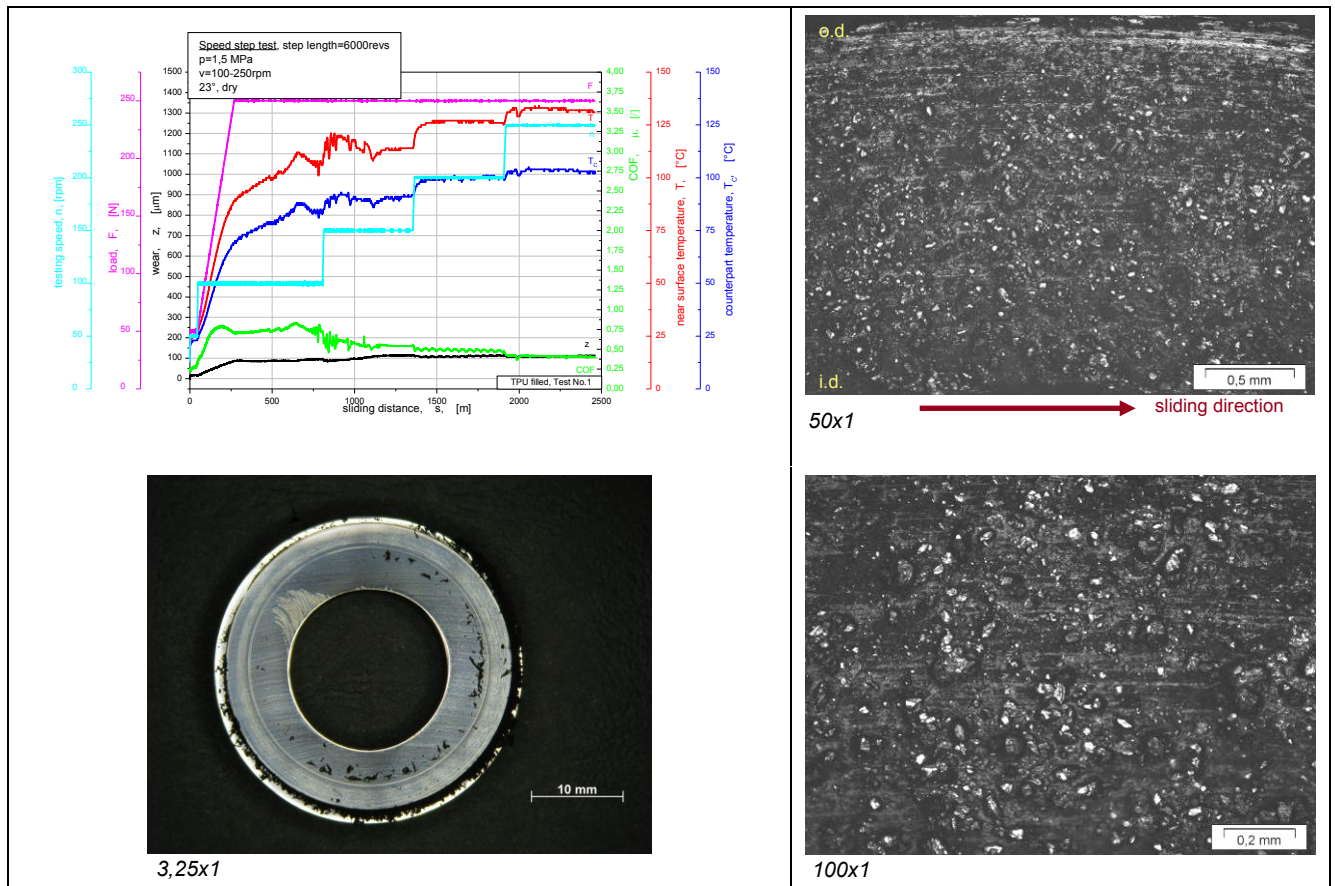


Figure 8.4-67: Speed Step test at 1,5 MPa of TPU filled, Test No.1

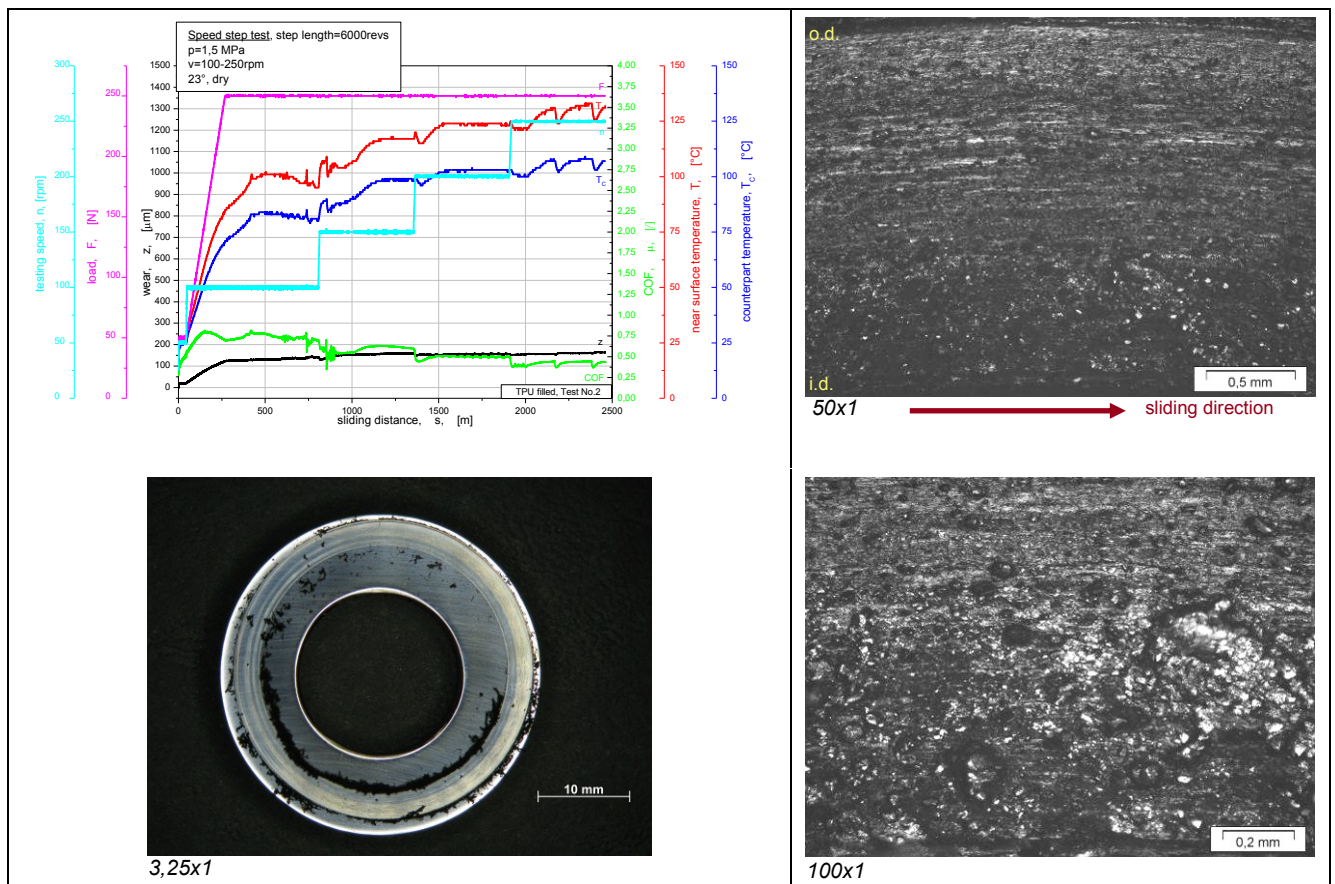


Figure 8.4-68: Speed Step test at 1,5 MPa of TPU filled, Test No.2

Gradually performed speed step tests of TPU filled

Table 8.4-15: Summary of gradually performed speed step tests for the filled material

Speed Step Test TPU filled,1 MPa, Step 1		100 rpm	150 rpm	200 rpm	250 rpm
Wear Parameters					
mass loss	[mg]	0,37			
overall wear rate K	[cm ³ /Nm]	2,66E-09			
linear wear rate	[µm/m]	0,00	x	x	x
Friction Parameters					
COF	[-]	0,91	x	x	x
near surface temperature	[°C]	91,14	x	x	x
counterpart temperature	[°C]	70,35	x	x	x
Speed Step Test TPU filled,1 MPa, Step 2		100 rpm	150 rpm	200 rpm	250 rpm
Wear Parameters					
mass loss	[mg]	2,94			
overall wear rate K	[cm ³ /Nm]	1,17E-08			
linear wear rate	[µm/m]	0,00	0,00	x	x
Friction Parameters					
COF	[-]	0,93	0,81	x	x
near surface temperature	[°C]	100,09	125,14	x	x
counterpart temperature	[°C]	75,04	96,38	x	x
Speed Step Test TPU filled,1 MPa, Step 3		100 rpm	150 rpm	200 rpm	250 rpm
Wear Parameters					
mass loss	[mg]	4,83			
overall wear rate K	[cm ³ /Nm]	1,33E-08			
linear wear rate	[µm/m]	0,00	0,00	0,00	x
Friction Parameters					
COF	[-]	0,87	0,79	0,63	x
near surface temperature	[°C]	89,25	109,64	122,60	x
counterpart temperature	[°C]	56,17	69,33	74,55	x
Speed Step Test TPU filled,1 MPa, Step 4		100 rpm	150 rpm	200 rpm	250 rpm
Wear Parameters					
mass loss	[mg]	4,55			
overall wear rate K	[cm ³ /Nm]	9,53E-09			
linear wear rate	[µm/m]	0,00	0,00	0,00	0,00
Friction Parameters					
COF	[-]	0,95	0,85	0,76	0,63
near surface temperature	[°C]	93,00	121,90	122,14	126,38
counterpart temperature	[°C]	68,09	85,14	86,93	88,90
Speed Step Test TPU filled,1 MPa, Step 4 , old specimen bracket		100 rpm	150 rpm	200 rpm	250 rpm
Wear Parameters					
mass loss	[mg]	3,39			
overall wear rate K	[cm ³ /Nm]	7,10E-09			
linear wear rate	[µm/m]	0,00	0,00	0,02	0,02
Friction Parameters					
COF	[-]	0,95	0,90	0,70	0,56
near surface temperature	[°C]	97,52	126,06	131,72	130,40
counterpart temperature	[°C]	76,35	96,12	101,24	99,20

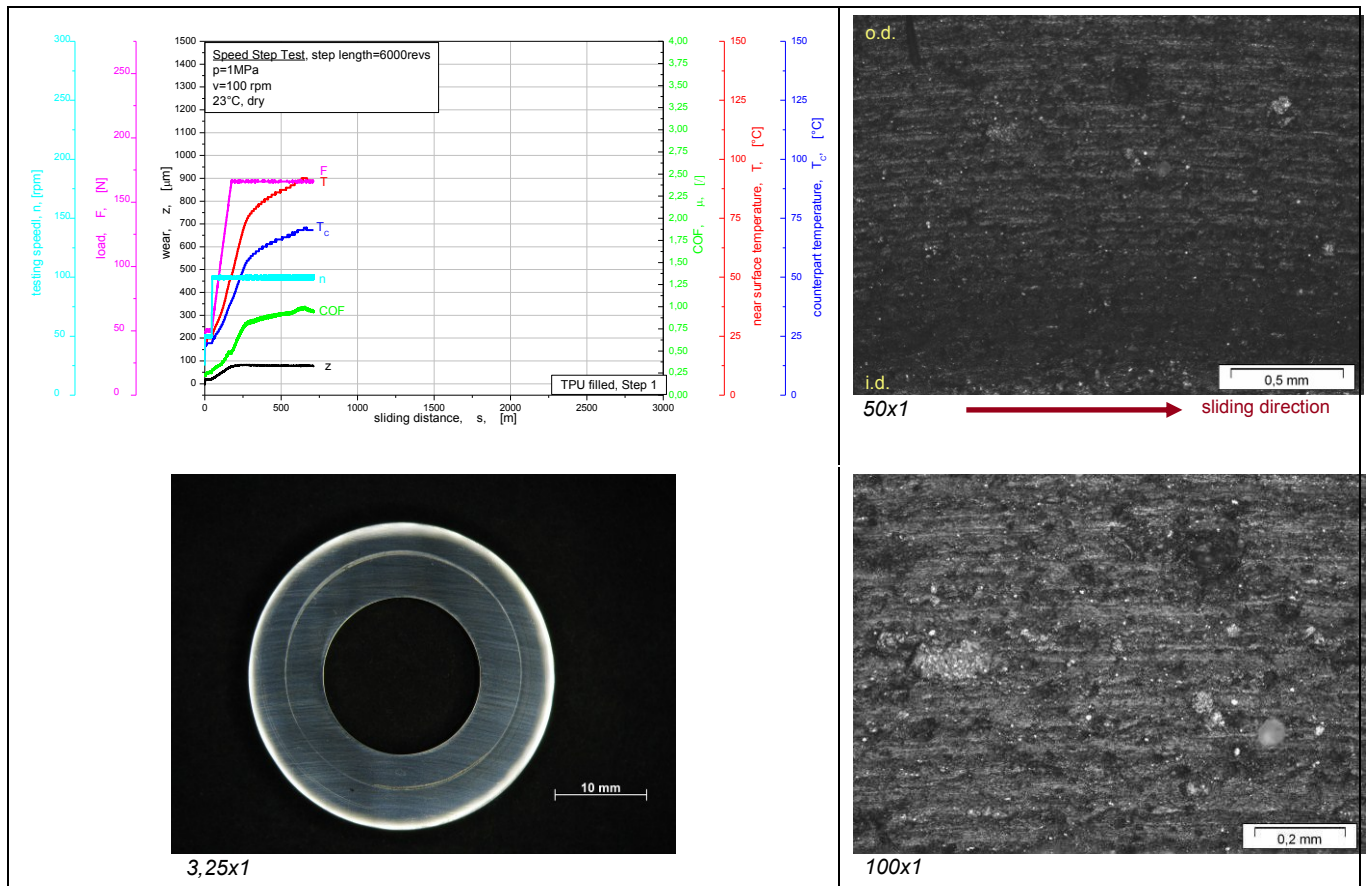


Figure 8.4-69: Gradually performed speed step test at 1 MPa of TPU filled, Step 1

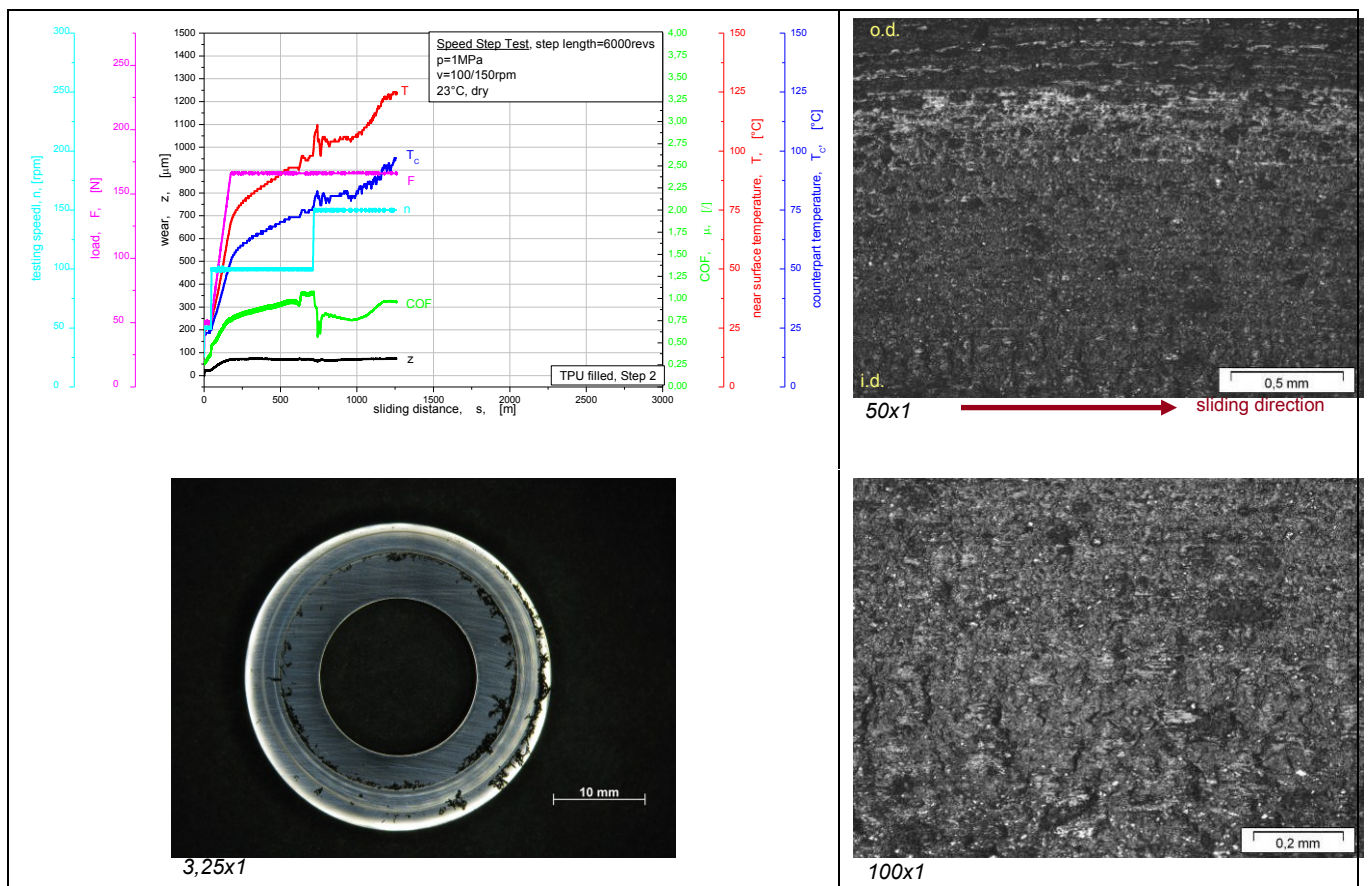


Figure 8.4-70: Gradually performed speed step test at 1 MPa of TPU filled, Step 2

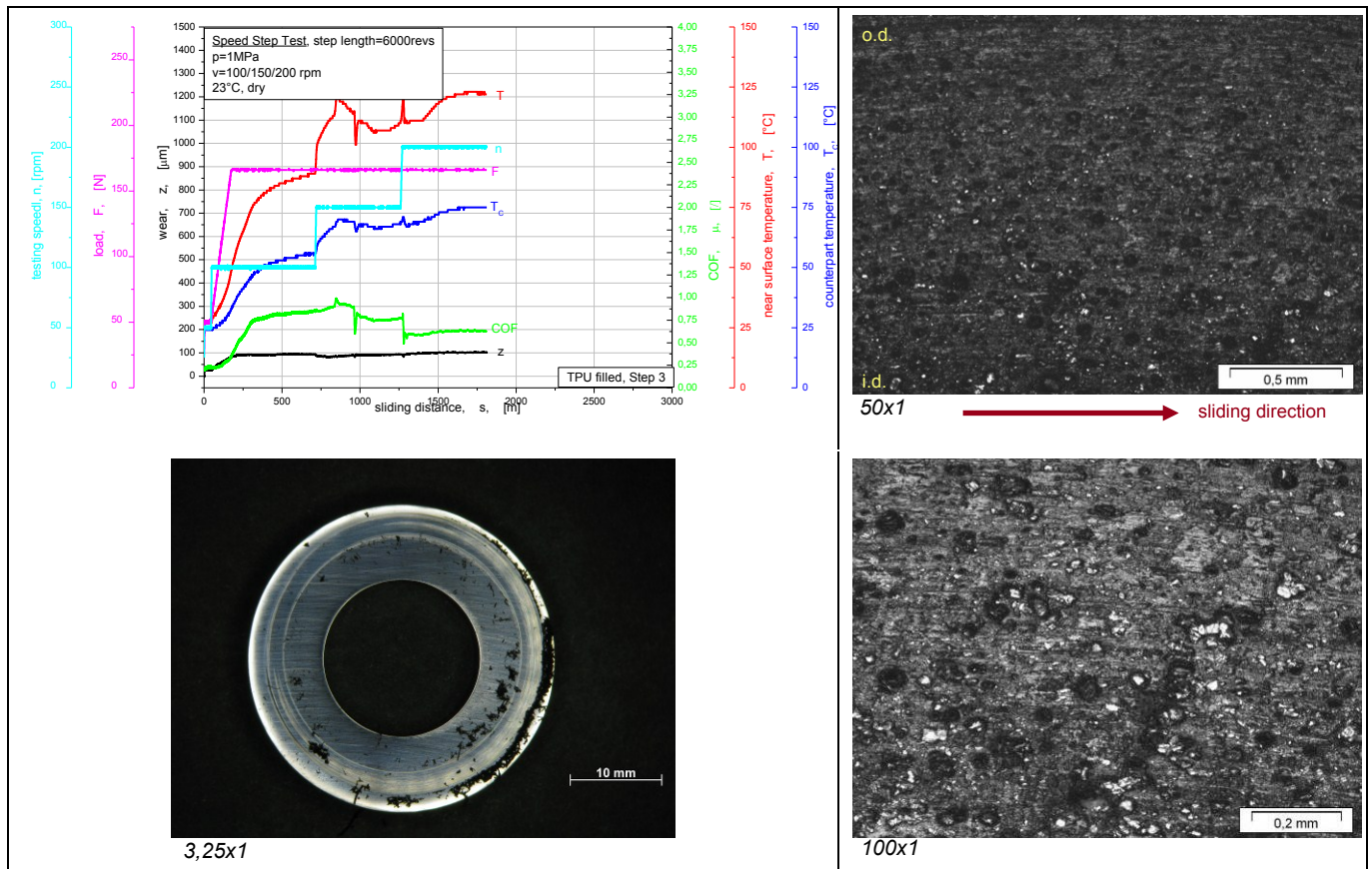


Figure 8.4-71: Gradually performed speed step test at 1 MPa of TPU filled, Step 3

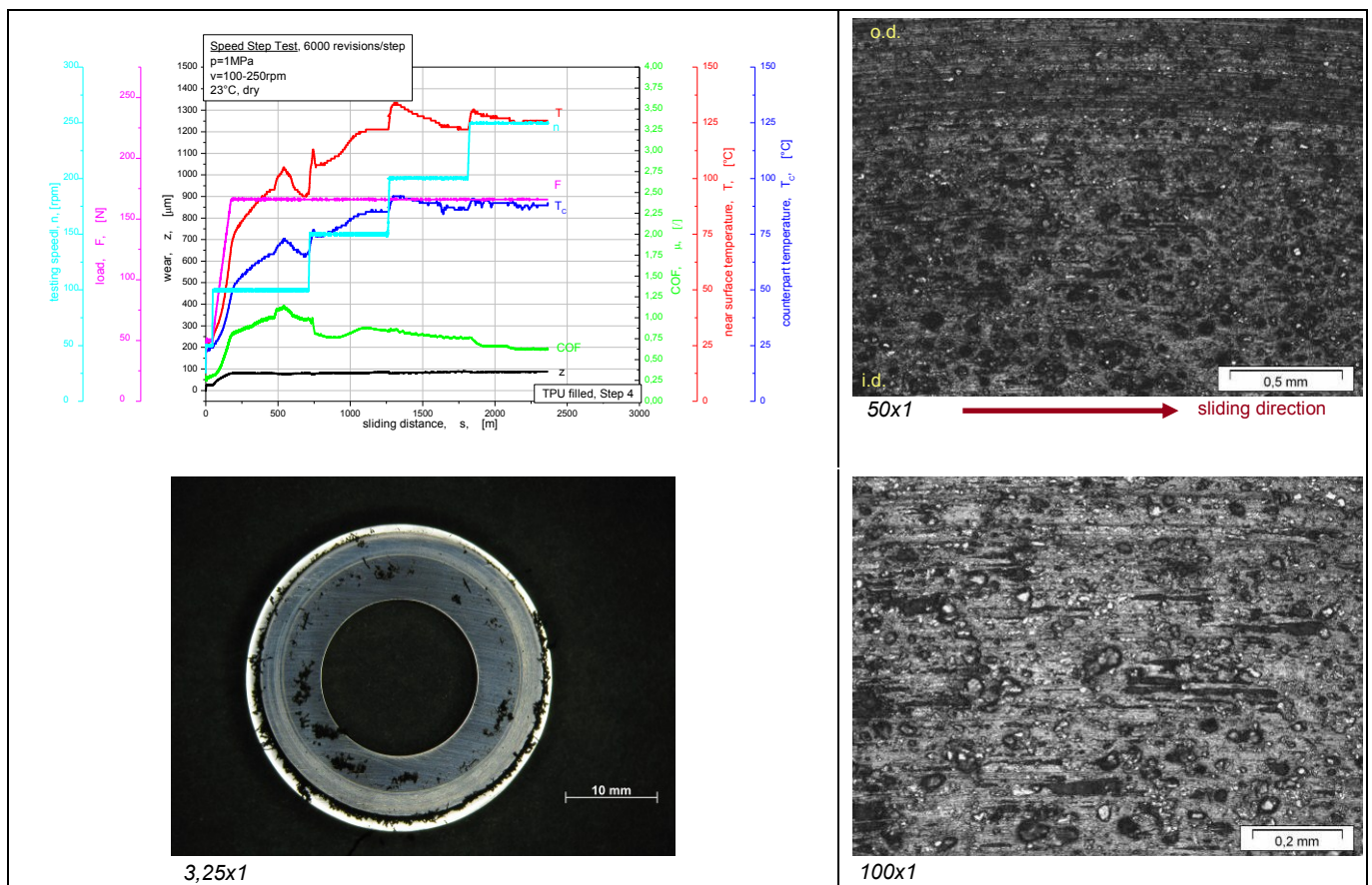


Figure 8.4-72: Gradually performed speed step test at 1 MPa of TPU filled, Step 4

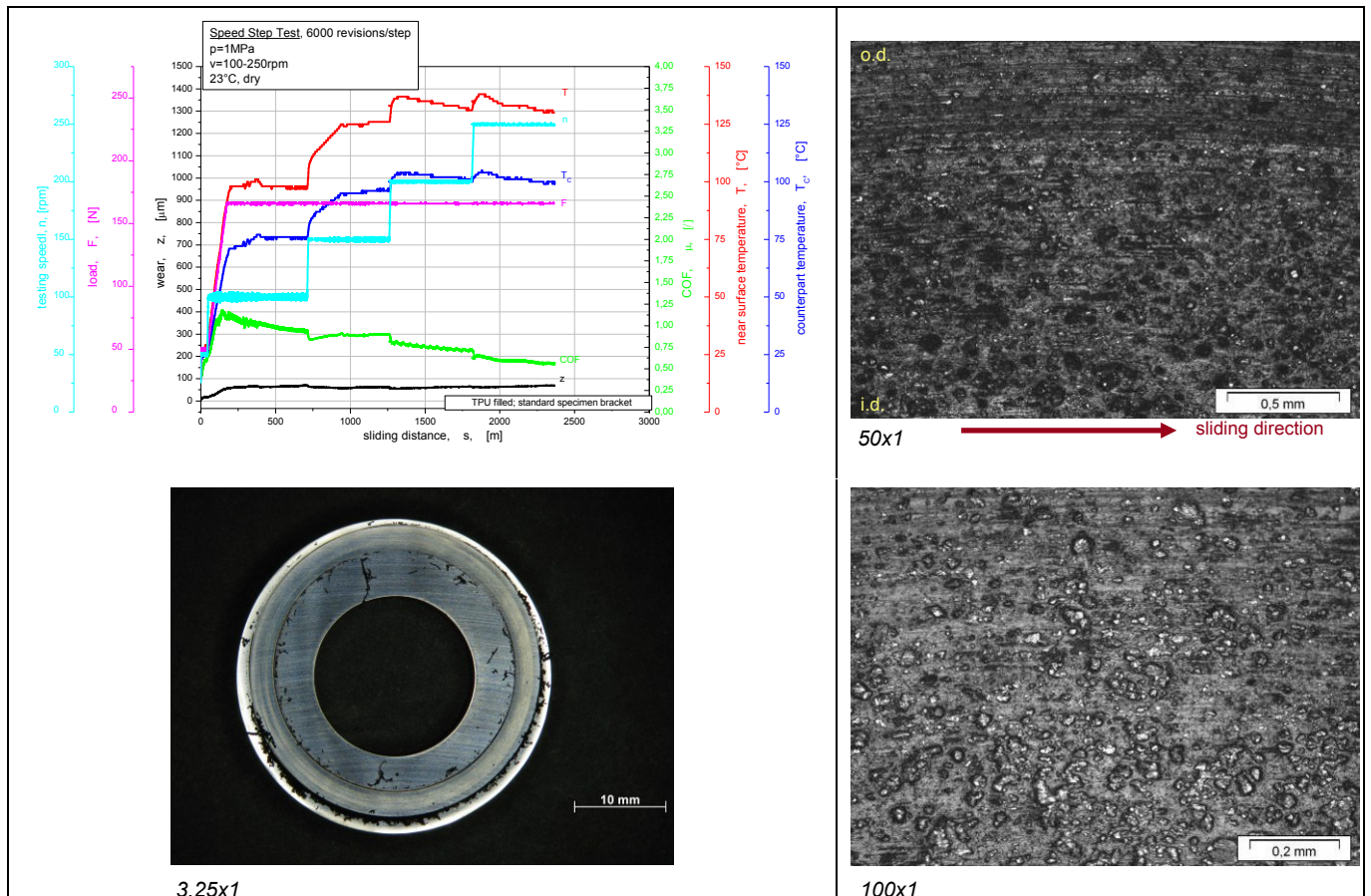


Figure 8.4-73: Gradually performed speed step test at 1 MPa of TPU filled, Step 4 (old specimen bracket)

8.4.7 Advanced PV-step tests of the filled material

Advanced load step tests of TPU filled

Table 8.4-16: Overview of the testing procedure of the advanced load step test

Advanced load step test TPU filled												
Test Parameters												
Step		Run in	1	2	3	4	5	6	7	8	9	10
Ramp time	[s]	x	1030,00	1260,00	1260,00	1260,00	1260,00	1260,00	1260,00	1260,00	1260,00	1260,00
Ramp distance	[m]	x	154,10	188,30	188,30	188,30	188,30	188,30	188,30	188,30	188,30	188,30
Testing force	[N]	50,00	83,00	125,00	166,00	208,00	250,00	292,00	334,00	376,00	418,00	460,00
Contact pressure	[MPa]	0,30	0,50	0,75	1,00	1,25	1,50	1,75	2,00	2,25	2,50	2,75
Testing speed	[rpm]	50,00	100/150/200									
Step length	[Revs]	x	6000,00									
Step distance	[m]	44,50	539,00	539,00	539,00	539,00	539,00	539,00	539,00	539,00	539,00	539,00
Testing temperature	[°C]	23,00										
Lubrication		dry										

Table 8.4-17: Summary of advanced load step tests for the filled material

Advanced Load Step Test TPU filled, 100 rpm, No. 1	0,5 MPa	0,75 MPa	1,00 MPa	1,25 MPa	1,50 MPa	1,75 MPa	2,00 MPa	2,25 MPa	2,50 MPa	2,75 MPa	
Wear Parameters											
mass loss	[mg]	12,15									
overall wear rate K	[cm ³ /Nm]	7,51E-10									
linear wear rate	[µm/m]	0,00	0,03	0,00	0,01	0,02	0,03	0,03	0,03	0,03	
Friction Parameters											
COF	[-]	1,15	0,76	0,61	0,70	0,71	0,64	0,59	0,56	0,53	
near surface temperature	[°C]	72,00	66,00	69,00	94,00	107,00	109,00	112,00	113,00	115,00	
counterpart temperature	[°C]	50,00	47,00	49,00	62,00	71,00	72,00	75,00	77,00	78,00	
Advanced Load Step Test TPU filled, 100rpm, No. 2	0,5 MPa	0,75 MPa	1,00 MPa	1,25 MPa	1,50 MPa	1,75 MPa	2,00 MPa	2,25 MPa	2,50 MPa	2,75 MPa	
Wear Parameters											
mass loss	[mg]	12,73									
overall wear rate K	[cm ³ /Nm]	7,87E-10									
linear wear rate	[µm/m]	0,01	0,02	0,03	0,02	0,02	0,03	0,02	0,02	0,02	
Friction Parameters											
COF	[-]	1,14	0,72	0,59	0,68	0,65	0,65	0,59	0,53	0,49	
near surface temperature	[°C]	72,00	66,00	70,00	95,00	102,00	108,00	109,00	112,00	113,00	
counterpart temperature	[°C]	57,00	54,00	65,00	75,00	79,00	85,00	85,00	88,00	89,00	

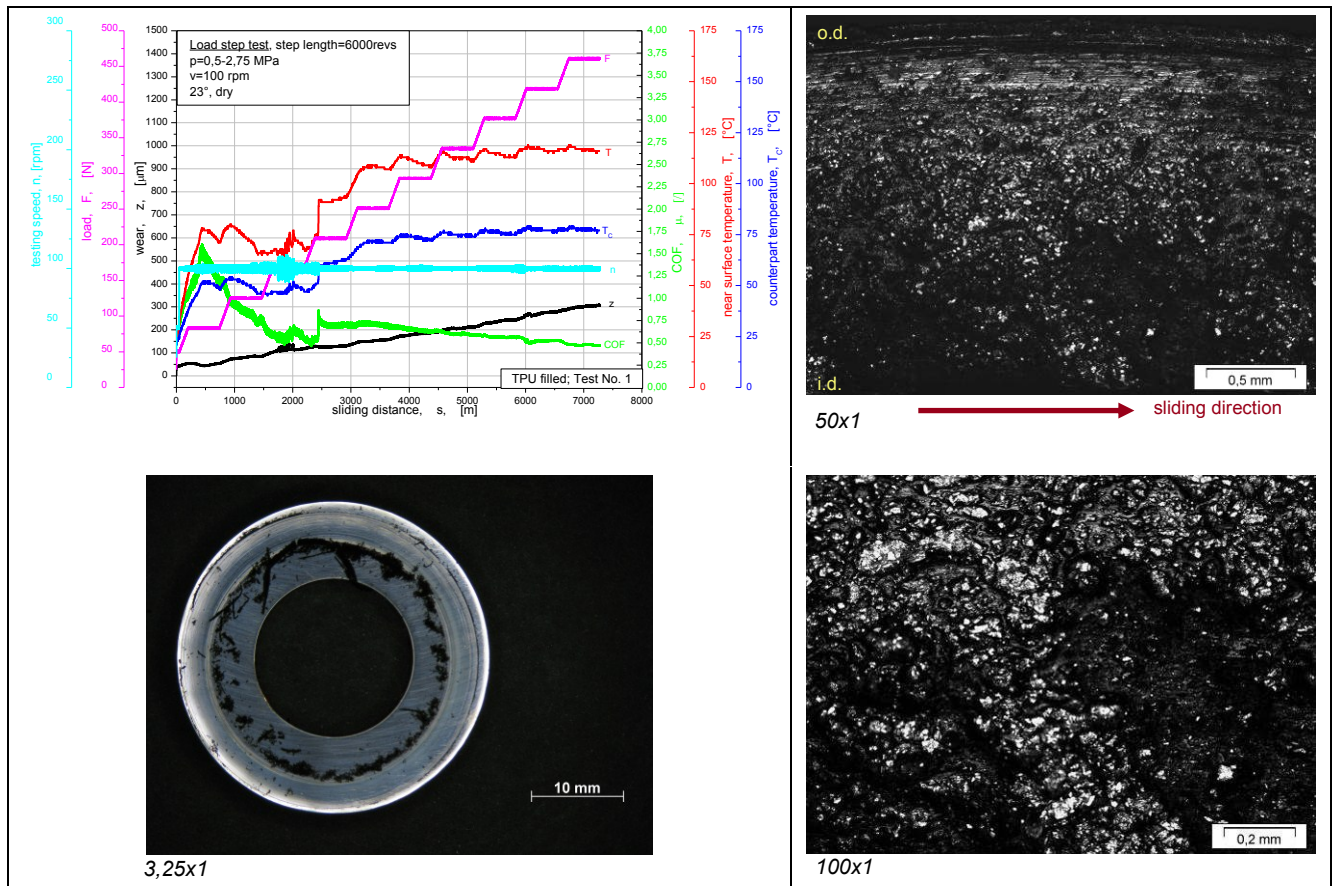


Figure 8.4-74: Advanced Load Step test at 100 rpm of TPU filled, Test No. 1

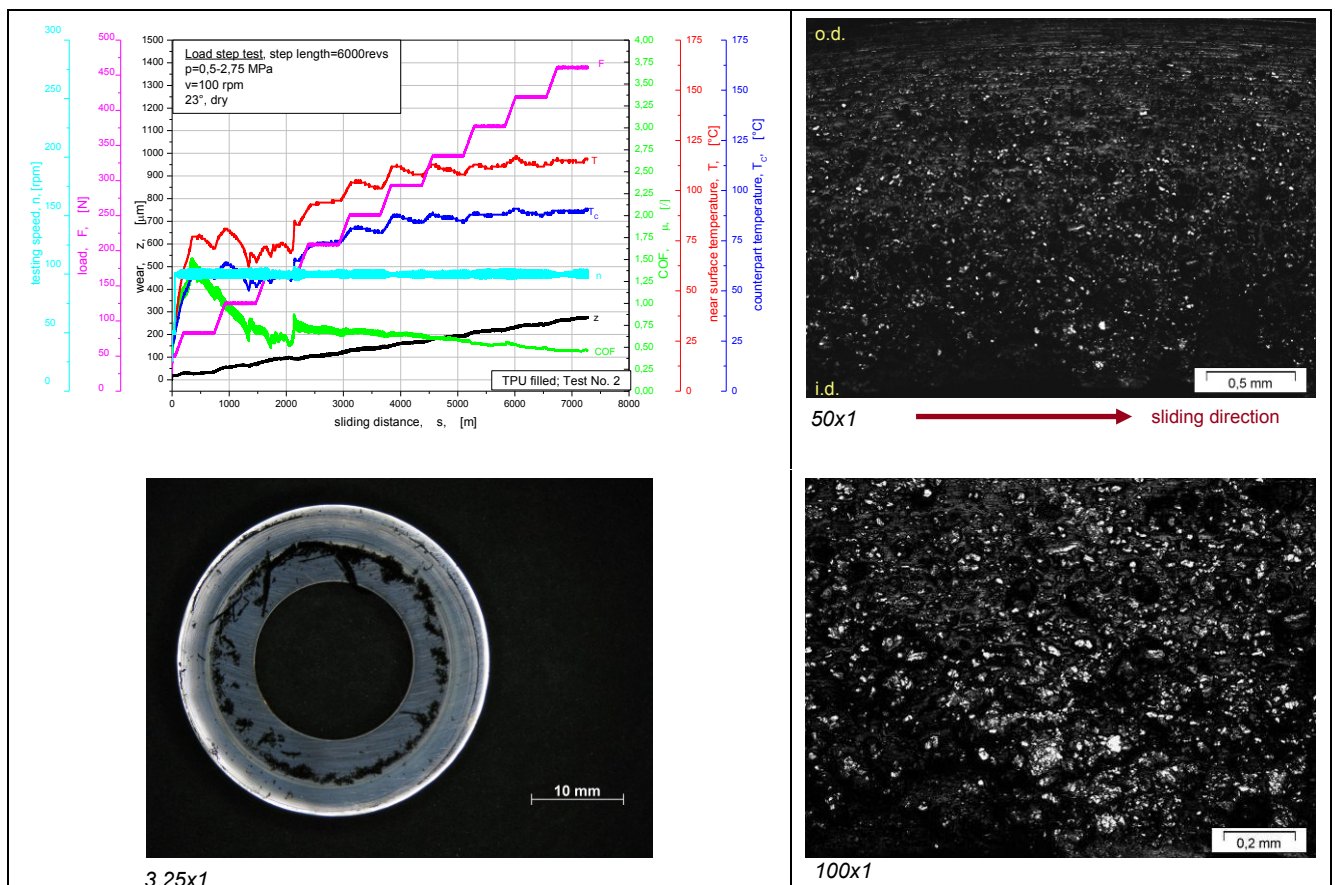


Figure 8.4-75: Advanced Load Step test at 100 rpm of TPU filled, Test No. 2

Advanced speed step tests for TPU filled

Table 8.4-18: Overview of the testing procedure of the advanced speed step test

Advanced speed step test TPU filled									
Test Parameters									
Step		Run in	1	2	3	4	5	6	7
Ramp time	[s]	x	237,90	43,21	44,77	45,71	47,36	48,83	50,30
Ramp distance	[m]	x	35,60	9,70	13,40	17,10	20,87	24,62	28,37
Testing force	[N]	50,00	83/166/250 N						
Contact pressure	[MPa]	0,30	0,50/1,00/1,50MPa						
Testing speed	[rpm]	50,00	100,00	150,00	200,00	250,00	300,00	350,00	400,00
Step length	[Revs]	x	6000,00						
Step distance	[m]	44,50	539,00	539,00	539,00	539,00	539,00	539,00	539,00
Testing temperature	[°C]	23,00							
Lubrication		dry							

Table 8.4-19: Summary of advanced speed step tests for the filled material

Advanced Speed Step Test TPU filled, 1 MPa, No. 1		100 rpm	150 rpm	200 rpm	250 rpm	300 rpm	350 rpm	400 rpm
Wear Parameters								
mass loss	[mg]	7,52						
overall wear rate K	[cm ³ /Nm]	2,69E-09						
linear wear rate	[µm/m]	0,06	0,01	0,02	0,00	0,01	0,01	0,01
Friction Parameters								
COF	[-]	0,80	0,76	0,67	0,56	0,57	0,50	0,46
near surface temperature	[°C]	81,00	106,00	119,00	123,00	134,00	142,00	154,00
counterpart temperature	[°C]	53,00	67,00	74,00	79,00	83,00	87,00	89,00
Advanced Speed Step Test TPU filled, 1 MPa, No. 2		100 rpm	150 rpm	200 rpm	250 rpm	300 rpm	350 rpm	400 rpm
Wear Parameters								
mass loss	[mg]	7,76						
overall wear rate K	[cm ³ /Nm]	2,78E-09						
linear wear rate	[µm/m]	0,03	0,00	0,02	0,01	0,01	0,01	0,02
Friction Parameters								
COF	[-]	0,80	0,83	0,65	0,55	0,54	0,51	0,48
near surface temperature	[°C]	88,00	118,00	123,00	126,00	136,00	145,00	157,00
counterpart temperature	[°C]	68,00	89,00	92,00	95,00	100,00	105,00	112,00

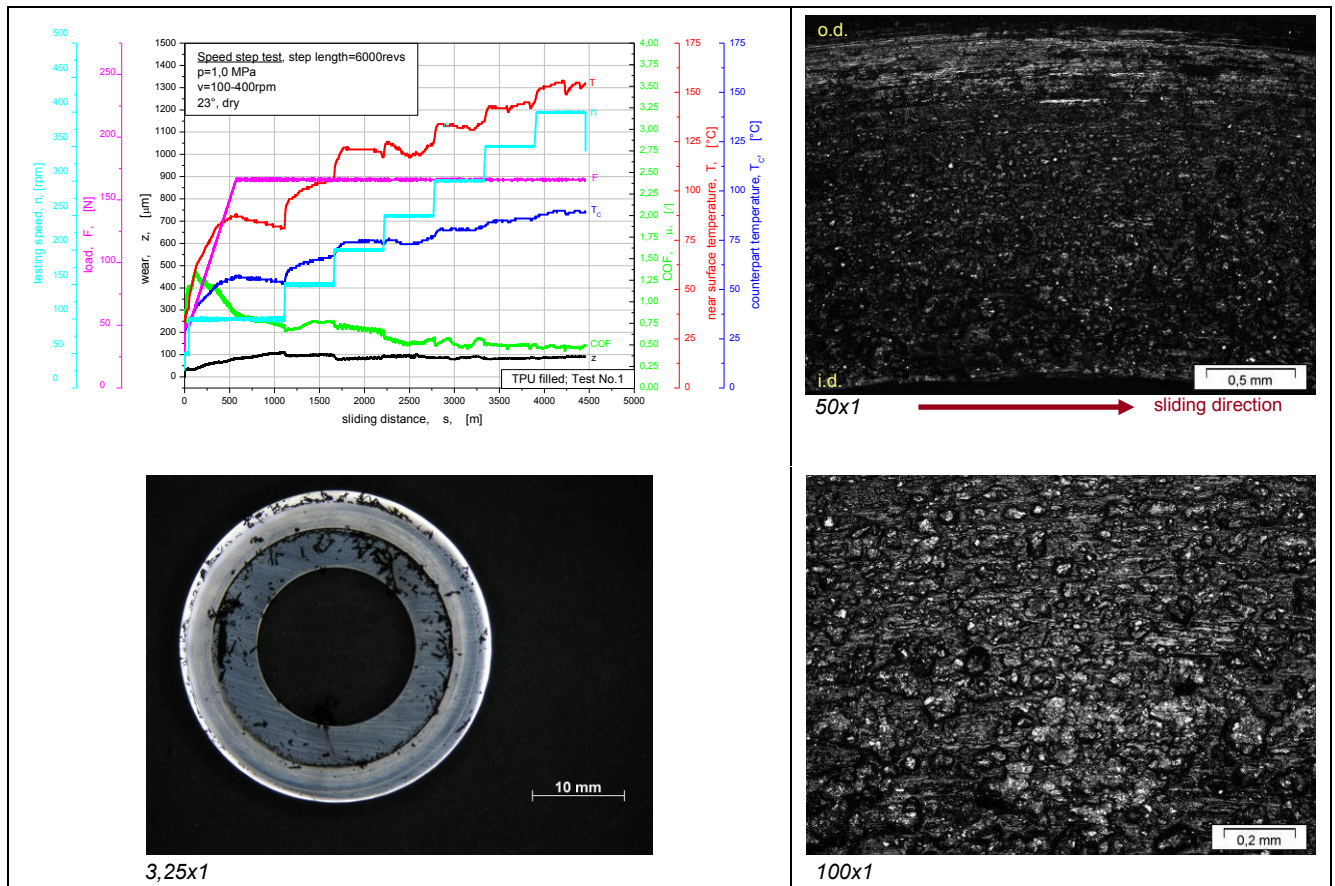


Figure 8.4-76: Advanced Speed Step test at 1,0 MPa of TPU filled, Test No.1

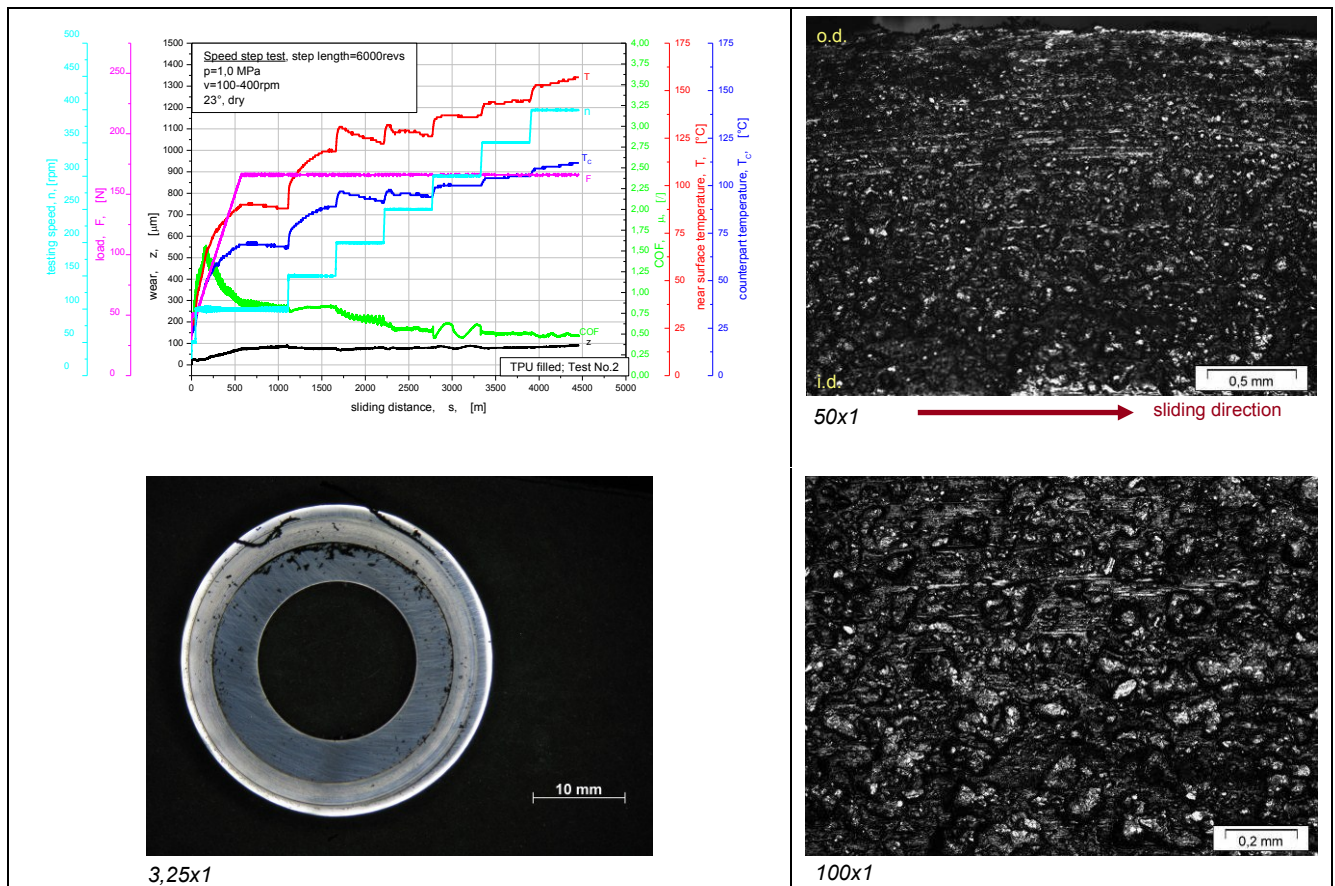


Figure 8.4-77: Advanced Speed Step test at 1,0 MPa of TPU filled, Test No.2